

Cover Page



Universiteit Leiden



The handle <http://hdl.handle.net/1887/20998> holds various files of this Leiden University dissertation.

Author: Smeden, Jeroen van

Title: A breached barrier : analysis of stratum corneum lipids and their role in eczematous patients

Issue Date: 2013-06-20

A BREACHED BARRIER
Analysis of stratum corneum lipids and their role
in eczematous patients

Jeroen van Smeden

The investigations described in this thesis were performed at the Division of Drug Delivery Technology of the Leiden Academic Centre for Drug Research, Leiden University, Leiden, The Netherlands. This research is supported by the Dutch Technology Foundation STW, which is part of the Netherlands Organisation for Scientific Research (NWO), and which is partly funded by the Ministry of Economic Affairs. In addition, the following companies provided substantial financial support to this research project: Astellas Pharma Inc., Evonik Industries AG, RiverD International B.V., and Unilever N.V.

© 2013, Jeroen van Smeden. All rights reserved. No part of this thesis may be reproduced or transmitted in any form or by any means without written permission of the author.

About the cover: The Great Wall of China is the largest man-made barrier in the world. With a total length of over 20,000 km, it was built as protection against invaders. Although it is clearly the most impressive barrier on earth made by men, its function as a barrier is nothing compared to the barrier function of humans largest organ, the skin. Although it is only about 0.0002 meter thick, it protects the body against continuous attacks from the environment. For example the number of bacteria that continuously try to breach the skin barrier, is estimated at 1,000,000,000,000 on an average human being, not taking into account other pathogens that may penetrate the skin. The skin barrier is located at the outermost layer of the skin, the horny layer (stratum corneum) and just like the Great Wall it is composed of a brick and mortar-like structure. In atopic eczema however, the skin barrier is impaired, and pathogens may penetrate the skin and cause an allergic reaction, often accompanied by red, dry, and itchy skin. This thesis describes several studies in which the skin barrier in eczematous patients is investigated.

Cover and part image: Photographs were legally purchased from iStockphoto and Janinja Olivier

Cover and thesis design by Melina Durinck

Printed by Gildeprint Drukkerijen (Enschede, The Netherlands)

A BREACHED BARRIER
Analysis of stratum corneum lipids and their role
in eczematous patients

Proefschrift

ter verkrijging van
de graad van Doctor aan de Universiteit Leiden,
op gezag van Rector Magnificus prof.mr. C.J.J.M. Stolker,
volgens besluit van het College voor Promoties
te verdedigen op donderdag 20 juni 2013
klokke 15:00 uur

door

Jeroen van Smeden
geboren te Leidschendam
in 1984

Promotiecommissie

Promotor: Prof. Dr. J. A. Bouwstra

Copromotor: Dr. R. J. Vreeken

Overige leden: Prof. Dr. M. Danhof
Prof. Dr. W. Jiskoot
Prof. Dr. J. van der Greef
Prof. Dr. J. M. Brandner
Dr. A. El Ghalbzouri

**To my loved ones,
Bianca, Lucas en Matthijs**



TABLE OF CONTENTS

9 PART I

35 PART II: METHOD DEVELOPMENT FOR DETAILED
STRATUM CORNEUM LIPID ANALYSIS

85 PART III: STRATUM CORNEUM LIPID COMPOSITION
IN ATOPIC ECZEMA AND ITS ROLE IN THE SKIN
BARRIER FUNCTION

155 PART IV: STUDIES ON STRATUM CORNEUM LIPIDS
FROM OTHER SKIN SOURCES SHOWING A BARRIER
DYSFUNCTION

199 PART V: SUMMARY AND APPENDICES

Chapter 1: General Introduction	10
Chapter 2: Aim and outline of this thesis	30
<hr/>	
Chapter 3: LC/MS analysis of stratum corneum lipids: ceramide profiling and discovery	36
Chapter 4: Combined LC/MS-Assay for Analysis of All Major Stratum Corneum Lipids, Focusing on Free Fatty Acids	58
<hr/>	
Chapter 5: Lamellar lipid organization and ceramide composition in the stratum corneum of patients with atopic eczema	86
Chapter 6: Increase in short-chain ceramides correlates with an altered lipid organization and decreased barrier function in atopic eczema patients	92
Chapter 7: The essence of free fatty acids and lipid chain length for the skin barrier function in patients with atopic eczema	116
Chapter 8: Lipid to protein ratio plays an important role in the skin barrier function atopic eczema patients	140
<hr/>	
Chapter 9: Skin barrier lipid composition and organization in Netherton Syndrome patients	156
Chapter 10: Increased Presence of Monounsaturated Fatty Acids in the Stratum Corneum of Human Skin Equivalents	176
<hr/>	
Summary and Perspectives	200
Nederlandse samenvatting	216
Curriculum vitae	236
List of publications	237
Dankwoord	238
List of abbreviations	240
<hr/>	



PART I

CHAPTER 1

GENERAL INTRODUCTION

Atopic eczema and its relation to the skin barrier

Atopic eczema (AE) is a multifactorial, chronic relapsing, pruritic, inflammatory skin disease. The disease is characterized by eczematous lesions as well as a broad spectrum of clinical manifestations, like xerosis (dry skin), erythema (red skin), and pruritus (itch) (Figure 1)¹. These symptoms affect the quality of life substantially, and patients often show difficulties in their social life². The incidence of AE in developed countries is rapidly increasing over the last two decennia to a current prevalence of 5-10% in adults and around 20% in children, making it one of the most common skin diseases³⁻⁸. The diagnosis of AE is based on a constellation of clinical findings, as there is no pathognomonic biomarker for diagnosis. Formerly, AE was considered as a solely inflammatory disease and therefore often referred to as atopic dermatitis (but also neurodermatitis and endogenous eczema). Patients show an increased reaction to antigens, thereby inducing a dominant T-cell response that upregulates the production of cytokines. Although the disease is called 'atopic', up



Figure 1: An example of a child with AE. In general, patients show the presence of lesional areas (affected, presence of erythema) as well as non-lesional sites (unaffected, which appear healthy).

to 60% of patients with the clinical phenotype of AE do not have elevation of total or allergen-specific IgE levels in serum. As only a subpopulation show increased levels of IgE antibodies and eosinophils (white blood cells associated with allergy), there is still a controversy in terminology⁹⁻¹¹.

However, a strong association between AE and loss-of-function mutations in the filaggrin gene (*FLG*) was observed in 2006¹²⁻¹⁶. Filaggrin is not directly related to the primary inflammatory response in AE, but is crucial for a proper formation of the outermost layer of the skin, the stratum corneum (SC), and SC hydration. The SC functions as the primary barrier of the skin¹⁷⁻¹⁹. Often referred to as a ‘brick and mortar’ structure, both the corneocytes (bricks) and lipids (mortar) are essential for the skin barrier. This finding created a paradigm shift in the understanding of the disease away from the inflammatory aspects towards AE as an epidermal barrier disorder^{11,20,21}. One of the current hypotheses is that defects in the barrier function of the SC may facilitate the transport of pathogens, allergens, and irritants across the skin, thereby provoking dysfunctional innate and adaptive immune responses (Figure 2)¹¹. This inflammation exacerbates the barrier defects, which allows successive pathogens to penetrate the skin, initiating a vicious circle. Recent studies corroborate this theory that a skin barrier dysfunction is causative for the risk of developing AE²¹⁻²⁶.

Human epidermis

Mammalian skin is divided into two layers, the dermis and epidermis (Figure 2). The former consists of predominantly collagen and elastin, but also contains fibroblasts and

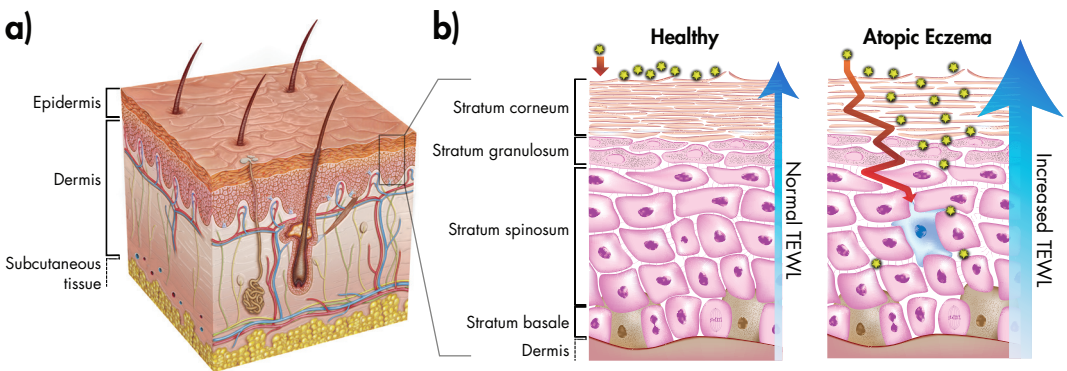


Figure 2: Schematic overview of the skin. **a)** Illustration resembling a cross-section of the skin showing the epidermis, dermis, and the subcutaneous tissue. A magnification of the epidermis is provided in. **b)** Under healthy conditions (left), the stratum corneum functions as the main barrier. However, a reduced barrier in AE patients (right) facilitates the transport of exogenous compounds into the deeper layers of the epidermis, thereby provoking an immune response. The reduced skin barrier function also leads to increased transepidermal water loss (TEWL).

the lymph vessels crucial for lymphocyte distribution in the dermis²⁷. Lymphocytes act as a second line of defense, and may induce a T-cell response when arrest of exogenous compounds occurs. In AE, lymphocyte activation leads to an inflammatory response resulting in skin lesions¹¹. The fact that exogenous compounds can reach the second line of defense means that it has already surpassed the epidermis.

The human epidermis can be divided into 4 layers (strata). The stratum basale is the deepest located layer that contains the epidermal stem cells. In this layer, proliferation of keratinocytes the major cell type takes place²⁸. Keratinocytes migrate upwards, and differentiate during this migration. This differentiation is a sequential process crucial for formation of the barrier function of the skin^{29,30}. First, keratinocytes are migrating to the stratum spinosum where the formation of lamellar bodies (LBs) is initiated³¹. LBs are secretory organelles that contain the precursors of the lipids essential for a proper skin barrier as well as many enzymes necessary to convert the lipids into their final structure in human SC³². The corneocytes are gradually differentiating and migrating towards the stratum granulosum, where numerous processes take place in a very short time period^{30,33,34}: Keratin filaments aggregate after interaction with filaggrin, and enzymes will start to degrade cell components like the nucleus and cell organelles. In addition, desmosomes that keep the keratinocytes together are transformed into corneodesmosomes, and a cornified envelope is formed around the plasma membrane of the keratinocytes³⁴. Lipids and enzymes of the LBs are extruded at the interface between the stratum granulosum and the uppermost layer of the skin, the SC³⁵⁻³⁷.

The stratum corneum as the primary skin barrier

The SC acts as the primary barrier against penetration of pathogens, allergens and other exogenous substances into the lower layers of the skin (the so-called outside-in barrier), and also prevent excessive transepidermal water loss (TEWL, Figure 2), the so-called inside-out barrier^{38,39}. The SC has a 'brick-and-mortar' like structure. The 'bricks' are corneocytes: flattened, terminally differentiated keratinocytes^{40,41}. The SC contains around 20 layers of corneocytes and is around 15-20 μm thick^{42,43}. The corneocytes are embedded in a lipid matrix that is the 'mortar' of the SC barrier. The mortar is formed at the interface of the stratum granulosum and SC: The lipid disks stored in the LBs are extruded into the intercellular space between the stratum granulosum and SC. These lipid disks fuse together and create the highly ordered lipid lamellae. Metabolism, transport and extrusion of the SC lipids will be discussed below.

The SC is constantly renewed. In human skin this occurs in approximately 2 to 4 weeks. At the surface, continuous shedding of the SC takes place at a rate of approximately $5 \cdot 10^8$

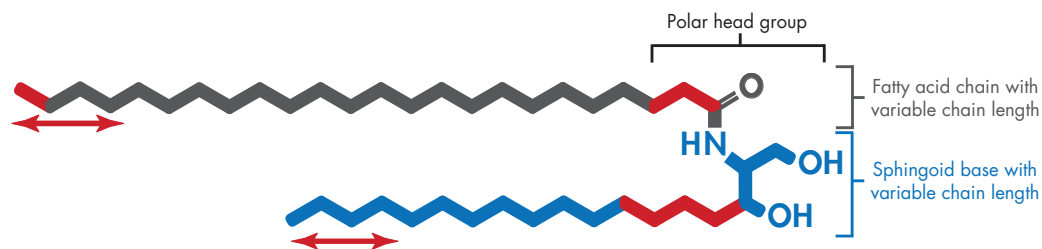
cells/day, a process called desquamation⁴⁴. It is an active process that depends on pH, enzyme activity, and also on SC water levels in which kallikreins (KLKs) and cathepsins degrade the strong cohesive links between the corneocytes, the corneodesmosomes⁴⁵⁻⁴⁹. Friction or sheer stress with the environment enhances the shedding of corneocytes at the skin surface.

The major penetration pathway of most molecules through the SC is along the intercellular pathway (i.e. penetration via the extracellular lipid matrix)^{50,51}. This emphasizes the importance of the SC lipids as the primary barrier components of the skin.

Extracellular lipid matrix in human stratum corneum

The lipids located in the extracellular matrix of the SC consist primarily of three lipid classes: ceramides (CERs), free fatty acids (FFAs), and cholesterol (CHOL), in approximately equimolar amounts⁵²⁻⁵⁵. The former two consist of carbon chains that are exceptionally heterogeneous in their molecular structure and are therefore classified into subclasses. Under healthy conditions, human SC FFAs are predominantly saturated, but mono-unsaturated FFAs (MUFAs) and trace amounts of poly-unsaturated FFAs (PUFAs) are present as well^{53,56,57}. FFAs with an additional hydroxyl-group (OH-FFAs) are occasionally reported too⁵⁷. Moreover, FFAs show an extensive variation in their carbon chain length. The most predominant FFAs have a chain length around 24 carbon atoms, but the full chain length distribution varies between 16 and 36 carbon atoms^{56,57}. The second lipid class, CERs, show even more structural diversity: They consist of a sphingoid base linked via an amide bond to a fatty acid (acyl) chain and are classified according to the different functional groups they have in both chains (Figure 3)⁵⁸: The sphingoid moiety can either be a sphingosine [S], dihydrosphingosine [DS], phytosphingosine [P] or 6-hydroxysphingosine [H]. The acyl chain is either non-hydroxylated [N], α -hydroxylated [A], or can even be ω -hydroxylated and successively linked to another fatty acid resulting in an esterified ω -hydroxylated [EO] acyl chain. The latter [EO] subclass (also named acyl-CER subclass) has an exceptionally long carbon chain which is unique for SC lipids. Different combinations in both carbon chains lead to the possibility of 12 different CER subclasses which have all been observed in human SC except for CER [EODs]⁵⁹. In addition to their variation in subclasses, CERs show a wide distribution in their total chain length (that is, the chain length of both the sphingosine base and the acyl chain together). CER chain lengths between 34 carbon atoms and 72 carbon atoms have been reported in healthy human subjects^{59,60}.

The SC lipid matrix is not only distinctive in its composition, but also shows a unique three-dimensional ordering (Figure 4)⁶¹. Lipids are organized in stacked layers, lamellae^{62,63}.



	Non-hydroxy fatty acid [N]	α -hydroxy fatty acid [A]	Esterified ω -hydroxy fatty acid [EO]
Dihydrosphingosine [dS]			
Sphingosine [S]			
Phytosphingosine [P]			
6-hydroxy sphingosine [H]			

Figure 3: Molecular structure and nomenclature of CERS. Containing a polar head group and two apolar tails, CERS are composed of a sphingoid base (depicted in blue) linked via an amide bond to an acyl chain (gray). Both chains can vary in their structure at the carbon positions indicated by the red arrows. In human SC, 4 different sphingoid bases (dihydrosphingosine [dS], sphingosine [S], phytosphingosine [P], 6-hydroxy sphingosine [H]) and 3 different acyl chains (non-hydroxy fatty acid [N], α -hydroxy fatty acid [A] and esterified ω -hydroxy fatty acid [EO]) are present. Together, this results in the presence of 12 subclasses of which all but CER [EOdS] have been identified in human SC.

The structures formed by these layers have a repeat distance (d) of approximately 6 nm or 13 nm, referred to as the short periodicity phase (SPP) and long periodicity phase (LPP), respectively⁶⁴⁻⁶⁶. In particular the LPP is considered to be important for the barrier function of the skin, as is demonstrated from *in vitro* studies using lipid membranes⁶⁷⁻⁶⁹. Approximately perpendicular to the lamellar organization, lipids are packed with certain density. This lateral lipid packing is also of high importance for a proper SC barrier function⁷⁰. At physiological temperature, human SC lipids are mainly present in a very dense orthorhombic organization. However, some lipid domains may be arranged in a less dense, hexagonal organization or even liquid organization, making the SC more permeable⁷¹⁻⁷⁵.

Epidermal lipid metabolism

SC lipids (viz. FFAs, CERS and CHOL) are either generated in viable keratinocytes by several enzymatic reactions (*de novo* synthesis) or taken up by keratinocytes from extracutaneous

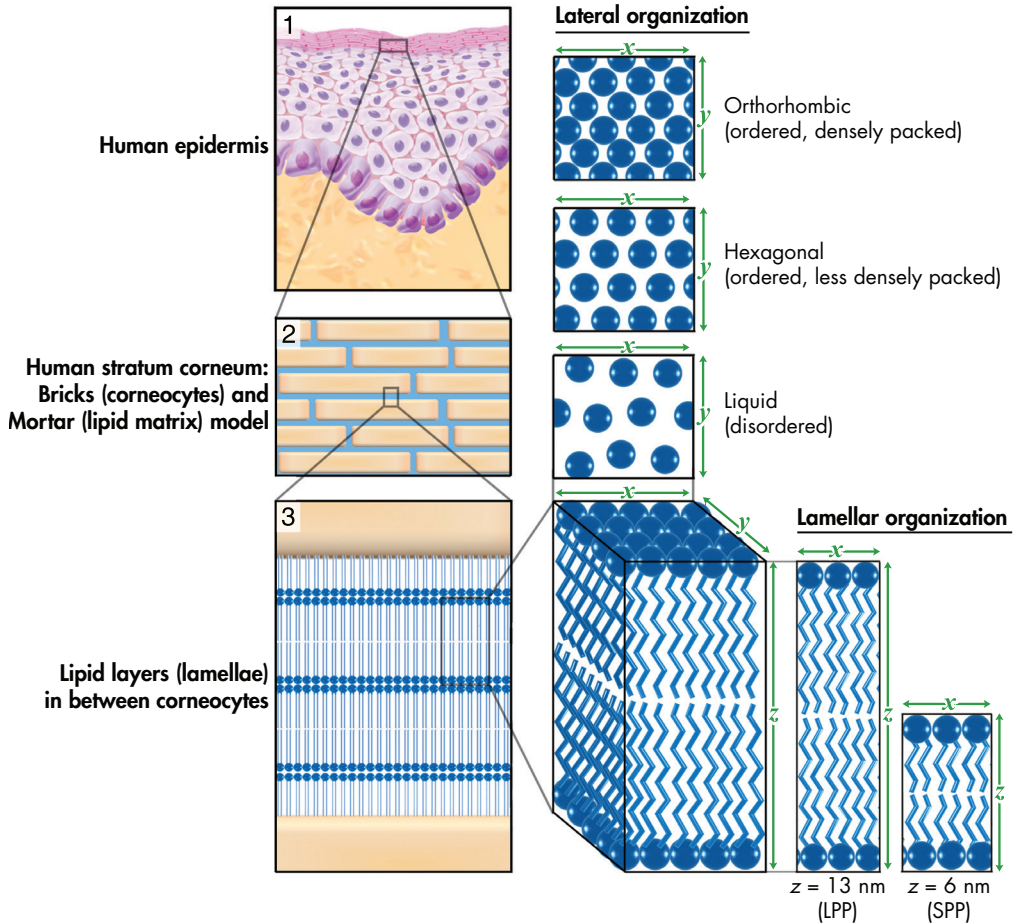


Figure 4: Descriptive illustration explaining the lamellar and lateral organization in human stratum corneum. **1)** The uppermost layer of the skin, the stratum corneum (SC), is composed of a 'brick' and 'mortar' structure of corneocytes and a highly ordered lipid matrix **2)** **3)** The lipids are arranged in stacked layers (lamellae), with two coexisting lamellar phases. These lamellar phases have a repeat distance of either 6 nm (SPP) or 13 nm (LPP). The lateral organization is the plane perpendicular to the direction of the lamellar organization. Three possible arrangements of the lipids are possible: a very dense, ordered orthorhombic organization, a less dense, ordered hexagonal organization, or a disordered liquid organization. The former is predominantly present in healthy human SC.

sources, such as the dietary lipids (e.g. essential FFAs) or lipids synthesized in other organs like the liver⁷⁶. Several enzymatic reactions are required for lipids synthesis and the subsequent lipid transport from the keratinocytes into the extracellular matrix of the SC, which will be discussed briefly (Figure 5).

Fatty acid synthase synthesizes FFAs to a chain length of 16 carbon atoms (palmitic acid) using acetyl-CoA and malonyl-CoA. Successively, FFAs can be elongated over 16 carbon atoms by a series of 7 elongases (ELOVLs)⁷⁷⁻⁷⁹. This results in a wide chain

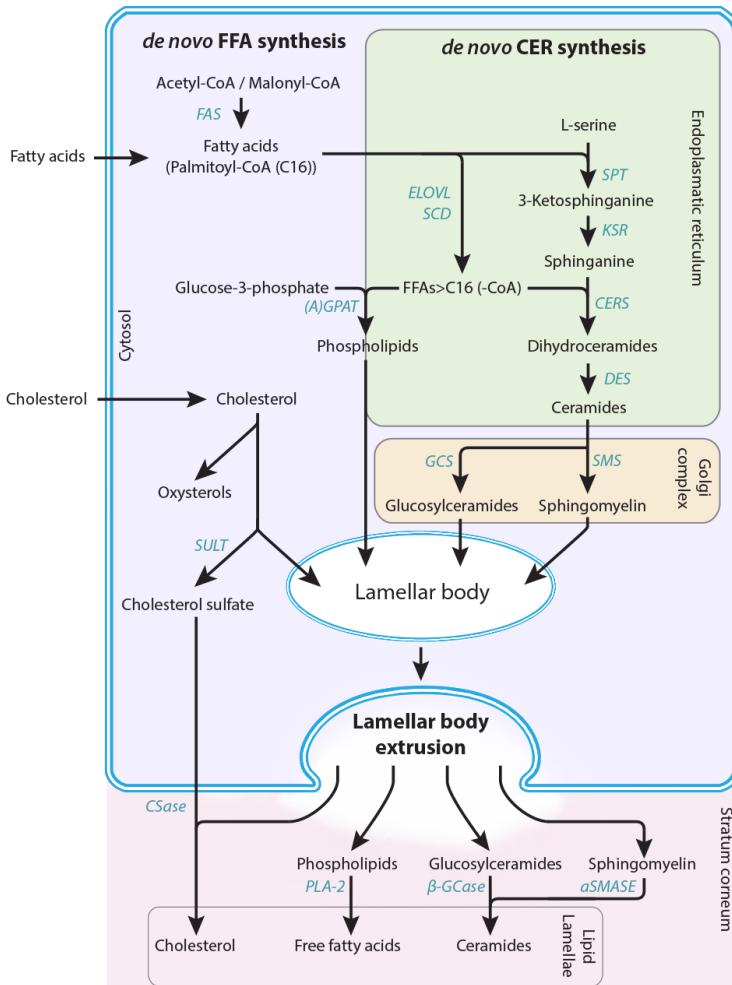


Figure 5: Schematic overview of main enzymatic processes involved in the formation of SC lipid lamellae. Arrows indicate the transport or conversion of lipids that are catalyzed by enzymes denoted by the abbreviations in blue. Abbreviations are as follows: FAS = fatty acid synthase; ELOVL = elongation of very long chain fatty acids family (1 to 7); SCD = stearoyl-CoA desaturase; SPT = serine palmitoyltransferase; KSR = 3-ketosphinganine reductase; (A)GPAT = (acyl)glycerol-3-phosphate acyltransferase; CERS = ceramide synthase family (1 to 6); DES = dihydroceramide desaturase (1 and 2); GCS = glucosylceramide synthase; SMS = sphingomyelin synthase; SULT = cholesterol sulfotransferase type 2B isoform 1b; CSase = cholesterol sulfatase; PLA-2 = phospholipase; β-GCcase = β-glucocerebrosidase; aSMASE = acid sphingomyelinase.

length distribution of FFAs. In addition to elongation, FFAs can be converted to mono-unsaturated FFAs (MUFAs) and poly-unsaturated FFAs (PUFAs) catalyzed by stearoyl-CoA desaturases (SCDs)⁸⁰. Subsequently, the synthesized FFAs can either be used for synthesis of CERS (described below) or transformed to phospholipids and stored into LBs.

CER synthesis occurs in the endoplasmic reticulum⁸¹⁻⁸³. The first step involves the enzyme serine palmitoyl transferase that catalyzes the condensation of serine and palmitoyl-CoA to form 3-keto-dihydrosphingosine, which is successively reduced to form dihydrosphingosine. The next enzymatic step acylates a FFA to dihydrosphingosine. In this step, 6 CER synthases are involved⁸⁴⁻⁸⁶. Each of the different CER synthases are more specific to certain FFA chain length and degree of unsaturation. The final step involves the conversion of the dihydrosphingosine into one of the several sphingoid subclasses

catalyzed by dihydroceramide desaturase (DES) enzymes. These subclasses of sphingoid bases are either sphingosine [S], dihydrosphingosine [DS], phytosphingosine [P], or 6-hydroxysphingosine [H]^{59,87}. The different CERS are then transported to the Golgi complex and converted to glucosyl-CERS and sphingomyelin, before transported into LBS^{86,88}.

CHOL is the third main component of the SC lipid matrix and needs no conversion for storage into the LBS. It can also be converted to oxysterol or CHOL-sulfate, which stimulates keratinocyte differentiation and plays a crucial role in the desquamation process by inhibiting the activity of proteases that promote the degradation of the desmosomes⁸⁹⁻⁹¹. Moreover, CHOL-sulfate is highly amphiphilic and can therefore cross the keratinocyte membrane and directly enter the stratum corneum where it will be partially converted back to CHOL by cholesterol sulfatase to be incorporated into the lipid lamellae^{76,92}.

The LBS generated in the stratum spinosum and stratum granulosum contain both the lipid precursors (CHOL, phospholipids, glucocylceramides and sphingomyelin) as well as the enzymes that convert the precursor-lipids into the final extracellular barrier lipids³¹. At the interface of the stratum granulosum and SC, secretion of the lipids from the LBS into the stratum corneum occurs. This process is called lamellar body extrusion, and is triggered by changes in the local calcium concentration⁷⁶. The lipids are then converted to their final substituents by enzymes that are cosecreted in the LBS^{32,93,94}: The phospholipids are converted back to FFAs (and glycerol) by phospholipases⁹⁵, whereas β -glucocerebrosidase and acidic sphingomyelinase convert respectively glucosylceramides and sphingomyelin back into CERS⁹⁶⁻⁹⁹.

Crucial for an optimal lipid synthesis and successive LB formation is a proper differentiation of keratinocytes. Important regulators of keratinocyte proliferation and differentiation are the nuclear hormone receptors like peroxisome proliferator-activated receptors (PPARs) and liver X receptor (LXR)^{92,100}. These transcription factors are designated as 'liposensors', as they can sense cellular lipid levels and adjust gene expression accordingly. PPARs are primarily activated by FFAs and their metabolic products, while LXR is activated by oxysterol metabolites¹⁰¹. Activation of PPARs and LXR stimulate expression of keratinocyte differentiation markers, such as loricrin, involucrin and filaggrin¹⁰²⁻¹⁰⁶. Consequently, as the amount of FFAs and CHOL necessary for LB formation increases, PPAR and LXR activation is also increased which stimulate corneocyte formation^{76,100}. In addition to their role in the formation of the SC 'bricks', PPARs and LXR also act directly on the SC lipids: They stimulate lipid synthesis, facilitates both LB formation and LB secretion, and promote extracellular lipid processing¹⁰⁷⁻¹¹⁰.

Stratum corneum hydration

The permeability, flexibility, and enzymatic activity of the SC is highly dependent on its water content. Proper SC hydration is regulated by (derivatives of) amino acids and specific salts, commonly referred to as the 'natural moisturizing factor' (NMF)^{111,112}. Reduced NMF levels in the SC may negatively affect the hydration level, but is also suggested to increase the local pH, as NMF are derived from amino acids. Sub-optimal SC hydration levels or pH can have an effect on hydrolytic enzymes and the aforementioned permeability and flexibility. This may thereby induce a negative effect on many processes like desquamation, keratinocyte differentiation, lipid synthesis, cornified envelope formation, and the SC barrier function^{111,113-119}. Most of the amino acid derived NMF are breakdown products of filaggrin. FLG mutations lead to reduced NMF levels which is associated with dry skin^{120,121}. This may explain the relation between AE, dry skin and FLG mutations¹²². Although loss-of-function mutations in the FLG gene are the foremost genetic risk factor for developing AE, a relatively large percentage of AE patients around 50-80% do not carry such a mutation^{123,124}. Besides, there is no convincing data that shows a clear relation between FLG mutations and a reduced skin barrier function in AE patients as measured by transepidermal water loss. Therefore, the role of filaggrin for an impaired SC barrier function remains indistinct, suggesting that other components of the epidermis and the skin barrier are likely to be involved as well¹²⁵⁻¹²⁷.

The cutaneous immune response in AE

The primary cause for inflammation in AE is related to penetration of antigens through the disrupted SC barrier. This leads to an acute Th2-driven inflammatory response in the early stage of AE, but can develop in a Th1-driven response when the disease becomes chronic^{11,20,128,129}. In addition, lesional epidermis (affected skin sites, Figure 1) in AE is characterized by infiltration of dermal dendritic cells, memory T cells, eosinophils, mast cells, lymphocytes and (IgE coated) macrophages^{11,130-134}. The Th2-response leads to increased expression of cytokines which play a crucial role in the cutaneous immune response. Among these are the pro-inflammatory interleukins (ILs), like IL-4, IL-5, IL-13, IL-17, IL-22 as well as IL-31, the initiator of the itch-response. These cytokines reduce the expression of filaggrin, thereby exaggerating AE^{11,135,136}. The production of these cytokines occurs in the T-cells, except for thymic stromal lymphopoietin (TSLP), which is produced by the keratinocytes. TSLP enhances the production of Th-2 cytokines by mast cells and mediates the dendritic cells towards a Th2-response^{137,138}.

The hydration of the skin is also of importance for the immune response. It is known that an increase in local pH induces the activity of serine proteases, leading to

the generation of primary cytokines, interleukin (IL)-1 α and IL-1 β ¹³⁹⁻¹⁴¹. These are considered to be important for triggering the cytokine cascade and are related to the skin barrier dysfunction¹⁴²⁻¹⁴⁴.

Studies on the SC barrier lipids in AE

The specific role of the lipid composition and organization with respect to AE has yet to be elucidated, though several studies show the importance of these aspects regarding AE. Concerning the lipid composition, there is conflicting information reported: some studies notice no change in the CER composition, whereas others demonstrate a decrease in total CER level as well as a decrease of CER subclasses [EOS], [EOH] and/or [NP], and increase in CER [AS]^{54,145-152}. A study by Ishikawa *et al.* tended to show differences in the chain length of some CER subclass in lesional skin only. In addition, they show that the levels of individual CER subclasses were altered even in non-lesional AE skin¹⁵³. With respect to FFAs, little is known on the changes in SC of AE compared to that in SC of control subjects. Results on the FFA lipid class in AE are scarce, but two studies report a decrease in SC FFAs longer than 24 or 26 carbon atoms in AE patients^{154,155}. With respect to the lipid organization in AE patients, almost no information is available. Pilgram *et al.* performed a limited study in 3 AE subjects in which they observe a significant increase in hexagonally ordered lipids compared to controls, as studied by electron diffraction. Fartasch *et al.* show that LB extrusion is delayed in AE, resulting in diminished delivery of the lipids into the intercellular regions¹⁵⁶. The metabolic enzymes involved in lipid synthesis have been studied as well, since these are involved in the underlying causes for possible changes in the SC lipids of AE patients. However, the data are scarce. For example: two studies report no changes in enzyme activity of sphingomyelinase and β -glucocerebrosidase in skin of AE patients compared to healthy controls^{157,158}. However, this is contradictory to a study published by Jensen *et al.*, who reported a reduced activity of sphingomyelinase in both lesional and non-lesional skin of AE patients¹⁵⁹. Hara *et al.* report that ceramide deficiency is related to another enzyme, sphingomyelin deacylase, which converts sphingomyelin into sphingosylphosphorylcholine and FFAs instead of CERS^{160,161}. Another example of important SC lipid modulators which are modified in AE are the PPARs. Lesional skin of AE patients showed an increased expression of PPAR β/δ , while the expression of PPAR α and PPAR γ was decreased^{162,163}. As discussed before, PPARs stimulate keratinocyte expression and have a direct effect on lipid synthesis, LB formation and its secretion, and promote extracellular lipid processing. Changes in these nuclear receptor proteins are therefore suggested to affect the SC lipid barrier. However, the changes in differentiation in relation to lipid biosynthesis and lipid composition are not fully established. One of the important

pieces in the puzzle is a comprehensive analysis of the barrier lipids, in which not only the lipid classes, but also the chain length distribution of the lipids is studied.

Analysis of the SC lipid composition

Analyzing the three main SC lipid classes (CHOL, FFA, CERS) can be challenging, as these lipids are very non-polar and show a large diversity¹⁶⁴. FFAs are most commonly analyzed by gas chromatography (GC) or gas liquid chromatography (GLC). Although the lipid composition can be examined in detail, the main draw-back of these methods is related to the labor intensive derivatization of the sample prior to analysis^{165,166}. Despite all technological improvements, identification and quantification of SC FFAs has only been reported twice by Ansari and Norlen in healthy human skin^{56,57}.

The structural variation is the main challenge for analysis of CERS. Usually, thin layer chromatography (TLC) is used to separate some of the CER subclasses, and quantification or additional structural information can be obtained by successive densitometry or nuclear magnetic resonance (NMR) spectroscopy^{58,150,167-170}. Main drawbacks are that TLC is usually cumbersome, cannot separate all subclasses at once, and has a low linear dynamic range in terms of quantification^{58,164}. Better separation of lipids can usually be achieved by GC, but CERS are non-volatile and unstable in the gas-phase, making GC only compatible for analysis of CERS when derivatized¹⁷¹⁻¹⁷⁴. Liquid chromatography (LC) in combination with light-scattering detection (LSD) has proven its potential for proper SC CER separation and analysis, but the inability for quantification is a major disadvantage¹⁷⁵⁻¹⁷⁹. Mass spectrometry (MS) is currently the most sensitive and powerful tool for identification of CERS, and although quantification is relatively difficult, technological developments over the last decennia have led to improvements on this major issue. In combination with LC, it allows for analysis of all CER subclasses and can distinguish between different chain lengths as well. Whereas TLC in combination with NMR demonstrates the presence of 9 CER subclasses, the introduction of LC/MS has led to the discovery and identification of 2 additional subclasses. MS can be a powerful tool as it gives information on the mass of a compound, a unique feature very useful for identification. However, the aforementioned quantification issue is a major drawback. Proper quantification is usually difficult as MS needs extensive validation, multiple internal standards per sample and quality controls. Nevertheless, reported data on SC CERS by LC/MS has proven its potential and its high sensitivity makes LC/MS the preferred method when small quantities of material are used^{59,60,180-185}.

The analysis of all lipid classes at once is currently limited to TLC only. This method has led to enormous advancements in the understanding of lipids in the SC, and is still

frequently used for SC lipid analysis. However, the aforementioned disadvantages makes this method not appropriate for detailed analysis, especially when focusing on the lipid chain length distribution or when using small lipid amounts. There is currently no method for detailed analysis of all SC lipids, in which chain lengths of individual FFAs and CERS as well as all their subclasses can be studied at once. One of the primary challenges that will be addressed in this thesis is regarding development of a robust and high-throughput method, using straightforward sample preparation that enables detailed analysis of all main SC lipid classes in a single setup using very limited sample amounts. LC in combination with MS seems most promising, as it can both separate lipid classes based on polarity (like TLC), and in addition on a second dimension: molecular mass.

The analytical methods reported in literature have also been used to study the SC lipids in AE, although the results remain inconclusive. For example, two (relatively recently) developed methods report contradictory information regarding AE. Farwanah *et al.* developed a high performance TLC method to compare the CER composition in non-lesional skin of 7 AE patients with 7 healthy control subjects¹⁴⁶. However, they observed no differences in any of the CER subclasses between the two groups. In contrast, Masukawa *et al.* developed an LC/MS method to study 8 AE patients and 7 control subjects¹⁵³. In contrast to Farwanah *et al.*, they observed significant changes in some of the CER subclasses of both lesional skin and non-lesional skin. They suggest that besides CER subclasses, CER chain length may be of importance for a proper SC lipid composition. These contradictory results show that more information is required to fully elucidate the lipid composition in these patients. To achieve this, there is a need for proper analytical methods enabling the analysis of all lipid classes in SC as well as the lipid chain length.

Analyzing the SC lipid organization

The SC lipids are organized in a highly ordered 3D-structure (Figure 4). The lamellar lipid organization can be studied by means of small angle x-ray diffraction (SAXD). The principle of SAXD is that x-rays are scattered by a sample (i.e. SC sheets). The scattered x-rays are recorded as a function of its scattering vector (q), defined as $q = 2\pi \cdot \sin \theta / \lambda$, in which λ is the wavelength of the x-rays and θ the angle of the scattered x-rays (Figure 6a). As the lamellar lipid organization is characterized by repeating lipid layers (periodicity phase), a typical SAXD profile of human SC (see Figure 6b) shows sequential maxima from which the repeat distance (d) of the LPP and SPP can be determined, according to the equation $d = n \cdot 2\pi / q_n$ ($n =$ order of diffraction peak)⁶⁴⁻⁶⁶.

The lateral lipid organization can be studied by Fourier transform infrared spectroscopy (FTIR). An infrared beam is emitted on a sample (i.e. SC sheet), and the amount of IR

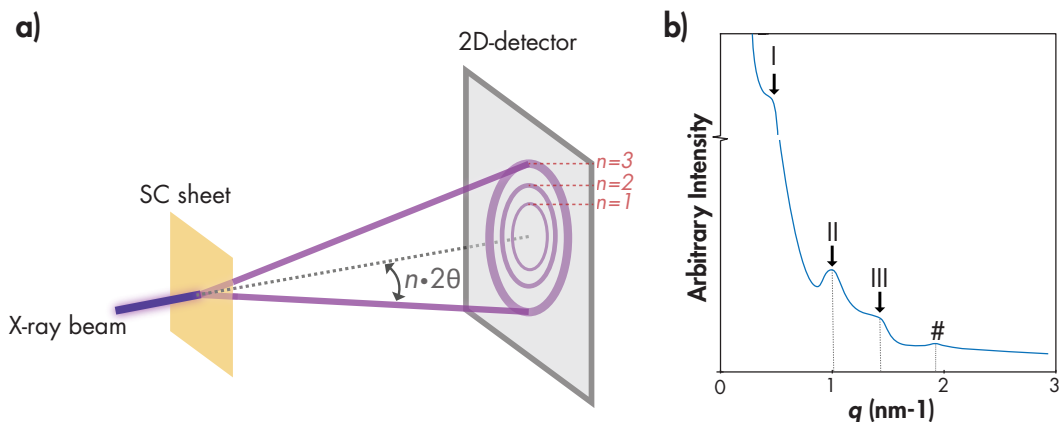


Figure 6: **a)** Principle of SAXD. An X-ray beam is scattered at a certain angle (θ) by the SC sheet, resulting in a 2D-SAXD image, which can be transformed into a typical SAXD plot shown in **b)**: A representative SAXD profile of human SC. The scattering intensity is plotted as a function of q , which is defined by $q = 2\pi \sin \theta / \lambda$. The X-ray diffraction graph of human SC is characterized by a high intensity at low q values due to keratin in the corneocytes and a series of peaks. The peaks indicated by I (weak peak), II (strong peak) and III (weak peak) are attributed to the LPP. Peak II is also attributed to the SPP. The peak indicated by # is due to CHOL.

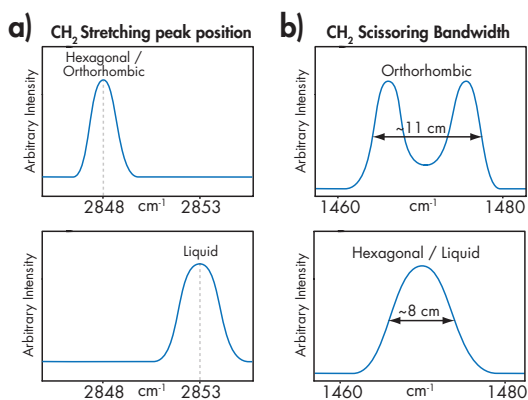


Figure 7: The lateral organization can be measured by FTIR. **a)** CH₂ stretching vibrations: At a lower frequency (~ 2848 cm⁻¹), CH₂ stretching vibrations indicate a high degree of conformational ordering of the lipids, whereas a high wavenumber (2853 cm⁻¹) is indicative for a liquid organization (low degree of conformational ordering). **b)** CH₂ scissoring vibrations (1460 - 1480 cm⁻¹): An orthorhombic organization results in a splitting of the scissoring vibrations, while a hexagonal packing results in a single vibration.

radiation that is absorbed due to resonating atom bond vibrations is recorded. Analyzing specific vibrations in different wavelength regions provide information on the 3-dimensional SC lipid organization. These are e.g. CH₂ symmetric stretching vibrations (2848 - 2053 cm⁻¹) and the CH₂ scissoring vibrations (1460 - 1480 cm⁻¹; Figure 7)⁷¹⁻⁷⁵. The former provides information on the conformational ordering of the lipids, and peak positions at a lower frequency (~ 2848 cm⁻¹) contribute to a higher degree of conformational ordering than peak positions located at a higher wavenumber (2853 cm⁻¹). The bandwidth of the CH₂ scissoring vibrations is indicative for the amount of orthorhombic domains

present in human SC. A small, single peak with a limited bandwidth is indicative for the presence of a hexagonal organization, whereas an increased bandwidth of the scissoring vibrations is indicative for an increased fraction of lipids present as orthorhombic lipid domains.

This thesis

The rapid increase in prevalence of AE urges for novel treatments, also with respect to SC barrier repair. However, the exact role of the SC lipids for the impaired skin barrier function in AE is inconclusive. This lack of knowledge hampers the development for restoring the SC barrier by e.g. topical treatments. The studies described in this thesis aim in providing detailed information on the SC lipid composition, the lipid organization, and the role of SC lipids for the skin barrier function. In other words: we want to study the role of the lipids in the impaired skin barrier in AE. To study these three basal parameters in a combined study is unique, but needs several scientific barriers to be breached before this can be realized. The next chapter will describe the objectives and aims that facilitate in realizing the main goal of the study.

References

- 1 Leung DY, Bieber T. Atopic dermatitis. *Lancet* 2003; 361: 151-60.
- 2 Kiebert G, Sorensen SV, Revicki D *et al.* Atopic dermatitis is associated with a decrement in health-related quality of life. *International Journal of Dermatology* 2002; 41: 151-8.
- 3 Alanne S, Nermes M, Soderlund R *et al.* Quality of life in infants with atopic dermatitis and healthy infants: a follow-up from birth to 24 months. *Acta Paediatrica* 2011; 100: e65-70.
- 4 Alvarenga TM, Caldeira AP. Quality of life in pediatric patients with atopic dermatitis. *J Pediatr (Rio J)* 2009; 85: 415-20.
- 5 Misery L, Finlay AY, Martin N *et al.* Atopic dermatitis: impact on the quality of life of patients and their partners. *Dermatology* 2007; 215: 123-9.
- 6 Mozaffari H, Pourpak Z, Poursayed S *et al.* Quality of life in atopic dermatitis patients. *Journal of microbiology, immunology, and infection = Wei mian yu gan ran za zhi* 2007; 40: 260-4.
- 7 Slattery MJ, Essex MJ, Paletz EM *et al.* Depression, anxiety, and dermatologic quality of life in adolescents with atopic dermatitis. *The Journal of allergy and clinical immunology* 2011; 128: 668-71.
- 8 van Valburg RW, Willemsen MG, Dirven-Meijer PC *et al.* Quality of life measurement and its relationship to disease severity in children with atopic dermatitis in general practice. *Acta Dermato-Venereologica* 2011; 91: 147-51.
- 9 Flohr C, Johansson SG, Wahlgren CF *et al.* How atopic is atopic dermatitis? *The Journal of allergy and clinical immunology* 2004; 114: 150-8.
- 10 Wollenberg A, Rawer HC, Schaubert J. Innate immunity in atopic dermatitis. *Clin Rev Allergy Immunol* 2011; 41: 272-81.
- 11 Oyoshi MK, He R, Kumar L *et al.* Cellular and molecular mechanisms in atopic dermatitis. *Adv Immunol* 2009; 102: 135-226.
- 12 Palmer CN, Irvine AD, Terron-Kwiatkowski A *et al.* Common loss-of-function variants of the epidermal barrier protein filaggrin are a major predisposing factor for atopic dermatitis. *Nature Genetics* 2006; 38: 441-6.
- 13 Brown SJ, McLean WH. One remarkable molecule: filaggrin. *The Journal of investigative dermatology* 2012; 132: 751-62.
- 14 Irvine AD, McLean WH, Leung DY. Filaggrin mutations associated with skin and allergic diseases. *The New England journal of medicine* 2011; 365: 1315-27.
- 15 McLean WH, Irvine AD. Heritable filaggrin disorders: the paradigm of atopi dermatitis. *The Journal of investigative dermatology* 2012; 132: E20-1.
- 16 O'Regan GM, Sandilands A, McLean WH *et al.* Filaggrin in atopic dermatitis. *The Journal of allergy and clinical immunology* 2008; 122: 689-93.
- 17 Elias PM, Choi EH. Interactions among stratum corneum defensive functions. *Experimental Dermatology* 2005; 14: 719-26.
- 18 Elias PM. Stratum corneum defensive functions: an integrated view. *The Journal of investigative dermatology* 2005; 125: 183-200.
- 19 Irvine AD, McLean WH. Breaking the (un)sound barrier: filaggrin is a major gene for atopic dermatitis. *The Journal of investigative dermatology* 2006; 126: 1200-2.
- 20 Elias PM, Hatano Y, Williams ML. Basis for the barrier abnormality in atopic dermatitis: outside-inside-outside pathogenic mechanisms. *The Journal of allergy and clinical immunology* 2008; 121: 1337-43.
- 21 Elias PM, Steinhoff M. "Outside-to-inside" (and now back to "outside") pathogenic mechanisms in atopic dermatitis. *The Journal of investigative dermatology* 2008; 128: 1067-70.
- 22 Elias PM. Barrier repair trumps immunology in the pathogenesis and therapy of atopic dermatitis. *Drug Discov Today Dis Mech* 2008; 5: e33-e8.
- 23 Seidenari S, Giusti G. Objective assessment of the skin of children affected by atopic dermatitis: A study of pH, capacitance and tewl in eczematous and clinically uninvolved skin. *Acta Dermato-Venereologica* 1995; 75: 429-33.
- 24 Elias PM, Schmutz M. Abnormal skin barrier in the etiopathogenesis of atopic dermatitis. *Current Opinion in Allergy and Clinical Immunology* 2009; 9: 437-46.
- 25 Werner Y, Lindberg M. Transepidermal water loss in dry and clinically normal skin in patients with atopic dermatitis. *Acta Derm Venereol* 1985; 65: 102-5.
- 26 Yoshiike T, Aikawa Y, Sindhvananda J *et al.* Skin barrier defect in atopic dermatitis: increased permeability of the stratum corneum using dimethyl sulfoxide and theophylline. *J Dermatol Sci* 1993; 5: 92-6.
- 27 Kielty CM, Shuttleworth CA. Microfibrillar elements of the dermal matrix. *Microsc Res Tech* 1997; 38: 413-27.
- 28 Barthel R, Aberdam D. Epidermal stem cells. *Journal of the European Academy of Dermatology and Venereology : JEADV* 2005; 19: 405-13.
- 29 Eckert RL. Structure, function, and differentiation of the keratinocyte. *Physiol Rev* 1989; 69: 1316-46.
- 30 Fuchs E. Epidermal differentiation: the bare essentials. *The Journal of cell biology* 1990; 111: 2807-14.
- 31 Feingold KR. Lamellar bodies: the key to cutaneous barrier function. *The Journal of investigative dermatology* 2012; 132: 1951-3.
- 32 Elias PM, Feingold KR. Epidermal lamellar body as a multifunctional secretory organelle. In: *Skin barrier* (Elias P, Feingold K, eds). New York: Taylor & Francis. 2006; 261-72.
- 33 Eckert RL, Rorke EA. Molecular biology of keratinocyte differentiation. *Environmental health perspectives* 1989; 80: 109-16.
- 34 Steven AC, Bisher ME, Roop DR *et al.* Biosynthetic pathways of filaggrin and lorincin--two major proteins expressed by terminally differentiated epidermal keratinocytes. *J Struct Biol* 1990; 104: 150-62.
- 35 Fartasch M, Bassukas ID, Diepgen TL. Structural relationship between epidermal lipid lamellae, lamellar bodies and desmosomes in human epidermis: an ultrastructural study. *The British journal of dermatology* 1993; 128: 1-9.
- 36 Menon GK, Ghadially R, Williams ML *et al.* Lamellar bodies as delivery systems of hydrolytic enzymes: implications for

- normal and abnormal desquamation. *The British journal of dermatology* 1992; 126: 337-45.
- 37 Menon GK, Feingold KR, Elias PM. Lamellar body secretory response to barrier disruption. *The Journal of investigative dermatology* 1992; 98: 279-89.
- 38 Madison KC. Barrier function of the skin: "la raison d'etre" of the epidermis. *The Journal of investigative dermatology* 2003; 121: 231-41.
- 39 Scheuplein RJ, Blank IH. *Permeability of the skin. Physiol Rev* 1971; 51: 702-47.
- 40 Elias PM. Epidermal lipids, barrier function, and desquamation. *The Journal of investigative dermatology* 1983; 80 Suppl: 44s-9s.
- 41 Elias PM. Epidermal lipids, membranes, and keratinization. *International Journal of Dermatology* 1981; 20: 1-19.
- 42 Blair C. Morphology and thickness of the human stratum corneum. *The British journal of dermatology* 1968; 80: 430-6.
- 43 Holbrook KA, Odland GF. Regional differences in the thickness (cell layers) of the human stratum corneum: an ultrastructural analysis. *The Journal of investigative dermatology* 1974; 62: 415-22.
- 44 Milstone LM. Epidermal desquamation. *Journal of dermatological science* 2004; 36: 131-40.
- 45 Egelrud T. Desquamation in the stratum corneum. *Acta dermato-venereologica. Supplementum* 2000; 208: 44-5.
- 46 Emami N, Diamandis EP. Human tissue kallikreins: a road under construction. *Clinica chimica acta; international journal of clinical chemistry* 2007; 381: 78-84.
- 47 Ishida-Yamamoto A, Kishibe M. Involvement of corneodesmosome degradation and lamellar granule transportation in the desquamation process. *Medical Molecular Morphology* 2011; 44: 1-6.
- 48 Ishida-Yamamoto A, Igawa S, Kishibe M. Order and disorder in corneocyte adhesion. *The Journal of dermatology* 2011; 38: 645-54.
- 49 Bouwstra JA, Groenink HW, Kempenaar JA *et al.* Water distribution and natural moisturizer factor content in human skin equivalents are regulated by environmental relative humidity. *The Journal of investigative dermatology* 2008; 128: 378-88.
- 50 Williams ML, Elias PM. The extracellular matrix of stratum corneum: role of lipids in normal and pathological function. *Crit Rev Ther Drug Carrier Syst* 1987; 3: 95-122.
- 51 Johnson ME, Blankschtein D, Langer R. Evaluation of solute permeation through the stratum corneum: lateral bilayer diffusion as the primary transport mechanism. *Journal of Pharmaceutical Sciences* 1997; 86: 1162-72.
- 52 Wertz PW, Downing DT. Epidermal lipids. In: *Physiology, biochemistry, and molecular biology of the skin* (Goldsmith LA, ed), 2nd edn. New York: Oxford University Press. 1991; 205-36.
- 53 Bouwstra JA, Gooris GS, Cheng K *et al.* Phase behavior of isolated skin lipids. *Journal of lipid research* 1996; 37: 999-1011.
- 54 Holleran WM, Takagi Y, Uchida Y. Epidermal sphingolipids: metabolism, function, and roles in skin disorders. *Febs Letters* 2006; 580: 5456-66.
- 55 Man MM, Feingold KR, Thornfeldt CR *et al.* Optimization of physiological lipid mixtures for barrier repair. *The Journal of investigative dermatology* 1996; 106: 1096-101.
- 56 Norlen L, Nicander I, Lundsjo A *et al.* A new HPLC-based method for the quantitative analysis of inner stratum corneum lipids with special reference to the free fatty acid fraction. *Archives of Dermatological Research* 1998; 290: 508-16.
- 57 Ansari MN, Nicolaides N, Fu HC. Fatty acid composition of the living layer and stratum corneum lipids of human sole skin epidermis. *Lipids* 1970; 5: 838-45.
- 58 Motta S, Monti M, Sesana S *et al.* Ceramide composition of the psoriatic scale. *Biochim Biophys Acta* 1993; 1182: 147-51.
- 59 Masukawa Y, Narita H, Shimizu E *et al.* Characterization of overall ceramide species in human stratum corneum. *J Lipid Res* 2008; 49: 1466-76.
- 60 Farwanah H, Wohlrab J, Neubert RH *et al.* Profiling of human stratum corneum ceramides by means of normal phase LC/APCI-MS. *Anal Bioanal Chem* 2005; 383: 632-7.
- 61 Bouwstra JA, Dubbelaar FE, Gooris GS *et al.* The lipid organisation in the skin barrier. *Acta dermato-venereologica. Supplementum* 2000; 208: 23-30.
- 62 Madison KC, Swartzendruber DC, Wertz PW *et al.* Presence of intact intercellular lipid lamellae in the upper layers of the stratum corneum. *The Journal of investigative dermatology* 1987; 88: 714-8.
- 63 Bouwstra JA, Gooris GS, van der Spek JA *et al.* Structural investigations of human stratum corneum by small-angle X-ray scattering. *The Journal of investigative dermatology* 1991; 97: 1005-12.
- 64 Groen D, Gooris GS, Bouwstra JA. New insights into the stratum corneum lipid organization by X-ray diffraction analysis. *Biophysical Journal* 2009; 97: 2242-9.
- 65 McIntosh TJ, Stewart ME, Downing DT. X-ray diffraction analysis of isolated skin lipids: reconstitution of intercellular lipid domains. *Biochemistry* 1996; 35: 3649-53.
- 66 Bouwstra J, Pilgram G, Gooris G *et al.* New aspects of the skin barrier organization. *Skin Pharmacology and Applied Skin Physiology* 2001; 14 Suppl 1: 52-62.
- 67 Groen D, Poole DS, Gooris GS *et al.* Is an orthorhombic lateral packing and a proper lamellar organization important for the skin barrier function? *Biochimica Et Biophysica Acta* 2011; 1808: 1529-37.
- 68 de Jager M, Groenink W, Bielsa i Guivernau R *et al.* A novel in vitro percutaneous penetration model: evaluation of barrier properties with p-aminobenzoic acid and two of its derivatives. *Pharm Res* 2006; 23: 951-60.
- 69 Grubauer G, Feingold KR, Harris RM *et al.* Lipid content and lipid type as determinants of the epidermal permeability barrier. *Journal of lipid research* 1989; 30: 89-96.
- 70 Bommannan D, Potts RO, Guy RH. Examination of stratum corneum barrier function in vivo by infrared spectroscopy. *The Journal of investigative dermatology* 1990; 95: 403-8.
- 71 Pilgram GS, Engelsma-van Pelt AM, Bouwstra JA *et al.* Electron diffraction provides new information on human stratum corneum lipid organization studied in relation to depth and temperature. *The Journal of investigative dermatology* 1999; 113: 403-9.
- 72 Damien F, Boncheva M. The extent of orthorhombic lipid

- phases in the stratum corneum determines the barrier efficiency of human skin *in vivo*. *The Journal of investigative dermatology* 2010; 130: 611-4.
- 73 Goldsmith LA, Baden HP. Uniquely oriented epidermal lipid. *Nature* 1970; 225: 1052-3.
- 74 de Jager MW, Gooris GS, Dolbnya IP *et al*. The phase behaviour of skin lipid mixtures based on synthetic ceramides. *Chemistry and physics of lipids* 2003; 124: 123-34.
- 75 Bouwstra JA, Gooris GS, Dubbelaar FE *et al*. Phase behavior of lipid mixtures based on human ceramides: coexistence of crystalline and liquid phases. *Journal of lipid research* 2001; 42: 1759-70.
- 76 Feingold KR. Thematic review series: skin lipids. The role of epidermal lipids in cutaneous permeability barrier homeostasis. *Journal of lipid research* 2007; 48: 2531-46.
- 77 Uchida Y. The role of fatty acid elongation in epidermal structure and function. *Dermato-endocrinology* 2011; 3: 65-9.
- 78 Kihara A. Very long-chain fatty acids: elongation, physiology and related disorders. *Journal of Biochemistry* 2012; 152: 387-95.
- 79 Ohno Y, Suto S, Yamanaka M *et al*. ELOVL1 production of C24 acyl-CoAs is linked to C24 sphingolipid synthesis. *Proc Natl Acad Sci U S A* 2010; 107: 18439-44.
- 80 Miyazaki M, Ntambi JM. Chapter 7 - Fatty acid desaturation and chain elongation in mammals. In: *Biochemistry of Lipids, Lipoproteins and Membranes (Fifth Edition)* (Dennis EV, Jean EV, eds). San Diego: Elsevier. 2008; 191-V.
- 81 Merrill AH, Jr. De novo sphingolipid biosynthesis: a necessary, but dangerous, pathway. *The Journal of biological chemistry* 2002; 277: 25843-6.
- 82 Futerman AH, Riezman H. The ins and outs of sphingolipid synthesis. *Trends Cell Biol* 2005; 15: 312-8.
- 83 Fagone P, Jackowski S. Membrane phospholipid synthesis and endoplasmic reticulum function. *Journal of lipid research* 2009; 50 Suppl: S311-6.
- 84 Levy M, Futerman AH. Mammalian ceramide synthases. *IUBMB Life* 2010; 62: 347-56.
- 85 Mizutani Y, Mitsutake S, Tsuji K *et al*. Ceramide biosynthesis in keratinocyte and its role in skin function. *Biochimie* 2009; 91: 784-90.
- 86 Sandhoff R. Very long chain sphingolipids: tissue expression, function and synthesis. *Febs Letters* 2010; 584: 1907-13.
- 87 Robson KJ, Stewart ME, Michelsen S *et al*. 6-Hydroxy-4-sphingenine in human epidermal ceramides. *Journal of lipid research* 1994; 35: 2060-8.
- 88 Hannun YA, Obeid LM. Principles of bioactive lipid signalling: lessons from sphingolipids. *Nat Rev Mol Cell Biol* 2008; 9: 139-50.
- 89 Denning MF, Kazanietz MG, Blumberg PM *et al*. Cholesterol sulfate activates multiple protein kinase C isoenzymes and induces granular cell differentiation in cultured murine keratinocytes. *Cell Growth Differ* 1995; 6: 1619-26.
- 90 Hanley K, Wood L, Ng DC *et al*. Cholesterol sulfate stimulates involucrin transcription in keratinocytes by increasing Fra-1, Fra-2, and Jun D. *Journal of lipid research* 2001; 42: 390-8.
- 91 Sato J, Denda M, Nakanishi J *et al*. Cholesterol sulfate inhibits proteases that are involved in desquamation of stratum corneum. *The Journal of investigative dermatology* 1998; 111: 189-93.
- 92 Feingold KR, Jiang YJ. The mechanisms by which lipids coordinately regulate the formation of the protein and lipid domains of the stratum corneum: Role of fatty acids, oxysterols, cholesterol sulfate and ceramides as signaling molecules. *Dermato-endocrinology* 2011; 3: 113-8.
- 93 Wertz PW, Downing DT, Freinkel RK *et al*. Sphingolipids of the stratum corneum and lamellar granules of fetal rat epidermis. *The Journal of investigative dermatology* 1984; 83: 193-5.
- 94 Freinkel RK, Traczyk TN. Lipid composition and acid hydrolase content of lamellar granules of fetal rat epidermis. *The Journal of investigative dermatology* 1985; 85: 295-8.
- 95 Mao-Qiang M, Feingold KR, Jain M *et al*. Extracellular processing of phospholipids is required for permeability barrier homeostasis. *Journal of lipid research* 1995; 36: 1925-35.
- 96 Holleran WM, Ginns EI, Menon GK *et al*. Consequences of beta-glucocerebrosidase deficiency in epidermis. Ultrastructure and permeability barrier alterations in Gaucher disease. *The Journal of clinical investigation* 1994; 93: 1756-64.
- 97 Holleran WM, Takagi Y, Menon GK *et al*. Processing of epidermal glucosylceramides is required for optimal mammalian cutaneous permeability barrier function. *The Journal of clinical investigation* 1993; 91: 1656-64.
- 98 Jensen JM, Schutze S, Forl M *et al*. Roles for tumor necrosis factor receptor p55 and sphingomyelinase in repairing the cutaneous permeability barrier. *The Journal of clinical investigation* 1999; 104: 1761-70.
- 99 Schmutz M, Man MQ, Weber F *et al*. Permeability barrier disorder in Niemann-Pick disease: sphingomyelin-ceramide processing required for normal barrier homeostasis. *The Journal of investigative dermatology* 2000; 115: 459-66.
- 100 Schmutz M, Jiang YJ, Dubrac S *et al*. Thematic review series: skin lipids. Peroxisome proliferator-activated receptors and liver X receptors in epidermal biology. *Journal of lipid research* 2008; 49: 499-509.
- 101 Cawla A, Repa JJ, Evans RM *et al*. Nuclear receptors and lipid physiology: opening the X-files. *Science* 2001; 294: 1866-70.
- 102 Komuves LG, Hanley K, Lefebvre AM *et al*. Stimulation of PPARalpha promotes epidermal keratinocyte differentiation *in vivo*. *The Journal of investigative dermatology* 2000; 115: 353-60.
- 103 Hanley K, Jiang Y, He SS *et al*. Keratinocyte differentiation is stimulated by activators of the nuclear hormone receptor PPARalpha. *The Journal of investigative dermatology* 1998; 110: 368-75.
- 104 Hanley K, Ng DC, He SS *et al*. Oxysterols induce differentiation in human keratinocytes and increase Ap-1-dependent involucrin transcription. *The Journal of investigative dermatology* 2000; 114: 545-53.
- 105 Mao-Qiang M, Fowler AJ, Schmutz M *et al*. Peroxisome-proliferator-activated receptor (PPAR)-gamma activation stimulates keratinocyte differentiation. *The Journal of investigative dermatology* 2004; 123: 305-12.
- 106 Schmutz M, Haqq CM, Cairns WJ *et al*. Peroxisome

- proliferator-activated receptor (PPAR)-beta/delta stimulates differentiation and lipid accumulation in keratinocytes. *The Journal of investigative dermatology* 2004; 122: 971-83.
- 107 Jiang YJ, Lu B, Kim P *et al*. PPAR and LXR activators regulate ABCA12 expression in human keratinocytes. *The Journal of investigative dermatology* 2008; 128: 104-9.
- 108 Jiang YJ, Lu B, Tarling EJ *et al*. Regulation of ABCG1 expression in human keratinocytes and murine epidermis. *Journal of lipid research* 2010; 51: 3185-95.
- 109 Man MQ, Choi EH, Schmutz M *et al*. Basis for improved permeability barrier homeostasis induced by PPAR and LXR activators: liposensors stimulate lipid synthesis, lamellar body secretion, and post-secretory lipid processing. *The Journal of investigative dermatology* 2006; 126: 386-92.
- 110 Rivier M, Castiel I, Safonova I *et al*. Peroxisome proliferator-activated receptor-alpha enhances lipid metabolism in a skin equivalent model. *The Journal of investigative dermatology* 2000; 114: 681-7.
- 111 Rawlings AV, Matts PJ. Stratum corneum moisturization at the molecular level: an update in relation to the dry skin cycle. *J Invest Dermatol* 2005; 124: 1099-110.
- 112 Tabachnick J, LaBadie JH. Studies on the biochemistry of epidermis. IV. The free amino acids, ammonia, urea, and pyrrolidone carboxylic acid content of conventional and germ-free albino guinea pig epidermis. *The Journal of investigative dermatology* 1970; 54: 24-31.
- 113 Harding CR. The stratum corneum: structure and function in health and disease. *Dermatol Ther* 2004; 17 Suppl 1: 6-15.
- 114 Elias PM. The epidermal permeability barrier: from Saran Wrap to biosensor. In: *Skin Barrier* (Elias PM, Feingold KR, eds). New York: Taylor & Francis. 2005; 25-32.
- 115 Del Rosso JQ. Moisturizers: function, formulation, and clinical applications. In: *Cosmeceuticals* (Draelos ZD, ed). Oxford: Elsevier. 2005; 97-102.
- 116 Bouwstra JA, de Graaff A, Gooris GS *et al*. Water distribution and related morphology in human stratum corneum at different hydration levels. *The Journal of investigative dermatology* 2003; 120: 750-8.
- 117 Del Rosso JQ, Levin J. The clinical relevance of maintaining the functional integrity of the stratum corneum in both healthy and disease-affected skin. *J Clin Aesthet Dermatol* 2011; 4: 22-42.
- 118 Tetsuji H. Cornified envelope. In: *Skin moisturization* (Rawlings AV, Leyden JJ, eds). New York: Informa Healthcare. 2009; 83-97.
- 119 Hachem JP, Man MQ, Crumrine D *et al*. Sustained serine proteases activity by prolonged increase in pH leads to degradation of lipid processing enzymes and profound alterations of barrier function and stratum corneum integrity. *The Journal of investigative dermatology* 2005; 125: 510-20.
- 120 Voegeli D. The role of emollients in the care of patients with dry skin. *Nursing standard* 2007; 22: 62, 4-8.
- 121 Takahashi M, Tezuka T. The content of free amino acids in the stratum corneum is increased in senile xerosis. *Archives of Dermatological Research* 2004; 295: 448-52.
- 122 Sandilands A, O'Regan GM, Liao H *et al*. Prevalent and rare mutations in the gene encoding filaggrin cause ichthyosis vulgaris and predispose individuals to atopic dermatitis. *The Journal of investigative dermatology* 2006; 126: 1770-5.
- 123 Irvine AD. Fleshing out filaggrin phenotypes. *The Journal of investigative dermatology* 2007; 127: 504-7.
- 124 Morar N, Cookson WO, Harper JI *et al*. Filaggrin mutations in children with severe atopic dermatitis. *The Journal of investigative dermatology* 2007; 127: 1667-72.
- 125 Jakasa I, Koster ES, Calkoen F *et al*. Skin barrier function in healthy subjects and patients with atopic dermatitis in relation to filaggrin loss-of-function mutations. *J Invest Dermatol* 2011; 131: 540-2.
- 126 Akiyama M. FLG mutations in ichthyosis vulgaris and atopic eczema: spectrum of mutations and population genetics. *The British journal of dermatology* 2010; 162: 472-7.
- 127 Proksch E, Jensen JM, Elias PM. Skin lipids and epidermal differentiation in atopic dermatitis. *Clin Dermatol* 2003; 21: 134-44.
- 128 Grewe M, Bruijnzeel-Koomen CA, Schopf E *et al*. A role for Th1 and Th2 cells in the immunopathogenesis of atopic dermatitis. *Immunol Today* 1998; 19: 359-61.
- 129 Scharschmidt TC, Segre JA. Modeling atopic dermatitis with increasingly complex mouse models. *The Journal of investigative dermatology* 2008; 128: 1061-4.
- 130 Leung DY, Bhan AK, Schneeberger EE *et al*. Characterization of the mononuclear cell infiltrate in atopic dermatitis using monoclonal antibodies. *The Journal of allergy and clinical immunology* 1983; 71: 47-56.
- 131 Bieber T. Atopic dermatitis. *The New England journal of medicine* 2008; 358: 1483-94.
- 132 Leung DY, Schneeberger EE, Siraganian Rp *et al*. The presence of IgE on macrophages and dendritic cells infiltrating into the skin lesion of atopic dermatitis. *Clin Immunol Immunopathol* 1987; 42: 328-37.
- 133 Zachary CB, Allen MH, MacDonald DM. In situ quantification of T-lymphocyte subsets and Langerhans cells in the inflammatory infiltrate of atopic eczema. *The British journal of dermatology* 1985; 112: 149-56.
- 134 Trautmann A, Akdis M, Schmid-Grendelmeier P *et al*. Targeting keratinocyte apoptosis in the treatment of atopic dermatitis and allergic contact dermatitis. *The Journal of allergy and clinical immunology* 2001; 108: 839-46.
- 135 Koga C, Kabashima K, Shiraishi N *et al*. Possible pathogenic role of Th17 cells for atopic dermatitis. *The Journal of investigative dermatology* 2008; 128: 2625-30.
- 136 Toda M, Leung DY, Molet S *et al*. Polarized in vivo expression of IL-11 and IL-17 between acute and chronic skin lesions. *The Journal of allergy and clinical immunology* 2003; 111: 875-81.
- 137 Allakhverdi Z, Comeau MR, Jessup HK *et al*. Thymic stromal lymphopoietin is released by human epithelial cells in response to microbes, trauma, or inflammation and potently activates mast cells. *The Journal of experimental medicine* 2007; 204: 253-8.
- 138 Bogiatzi SI, Fernandez I, Bichet JC *et al*. Cutting Edge: Proinflammatory and Th2 cytokines synergize to induce thymic stromal lymphopoietin production by human skin

- keratinocytes. *Journal of Immunology* 2007; 178: 3373-7.139
- Nylander-Lundqvist E, Back O, Egelrud T. IL-1 beta activation in human epidermis. *Journal of Immunology* 1996; 157: 1699-704.
- 140 Elias PM. Stratum corneum defensive functions: An integrated view. *Journal of Investigative Dermatology* 2005; 125: 183-200.
- 141 Elias PM, Schmutz M. Abnormal skin barrier in the etiopathogenesis of atopic dermatitis. *Current Allergy and Asthma Reports* 2009; 9: 265-72.
- 142 Elias PM, Wood lc, Feingold KR. Epidermal pathogenesis of inflammatory dermatoses. *Am J Contact Dermat* 1999; 10: 119-26.
- 143 Elias PM, Feingold KR. Does the tail wag the dog? Role of the barrier in the pathogenesis of inflammatory dermatoses and therapeutic implications. *Archives of dermatology* 2001; 137: 1079-81.
- 144 Badertscher K, Bronnimann M, Karlen S *et al.* Mast cell chymase is increased in chronic atopic dermatitis but not in psoriasis. *Archives of Dermatological Research* 2005; 296: 503-6.
- 145 Bleck O, Abeck D, Ring J *et al.* Two ceramide subfractions detectable in Cer(AS) position by HPTlc in skin surface lipids of non-lesional skin of atopic eczema. *J Invest Dermatol* 1999; 113: 894-900.
- 146 Farwanah H, Raith K, Neubert RH *et al.* Ceramide profiles of the uninvolved skin in atopic dermatitis and psoriasis are comparable to those of healthy skin. *Arch Dermatol Res* 2005; 296: 514-21.
- 147 Angelova-Fischer I, Mannheimer AC, Hinder A *et al.* Distinct barrier integrity phenotypes in filaggrin-related atopic eczema following sequential tape stripping and lipid profiling. *Exp Dermatol* 2011; 20: 351-6.
- 148 Ishibashi M, Arikawa J, Okamoto R *et al.* Abnormal expression of the novel epidermal enzyme, glucosylseramide deacylase, and the accumulation of its enzymatic reaction product, glucosylsphingosine, in the skin of patients with atopic dermatitis. *Laboratory investigation; a journal of technical methods and pathology* 2003; 83: 397-408.
- 149 Matsumoto M, Umemoto N, Sugiura H *et al.* Difference in ceramide composition between "dry" and "normal" skin in patients with atopic dermatitis. *Acta Dermato-Venereologica* 1999; 79: 246-7.
- 150 Di Nardo A, Wertz P, Giannetti A *et al.* Ceramide and cholesterol composition of the skin of patients with atopic dermatitis. *Acta Derm Venereol* 1998; 78: 27-30.
- 151 Jungersted JM, Scheer H, Mempel M *et al.* Stratum corneum lipids, skin barrier function and filaggrin mutations in patients with atopic eczema. *Allergy* 2010; 65: 911-8.
- 152 Imokawa G, Abe A, Jin K *et al.* Decreased level of ceramides in stratum corneum of atopic dermatitis: an etiologic factor in atopic dry skin? *J Invest Dermatol* 1991; 96: 523-6.
- 153 Ishikawa J, Narita H, Kondo N *et al.* Changes in the ceramide profile of atopic dermatitis patients. *J Invest Dermatol* 2010; 130: 2511-4.
- 154 Macheleidt O, Kaiser HW, Sandhoff K. Deficiency of epidermal protein-bound omega-hydroxyceramides in atopic dermatitis. *J Invest Dermatol* 2002; 119: 166-73.
- 155 Takigawa H, Nakagawa H, Kuzukawa M *et al.* Deficient production of hexadecenoic acid in the skin is associated in part with the vulnerability of atopic dermatitis patients to colonization by *Staphylococcus aureus*. *Dermatology* 2005; 211: 240-8.
- 156 Fartasch M, Bassukas ID, Diepgen TL. Disturbed extruding mechanism of lamellar bodies in dry non-eczematous skin of atopics. *Br J Dermatol* 1992; 127: 221-7.
- 157 Jin K, Higaki Y, Takagi Y *et al.* Analysis of beta-glucocerebrosidase and ceramidase activities in atopic and aged dry skin. *Acta Dermato-Venereologica* 1994; 74: 337-40.
- 158 Kusuda S, Cui CY, Takahashi M *et al.* Localization of sphingomyelinase in lesional skin of atopic dermatitis patients. *The Journal of investigative dermatology* 1998; 111: 733-8.
- 159 Jensen JM, Folster-Holst R, Baranowsky A *et al.* Impaired sphingomyelinase activity and epidermal differentiation in atopic dermatitis. *The Journal of investigative dermatology* 2004; 122: 1423-31.
- 160 Hara J, Higuchi K, Okamoto R *et al.* High-expression of sphingomyelin deacylase is an important determinant of ceramide deficiency leading to barrier disruption in atopic dermatitis. *The Journal of investigative dermatology* 2000; 115: 406-13.
- 161 Higuchi K, Hara J, Okamoto R *et al.* The skin of atopic dermatitis patients contains a novel enzyme, glucosylseramide sphingomyelin deacylase, which cleaves the N-acyl linkage of sphingomyelin and glucosylseramide. *The Biochemical journal* 2000; 350 Pt 3: 747-56.
- 162 Westergaard M, Henningsen J, Johansen C *et al.* Expression and localization of peroxisome proliferator-activated receptors and nuclear factor kappaB in normal and lesional psoriatic skin. *The Journal of investigative dermatology* 2003; 121: 1104-17.
- 163 Plager DA, Leontovich AA, Henke SA *et al.* Early cutaneous gene transcription changes in adult atopic dermatitis and potential clinical implications. *Experimental Dermatology* 2007; 16: 28-36.
- 164 Cremesti ae, Fischl AS. Current methods for the identification and quantitation of ceramides: an overview. *Lipids* 2000; 35: 937-45.
- 165 Blau K, Halket JM. *Handbook of derivatives for chromatography*, 2nd edn. Chichester ; New York: Wiley. 1993.
- 166 Gutnikov G. Fatty acid profiles of lipid samples. *J Chromatogr B Biomed Appl* 1995; 671: 71-89.
- 167 Robson KJ, Stewart ME, Michelsen S *et al.* 6-Hydroxy-4-sphingenine in human epidermal ceramides. *J Lipid Res* 1994; 35: 2060-8.
- 168 Stewart ME, Downing DT. A new 6-hydroxy-4-sphingenine-containing ceramide in human skin. *J Lipid Res* 1999; 40: 1434-9.
- 169 Wertz PW, Miethke MC, Long SA *et al.* The composition of the ceramides from human stratum corneum and from comedones. *J Invest Dermatol* 1985; 84: 410-2.
- 170 Bose R, Chen P, Loconti A *et al.* Ceramide generation by the Reaper protein is not blocked by the caspase inhibitor, p35. *J Biol Chem* 1998; 273: 28852-9.

- 171 Gaver RC, Sweeley CC. Methods for Methanolysis of Sphingolipids and Direct Determination of Long-Chain Bases by Gas Chromatography. *J Am Oil Chem Soc* 1965; 42: 294-8.
- 172 Murphy RC, Fiedler J, Hevko J. Analysis of nonvolatile lipids by mass spectrometry. *Chem Rev* 2001; 101: 479-526.
- 173 Raith K, Darius J, Neubert RH. Ceramide analysis utilizing gas chromatography-mass spectrometry. *J Chromatogr A* 2000; 876: 229-33.
- 174 Bleton J, Gaudin K, Chaminade P *et al.* Structural analysis of commercial ceramides by gas chromatography-mass spectrometry. *J Chromatogr A* 2001; 917: 251-60.
- 175 Christie WW, Urwin RA. Separation of Lipid Classes from Plant-Tissues by High-Performance Liquid-Chromatography on Chemically Bonded Stationary Phases. *Hrc-J High Res Chrom* 1995; 18: 97-100.
- 176 Christie WW. Rapid Separation and Quantification of Lipid Classes by High-Performance Liquid-Chromatography and Mass (Light-Scattering) Detection. *Journal of Lipid Research* 1985; 26: 507-12.
- 177 Gildenast T, Lasch J. Isolation of ceramide fractions from human stratum corneum lipid extracts by high-performance liquid chromatography. *Biochim Biophys Acta* 1997; 1346: 69-74.
- 178 Gaudin K, Chaminade P, Ferrier D *et al.* Analysis of commercial ceramides by non-aqueous reversed-phase liquid chromatography with evaporative light-scattering detection. *Chromatographia* 1999; 49: 241-8.
- 179 Gaudin K, Chaminade P, Baillet A *et al.* Contribution to liquid chromatographic analysis of cutaneous ceramides. *J Liq Chromatogr R T* 1999; 22: 379-400.
- 180 Farwanah H, Wirtz J, Kolter T *et al.* Normal phase liquid chromatography coupled to quadrupole time of flight atmospheric pressure chemical ionization mass spectrometry for separation, detection and mass spectrometric profiling of neutral sphingolipids and cholesterol. *J Chromatogr B Analyt Technol Biomed Life Sci* 2009; 877: 2976-82.
- 181 Farwanah H, Pierstorff B, Schmelzer CE *et al.* Separation and mass spectrometric characterization of covalently bound skin ceramides using lc/Apci-ms and Nano-ESI-ms/ms. *J Chromatogr B Analyt Technol Biomed Life Sci* 2007; 852: 562-70.
- 182 Masukawa Y, Narita H, Sato H *et al.* Comprehensive quantification of ceramide species in human stratum corneum. *J Lipid Res* 2009; 50: 1708-19.
- 183 Vietzke JP, Brandt O, Abeck D *et al.* Comparative investigation of human stratum corneum ceramides. *Lipids* 2001; 36: 299-304.
- 184 Raith K, Neubert RHH. Liquid chromatography-electrospray mass spectrometry and tandem mass spectrometry of ceramides. *Analytica Chimica Acta* 2000; 403: 295-303.
- 185 Hinder A, Schmelzer CEH, Rawlings AV *et al.* Investigation of the Molecular Structure of the Human Stratum Corneum Ceramides [NP] and [EOS] by Mass Spectrometry. *Skin Pharmacology and Physiology* 2011; 24: 127-35.

Figure 1 was used with permission from Rachmat Tubagus, doktermudatrader.blogspot.nl (2012)

Figure 2a was purchased from iStockphoto

Figure 2b was purchased from Shutterstock

CHAPTER 2

AIM AND OUTLINE OF THIS THESIS

Background

Human skin forms a protective barrier against penetration of exogenous compounds into the body and prevents excessive transepidermal water loss (TEWL)¹⁻³. This skin barrier function is primarily located in the uppermost layer of the skin, the stratum corneum (SC). Human SC consists of corneocytes embedded in a highly structured lipid matrix. The SC lipid matrix is comprised of ceramides (CERs), free fatty acids (FFAs) and cholesterol (CHOL)^{4,5}. The lipids are crucial for the skin barrier function. In atopic eczema (AE), the skin barrier is impaired, and allergens and irritants can penetrate through the SC into the lower epidermal layers thereby provoking an immune response⁶⁻⁸. Previous studies demonstrated that SC lipid composition in AE patients is changed, although the role of the lipids is not fully understood.

Objectives

The primary aim of this thesis is to study in detail the SC lipid composition and organization as well as their role in the skin barrier function in eczematous patients. This is achieved by pursuing the following challenges:

1. Developing robust methods that enables quantitative analysis of all main SC lipid classes in detail.
2. Determine the comprehensive SC lipid composition of both lesional and non-lesional skin in AE patients and compare the lipid profile to healthy controls.
3. Establish how changes in the SC lipid composition of AE patients are related to changes observed in the lipid organization, and how those affect the skin barrier function.
4. Determine the relationship between SC lipid

composition and organization with respect to other SC sources that show a reduced skin barrier function, i.e. Netherton syndrome (NTS) and human skin equivalents (HSEs).

Outline

This thesis is divided into three parts that will address the aforementioned objectives:

- Part II (Chapters 3-4) covers the development of a novel method for analysis of CHOL, CERs and FFAs, by means of liquid chromatography coupled to mass spectrometry (LC/MS).
- Part III (Chapters 5-8) describes the use of the developed LC/MS methods to examine the SC lipid composition in AE patients and control subjects. The observed changes in the SC lipid composition in skin of AE patients will be related to changes in the lipid organization and reduced skin barrier function.
- Part IV (Chapters 9-10) focuses on the relationship between lipid composition and lipid organization of two different skin sources: SC from NTS patients and SC from HSEs.

Chapter overview

Chapter 3 describes the development of a normal phase LC/MS method for analysis of all CER subclasses and their chain length distribution in human SC. A short validation assay is presented and comparisons are made between *ex-vivo* human SC and SC harvested from tape strips. It also reports on the identification of a new CER subclass by means of fragmentation studies (MS/MS) and high mass accuracy MS.

LC/MS method development continues in **Chapter 4**, in which the analysis of FFAs is described. Reverse phase LC/MS in negative ion mode is used. Method validation shows the robustness, linearity, and sensitivity of the method, and demonstrates the use of chloride adducts for increased ionization efficiency. The FFA method was successively coupled to the method for CER analysis explained in the previous chapter, which was improved to enable analysis of CHOL as well. The combined method was then applied on SC samples from different skin sources: human SC from *ex vivo* skin, human SC harvested by tape stripping, porcine skin, and skin obtained from HSEs.

Part II focuses on the application of the developed LC/MS methods for analysis of the SC lipid in AE patients. **Chapter 5** describes a short study in 6 AE patients and 6 healthy subjects. The CER composition is examined and related to the lamellar lipid organization studied by small-angle x-ray diffraction (SAXD).

In **Chapter 6**, data are presented on the CER composition of non-lesional SC of 28 AE patients and healthy subjects. The CER composition is related to the lamellar lipid

organization (SAXD studies) and lateral lipid organization (Fourier transform infrared spectroscopy (FTIR) studies). In addition, changes in the CER composition and lipid organization were associated to changes in skin barrier function (monitored by TEWL) and disease severity (SCORAD). Finally, the influence of loss-of-function mutations in the flaggrin gene as well as the level of natural moisturizing factor is studied in relation to the SC lipids and skin barrier function.

Chapter 7 reports the continuation on examining the SC in AE, in which both the FFA and CER composition was determined and compared to healthy subjects. In addition, the effect of inflammation on the lipid parameters is discussed, as both lesional and non-lesional skin sites are examined. Changes observed in the SC FFAs and CERs are discussed in relation to the lipid organization and skin barrier function, and finally linked to epidermal lipid metabolism.

In contrast to the previous three chapters, which report on the relative levels of the various lipids in SC lipid in AE patients, **Chapter 8** demonstrates the importance of the lipid/protein ratio with respect to the SC barrier function. This is examined by Raman spectroscopy, whereas the barrier is monitored by TEWL.

Part III reports on SC lipid studies from two different skin sources. **Chapter 9** focuses on the SC lipids in patients with NTS, a severe skin disease in which a mutation in the SPINK5 gene leads to hyperactivity of epidermal proteases resulting in SC detachment. The observed changes in lipid composition are compared to changes in lipid organization. These changes are also discussed in view of the results obtained from AE patients described in the previous chapters.

In **Chapter 10**, data are shown on the lipid composition of SC obtained from HSEs. The lipid composition, examined by the newly developed LC/MS method, is compared to the lipid composition using thin layer chromatography. In addition, the lipid organization and the activity of several enzymes involved in epidermal lipid synthesis are determined and discussed with respect to the lipid composition.

Chapter 11 summarizes the results, presents overall conclusions, and elaborates on the perspectives.

An overview of the main parameters described in this thesis as well as the respective analytical methods used to collect these data are presented in Figure 1: The SC lipid composition, lipid organization, and (to a less extend) lipid amount are the most prominently discussed parameters in relation to the SC barrier function. In addition, the disease severity and flaggrin content are also related to the SC barrier function in several chapters.

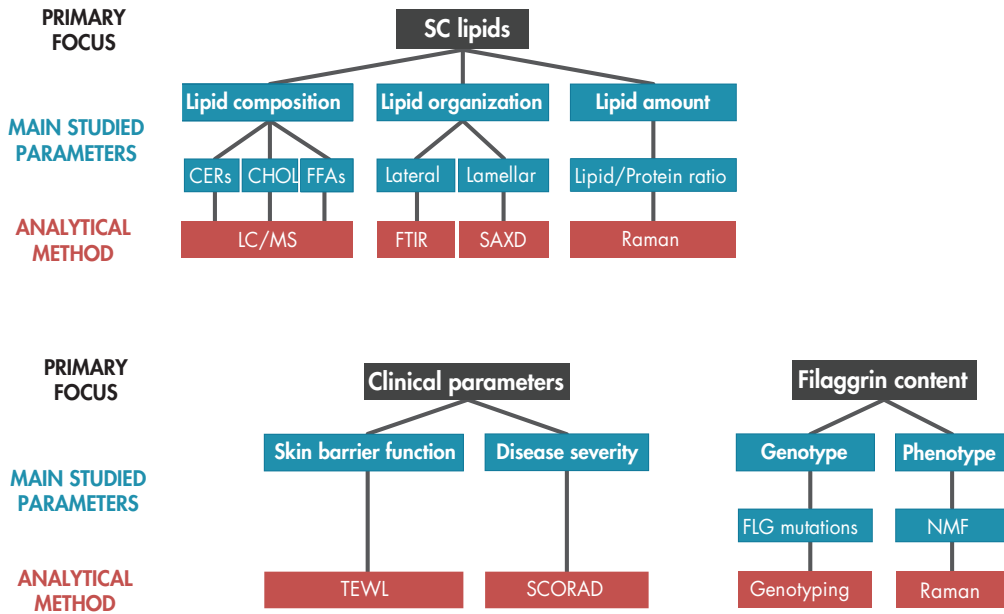


Figure 1: Schematic overview, illustrating the primary focus of the studies described throughout this thesis (in black); the main studied parameters (in blue); and the analytical methods used to examine these parameters (in red).

References

- Madison KC. Barrier function of the skin: "la raison d'être" of the epidermis. *The Journal of investigative dermatology* 2003; 121: 231-41.
- Scheuplein RJ, Blank IH. Permeability of the skin. *Physiol Rev* 1971; 51: 702-47.
- Elias PM. Stratum corneum defensive functions: an integrated view. *The Journal of investigative dermatology* 2005; 125: 183-200.
- Wertz PW. Lipids and barrier function of the skin. *Acta Derm Venereol Suppl (Stockh)* 2000; 208: 7-11.
- Downing DT, Stewart ME, Wertz PW *et al*. Skin lipids: an update. *J Invest Dermatol* 1987; 88: 2s-6s.
- Oyoshi MK, He R, Kumar L *et al*. Cellular and molecular mechanisms in atopic dermatitis. *Adv Immunol* 2009; 102: 135-226.
- Elias PM, Hatano Y, Williams ML. Basis for the barrier abnormality in atopic dermatitis: outside-inside-outside pathogenic mechanisms. *The Journal of allergy and clinical immunology* 2008; 121: 1337-43.
- Elias PM, Steinhoff M. "Outside-to-inside" (and now back to "outside") pathogenic mechanisms in atopic dermatitis. *The Journal of investigative dermatology* 2008; 128: 1067-70.



METHOD DEVELOPMENT FOR
DETAILED STRATUM CORNEUM
LIPID ANALYSIS

PART II

CHAPTER 3

LC/MS ANALYSIS OF STRATUM CORNEUM LIPIDS: CERAMIDE PROFILING AND DISCOVERY

Jeroen van Smeden¹, Louise Hoppel²,
Rob van der Heijden²,
Thomas Hankemeier^{2,3}, Rob J. Vreeken^{2,3},
Joke A. Bouwstra¹

¹ Division of Drug Delivery Technology;
Leiden Academic Centre for Drug
Research, Leiden University, Leiden,
The Netherlands

² Division of Analytical Biosciences;
Leiden Academic Centre for Drug
Research, Leiden University, Leiden,
The Netherlands

³ Netherlands Metabolomics Centre;
Leiden Academic Centre for Drug
Research, Leiden University, Leiden,
The Netherlands

Adapted from *Journal of Lipid Research*.
2011. 52: 1211–1221.

Abstract

Ceramides (CERs) in the upper layer of the skin, the stratum corneum (SC), play a key role in the skin barrier function. In human SC, the literature currently reports 11 CER subclasses that have been identified. In this paper, a novel quick and robust liquid chromatography coupled to mass-spectrometry (LC/MS) method is presented that allows the separation and analysis of all known human SC CER subclasses using only limited sample preparation. Besides all 11 known and identified subclasses, a 3D multi-mass chromatogram shows the presence of other lipid subclasses. Using LC/MS/MS with both an ion trap (IT) system, a Fourier transform-ion cyclotron resonance (FT-ICR) system, and a triple quadruple (TQ) system, we were able to identify one of these lipid subclasses as a new CER subclass: the ester-linked ω -hydroxy fatty acid with a dihydrosphingosine base (CER [EOds]). Besides the identification of a new CER subclass, this paper also describes the applicability and robustness of the developed LC/MS method by analyzing three (biological) SC samples: SC from human dermatomed skin, human SC obtained by tape stripping, and SC from full-thickness skin explants. All three biological samples showed all known CER subclasses and slight differences were observed in CER profile.

Introduction

The outermost layer of mammalian skin, the stratum corneum (SC), consists of corneocytes embedded in a lipid matrix. This layer serves as the main barrier for diffusion of substances across the skin. As the lipid matrix is the only continuous pathway in the SC, the composition and organization of these lipids are of major importance for a

competent skin barrier function¹⁻⁴. The major lipid classes in human SC are cholesterol, free fatty acids, and ceramides (CERs). In particular the CERs have drawn much attention and several reported studies demonstrate that changes in CER composition may play a role in an impaired skin barrier⁵⁻¹¹. The various CERs consist of a sphingoid base linked via an amide bond to a fatty acid. Both variations in the fatty acid carbon chain and the sphingoid base architecture results in a large number of CER subclasses with a wide variation in chain length distribution. The molecular architecture of these subclasses is depicted in Figure 1. Over the years, important information about CER composition in human SC has been obtained using high performance thin layer chromatography (HPTLC) in conjunction with nuclear magnetic resonance (NMR). This resulted in a gradual increase in the number of identified subclasses. By use of these methods, 9 different human CER subclasses have been identified in the SC of healthy human skin¹²⁻¹⁶. As HPTLC is easily accessible, it is still frequently used in various fields with respect to skin lipid research to determine the CER subclasses in human SC^{11,17,18}. However, these approaches are very time consuming and a high quantity of material is required, which is not always available. The application of liquid chromatography coupled to mass spectrometry (LC/MS) results in a much more detailed profile of each individual subclass using only small quantities of material¹⁹⁻²⁸. Besides their important role in human skin, CERs are also key molecules with respect to cell signaling, growth, differentiation, and apoptosis²⁹⁻³⁸. Also in these research areas, the introduction of MS has shown a tremendous boost in the identification

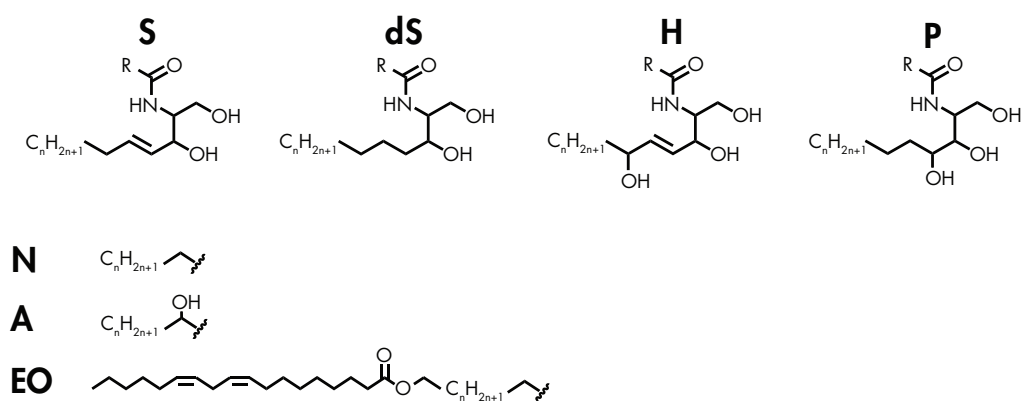


Figure 1: Ceramide structures: Four possible sphingosine related chains (S: sphingosine; ds: dihydrosphingosine; H: 6-hydroxy-sphingosine; P: phyto-sphingosine) are linked via an amide bond to either of three different fatty acid components (N: non-hydroxy fatty acid; A: α-hydroxy fatty acid; EO: esterified ω-hydroxy fatty acid) resulting in theoretically 12 different CER subclasses. Literature has reported the presence of all but CER [EOds] in human SC. Note: R represents one of the three different fatty acid chains.

of CERs in biological matrices.

With respect to human SC, two novel CER subclasses were reported recently³⁹, showing that the number of subclasses in human SC is still expanding. However, several of the LC/MS methods currently reported cannot analyze all CER subclasses in a single run. Also, almost all LC/MS methods reported so far are time consuming; multiple sample preparation steps are necessary and many methods require a solid phase extraction step beforehand. Moreover, the total analysis time of a single sample always exceeds 20 minutes and often more than one hour, which is less attractive for analysis of a large number of samples. Therefore, the aims of our study were to *i*) minimize analysis time to allow quick sampling and analysis of total CER content; *ii*) use a minimal number of sample preparation steps to keep the method accessible while minimizing degradation during these steps, and *iii*) maintain a high CER sensitivity. To achieve these goals, we decided to use a normal phase LC (NPLC) setup in combination with an atmospheric pressure chemical ionization (APCI) source. Regarding CER analysis, this choice offers some advantages over the commonly used reversed phase LC (RPLC) combined with electrospray ionization (ESI) MS, such as *i*) considerably lower ion suppression⁴⁰⁻⁴²; *ii*) APCI experiments are usually performed at higher flow rates compared with ESI, allowing for a shorter analysis time⁴³, and *iii*) APCI permits the use of a nonpolar mobile phase, enhancing the ionization efficiency for non-polar compounds, i.e. CERs (in particular the higher mass subclasses)^{21,44}.

Analysis of human SC CERs using this developed method resulted in the appearance of new lipid classes in a 3D-chromatogram. To obtain structural information about some of these new species, we performed fragmentation (MS/MS) on relevant ions (see Table III), which led to the identification of one new CER subclass. The robustness of the LC/MS method was also demonstrated by measuring CERs from three different biological matrices: extracted lipids of isolated SC from native human skin, SC harvested with tape-strips, or SC obtained from the outgrowth of full-thickness human skin explants, referred to as the human skin explant model⁴⁵. We chose these three different biological matrices to demonstrate the applicability of this methodology for future studies.

Materials and Methods

CER classification

In this paper, we use the most recently introduced CER classification system according to Motta *et al.*⁴⁶, which was extended by Masukawa *et al.*³⁹. The CERs consist of either a sphingosine (S), a phyto-sphingosine (P), a 6-hydroxy sphingosine (H) or a dihydrosphingosine (ds) base. This base is chemically linked to either a non-hydroxy

fatty acid (N), α -hydroxy fatty acid (A), or an esterified ω -hydroxy fatty acid (EO). Current literature reports 11 different CER subclasses, viz. CERs denoted by [NS], [Nds], [NP], [NH], [AS], [Ads], [AP], [AH], [EOS], [EOP], and [EOH]. Figure 1 gives an overview of the molecular structures of all known CER subclasses. With respect to the fragmentation studies of CER species in this report, a more detailed nomenclature is used and shows as well, in parentheses, the number of carbon atoms for the specific ester, fatty acid, or carbon chain. For example, CER [E(18:2)O(30)S(18)] corresponds to a CER species containing a C18 sphingosine carbon backbone linked via an amide bond to a ω -hydroxy triacontanoic acid, which is ester-linked to a linoleic moiety.

Chemicals

Ethanol (EtOH), isopropyl alcohol (IPA), methanol (MeOH), and n-heptane of HPLC grade or higher were purchased from Biosolve (Valkenswaard, The Netherlands). HPLC grade chloroform was obtained from Lab-Scan (Dublin, Ireland). Ultra purified water was prepared using a Purelab Ultra purification system (Elga Labwater, High Wycombe, UK). Trypsin and trypsin inhibitor were purchased from Sigma-Aldrich Chemie GmbH (Steinheim, Germany). Synthetic CER [N(24)ds(18)] was purchased from Avanti Polar Lipids (Alabaster, AL). All other synthetic CERs were kindly provided by Cosmoferm (Delft, The Netherlands): CER [EOS] (E(18:2)O(30)S(18)), CER [NS] (N(24)S(18)), CER [NP] (N(24)P(18)), CER [AS] (A(24)S(18)), CER [AP] (A(24)P(18)), and CER [EOP] (E(18:2)O(30)P(18)).

Isolation of SC from human skin, tape stripping and cultured full-thickness explants

Within 24 hours after surgery, residual subcutaneous fat was removed from the skin. The preparation of human SC was performed according to the procedure described by Nugroho *et al.*⁴⁷. In short, skin was stretched on Styrofoam and dermatomed to a thickness of around 300 μ m (Deca Dermatome, DePuy Healthcare, Leeds, UK). Then, the skin was put on Whatman filters soaked in a solution of 0.1 % trypsin in 150 mM Phosphate Buffered Saline (PBS) solution pH 7.4 (8 g/L NaCl, 2.86 g/L Na₂HPO₄, 0.2 g/L KH₂PO₄, 0.19 g/L KCl). After overnight storage at 4 °C, the skin was incubated for 1 h at 37 °C followed by peeling off the SC from the epidermis. The SC was washed once in a 0.1% trypsin inhibitor in PBS pH 7.4 solution, twice in water, and stored in a dry, argon gas containing environment to inhibit oxidation of the SC lipids. Lipids from the full-thickness skin explants model were also collected: Six cultured samples were combined into two pools of three samples and treated analogous to the samples obtained from surgical skin described above, excluding

the dermatome step. Lipids obtained from tape stripping were harvested according to the following procedure: tape stripping (area 4.5 cm²) was performed on the ventral forearm of a healthy volunteer (male, age 33). Ten consecutive Poly(phenylene sulfide) tape strips (Nichiban, Tokyo, Japan) were taken at the same spot. All tapes were pressed to the targeted skin (450 g/cm²) and peeled off with tweezers in one fluid stroke using alternating directions for each tape strip. The 5th to 8th tape strips were selected for lipid extraction. The tapes were punched to an area of 2 cm², and each punched area was put separately in a glass vial filled with 1 mL chloroform/methanol/water (1:2:½). All vials were stored at -20°C under argon atmosphere.

Lipid extraction

Lipids from tape strips, SC isolated from dermatomed human skin, and cultured full-thickness skin explants were all extracted according to the method of Bligh and Dyer⁴⁸ with some small modifications described by Thakoersing *et al*⁴⁹. Briefly, liquid-liquid extraction of the lipids from either human SC or tape strips was performed sequentially using 3 different ratios of solvent mixtures chloroform/MeOH/water (1:2:½; 1:1:0; 2:1:0). A solution of 0.25 M KCl was added to extract polar lipids. After drying to N₂ gas, lipids were dissolved in a solution of heptane/chloroform/MeOH (95:2½:2½): Regarding the lipids isolated from SC of dermatomed skin, 1 mL of solvent was appropriate to obtain a proper sample concentration for optimal LC/MS analysis. SC lipid samples obtained from the 4 tape strips were pooled prior to drying, and afterwards reconstituted in 0.1 mL to concentrate the lipids. Lipids extracted from cultured full-thickness skin explants were also reconstituted to a final volume of 0.1 mL.

CER analysis by LC/MS

NPLC was performed using a binary gradient solvent system of heptane (solvent A) and heptane/IPA/EtOH (2:1:1, solvent B) using a flow rate of 0.8 mL/min (see Table I for

Time (min)	A / B (% / %)
0.00	93 / 7
2.50	93 / 7
2.55	90 / 10
5.00	90 / 10
10.00	50 / 50
10.50	93 / 7
12.00	93 / 7

Table I: Applied LC gradient setup of a single run. Solvent A corresponds to 100% heptane; Solvent B contains 50% heptane, 25% isopropanol, 25% ethanol.

detailed gradient description). Separation was performed using a polyvinyl alcohol (PVA)-sil column (PVA-bonded column; 5 μm particle size, 100 \times 2.1 mm i.d.) purchased from YMC (Kyoto, Japan). The HPLC (Alliance 2695, Waters Corp., Milford, MA) was coupled to one of several mass spectrometers, depending on the aim of the study. Additional details on the individual studies are described below. In general all mass spectrometers were equipped with an APCI source set to 450°C. Synthetic CERs had a final concentration ranging from nanomolar up to micromolar, depending on the experiment. Biological samples were concentrated to a final total lipid concentration around 0.1 mg/mL, determined by weighing. The injection volume of all samples was set to 10 μL . The analysis was performed using Thermo Finnigan Xcalibur software (version 2.0).

Profiling of CERs in synthetic and biological mixtures

Profiling of CERs in synthetic mixtures as well as in samples from dermatomed skin, tape strips, and full-thickness skin explants was performed with the LC system described above coupled to a triple quadrupole (TQ) mass spectrometer (TSQ Quantum, Thermo Finnigan, San Jose, CA) equipped with an APCI source operated in the positive ion mode. The temperature of the source heater was set to 450°C and the heated capillary was set to 250°C. The capillary voltage was maintained at 3 kV, and the discharge current was set to 5 μA . The flow rates of the nitrogen sheath and auxiliary gas were set to 0.4 and 2.4 L/min, respectively. To obtain a full CER profile including all CER chain lengths, the scan range was set from 600-1200 atomic mass units (amu). The resolution full width at half maximum (FWHM) was set to 0.7 amu. The analysis time was set to 8 minutes with an addition of 4 minutes of column washing and equilibration afterwards, leading to a total run time of 12 minutes. Synthetic CERs were used for development of the method, fragment analysis (see below), and limit-of-detection/limit of quantification (LOD/LOQ) determination. Regarding the development of the method, an equimolar synthetic mixture of 250 fmol/CER was prepared and analyzed. For LOD/LOQ determination, a range from micromolar to nanomolar was used, resulting in amounts on-column ranging from picomol to femtomol levels.

Identification of CER using (LC/MS/MS)

Fragmentation spectra (MS/MS) of synthetic CERs and human SC CERs were obtained using an ion trap (IT) system (LCQ Deca, Thermo Finnigan) combined with a Surveyor LC system (Thermo Finnigan). Synthetic CERs were infused (in chloroform-MeOH 2:1) using a postcolumn low dead volume T-piece at a rate of 5 $\mu\text{L}/\text{min}$ while maintaining a continuous flow of solvent A:B (93:7), as described above, at 0.8 mL/min. The normalized collision

energy for MS/MS was set between 40% and 70%, depending on the specific fragments which appeared to be indicative of a specific CER structure (more detail below). The sheath gas and auxiliary gas were set to consecutively 50 and 5 AU, which were slightly different settings compared with the setup used for general profiling of CERs described earlier but showed better results with respect to fragmentation of CERs. The scan time was set to 50 ms. All other parameters were similar to the setup of the TQ system described above. A drawback of MS/MS using an IT system is the limitation of the scan range that can be selected once the parent ion is set: in our studies, species over 1020 amu were fragmented. Using the IT system described above, the product scan range resulted in a low-mass cut-off at m/z 285 amu. Because we also wanted to acquire information on fragments in the range between 250 and 280 amu, MS/MS was performed on the TQ system, analyzing in the product scan mode while the collision energy was set to 40V. All other parameters were identical to the setup described for the TQ system.

High mass accuracy analysis

Accurate mass analysis of all synthetic CERs as well as the unidentified species observed in the lipid mixture isolated from native human SC was performed using a Fourier transform-ion cyclotron resonance system (LTQ FT Ultra, Thermo Electron) interfaced with a Surveyor LC pump and injector system equivalent to the one used for MS/MS analysis described above. The analysis time was set to 100 ms for mass accuracy up to 4 digits (deviation < 1ppm) and the resolution was set at 100,000. All other parameters were comparable to the setup used for fragment analysis described above.

Results and Discussion

Analysis and optimization of HPLC/APCI-MS

Prior to analysis of biological samples, the method was developed and optimized for all 6 synthetic CERs, resulting in applied parameters which were described in the Materials and Methods section (Profiling of CERs in synthetic and biological mixtures). To analyze each individual synthetic CER with uniform chain length, NPLC was chosen over reverse phase LC because this mode allows for separation of individual CER subclasses. We chose to use a PVA column as it has advantages in terms of separation and peak shape compared with commonly used silica and diol columns^{50,51}. Although ESI is mainly used for the analysis of CERs, the APCI mode is also used frequently. The latter permits a higher flow rate (in our studies 0.8 mL/min) that results in a significantly shorter elution time of the CERs⁴³, thereby decreasing the overall LC/MS analysis time. The total ion chromatogram of the synthetic CERs is provided in Figure 2a and shows that with this high flow rate, the

CER subclasses are excellently separated. Because APCI was used, only single positively charged ions were present and could under our conditions be identified as either $[M+H]^+$ or $[M+H-H_2O]^+$ ions. The LOD and LOQ of all six synthetic CERs were determined and are listed in Table II. These were calculated from ion extracted chromatograms (IECs) obtained from full scan MS (m/z 600-1200 amu). The LOD and LOQ were defined by the signal-to-noise ratio (S/N), being 3 and 10, respectively.

This LC/MS method shows several advantages over others with regard to analysis time, sample preparation and sensitivity. Qualitative analysis as well as relative comparability studies may be carried out easily. However, complete quantitative analysis of CERs is only possible when the effect of different ionization efficiencies between CER subclasses and chain lengths has been studied. Moreover, ion suppression effects (although they are expected to be of limited effect during APCI-MS) as well as sample preparation effects should also be taken into account. Ideally, each analyte should have its own isotopically labeled internal standards (^{13}C , ^{15}N and 2D isotopes) added at different stages of the sample preparation and the analysis. This should allow for correction of the mentioned effects resulting in quantitative data of these CERs. However, such internal standards are not, or very limitedly, available. Therefore, a practical approach is to use a limited number of such standards that correct for these effects per CER subclass. Future studies will include several of these standards to make this assay (semi-)quantitative. The use of several nonisotopically labeled internal standards to correct for chain length and CER subclass regarding human SC is described in the literature only once²³.

CER analysis of human SC

To separate and analyze the CER subclasses from isolated human SC, a crude human SC lipid mixture was injected using an identical setup as was used for synthetic CERs. The CER total ion chromatogram of the human SC sample is shown in Figure 2b and shows elution and group separation of all CER subclasses within 8 minutes. The chromatographic resolution of the peaks was considerably lower compared with the synthetic CER mixture. This, however, can be fully explained by the presence of a wide range of both fatty acid and sphingosine chain lengths in each CER subclass, resulting in a relatively broad chromatographic peak per class: the total carbon chain length of the CER has a small effect on the polarity of the species thereby changing the retention time slightly. For example, both synthetic $[N(18)P(24)]$ and its human SC counterpart elutes at 4.10 minutes and show similar peak shapes (Figure 2a and Supplementary Figure 1). However, human CER $[NP]$ with a total chain length of 54 carbon atoms elutes at 3.72 minutes, whereas a total chain length of 40 shows a retention time at 4.18 minutes. This illustrates that the

Table II: Accurate mass LC-MS analysis and LOD/LOQ values of 6 synthetic ceramides.

Ceramide	Main ion measured	Main ion mass measured (amu) ^a	LOD (fmol) ^b	LOQ (fmol) ^b
E(18:2)O(30)S(18)	[M+H-H ₂ O] ⁺	994.953	9	29
E(18:2)O(30)P(18)	[M+H] ⁺	1030.974	1	5
N(24)S(18)	[M+H-H ₂ O] ⁺	632.634	13	45
N(24)P(18)	[M+H] ⁺	668.655	18	60
A(24)S(18)	[M+H-H ₂ O] ⁺	648.629	28	94
A(24)P(18)	[M+H] ⁺	684.650	19	64
N(24)dS(18)	[M+H] ⁺	652.661	6	21

Amu: atomic mass unit; LOD: limit of detection, defined as $S/N=3$; LOQ: Limit of quantification, defined as $S/N=10$.
a: measured with FT-ICR MS, resolution 100,000. b: measured with TQ MS: resolution FWHM (Full Width at Half Maximum) = 0.7 amu.

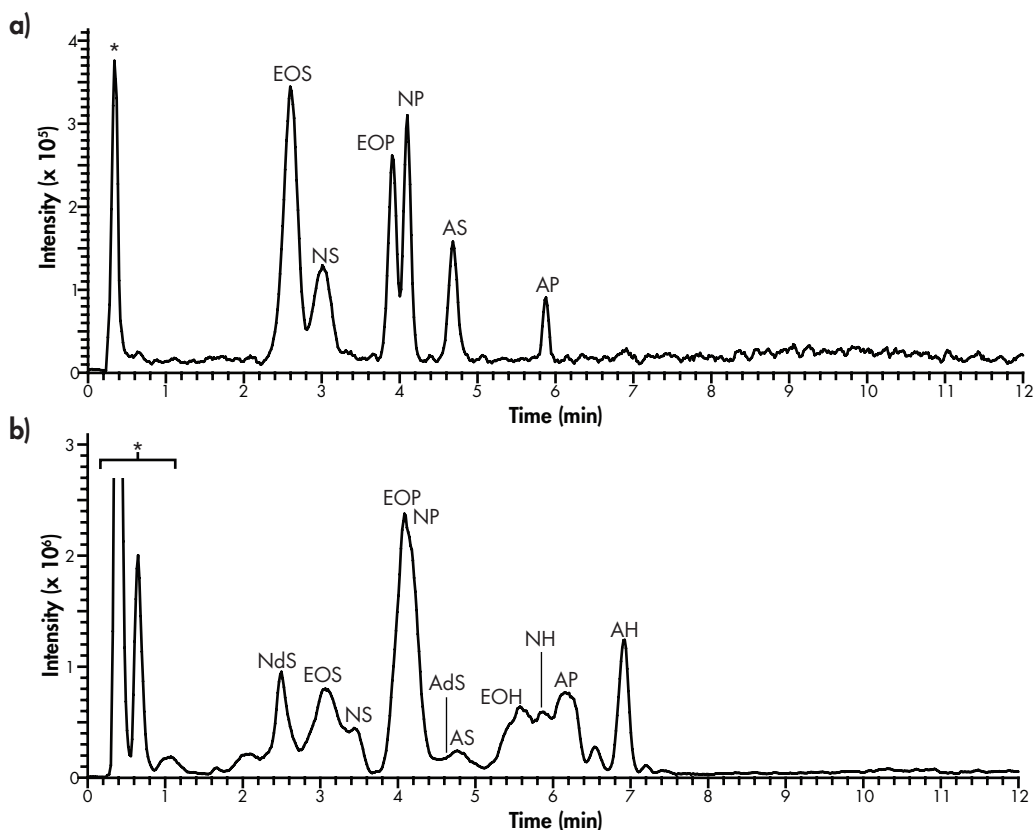


Figure 2: NPLC/APCI-MS total ion current of **a)** equimolar (250 fmol/CER) synthetic human CER mixture containing CER [EOS], [NS], [EOP], [NP], [AS] and [AP]; **b)** crude lipid extract of human SC (abbreviations as in Figure 1). Peaks noted with a * contain other SC lipid classes (e.g. triglycerides, cholesterol) and do not interfere with the CER analysis.

distribution in total number of carbon atoms results in the broadening of the total ion current peak as depicted in Figure 2b. Nevertheless, this apparent ‘loss in resolution’ can be fully overcome by adding the mass/charge (m/z) axis as a third dimension. The peaks that did show overlap in the human CERs total ion current chromatogram can therefore easily be distinguished in the 3D multi-mass chromatogram as shown in Figure 3. This plot shows each separated CER class with multiple peaks from which each total carbon chain length could be derived. From this 3D plot the variation in chain lengths and therefore the slight difference in polarity (i.e. retention time) can be seen clearly. An overview of the total carbon chain lengths of all CER subclasses is listed in the inset of Figure 3. The calculated total chain length distribution is in line with those reported by Masukawa *et al*³⁹. However, due to the high sensitivity of our method and the specific tuning for high mass CERs, it shows an even broader range of chain lengths for, in particular, the [EO] subclasses. This results in the detection of CER subclasses with molecular masses over 1100 amu corresponding to very long total carbon chain lengths up to 76 carbon atoms.

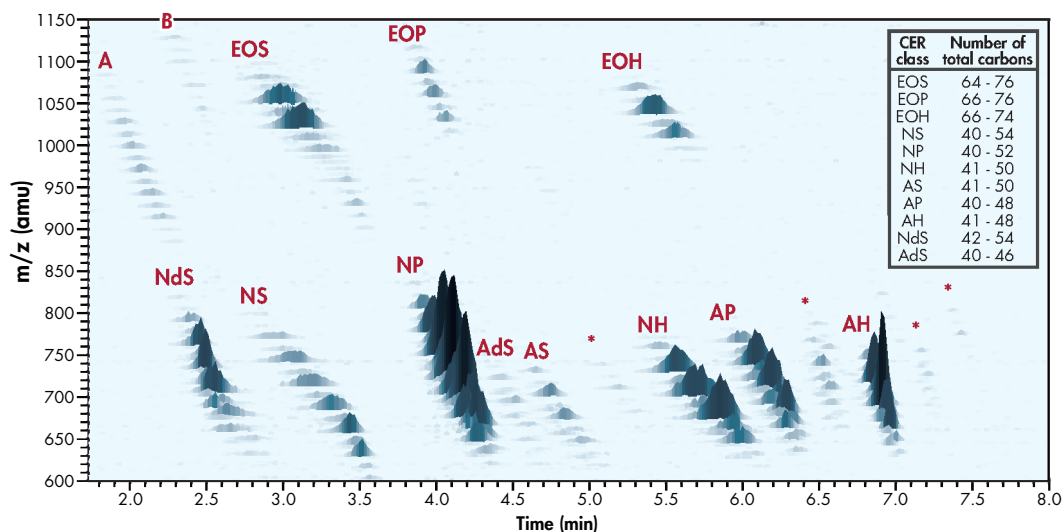


Figure 3: 3D multi-mass chromatogram of dermatomed human SC. Positive ions of CER species using NPLC/APCI-MS. X-axis shows the retention time. Y-axis represents the m/z ratio (in amu). Z-axis depicts the relative intensity of the CER species. Classes noted by either an A, B, or * are unknown species. The inset in the upper right corner shows the range in which the various chain lengths of every CER class were observed.

Ms/ms of the unknown CER class

Besides 11 CER subclasses known to be present in human SC, Figure 3 also shows the presence of other lipid subclasses, marked as *, A, and B, which are unidentified so far. Currently, four sphingoid base chains and three acyl chain variations have been identified in CERs isolated from human SC, which results in theoretically 12 different CER subclasses (Figure 1)^{23,39}. CER [EODs] has been previously observed by gas-liquid chromatography in pig skin and epidermal cysts as a variant of CER [EOS]^{16,52}. However, its presence in human SC as a separate subclass has never been confirmed and recent literature on human SC only mentions 11 different subclasses, not pointing out CER [EODs]. Therefore, our aim was to seek for the presence of this CER subclass [EODs] in the 3D mass chromatogram. Because this CER bears an esterified fatty acid, its m/z -value should be in the range of other [EO] subclasses (i.e. over 900 amu). Figure 3 depicts two unidentified lipid classes located in this high m/z range: A and B. To obtain more information about the unknown classes, LC/FT-ICR MS was used to determine the m/z of all peaks of both unidentified classes with high mass accuracy. From the high mass accuracy data it was concluded that the masses of the unidentified group labeled B in Figure 3 correspond to the theoretical masses of the CER subclass [EODs], and a combined mass spectrum of this unknown lipid class is shown in Figure 4, including the accurate masses and the total number of C-atoms the species should bear. Another indication that this unidentified lipid class may correspond to CER [EODs] was obtained from the observed elution/retention times: It is

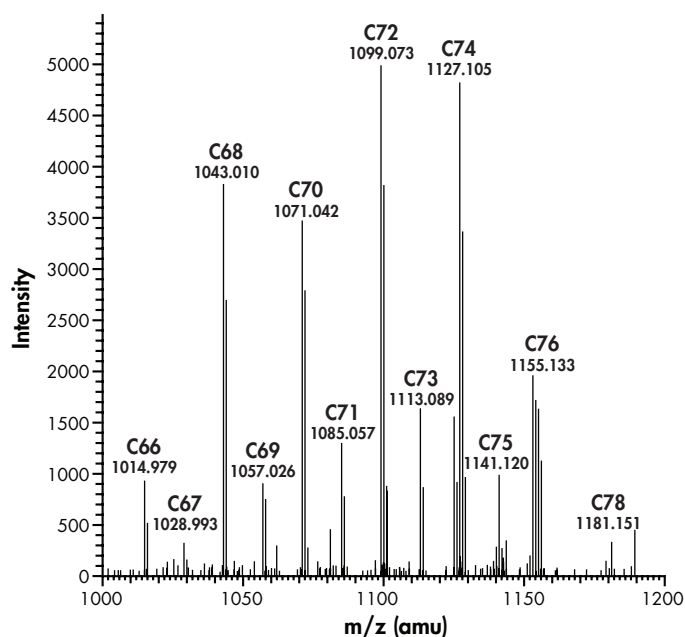


Figure 4: Average mass spectrum (retention time range: 2.1-2.7 min; positive ion mode) of unidentified lipid class, performed by high mass accuracy FT-ICR-MS. C-numbers correspond to the theoretical total number of carbon atoms the species should bear, i.e. the chain length of the proposed CER [EODs].

expected that CER [EODs] elutes prior to the [EOS] subclass, as [Nds] and [Ads] both elute prior to their unsaturated non-hydroxy and ω -hydroxy sphingosine analogs, [NS] and [AS] respectively. This expectation is in accordance to the elution sequence of the unknown CER class and CER [EOS]. Therefore, both on the basis of the close agreement between the theoretical mass of the expected compound and the observed exact mass with matching elemental formulae as well as their relative retention times there is a strong indication that this unknown subclass is indeed the CER [EODs].

To confirm the hypothesis that this unknown CER subclass is indeed the proposed CER [EODs], MS/MS experiments were performed to obtain structural information on the fragments of both known as well as the unknown CERS. Because no synthetic variant of CER [EODs] is commercially available, synthetic CERS, viz. [N(24)S(18)], [N(24)ds(18)], and [E(18:2)O(30)S(18)] were fragmented to obtain product ions that could be characteristic for their structure. This data was compared with that reported before^{39,53-58}. Following the synthetic CERS, CER fragment-ions of relevant human SC were analyzed. Subsequently, the above derived fragmentation reactions were used to identify fragments of the unknown SC CER subclass. The results of these fragmentation studies are shown in Figure 5a-e and Table III, and will be explained below. (It is not in the scope of this publication to fully interpret the observed spectra and identify all observed (fragment-)ions, as this requires additional studies.)

When focusing on the synthetic CER [N(24)S(18)] (Figure 5a), very characteristic fragments were observed for both the sphingosine base as well as the fatty acid chain, which have also been reported in earlier studies^{39,54,56,58}. In particular fragments at m/z 252.3, 264.3, and 282.2 amu corresponding to [(M+H)-(FA chain)-CH₃OH]⁺, [(M+H)-(FA chain)-H₂O]⁺ and [(M+H)-(FA chain)]⁺ respectively, are descriptive for a sphingosine base of 18 carbon atoms. Also, a fatty acid chain of 24 carbon atoms shows typical fragments at m/z 368.3 and 392.4 amu, which can be recognized as [(M+H)-(sphingosine chain)]⁺ and [(M+H)-(C¹⁶H³¹OH)]⁺ respectively. Also fragments without individual chain length information were observed: ions at m/z 602.4 and 614.6 amu, matching respectively [(M+H)-H₂O-CH₃OH]⁺ and [(M+H)-H₂O]⁺ ions, are also present in Figure 5a. Subsequently, MS/MS experiments were conducted on CER [N(24)ds(18)], resulting in the mass spectrum shown in Figure 5b. Again, fragments corresponding to the fatty acid chain and the sphingosine base were observed^{54,56,58}: the fatty acid related fragments of CER [Nds] are similar to their CER [NS] counterparts (m/z 368.3 and 392.4 amu). This is expected because both structures contain a non-hydroxy fatty acid and are therefore identical. Fragments related to the sphingosine base are shifted +2 amu (m/z 254.3, 266.3 and 284.2 amu). This is also in agreement as CER [ds] contains one degree of

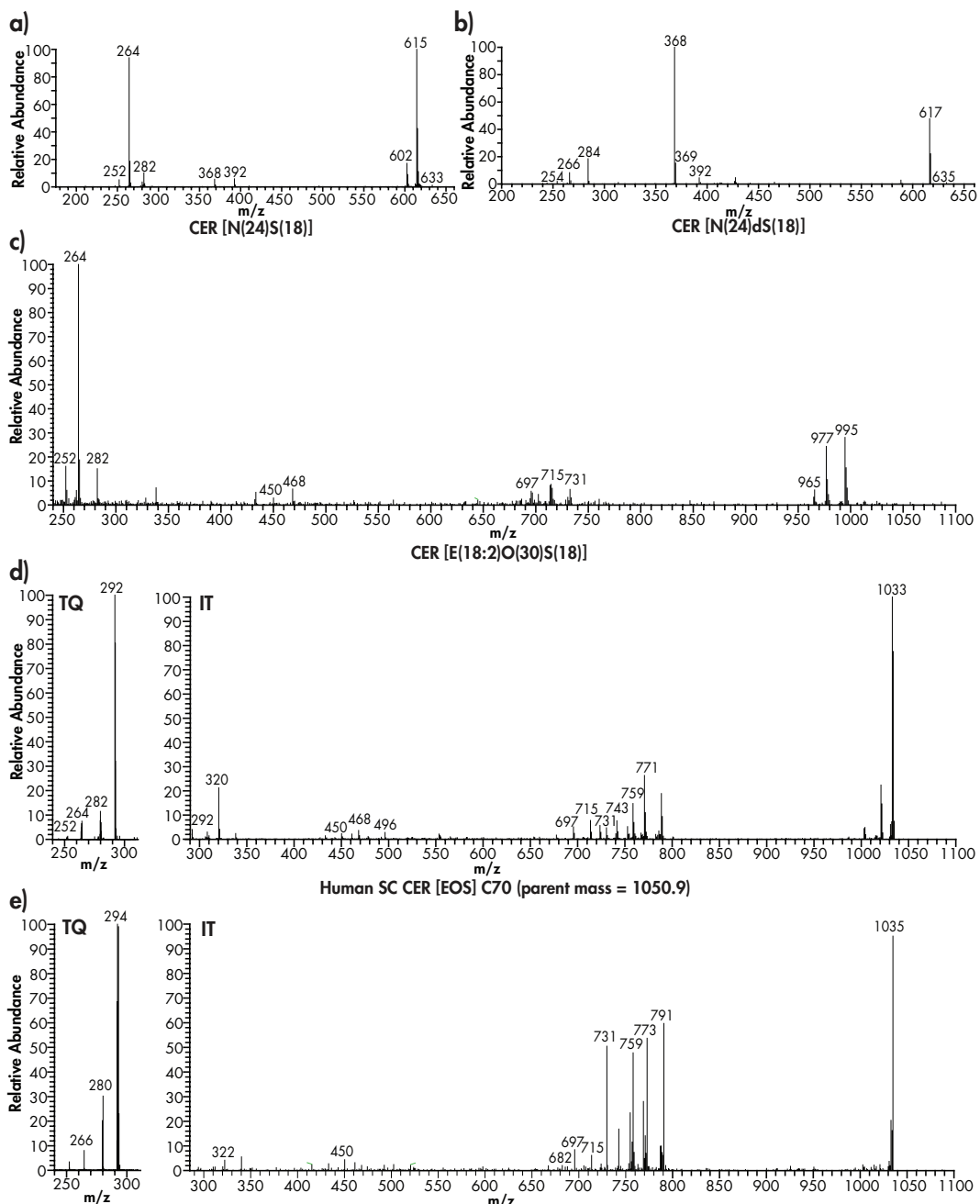


Figure 5: MS/MS spectra of synthetic CERS using an Ion Trap (IT) system: **a)** CER [N(18)S(24)]; **b)** CER [N(18)ds(24)]; **c)** CER [E(18:2)O(30)S(18)]; **d)** human SC CER subclass [EOS] C70, parent m/z 1050.9 amu; **e)** unknown human SC CER, parent m/z 1052.9 amu. Because of the low m/z cut off and range limitations of MS/MS using an IT system (see text), a Triple Quad (TQ) MS was used to obtain fragment ion spectra in the low mass range (250-300 amu) of human SC CER [EOS] (**d**) and the unknown CER (**e**).

saturation less, i.e. two hydrogen atoms more. Hereafter, the more complicated CER [EOS] – consisting of a sphingosine base 18 carbon atoms long and a fatty acid chain 30 carbon atoms long, with a linoleic acid moiety esterified to it – was studied. Fragmentation of this CER resulted in a mass spectrum present in Figure 5c. Since this CER also bears a sphingosine base, fragments with respect to the sphingosine chain are similar to CER [NS] and CER [Nds] (viz. ions at m/z 252.3, 264.3, 282.2 amu). The fragments at m/z 450.5, 730.7 and 964.9 amu correspond to fragments related to the fatty acid chain. The MS/MS spectrum of CER [EOS] contains additional fragments compared with CER [NS] and [Nds] because the esterified linoleic acid may fragment as well. Fragments at m/z 696.7 and 714.7 amu indicate the loss of a linoleic moiety with and without the loss of a water molecule, respectively.

Subsequently, MS/MS spectra of the human SC variant of CER [EOS] were studied to confirm that their fragmentation is in agreement with these observations. The precursor ion of CER [E(18:2)O(34)S(18)] at m/z 1050.9 amu was fragmented and the result is shown in Figure 5d. Indeed, fragments corresponding to the loss of the fatty acid chain, the sphingosine chain, as well as fragments without the ester chain were observed (see Table III). In addition, fragments showed individual chain lengths of either the fatty acid or sphingosine chain. The characteristic sphingosine fragment of m/z 264.3 amu for example (C18 sphingosine), also showed fragments of m/z 292.3 and 320.3 amu (respectively C20 and C22). The same phenomenon was observed for esterified fatty acid fragments like 730.7 and 758.7 (C48 and C50). Finally, we performed MS/MS on the hypothesized CER [EODs] observed in human SC. Because human CERs contain various chain lengths in a single subclass, the precursor ion of the proposed CER [E(18:2)O(34)ds(18)], at m/z 1052.9 was selected for fragmentation studies. This precursor ion should, following observations described above, lead to fragments best comparable to the CER [E(18:2)O(34)S(18)] counterpart. Figure 5e shows the MS/MS spectrum obtained from this precursor ion. Very indicative fragments, which were observed in both CER [EOS] as well as in CER [Nds], also appear in this spectrum, indicating that this unidentified species indeed contains an esterified ω -hydroxy fatty acid moiety and also bears a dihydrosphingosine chain (i.e. 266.3, 450.5, 730.7, 772.7, 790.8). This strongly supports the hypothesis that the unknown CER class is indeed CER [EODs]. From Figure 4 it can be concluded that the mass range of this newly identified CER [EODs] ranges from m/z 1015.0 to 1181.1 amu and corresponds exactly with a CER [EODs] having a total chain length ranging from 66 to 78 carbon atoms long. Besides, it is known from literature that the CERs containing an even number of carbon atoms are more abundantly present than odd chain length CERs^{21,23}, which is also the case in our mass spectrum of Figure 4, again

Table III: Overview of MS fragments of both synthetic and biological ceramides and its structural correlation.

Ceramide subclass	Molecular structure including locations of possible fragmentation	m/z (amu)	Loss of functional group					
			H ₂ O	FA chain 1	Sph chain 2	CH ₂ OH 3	C ₁₆ H ₁₃ OH 4	Ester chain 5
[N(24)S(18)] Parent ion = 651 (synthetic)		252	X			X		
		264	X	X				
		282	X		X			
		368					X	
		392	X			X		X
		602	XX					
		615	X					
633	X							
[N(24)S(18)] Parent ion = 653 (synthetic)		254		X				
		266	X	X				
		284	X	X				
		368			X			
		392	XX				X	
		617	X					
		635	X					
[E(18:2)O(30)S(18)] Parent ion = 1013 (synthetic)		252		X				
		264	X	X				
		282	X	X				
		450			X			X
		468	XX		X			X
		697	X					X
		715	X		X			X
		731	X					
		965	XX					
		977	X					
		995	X					
[EOS] C70 parent ion = 1051 (human SC)		264/292/320 ^{a,b}	X	X				
		282 ^a			X			
		450			X			X
		468/496	XX		X			X
		715/743/771 ^b	X			X		X
731/759 ^b	XX							
1033								
[EOdS] (proposed) parent ion = 1053 (human SC)		266/280/294/322 ^{a,b}	X	X				
		450			X			X
		731/759 ^b	X		X			X
		773	X					
		791	X					
1035	XX							

Dotted lines with their corresponding numbers depict the location of fragmentation, viz. which functional group is lost. The variables m and n located in the molecular structure indicate variations in chain length. FA chain means fatty acid chain; Sph chain means sphingosine chain. 'X' indicates that the particular functional group is lost for that particular mass. 'XX' means that functional group is lost twice. 'a' Indicates these fragments were measured using a Triple Quad (TQ) system. All other fragments are observed using an Ion Trap (IT) mass spectrometer. 'b' Indicates that besides this particular m/z value, also values that lost the same functional group but show different masses were observed. This is due to the variation in total chain length in human SC, so a different length in carbon backbone results in mass peaks located exactly one or more CH_2 masses shifted. In example: fragment m/z 280 amu lost the same functional group as 266 amu, the only difference is the chain length of the fatty acid backbone, which is one CH_2 group longer.

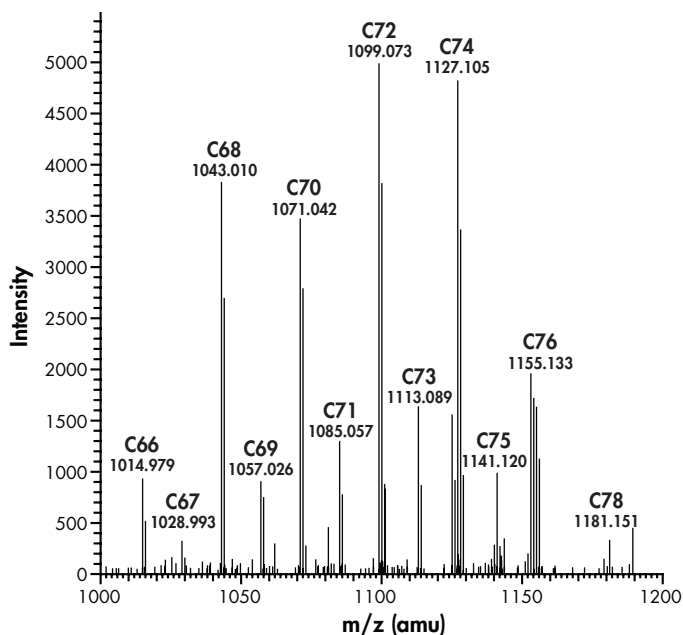


Figure 6: Average mass spectrum (retention time range: 1.8-2.4 min; positive ion mode) of unidentified lipid class, performed by high mass accuracy FT-ICR-MS, including mass table with the differences (Δ) of the observed and theoretical mass of the proposed molecular formulae in parts per million (ppm).

confirming that the unknown CER subclass is CER [EODs].

Finally, we also hypothesized on the possible molecular structure of the unknown lipid class noted as 'A' in Figure 3. Although we cannot make any firm conclusion because no extensive MS/MS studies were performed, it can be pointed out that this lipid species bears a mass in similar ranges as the CER [EO] subclasses. Moreover, from the early elution time it can be concluded that this lipid class is more apolar than all known CERs subclasses. Figure 6 shows the mass spectrum result of high mass accuracy analysis performed on these species by FT-ICR-MS, including the respective molecular formulae for every peak observed. These molecular formulae are quite conclusive, as the difference between the observed and theoretical mass is low: between -0.17 and 1.06 parts per million. Although it is highly speculative what the molecular structure of this lipid class is, the arguments mentioned above, in combination with the exact mass data, may point to a lipid structure comparable to CER [EODs], but with one OH-group less. More extensive research and repeated measurements will address this lipid in future studies.

Human skin CER analysis harvested by using tape strips

Our aim was to develop a method for CER analysis that could also provide a CER profile when harvesting *in vivo* SC using tape strips. Because tape strips usually contain substantial amounts of contaminants like polymers, most of them are incompatible with

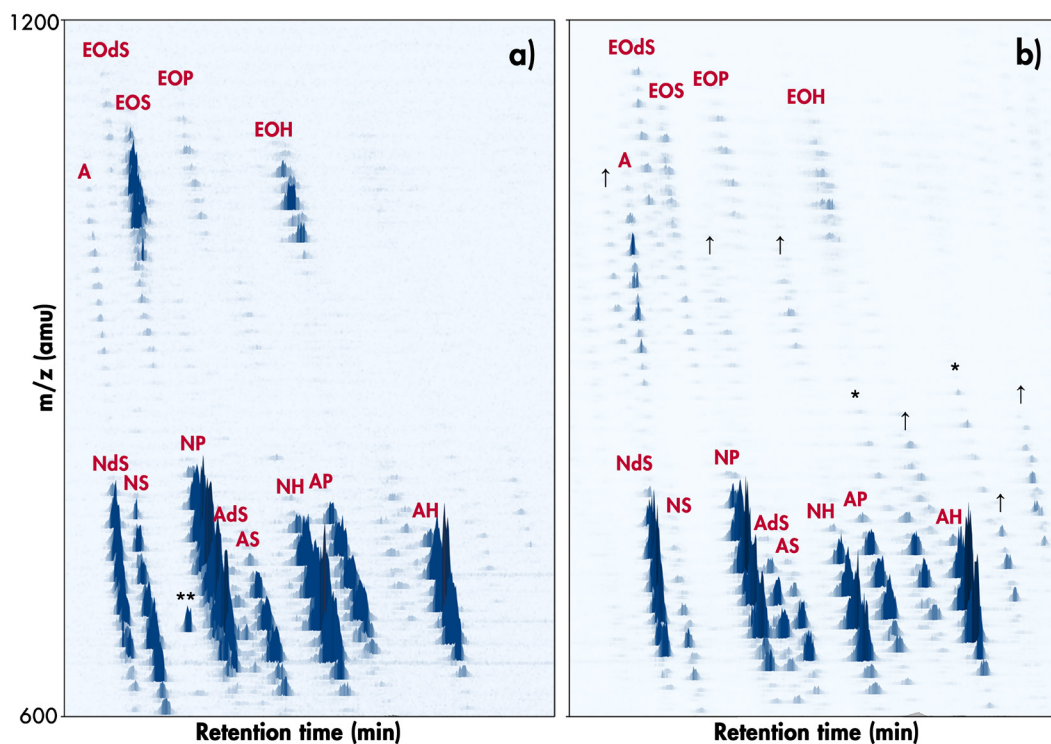


Figure 7: 3D multi-mass chromatogram of **a)** tape strips from human SC; **b)** cultured full-thickness skin explants. “A” represent the same unknown lipid mass as was shown in human SC from dermatomed skin (Figure 3). Compared to human SC from dermatomed skin, some lipid species in cultured full-thickness skin explants show either higher abundance (noted by ↑), or did not show up in dermatomed skin at all and might therefore possibly be different CER species (noted by *). Probable contamination caused by the tape strip is depicted as **.

LC/MS. To circumvent these issues, we decided to use poly(phenylene sulfide) tape strips obtained from Nichiban. These tape strips were also used in studies for CER analysis by Masukawa *et al.*^{23,39}. After lipid extraction and the additional concentration step (see Material and Methods), samples were injected and the 3D CER profile is shown in Figure 7. All the CER subclasses with varying chain length distributions could be identified and possible contaminants from the tape did not interfere with the results. All known CER classes can be observed in tape strip harvested SC and only minor deviations from the profile were observed. The nature of these differences remains to be investigated in future studies.

CER analysis of a human skin explant model

The extracted lipids from a cultured full-thickness skin explants model were analyzed using the same method as used for dermatomed skin and skin harvested from tape strips.

The results of the two individual pools were comparable and one of these 3D multi-mass chromatograms is presented in Figure 7b. Although it is not the purpose of this study to thoroughly investigate the exact differences between human skin and the cultured full-thickness skin explant model, from Figure 7b it can be concluded that this model contains several differences, including additional lipid subclasses compared with native human skin, possibly CERS.

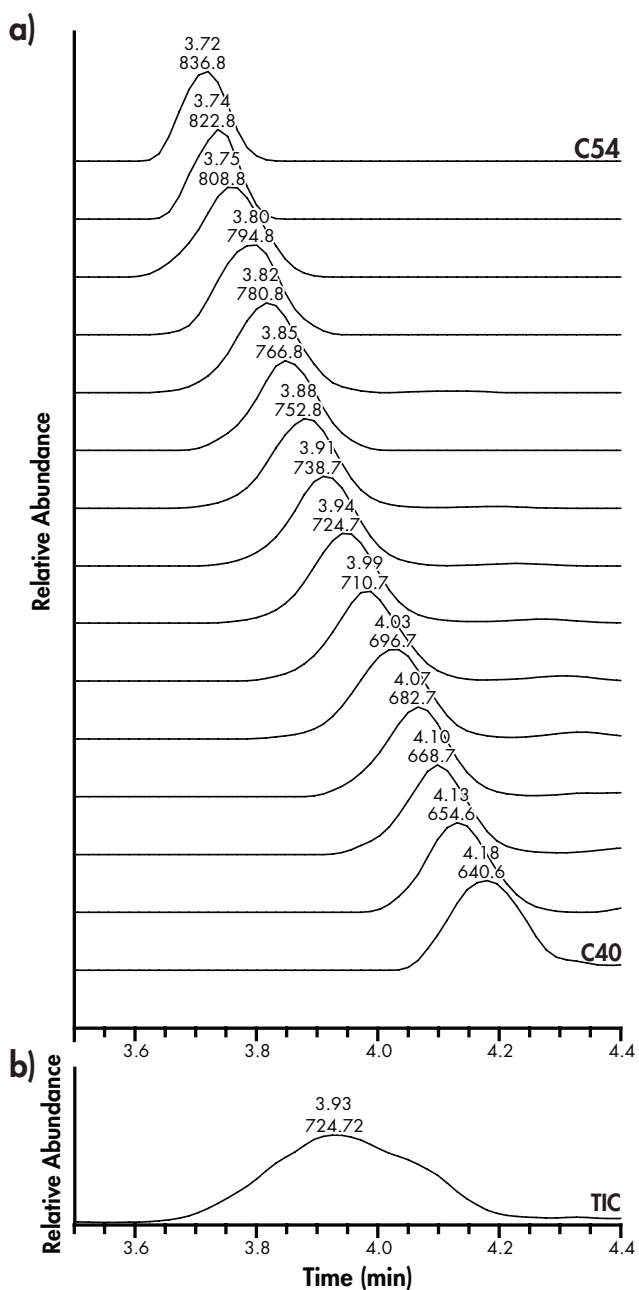
Conclusion

In this paper, we describe a new method for effectively profiling SC CERS with high sensitivity and only a very limited number of sample preparation steps, making this method very approachable for the analysis of different sorts of SC samples. The high sensitivity of our method – in particular for CERS with a higher mass range – resulted in the detection of additional lipid classes of which one could be identified as CER [EODs]. This is the fourth CER linoleic moiety esterified to a very long fatty acid chain confirmed to be present in human skin by LC/MS. We also successfully applied this method to CERS extracted from human SC harvested using tape strips. Because low quantities of lipids are obtained by tape stripping, an LC/MS method with high sensitivity is required. Also regarding these tape strip samples, the developed method was robust enough to detect all CERS. Finally, samples from a cultured full-thickness skin explant model could also be analyzed using this developed method and sensitivity seems no issue. Future research on CER analysis may benefit from this new method, showing an easy, robust, quick, and sensitive method for analysis of these lipid species.

Acknowledgements

This research is supported by the Dutch Technology Foundation STW, which is part of the Netherlands Organisation for Scientific Research (NWO), and which is partly funded by the Ministry of Economic Affairs. The authors gratefully acknowledge Cosmoferm for the provision of the synthetic CERS. This study was also supported by the research program of the Netherlands Metabolomics Centre (NMC) which is part of The Netherlands Genomics Initiative/Netherlands Organization for Scientific Research. Finally, the authors thank Robert Rissmann and Judith van Dommellen for their contribution to the development of the LC/MS method, and Varsha Thakoersing for providing cultured full-thickness skin explants.

Supplemental data



Supplementary Figure 1: a) Stacked chromatograms (IEC) of the human stratum corneum CER subclass [NS]. The wide distribution in chain lengths of a single ceramide subclass (40 to 54 carbon atoms) causes the wide total ion current profile of all CER [NS] shown in **b)**.

References

- Madison KC. Barrier function of the skin: "la raison d'etre" of the epidermis. *J Invest Dermatol* 2003; 121: 231-41.
- Wertz PW, van den Bergh B. The physical, chemical and functional properties of lipids in the skin and other biological barriers. *Chem Phys Lipids* 1998; 91: 85-96.
- Coderch L, Lopez O, de la Maza A *et al.* Ceramides and skin function. *Am J Clin Dermatol* 2003; 4: 107-29.
- Elias PM, Friend DS. The permeability barrier in mammalian epidermis. *J Cell Biol* 1975; 65: 180-91.
- Di Nardo A, Wertz P, Giannetti A *et al.* Ceramide and cholesterol composition of the skin of patients with atopic dermatitis. *Acta Derm Venereol* 1998; 78: 27-30.
- Farwanah H, Raith K, Neubert RH *et al.* Ceramide profiles of the uninvolved skin in atopic dermatitis and psoriasis are comparable to those of healthy skin. *Arch Dermatol Res* 2005; 296: 514-21.
- Imokawa G, Abe A, Jin K *et al.* Decreased level of ceramides in stratum corneum of atopic dermatitis: an etiologic factor in atopic dry skin? *J Invest Dermatol* 1991; 96: 523-6.
- Ishikawa J, Narita H, Kondo N *et al.* Changes in the Ceramide Profile of Atopic Dermatitis Patients. *J Invest Dermatol* 2010; 130: 2511-4.
- Raith K, Farwanah H, Wartewig S *et al.* Progress in the analysis of Stratum corneum ceramides. *European Journal of Lipid science and Technology* 2004; 106: 561-71.
- Jungersted JM, Hellgren LI, Jemec GBE *et al.* Lipids and skin barrier function - a clinical perspective. *Contact Dermatitis* 2008; 58: 255-62.
- Jungersted JM, Scheer H, Mempel M *et al.* Stratum corneum lipids, skin barrier function and filaggrin mutations in patients with atopic eczema. *Allergy* 2010; 65: 911-8.
- Ponec M, Weerheim A, Lankhorst P *et al.* New acylceramide in native and reconstructed epidermis. *J Invest Dermatol* 2003; 120: 581-8.
- Robson KJ, Stewart ME, Michelsen S *et al.* 6-Hydroxy-4-sphinganine in human epidermal ceramides. *J Lipid Res* 1994; 35: 2060-8.
- Stewart ME, Downing DT. Free sphingosines of human skin include 6-hydroxysphingosine and unusually long-chain dihydrosphingosines. *J Invest Dermatol* 1995; 105: 613-8.
- Stewart ME, Downing DT. A new 6-hydroxy-4-sphinganine-containing ceramide in human skin. *J Lipid Res* 1999; 40: 1434-9.
- Wertz PW, Downing DT. Ceramides of pig epidermis: structure determination. *J Lipid Res* 1983; 24: 759-65.
- Higuchi H, Nakamura M, Kuwano A *et al.* Quantities and types of ceramides and their relationships to physical properties of the horn covering the claws of clinically normal cows and cows with subclinical laminitis. *Canadian Journal of Veterinary Research-Revue Canadienne De Recherche Veterinaire* 2005; 69: 155-8.
- Shimada K, Yoon JS, Yoshihara T *et al.* Increased transepidermal water loss and decreased ceramide content in lesional and non-lesional skin of dogs with atopic dermatitis. *Veterinary Dermatology* 2009; 20: 541-6.
- Farwanah H, Pierstorff B, Schmelzer CE *et al.* Separation and mass spectrometric characterization of covalently bound skin ceramides using lc/apci-ms and Nano-esi-ms/ms. *J Chromatogr B Analyt Technol Biomed Life Sci* 2007; 852: 562-70.
- Farwanah H, Wirtz J, Kolter T *et al.* Normal phase liquid chromatography coupled to quadrupole time of flight atmospheric pressure chemical ionization mass spectrometry for separation, detection and mass spectrometric profiling of neutral sphingolipids and cholesterol. *J Chromatogr B Analyt Technol Biomed Life Sci* 2009; 877: 2976-82.
- Farwanah H, Wohlrab J, Neubert RH *et al.* Profiling of human stratum corneum ceramides by means of normal phase lc/apci-ms. *Anal Bioanal Chem* 2005; 383: 632-7.
- Masukawa Y, Narita H, Imokawa G. Characterization of the lipid composition at the proximal root regions of human hair. *J Cosmet Sci* 2005; 56: 1-16.
- Masukawa Y, Narita H, Sato H *et al.* Comprehensive quantification of ceramide species in human stratum corneum. *J Lipid Res* 2009; 50: 1708-19.
- Masukawa Y, Tsujimura H. Highly sensitive determination of diverse ceramides in human hair using reversed-phase high-performance liquid chromatography-electrospray ionization mass spectrometry. *Lipids* 2007; 42: 275-90.
- Vietzke JP, Brandt O, Abeck D *et al.* Comparative investigation of human stratum corneum ceramides. *Lipids* 2001; 36: 299-304.
- Hinder A, Schmelzer CE, Rawlings AV *et al.* Investigation of the Molecular Structure of the Human Stratum Corneum Ceramides [NP] and [EOS] by Mass Spectrometry. *Skin Pharmacol Physiol*; 24: 127-35.
- Raith K, Neubert RHH. Liquid chromatography-electrospray mass spectrometry and tandem mass spectrometry of ceramides. *Analytica Chimica Acta* 2000; 403: 295-303.
- Cremer AE, Fischl AS. Current methods for the identification and quantitation of ceramides: an overview. *Lipids* 2000; 35: 937-45.
- Hannun YA, Obeid LM. Principles of bioactive lipid signalling: lessons from sphingolipids. *Nat Rev Mol Cell Biol* 2008; 9: 139-50.
- Taha TA, Mullen TD, Obeid LM. A house divided: ceramide, sphingosine, and sphingosine-1-phosphate in programmed cell death. *Biochim Biophys Acta* 2006; 1758: 2027-36.
- Kitatani K, Idkowiak-Baldys J, Hannun YA. The sphingolipid salvage pathway in ceramide metabolism and signaling. *Cell Signal* 2008; 20: 1010-8.
- Vaena de Avalos S, Jones JA, Hannun YA. Ceramides. In: *Bioactive Lipids* (Nicolau A, GKokotos G, eds), Vol. 17. *Bridgewater: The Oily Press*. 2004; 135-67.
- Jayadev S, Liu B, Bielawska AE *et al.* Role for ceramide in cell cycle arrest. *J Biol Chem* 1995; 270: 2047-52.
- Hannun YA, Luberto C. Ceramide in the eukaryotic stress response. *Trends Cell Biol* 2000; 10: 73-80.
- Kolesnick RN, Kronke M. Regulation of ceramide production and apoptosis. *Annu Rev Physiol* 1998; 60: 643-65.
- Riboni L, Prinetti A, Bassi R *et al.* A mediator role of ceramide in the regulation of neuroblastoma Neuro2a cell

- differentiation. *J Biol Chem* 1995; 270: 26868-75.
- 37 Venable ME, Lee JY, Smyth MJ *et al.* Role of ceramide in cellular senescence. *J Biol Chem* 1995; 270: 30701-8.
- 38 Pena LA, Fuks Z, Kolesnick R. Stress-induced apoptosis and the sphingomyelin pathway. *Biochem Pharmacol* 1997; 53: 615-21.
- 39 Masukawa Y, Narita H, Shimizu E *et al.* Characterization of overall ceramide species in human stratum corneum. *J Lipid Res* 2008; 49: 1466-76.
- 40 Jessome, Lee L, Volmer DA. Ion suppression: A major concern in mass spectrometry. In, Vol. 24. Duluth, MN, United States: Advanstar Communications. 2006; 498-511.
- 41 Matuszewski BK, Constanzer ML, Chavez-Eng CM. Matrix effect in quantitative lc/ms/ms analyses of biological fluids: a method for determination of finasteride in human plasma at picogram per milliliter concentrations. *Anal Chem* 1998; 70: 882-9.
- 42 Bruins CH, Jeronimus-Stratingh CM, Ensing K *et al.* On-line coupling of solid-phase extraction with mass spectrometry for the analysis of biological samples. I. Determination of clenbuterol in urine. *J Chromatogr A* 1999; 863: 115-22.
- 43 de Hoffmann E, Stroobant V. *Mass Spectrometry, Principles and Applications, 3rd edn.*: Wiley.
- 44 Ashcroft AE. Atmospheric Pressure Chemical Ionization. In: *Ionization Methods in organic mass spectrometry (Barnett NW, ed)*. Cambridge (UK): The Royal Society of Chemistry. 1997.
- 45 Lebonvallet N, Jeanmaire C, Danoux L *et al.* The evolution and use of skin explants: potential and limitations for dermatological research. *Eur J Dermatol*; 20: 671-84.
- 46 Motta S, Monti M, Sesana S *et al.* Ceramide composition of the psoriatic scale. *Biochimica et Biophysica Acta (BBA) - Molecular Basis of Disease* 1993; 1182: 147-51.
- 47 Nugroho AK, Li L, Dijkstra D *et al.* Transdermal iontophoresis of the dopamine agonist 5-OH-DPAT in human skin *in vitro*. *Journal of Controlled Release* 2005; 103: 393-403.
- 48 Bligh EG, Dyer WJ. A rapid method of total lipid extraction and purification. *Can J Biochem Physiol* 1959; 37: 911-7.
- 49 Thakoersing VS, Ponec M, Bouwstra JA. Generation of human skin equivalents under submerged conditions-mimicking the in utero environment. *Tissue Eng Part A*; 16: 1433-41.
- 50 Christie WW, Gill S, Nordbäck J *et al.* New procedures for rapid screening of leaf lipid components from Arabidopsis. *Phytochemical Analysis* 1998; 9: 53-7.
- 51 Quinton L, Gaudin K, Baillet A *et al.* Microanalytical systems for separations of stratum corneum ceramides. *J Sep Sci* 2006; 29: 390-8.
- 52 Wertz PW, Swartzendruber DC, Madison KC *et al.* Composition and morphology of epidermal cyst lipids. *J Invest Dermatol* 1987; 89: 419-25.
- 53 Schiffmann S, Sandner J, Birod K *et al.* Ceramide synthases and ceramide levels are increased in breast cancer tissue. *Carcinogenesis* 2009; 30: 745-52.
- 54 Masukawa Y, Tsujimura H, Narita H. Liquid chromatography-mass spectrometry for comprehensive profiling of ceramide molecules in human hair. *J Lipid Res* 2006; 47: 1559-71.
- 55 Hsu FF, Turk J, Stewart ME *et al.* Structural studies on ceramides as lithiated adducts by low energy collisional-activated dissociation tandem mass spectrometry with electrospray ionization. *J Am Soc Mass Spectrom* 2002; 13: 680-95.
- 56 Yoo HH, Son J, Kim DH. Liquid chromatography-tandem mass spectrometric determination of ceramides and related lipid species in cellular extracts. *J Chromatogr B Analyt Technol Biomed Life Sci* 2006; 843: 327-33.
- 57 Schiffmann S, Sandner J, Schmidt R *et al.* The selective COX-2 inhibitor celecoxib modulates sphingolipid synthesis. *J Lipid Res* 2009; 50: 32-40.
- 58 Shaner RL, Allegood JC, Park H *et al.* Quantitative analysis of sphingolipids for lipidomics using triple quadrupole and quadrupole linear ion trap mass spectrometers. *J Lipid Res* 2009; 50: 1692-707.

CHAPTER 4

COMBINED LC/MS- ASSAY FOR ANALYSIS OF ALL MAJOR STRATUM CORNEUM LIPIDS, FOCUSING ON FREE FATTY ACIDS

Jeroen van Smeden,¹ Walter A. Boiten,¹
Thomas Hankemeier,^{2,3} Robert Rissmann,⁴
Joke A. Bouwstra¹ and Rob J. Vreeken^{2,3}

¹ Division of Drug Delivery Technology,
Leiden Academic Centre for Drug
Research, Leiden University, Leiden,
The Netherlands.

² Division of Analytical Biosciences,
Leiden Academic Centre for Drug
Research, Leiden University, Leiden,
The Netherlands.

³ Netherlands Metabolomics Centre,
Leiden Academic Centre for Drug
Research, Leiden University, Leiden,
The Netherlands.

⁴ Centre for Human Drug Research, Leiden,
The Netherlands.

Submitted

Abstract

Ceramides (CERS), cholesterol (CHOL), and free fatty acids (FFAs) are the main lipid classes in human stratum corneum (SC, outermost layer of the skin), but there are no studies that report on the detailed analysis of these classes in a single setup. The primary aims of this present study were to 1) develop a LC/MS method for quantitative analysis of FFAs; and 2) combine this method with the analysis of CHOL and with our recently reported method for CER analysis. This combined method detects all major SC lipids in a single setup using NPLC and positive ion mode APCI-MS for detection of CERS and CHOL, and RPLC using negative ion mode APCI-MS to analyze FFAs. Validation showed this method to be robust, reproducible, sensitive, and fast. It is, to our knowledge, the first study that permits the analysis of SC FFAs by LC/MS. The method was successfully applied on *ex vivo* human SC, human SC obtained from tape stripping and human skin substitutes (porcine SC and human skin equivalents). In conjunction with CER profiles, clear differences in FFA profiles were observed between these different SC sources. For future research, this provides an excellent method for quantitative, ‘high-throughput’ profiling of SC lipids with more than adequate sensitivity.

Introduction

Lipid analysis is currently of main interest in many research areas, as these compounds are crucial to unveil biological mechanisms in e.g. cell signaling, energy storage, enzyme activation, apoptosis, metabolism and functioning of cell membranes¹⁻⁷. Particularly in dermatological research, lipidomics has had increased attention since its importance regarding human dermatological disorders has

recently been demonstrated⁸⁻¹³. The lipids located in the uppermost layer of the skin – the stratum corneum (SC) – fulfill a primary role in the skin barrier function^{9,14-17}. Human SC lipids consist of mainly 3 classes: free fatty acids (FFAs), ceramides (CERS) and cholesterol (CHOL)¹⁸⁻²⁴. Based on their variations in chemical structure, CERS are divided into subclasses²⁵ (in Supplementary Figure 1 the CER subclasses are provided), which are important for a proper barrier function²⁶⁻²⁹.

The recent increment in more detailed knowledge about SC lipid composition can, to a large extent, be attributed to the upcoming use of liquid chromatography coupled to mass spectrometry (LC/MS). LC/MS provides both information on lipid subclasses as well as the chain length distribution in each of the subclasses, which is not possible using the common technique of thin layer chromatography (TLC)³⁰⁻³². However, no study reports on LC/MS analysis of all three SC lipid classes in a single setup. One of the main reasons is the lack of a proper LC/MS method for analyzing SC FFAs. The most frequently used method to analyze this particular lipid class is gas chromatography (GC). This method, however, is labor intensive as derivatization of the FFAs is required prior to analysis³³⁻³⁵. Moreover, GC is rarely used for analysis of the CERS simultaneously, as these non-volatile compounds are unstable in the gas-phase (if not derivatized, which is cumbersome as well)³⁶⁻³⁸. On the contrary, LC/MS has the potential to analyze the CERS, FFAs, and CHOL in a single setup.

Therefore, the first aim of the study was to develop and validate an LC/MS method that enables quantitative analysis of FFAs present in human SC. Once validated, the second aim was to combine this method with our recently reported LC/MS method for analysis of CERS (see previous chapter)³⁹, and to improve this method to enable the analysis of CHOL as well. The two combined methods would permit the analysis of all main SC lipid classes. Sample collection and preparation should be kept to a minimum to prevent degradation and allow for high-throughput analysis⁴⁰. Analysis of underivatized lipids is therefore preferable.

After the development of the LC/MS method, we validated and successively tested the method on SC from *ex vivo* human SC and compared it to three scientifically relevant samples: 1) analysis of human SC obtained from tape stripping (tape stripping is a non-invasive way to obtain SC from which the lipids can be extracted) and 2) SC from two human skin substitutes, i.e. porcine skin and human skin equivalent (HSE). The latter is generated from keratinocytes and fibroblasts, the most abundant cell types in the skin.

Materials and Methods

Chemicals

HPLC grade (or higher) methanol (MeOH), n-heptane, isopropanol (IPA), acetonitrile (ACN), ethanol (EtOH), and acetic acid (HAc) were purchased from Biosolve (Valkenswaard, The Netherlands). Chloroform (CHCl₃) was attained from Lab-Scan (Dublin, Ireland). Ultra purified water was prepared using a Purelab Ultra purification system (Elga Labwater, High Wycombe, UK). Potassium chloride was obtained from Merck (Darlctadt, Germany). FFA 22:0-OH and deuterated CHOL-D7 were obtained from Larodan AB (Malmö, Sweden). Trypsin, trypsin inhibitor, CHOL as well as FFAs 16:0, 16:1, 18:0, 18:1, 18:2, 20:0, 22:0, 22:1, 24:0, 24:1 and 28:0 were obtained from Sigma-Aldrich GmbH (Steinheim, Germany). Deuterated FFAs 18:0-D35 and 24:0-D47 acids were purchased from Cambridge Isotope Laboratories (Andover, MA). Synthetic CER [Nds] was purchased from Avanti Polar Lipids (Alabaster, AL). All other synthetic CERS, viz. [EOS], [NS], [NP], [AS], [AP], [EOP], deuterated [EOS]-D31, and deuterated [NS]-D47, were kindly provided by Evonik (Essen, Germany). A more specified description of the chemicals is located in the Supplementary Materials and Methods.

SC sample collection and lipid extraction

Synthetic lipids as well as SC lipids from human *ex vivo* surgical skin were used to develop and validate the LC/MS method. To study the applicability of the developed method, 3 different skin sources (viz. human SC obtained from tape stripping, SC from HSEs, and SC from porcine skin) were analyzed and compared to human *ex vivo* SC. The collection and processing of skin samples is in accordance to the Declaration of Helsinki and all human subjects gave written informed consent. The whole sample collection (by means of tape stripping)^{39,41,42} and lipid extraction procedures (extended Bligh and Dyer)^{43,44} are described previously, and also added to the supporting Materials and Methods. Afterwards, samples were reconstituted in heptane/CHCl₃/MeOH (95:2½:2½) to a final concentration of ~1.0 mg/ml. When sample storage was necessary, samples were stored under argon atmosphere, at -20°C, in a dark environment. The heptane/CHCl₃/MeOH solution is stable at 21°C, but phase separation occurs over time at lower temperatures (e.g. <7°C). Heating the solution for 1 hour at 34°C results in a single phase. The solution can be used afterwards at room temperature. This single solution was suitable for lipid analysis of both FFAs as well as CERS and CHOL.

Lipid analysis by LC/MS

All SC lipids were analyzed using a single setup of an HPLC (either an Alliance 2695,

Waters Corp., Milford, MA; or Surveyor Thermo Finnigan, San Jose, CA) coupled to an APCI source equipped on a triple quadrupole (TQ) mass spectrometer (TSQ Quantum, Thermo Finnigan) operating in full scan mode. Separation of FFAs by chain length and degree of unsaturation can be achieved on a reverse phase column. Using APCI-MS, underivatized FFAs are most effectively analyzed in negative ion mode^{45,46}, whereas CERS and CHOL are best separated on a normal phase column and result in abundant protonated species in the positive ion mode^{47,48}. Therefore, we use two injections of 10 μ l to analyze all SC lipids: one injection for the separation of FFAs on a RPLC column (Purospher Star LiChroCART, Merck) and another injection for the analysis of both CERS and CHOL by separation on a NPLC column (PVA-Sil, YMC, Kyoto, Japan). A switching valve (Rheodyne MXP9900-000, IDEX Corporation, Rohnert Park, CA) was used to change the flow to either the NPLC- or RPLC-column. Another switching valve directed the flow to either the APCI-MS or to the waste to prevent ionization effects caused by excessive contamination originating from e.g. tape strips. A schematic illustration of the setup is shown in Supplementary Figure 2.

Regarding the FFA analysis, the vaporizer and capillary temperature were set to 450 and 250°C, respectively. Ionization was performed in negative ion mode, scanning from 200-600 amu using a nitrogen flow of 3 and 0.8 L/min for auxiliary and sheath gas, respectively. The discharge current was set at 6 μ A while the capillary voltage was maintained at 2kV. The peak width at nominal resolution, determined by full width at half maximum, was set to 0.7 amu. Chromatographic separation of all FFAs (C₁₄-C₃₆) was achieved within 7 minutes at a flow rate of 0.5 mL/min using a binary gradient from ACN/H₂O (90:10) to MeOH/heptane (90:10). 1% CHCl₃ and 0.1% HAC were added to both mobile phases to greatly enhance the ionization efficiency and boost the formation of the [M+Cl]⁻ adduct, which appeared to be the main ion present for all FFA(-related) compounds (see 'FFA method development' in results and discussion section). For the analysis of CERS and CHOL, the method published previously was used with some small adaptations to the gradient, sheath gas flow rate, and scan range (360-1200 amu), to permit analysis of CHOL. The full method development and explanation of CER analysis is described elsewhere³⁹. A summary of all LC and MS parameters is presented in Supplementary Table I.

Data processing

Automated peak detection and area integration was performed using Quan Browser software version 2.0.7 (Thermo Fisher Scientific, Bremen, Germany), but all data were manually inspected and corrected when necessary. Peak areas were corrected for their appropriate internal standard (ISTD).

Method validation.

An in-house protocol was used to determine the linear dynamic range, limit of detection and quantification (LOD and LOQ), and inter-day and inter-batch reproducibility. The linear dynamic range of each analyte was determined from calibration curves prepared as an academic sample as well as in human SC matrix. Standards were prepared in duplicate and injected in triplicate. Linear regression on the calibration curves was performed (on data points >LOQ), except for CHOL, where a non-linear fit was more appropriate since ion suppression played a significant role at higher concentration ranges. LODs and LOQs of each FFA ([M+Cl]⁻) were determined by the signal to noise ratio (S/N) of 3 and 10, respectively. Matrix effects (e.g. ion suppression) were studied by calibration curves of deuterated internal standards (FFA 18:0-D35 and 24:0-D47) which were prepared with and without spiked lipids from pooled (*n*=6) human *ex vivo* SC. Regarding the FFAs, 8 different FFAs in 7 different concentrations ranging between 0.01 μM up to 900 μM (corresponding to levels of 0.1 pmol to 9 nmol) per FFA were assessed. For CHOL, deuterated and non-deuterated CHOL in 12 different concentrations ranging between 25 pmol and 25 nmol were analyzed. Regarding the CERS, adaptations to the original method did only influence the retention time, not the LOD/LOQ values. As a consequence, the latter is adapted from the previously reported values and listed in Supplementary Table II³⁹. Regarding the reproducibility, both the inter-day variation and inter-batch variation were examined. The former was calculated from a triplicate measurement over 3 different days (intra-batch/inter-day), while the latter was calculated from 3 different batches analyzed on a single day (inter-batch/intra-day).

Results and Discussion

FFA method development

No LC/MS method is available for FFA analysis of SC, but several reports exist for FFA analysis from other lipid sources. However, LC puts some limitations on the choice of the mobile phase^{49,50}. APCI may in our case be appreciated over other ionization techniques as we also use APCI in our setup to detect CERS and CHOL, and it is desirable to use a single setup for the detection of all SC lipid classes at once. Besides, it shows less dependency on ion suppression⁵¹⁻⁵⁶. For the reasons mentioned above – and the expectation of the presence of very long carbon chains (>30 carbon atoms) in SC FFAs – we used the analytical method of Nagy *et al.* as a starting point, since that method focused on analyzing long chain FFAs from dried blood spots and plant oils⁴⁵. We modified and optimized the method, as it was not able to detect and separate most SC FFAs. The first challenge was to enhance ionization efficiency, because signal to noise ratios were too low for real-life

applications. Post-column addition of $\text{CHCl}_3/\text{MeOH}$ (2:1, 20 $\mu\text{l}/\text{min}$) resulted in a drastic increase in signal intensity of around 2900% (see Supplementary Figure 3) for every FFA with mass $[\text{M}+35]^-$. This chloride adduct, being reported in various applications based on LC/MS analysis⁵⁷⁻⁵⁹, originated from the CHCl_3 which was subsequently added to the mobile phase (1% v/v proved optimal). Also a small amount of acetic acid (0.1% v/v) was added to assure that all FFAs are fully non-dissociated⁶⁰, allowing proper chromatography and chloride adduct formation ($[\text{M}+\text{Cl}]^-$). This favored the ionization towards a consistent chloride adduct which accounted for >99% of the total signal for all observed FFAs (see Supplementary Table III).

A second challenge was to increase the separation between different FFAs. The initial method separated FFAs based on their chain length. However, FFAs differing in degree of unsaturation (e.g. 18:0 vs. 18:1 vs. 18:2) were not separated. Separation by retention time was necessary since the chloride isotope peaks $[\text{M}+^{37}\text{Cl}]^-$ of C18:1 and C18:2 overlapped with the base peaks $[\text{M}+^{35}\text{Cl}]^-$ of C18:0 and C18:1, respectively. Replacing $\text{MeOH}/\text{H}_2\text{O}$ by MeOH/ACN resulted in an additional separation between different degrees of unsaturation, as is illustrated in Figure 1. For example, the resolution between C18:0 and C18:1 – as defined by $R = 2(t_{R18:0} - t_{R18:1}) / (w_{C18:0} + w_{C18:1})$ – increased from 0.12 to 1.36. However,

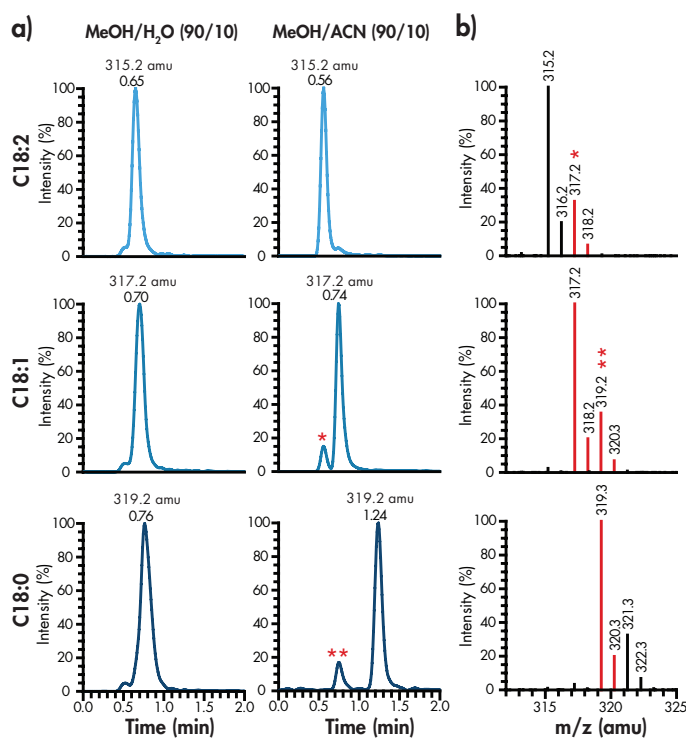


Figure 1: a) LC/MS chromatogram of a mixture of synthetic FFAs C18:0, C18:1, and C18:2 using either $\text{MeOH}/\text{H}_2\text{O}$ (left) or MeOH/ACN (right) as the mobile phase. Numbers correspond to the mass and retention time of that ion. * and ** indicate the chloride isotope peak that corresponds to an FFA with one degree of unsaturation more, shown in the mass spectra of **b**). These peaks that are overlapping in mass (due to the chloride isotope) and significantly interfere (>5% with the results (if not separated by their retention time) are shown in red, while non-interfering peaks are shown in black.

since 100% ACN was immiscible with heptane, phase separation occurred and no proper analysis could be performed. Therefore a gradient of ACN/H₂O (90:10) to MeOH/heptane (90:10) was used that proved to be optimal and resulted in the proper separation of all FFAs.

After optimization, the method was validated. All quantitative parameters will be discussed below, primarily focusing on FFAs. Individual chromatograms of saturated and unsaturated FFAs detected in human SC are provided in Figure 2. All FFAs that are predominantly present in human skin (FFA C24-C28) appear as clear, well separated peaks. However, early eluting FFAs which are less abundant in human SC (C14:0-C17:0, C19:0, C16:1-C18:2) show less defined peak shapes. This could be improved by increasing the retention time, but the increase in a slightly better peak profile does not outweigh our

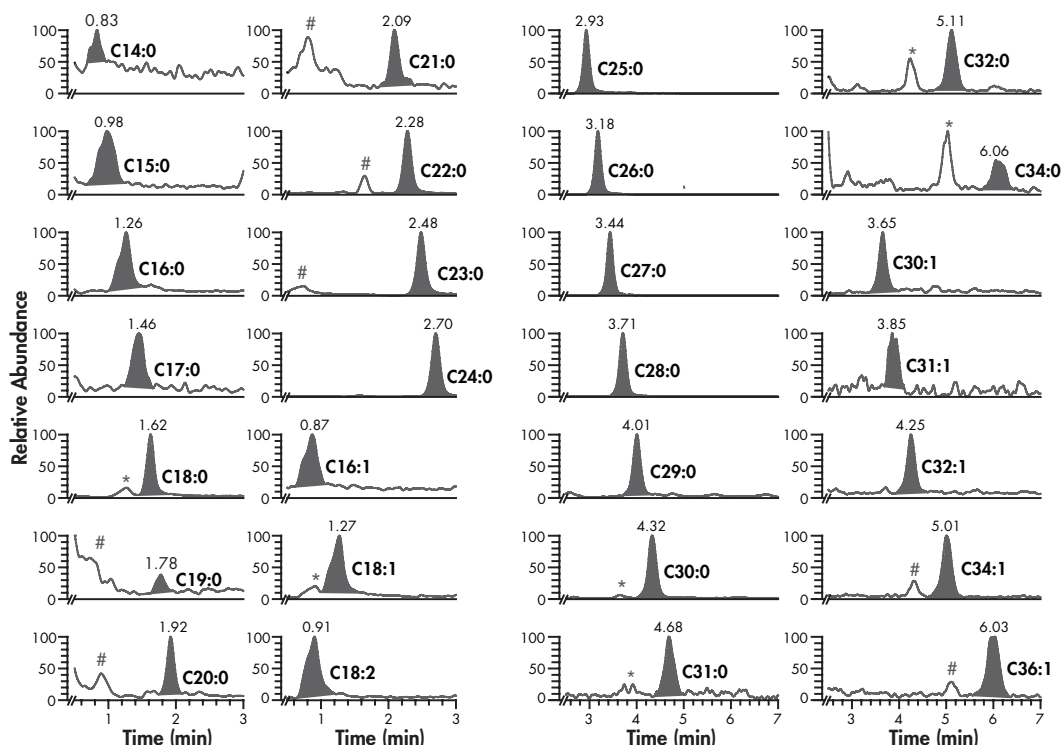


Figure 2: Chromatograms of $[M+Cl]^-$ ions of FFAs observed in human SC (range C14:0-C36:1). Left two columns show FFAs with short to medium chain length that elute at an early stage from the column (<3 minutes), while the right two columns show medium and long chain length FFAs. Values above the respective FFA peaks correspond to the retention time. * indicates the ³⁷Cl isotope peak that correspond to an FFA with one degree of unsaturation more than the peak of interest. # indicate peaks which belong to either CERS or are unknown.

primary aim to enable high-throughput screening for FFAs. Besides, we focused on the most abundant FFAs, in which we did not encounter these problems.

FFA method validation.

Validation measurements were performed according to an in-house developed protocol, and the chromatographic robustness, linearity, sensitivity (LOD/LOQ), reproducibility and matrix effects were determined and described in more detail below (Table I).

Chromatographic robustness. The variation of the retention time of each analyte was investigated. In general, the average RSD of the retention time was 4.7%, but differed among the various FFAs. FFAs with less than 20 carbon atoms showed more variation (RSD= \sim 7-8%), while later eluting FFAs, having more than 20 carbon atoms (which are most abundant in human SC), showed a more robust retention time (RSD= \sim 2%). All analytes showed acceptable capacity factors (k' >1.5) ranging between 1.7-10.0 for the earliest and latest eluting synthetic FFA (C18:2 / C28:0), respectively. Additional information on the robustness was obtained by transferring the method to a different HPLC system (Alliance 2695, Waters): No significant changes in any of the parameters was observed.

Sensitivity and linear dynamic range. LOD/LOQ values of each synthetic reference compound were determined using both academic solutions (CHCl₃/MeOH/heptane, 95:2½:2½) and *ex vivo* SC matrix solution (academic solution plus 1 mg/ml isolated SC). The linearity (R^2) of all analytes ranged from 0.990-0.999 over the range of 0.1-9000 pmol (7 data points, Table I and Supplementary Figure 4). Regarding the LOD and LOQ, a log-linear relationship was observed between the chain length (i.e. mass) of the FFA and the response factor (Figure 3). To cross-validate this relationship, we used synthetic FFAs

Table I: Validation results of synthetic FFAs, measured in full scan mode. Capacity factors (k'), linearity (R^2), sensitivity (LOD/LOQ), precision (RSDs) and inter batch and inter day variations are shown.

FFA	Base peak (amu)	Rt (min)	k'	LOD (nM)	LOQ (nM)	Inter-day RSD%*	Inter-batch RSD%*	R^2 values**
C18:0	319.3	1.62 ± 0.11	3.8	100	335	1.5-16.3	4.2-7.6	0.992
C18:1	317.3	1.27 ± 0.11	2.8	73	242	5.8-15.0	2.8-8.0	0.990
C18:2	315.2	0.91 ± 0.07	1.7	60	201	6.6-14.5	3.5-9.6	0.991
C22:0	375.3	2.28 ± 0.06	5.8	21	68	3.2-10.0	2.3-7.8	0.991
C24:0	403.4	2.70 ± 0.06	7.0	12	41	3.3-7.6	2.6-3.3	0.997
C28:0	459.4	3.71 ± 0.07	10.0	7	23	2.1-4.1	1.6-4.0	0.996
C18:0D35	354.4	1.38 ± 0.07	3.1	51	169	ND	ND	0.997
C24:0D47	450.6	2.57 ± 0.06	6.6	17	58	ND	ND	0.999

The capacity factor (k') was calculated using $T_{\text{injection peak}} = 0.34$ minutes*. RSD% presented here are those measured over the full range of concentrations. ND means not determined. **: calculated from all combined data points of 3 days, 3 batches.

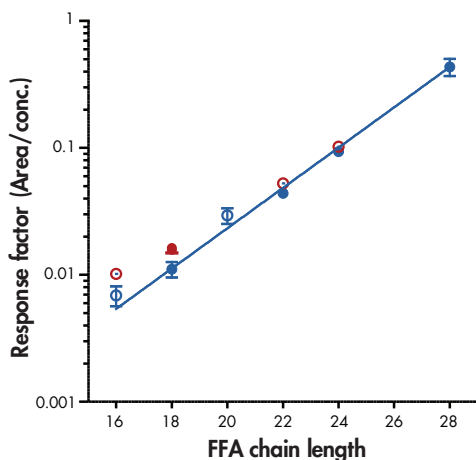


Figure 3: Dot plot showing the relation between the chain length of FFAs and the response factor (10^0 Log scale), defined as the AUC/concentration. Blue and red dots represent saturated and unsaturated FFAs, respectively. Closed dots correspond to the values calculated from the validation protocol (C18:0, C18:1, C18:2, C22:0, C24:0 and C28:0), while open dots represent samples that were analyzed on a different day to cross-validate the protocol (C16:0, C16:1, C20:0, C22:1 and C24:1). The exponential fit of this curve showed $R^2=0.984$.

(16:0, 16:1, 20:0, 22:1, 24:1) and calculated their response factors. The values fit very well in between the other data points. Thus, FFAs with a higher chain length showed lower LOD and LOQ values. Both higher noise and lower response levels at lower mass ranges as well as short retention times contribute to this change in LOD/LOQ phenomenon. LOD and LOQ values were determined by S/N 3 and 10, respectively for the individual ion traces $[M+Cl]^-$ for each lipid by using full scan MS acquisition. LODs range from 100 to 7 nM (1 to 0.07 pmol) for C18:0 to C28:0, respectively. LOQ values of C18:0 to C28:0 range from 335 to 23 nM (3.4 to 0.23 pmol). These LODs and LOQs are suitable for the analysis of all common SC samples (e.g. *ex vivo* SC, tape stripped SC, etcetera) and this makes the method very competitive with time-consuming GC or GC/MS procedures.

Reproducibility. The reproducibility was examined by determining inter-day and inter-batch variability for all synthetic analytes (Table I). Batch to batch variation among the various FFAs and their concentrations was on average 4.5%, ranging between 1.6 and 9.6%. The inter-day variability varied depending on the FFA chain length and the concentration used. An average variability of 7.7% was achieved, but higher mass FFAs and high concentrations generally reduced the variability to 4% or lower. For instance, the inter-day variability of C24:0 was ~3% at a concentration ≥ 3 nmol. In contrast, FFA 18:0 showed an inter-day RSD of 1.5% at a concentration of 900 μ M, but this value was increased to 16.3% at concentrations just above the LOQ. The variation in chromatographic robustness is a second reason for the increase in RSD: lower mass FFAs show more variation in elution time, thereby affecting the peak area to some extent.

Matrix effects. By comparing calibration curves between an academic solution and a SC matrix solution, we observed only very small differences for our internal standards:

Table II: Lipids present in *ex vivo* human SC, human SC harvested by tape stripping, HSEs and porcine skin.

Compound	Human SC	Tape	HSE	Porcine
FFAs				
<i>Saturated</i>				
C14:0	x	x	x	x
C16:0	x	x*	x	x
C16:1	x	x*	x	x
C18:0	x	x*	x	x
C18:1	x	x*	x	x
C18:2	x	x	x	x
C20:0	x	x	x	x
C21:0	x	x	-	x
C22:0	x	x	x	x
C23:0	x	x	-	x
C24:0	x	x	x	x
C25:0	x	x	x	x
C26:0	x	x	x	x
C27:0	x	x	-	x
C28:0	x	x	x	x
C29:0	x	x	-	x
C30:0	x	x	x	x
C31:0	x	x	-	x
C32:0	x	x	-	x
C33:0	x	-	-	-
C34:0	x	-	-	-
<i>Unsaturated</i>				
C16:1	x	x	x	x
C18:1	x	x	x	x
C18:2	x	x	x	x
C18:3	-	-	-	x
C20:1	-	-	x	x
C22:1	-	-	x	x
C24:1	-	-	x	x
C26:1	-	-	x	x
C28:1	-	-	x	x
C30:1	x	x	x	x
C32:1	x	x	x	x
C34:1	x	x	x	x
C36:1	x	-	x	x
C38:1	-	-	x	x
<i>Hydroxy</i>				
C22:0-OH	x	x	-	-
C23:0-OH	x	x	-	-
C24:0-OH	x	x	x	x
C25:0-OH	x	x	-	-
C26:0-OH	x	x	x	x
C27:0-OH	x	x	-	-
C28:0-OH	x	x	-	-
CERs				
[EOS]	64-76	65-76	66-76	60-74
[EOP]	63-76	64-76	64-76	64-70
[EOH]	63-72	64-72	66-72	-
[EOdS]	66-78	66-78	66-78	62-72
[NS]	34-56	34-54	34-54	32-52
[NP]	34-54	34-54	34-54	33-52
[NH]	34-52	34-52	32-48	-
[NdS]	34-58	34-56	34-56	33-52
[AS]	34-52	33-52	32-50	31-52
[AP]	34-51	34-52	34-50	36-52
[AH]	32-51	34-50	32-48	-
[AdS]	34-52	33-52	34-50	32-46
CHOL				
CHOL	x	x	x	x

x = Detected. - = Not detected. * = Present in blank tape strips. Numbers in the CER section correspond to the range in carbon chain length (i.e. total number of carbon atoms from the sphingosine chain and fatty acid chain).

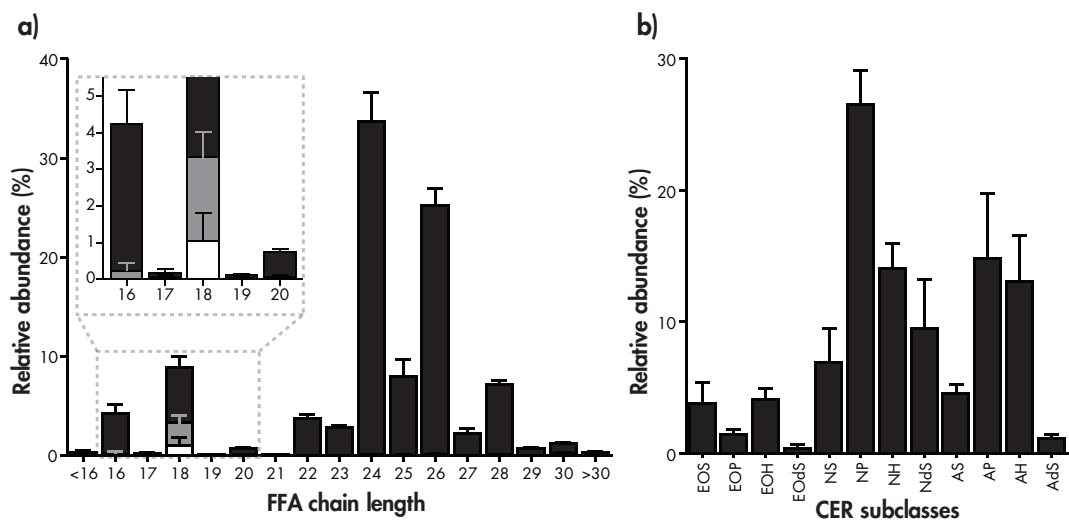


Figure 4: Barplots (mean \pm SD, $n=13$) of the relative abundances of **a)** human SC FFAs and **b)** all 12 CER subclasses. With respect to the FFAs, predominantly saturated FFAs are present (black bars). However, monounsaturated FFAs (gray bars) and diunsaturated FFAs (white bars) are observed as well – for FFA C18 primarily – as is shown from the inset.

compared to academic solutions, matrix samples showed 99.6% and 100.7% response for the C18:0-D35 and C24:0-D47 internal standards. As we observed a higher variation between inter-batch samples, we neglect this relatively small error.

Detection of FFAs in human SC samples.

Human *ex vivo* SC shows roughly 30 known FFAs, both saturated (odd and even chain lengths ranging from C14:0-C34:0) and unsaturated (even chain lengths ranging from C16:1-C18:1, C30:1-C36:1, C18:2). Overall, C24:0 and C26:0 are the most abundantly present FFAs in human SC, accounting for >50% to the total FFA content, whereas the presence of unsaturated FFAs was low (Figure 4a-c). FFAs with even chain length account for ~80% to the total FFA level present in human skin. The results are in excellent agreement to the results obtained by GC analysis published by Ponec *et al.* and Norlen *et al.*^{32,61} As a result of the increased sensitivity of the newly developed method (largely due to the use of CHCl₃ as an ionization enhancer), the carbon chain length range in which we were able to observe FFAs is similar or even broader than reported so far^{32,61-65}, as chain lengths over 32 carbon atoms could be detected (Figure 5a and Table II). Also the total analysis time is noticeably reduced from >50 minutes using the GC/MS method to 8 minutes for the new LC/MS method. Besides the unsaturated and saturated FFAs observed in human SC, we were also interested in hydroxy-FFAs that are rarely taken into account

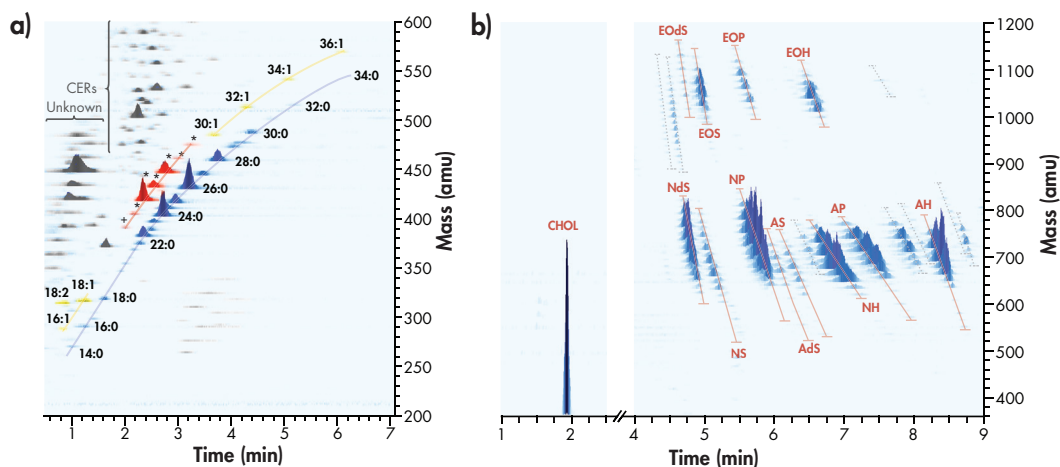


Figure 5: 3D multi-mass chromatograms of **a)** RPLC-MS on human SC FFAs. Saturated and unsaturated FFAs are marked in blue and yellow respectively. Ions shown in red and labeled */+ are unknown FFAs hypothesized as hydroxy-FFAs. These lipids ranged from 22 carbon atoms (labeled +) to 28 carbon atoms (see Supplementary Figure 5). Other lipid (related) peaks are shown in grey. **b)** NPLC-MS on human SC CHOL and CERs. All 12 CER subclasses present in human SC are detected, all with variation in chain length. Red lines and gray dotted lines indicate the chain length distribution for identified and unidentified CER subclasses, respectively.

but have shown to be present in human SC⁶². Identification by LC/MS did not reveal any informative ions and could therefore not be used to obtain structural information. Therefore, synthetic C22:0-OH was analyzed and showed a retention time (2.0 min), m/z (391.3 amu), and chloride-adduct pattern which is similar to one of the unknown peaks in human SC (Figure 5a, labeled '+'). These three parameters indicate that this unknown peak is indeed C22:0-OH. In fact, more unidentified peaks (noted by *) are observed in human SC. It is highly probable that these are hydroxy-FFAs as they differ exactly 14 amu in mass (one CH₂ group) from each other, elute at retention times similar to the extrapolated synthetic C22:0-OH FFA, and show a chloride-adduct pattern (Supplementary Figure 5). As is the case for saturated FFAs, even chain length OH-FFAs are much more abundant than odd chain length OH-FFAs, C24:0-OH and C26:0-OH being the most prominent ions observed.

CER and CHOL analysis and its detection in human SC samples

Small adaptations to the previously reported method for CER analysis (provided in Supplementary Table I) enabled the analysis of CHOL, eluting as a very intense peak prior to all CER subclasses at 1.9 min (Figure 5b and Supplementary Table II) at m/z of 369 amu, corresponding to the $[M+H-H_2O]^+$ ion. The LOD for CHOL and deuterated CHOL was 280

and 150 nM (2.8 pmol and 1.5 pmol, injected on column), respectively. A linear dynamic range was achieved below 300 μ M (3 nmol, injected on column), but above this amount the linear dynamic range was lost (Supplementary Figure 4) due to limited ionization capability. This resulted in a reduction of effective voltage for the corona discharge and hence a lower electric field strength. We note that this dynamic range of CHOL is reduced after analysis of large series (> 150 human SC samples of 1 mg/mL): the upper limit will be restricted due to limited ionization efficiency as a result of carbonaceous deposit on the tip of the discharge needle limiting the electric field strength. When continuing analysis on an unclean APCI needle, sensitivity is lost for subsequently CHOL, FFAs, and finally CERS. As this effect starts off with a reduction in dynamic range of CHOL, it can be used as a marker for corona discharge needle condition (i.e. system performance).

Regarding CERS, separation and sensitivity was similar as published previously³⁹. In fact, extending the mass range below 600 amu revealed additional CER species (see Applications section). The CER profile depicted in Figure 4b closely resembles that of the earlier quantitative publication by Masukawa *et al.*⁶⁶, in which various synthesized internal standards were used to correct every CER subclass for their relative ionization efficiency. The LC/APCI-MS method described in this manuscript makes use of 2 internal standards which are commercially available. Nevertheless, the results of both methods are very similar, indicating that our APCI-MS method is not biased towards certain CER subclasses, and by the addition of 2 internal standards, one can correct successfully for differences in e.g. ionization efficiencies between high mass and low mass CERS.

Applications on the combined LC/MS method for analysis of FFAs, CERS and CHOL

Besides the already discussed human *ex vivo* SC lipid profile, the applicability of the developed LC/MS method is illustrated by applying this method to obtain a lipid profile from three different biological samples, e.g. 1) tape stripped human SC, 2) HSEs and 3) porcine skin. The 3D multi-mass chromatograms and identified SC lipids in the respective samples are shown in Figure 6 and Table II respectively. The main advantage of plotting 3D multi-mass chromatograms is that it is easy to show full lipid profiles in a single picture, thereby comparing various samples on a relative scale. A disadvantage is that no conclusion can be drawn on an absolute quantitative level. For the purpose of this study, a relative comparison of lipid profiles by these 3D plots is sufficient, and Figure 6 illustrates the applicability of the developed method. Pictures are for comparison purposes normalized towards the most prominent endogenic FFA or CER peak (marked in purple). Key differences will be discussed below.

Tape stripped human SC: The amount of lipids from a tape stripped sample is much lower

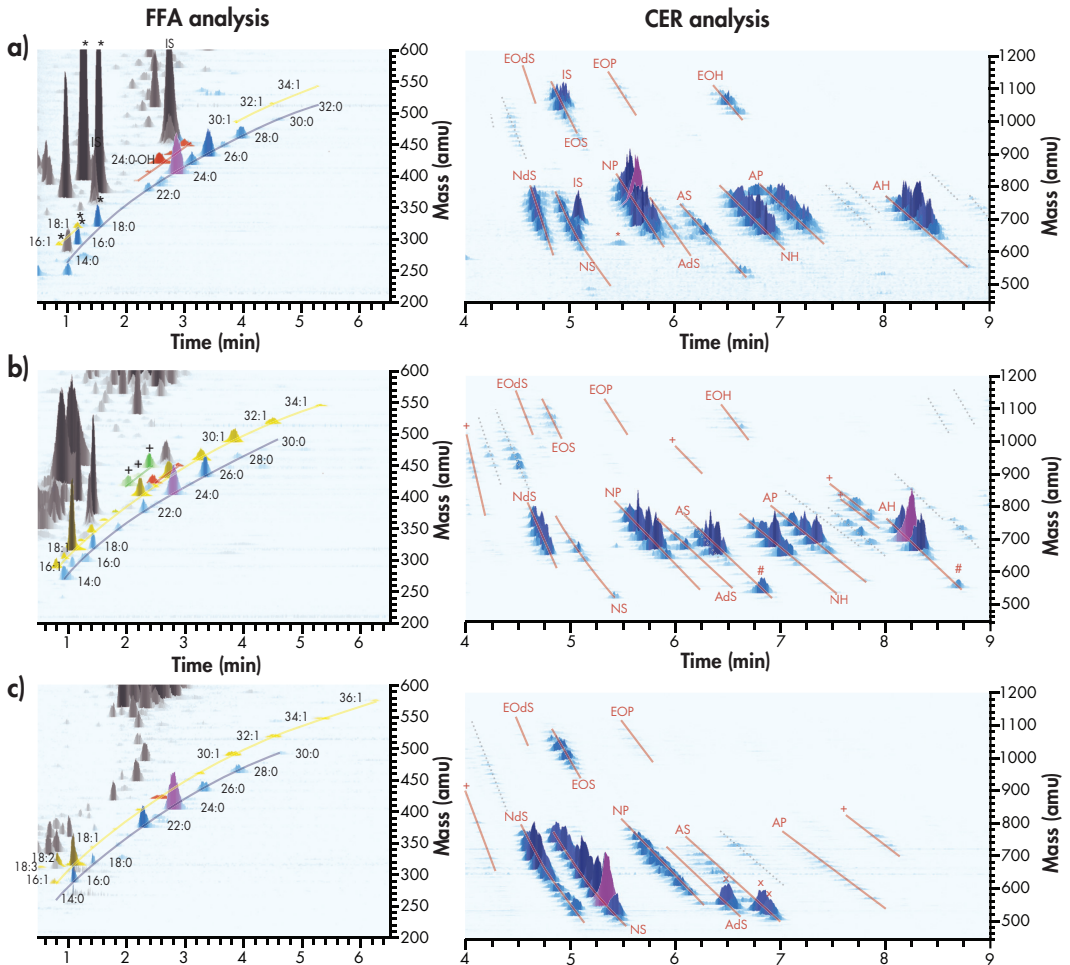


Figure 6: Representative, normalized 3D multi-mass chromatograms for both FFA analysis (left) and CER analysis (right) of **a)** Tape stripped SC; **b)** HSE SC; **c)** Porcine SC. Chromatograms are normalized to the peak marked in purple (the most abundant endogenous FFA or CER in their respective plots). Saturated, unsaturated and hydroxy-FFAs are marked in blue, yellow and red, respectively. Unidentified peaks or peaks belonging the CER lipid class are shown in gray. Ions shown in green and labeled '+' are unknown FFAs specific for the skin substitutes. * indicate contamination from tape strips. Internal standards are labeled 'IS'. # and × note the increased abundance of the very short CERs in HSE and porcine skin, respectively.

compared to *ex vivo* SC: It takes between 20-50 Nichiban PPS tape strips to fully remove the SC, thus 1 tape strip removes about 2-5% of the total SC amount (unpublished data, J. van Smeden 2010). Nevertheless, almost all FFAs and CERs are still detectable (Figure 6a and Table II) and show comparable lipid profiles: The CER profile closely resembles the *ex vivo* SC pattern, and all 12 subclasses and chain lengths are observed. Also the FFA profile shows great similarities to the *ex vivo* SC lipid profile, except for short chain FFAs

C16 and C18. The increased abundance of these particular FFAs by using tape stripping as sampling method, was caused by the presence of high levels of these FFAs in the tape itself (marked as *), as was confirmed by analysis of blank tape strips (not shown). This 'contamination' of lipids from tape is a very common problem, and of all investigated tapes, this Nichiban PPS tape showed the least amount of lipid content.

HSEs: There are many similarities between *ex vivo* SC (Figure 5 and Table II) and the HSEs (Figure 6b and Table II): All 12 CER classes are present and saturated, unsaturated and hydroxy-FFAs are observed. However, there are also some major differences: First of all, the FFA lipid profile (left picture Figure 6b) of HSEs shows the increased appearance of unsaturated FFAs, covering a broader range than present in human SC, ranging from C16:1 up to C38:1. Second, very few hydroxy-FFAs are observed (labeled in red). Third, the FFA chain length distribution is shifted to shorter chain length, as FFAs longer than C30:0 are reduced and short chain FFAs (C16:0, C16:1, C18:0 and C18:1) are increased. Fourth, there are multiple additional (unknown) lipids observed, of which the ones marked by a '+' are noteworthy to mention: These have a mass of 2 amu less than the slightly later eluting OH-FFAs. As there is an increase in monounsaturated FFAs (MUFAs) compared to *ex vivo* SC, it may be that these lipids are MUFA OH-FFAs. Indeed, the shorter retention times as well as the masses of these lipids may suggest the presence of MUFA OH-FFAs, although more studies are necessary to confirm this. At last, the 3D multi-mass chromatogram indicates a reduced presence of odd chain FFAs compared to *ex vivo* SC.

With respect to the CER profile (right picture in Figure 6b), additional unidentified subclasses are observed which are marked by '+'. There is a relative increase in the presence of hydrophilic lipids, in particular CER [AH] and some unidentified compounds that elute near CER [AH]. In addition, low mass CERS (marked by #) are increased which is in line with the FFA profile: as previously stated, a higher abundance of shorter chain length FFAs are observed in HSEs compared to *ex vivo* SC. Finally, CER [NP] and [NS] are largely reduced, which is in line with previous HPTLC research. The nature and possible biological causes for these differences are discussed in detail elsewhere by Thakoersing *et al.*⁶⁷, but it was concluded that biological pathways in which FFA elongation and desaturation are involved, may likely be altered.

Porcine skin: Regarding FFAs, almost no hydroxy-FFAs or odd chain length FFAs are observed (Figure 6c and Table II). For the CER profile, non-polar CERS (i.e. CER [Nds] and [NS]) are relatively much more abundant than the most hydrophilic CER subclasses compared to human SC. Some of these hydrophilic CERS are strongly reduced (i.e. CER [AP] and [EOP]) and some subclasses are fully absent (CER [AH], [NH] and [EOH]), which is in agreement to literature⁶⁸⁻⁷⁰. This is in contrast to the HSE profile, which shows increased

abundance of polar CERS. In addition, there is a shift to a shorter CER chain length, which can be observed from the drastic increase in CERS with a shorter chain length (mass <600 amu), in particular 3 extraordinary high peaks (marked by ×): CER [AdS] C₃₄ and both CER [AS] C₃₃ and C₃₄.

In summary, our results show that tape stripping is an appropriate method to be used for LC/MS analysis of *in vivo* SC lipids, and the obtained lipid profile closely resembles the lipid profile from full-thickness *ex vivo* SC. The skin substitutes show drastic changes in the FFA composition, which also affected the CER composition. HSEs show a lipid profile which is more comparable to human skin than porcine skin, in particular for the CER profile. This could be relevant for near-future studies, as animal testing for cosmetic purposes is banned throughout the European Union by 2013 and proper skin substitutes are necessary⁷¹. Although the HSEs do not fully mimic the lipid composition in human SC, changes in culture conditions may improve the lipid composition, as recently reported by Thakoersing *et al.*⁴¹

Conclusions

An LC/MS method was developed that is able to detect and quantify CHOL, CERS and FFAs using a single setup with two injections. This method is fast, allowing for high throughput analysis, and requires no derivatization steps. It is sensitive enough to analyze small sample amounts (i.e. tape stripping), but also permits analysis of samples with much higher sample concentration (e.g. *ex vivo* SC) due to its high linear dynamic range. Regarding the analysis of FFAs, this is – to the best of our knowledge – the first time that LC/MS enables the analysis of underivatized FFAs from SC. The addition of chloroform as an ionization agent resulted in the formation of [M+Cl]⁻ adducts which enabled analysis of saturated, unsaturated and hydroxy FFAs in SC with a wide chain length range (14-38 carbon atoms). The method proved to be robust, as can be deduced from the validation parameters. The method was successfully applied on human *ex vivo* SC, human SC obtained from tape stripping, and SC obtained from 2 human skin substitutes. In these skin substitutes, all 3 lipid classes are present, but its lipid profile differs substantially from that in human SC when analyzed in detail by LC/MS. In addition to the identified FFAs and CERS which were profiled for the different SC sources, many unknown lipids were observed as well. Upcoming studies will surely focus on the identification of these compounds. This LC/MS method can be used to obtain lipid profiles of numerous different SC samples. In particular lipidomics on skin diseases is currently of high interest, and future studies will exploit the detailed SC lipid analysis by LC/MS presented here.

Acknowledgements

This research is supported by the Dutch Technology Foundation STW, which is part of the Netherlands Organisation for Scientific Research (NWO), and which is partly funded by the Ministry of Economic Affairs. The authors thank STW partners Astellas Pharma Inc. and Unilever N.V. for (co)financing this project (No. 10064) as well as Evonik (Essen) for the provision of the synthetic CERS. The project was supported by the Netherlands Metabolomics Centre (NMC) which is part of the Netherlands Genomics Initiative/ Netherlands Organisation for Scientific Research and the European Cooperation in Science and Technology (COST). Finally, the authors would like to thank Hannah Scott and Edward Kaye for their technical assistance.

References

- 1 Wymann MP, Schneider R. Lipid signalling in disease. *Nat Rev Mol Cell Biol* 2008; 9: 162-76.
- 2 Taha TA, Mullen TD, Obeid LM. A house divided: ceramide, sphingosine, and sphingosine-1-phosphate in programmed cell death. *Biochim Biophys Acta* 2006; 1758: 2027-36.
- 3 Futerman AH, Hannun YA. The complex life of simple sphingolipids. *EMBO Rep* 2004; 5: 777-82.
- 4 Gurr MI, Harwood JL, Frayn KN. *Lipid biochemistry*, 5th edn. Malden, Mass.: Blackwell Science. 2002.
- 5 Hannun YA. Functions of ceramide in coordinating cellular responses to stress. *Science* 1996; 274: 1855-9.
- 6 Pettus BJ, Chalfant CE, Hannun YA. Ceramide in apoptosis: an overview and current perspectives. *Biochim Biophys Acta* 2002; 1585: 114-25.
- 7 Stryer L. *Biochemistry*, 4th edn. New York: W.H. Freeman. 1995.
- 8 Chamlin SL, Kao J, Frieden IJ *et al.* Ceramide-dominant barrier repair lipids alleviate childhood atopic dermatitis: changes in barrier function provide a sensitive indicator of disease activity. *J Am Acad Dermatol* 2002; 47: 198-208.
- 9 Proksch E, Folster-Holst R, Jensen JM. Skin barrier function, epidermal proliferation and differentiation in eczema. *J Dermatol Sci* 2006; 43: 159-69.
- 10 Elias PM, Crumrine D, Paller A *et al.* Pathogenesis of the cutaneous phenotype in inherited disorders of cholesterol metabolism: Therapeutic implications for topical treatment of these disorders. *Dermatoendocrinol* 2011; 3: 100-6.
- 11 Elias PM, Schmuth M. Abnormal skin barrier in the etiopathogenesis of atopic dermatitis. *Curr Opin Allergy Clin Immunol* 2009; 9: 437-46.
- 12 Jungersted JM, Helligren LI, Jemec GB *et al.* Lipids and skin barrier function—a clinical perspective. *Contact Dermatitis* 2008; 58: 255-62.
- 13 Imokawa G. Lipid abnormalities in atopic dermatitis. *J Am Acad Dermatol* 2001; 45: S29-32.
- 14 Elias PM, Goerke J, Friend DS. Mammalian epidermal barrier layer lipids: composition and influence on structure. *J Invest Dermatol* 1977; 69: 535-46.
- 15 Elias PM, Menon GK. Structural and lipid biochemical correlates of the epidermal permeability barrier. *Adv Lipid Res* 1991; 24: 1-26.
- 16 Holleran WM, Feingold KR, Man MQ *et al.* Regulation of epidermal sphingolipid synthesis by permeability barrier function. *J Lipid Res* 1991; 32: 1151-8.
- 17 Schurer NY, Elias PM. The biochemistry and function of stratum corneum lipids. *Adv Lipid Res* 1991; 24: 27-56.
- 18 Coderch L, Lopez O, de la Maza A *et al.* Ceramides and skin function. *Am J Clin Dermatol* 2003; 4: 107-29.
- 19 Downing DT, Stewart ME, Wertz PW *et al.* Skin lipids: an update. *J Invest Dermatol* 1987; 88: 28-68.
- 20 Elias PM. Lipids and the epidermal permeability barrier. *Arch Dermatol Res* 1981; 270: 95-117.
- 21 Elias PM. Epidermal lipids, barrier function, and desquamation. *J Invest Dermatol* 1983; 80: 448-98.
- 22 Elias PM, Friend DS. The permeability barrier in mammalian epidermis. *J Cell Biol* 1975; 65: 180-91.
- 23 Grubbauer G, Feingold KR, Harris RM *et al.* Lipid content and lipid type as determinants of the epidermal permeability barrier. *J Lipid Res* 1989; 30: 89-96.
- 24 Madison KC. Barrier function of the skin: "la raison d'etre" of the epidermis. *J Invest Dermatol* 2003; 121: 231-41.
- 25 Motta S, Monti M, Sesana S *et al.* Ceramide composition of the psoriatic scale. *Biochim Biophys Acta* 1993; 1182: 147-51.
- 26 Bouwstra JA, Gooris GS, Dubbelaar FE *et al.* Role of ceramide 1 in the molecular organization of the stratum corneum lipids. *J Lipid Res* 1998; 39: 186-96.
- 27 de Jager M, Gooris G, Ponec M *et al.* Acylceramide head group architecture affects lipid organization in synthetic ceramide mixtures. *J Invest Dermatol* 2004; 123: 911-6.
- 28 Di Nardo A, Wertz P, Giannetti A *et al.* Ceramide and cholesterol composition of the skin of patients with atopic dermatitis. *Acta Derm Venereol* 1998; 78: 27-30.
- 29 Norlen L, Nicander I, Lundh Rozell B *et al.* Inter- and intra-individual differences in human stratum corneum lipid content related to physical parameters of skin barrier function in vivo. *J Invest Dermatol* 1999; 112: 72-7.
- 30 Christie WW. *Lipid analysis: isolation, separation, identification and structural analysis of lipids*. Bridgewater: Oily Press [u.a.]. 2003.
- 31 Ponec M, Boelsma E, Weerheim A. Covalently bound lipids in reconstructed human epithelia. *Acta Derm Venereol* 2000; 80: 89-93.
- 32 Ponec M, Weerheim A, Lankhorst P *et al.* New acylceramide in native and reconstructed epidermis. *J Invest Dermatol* 2003; 120: 581-8.
- 33 Blau K, Halket JM. *Handbook of derivatives for chromatography*, 2nd edn. Chichester; New York: Wiley. 1993.
- 34 Gutnikov G. Fatty acid profiles of lipid samples. *J Chromatogr B Biomed Appl* 1995; 671: 71-89.
- 35 Kotani A, Kusu F, Takamura K. New electrochemical detection method in high-performance liquid chromatography for determining free fatty acids. *Analytica Chimica Acta* 2002; 465: 199-206.
- 36 Gaver RC, Sweeley CC. Methods for Methanolysis of Sphingolipids and Direct Determination of Long-Chain Bases by Gas Chromatography. *J Am Oil Chem Soc* 1965; 42: 294-8.
- 37 Murphy RC, Fiedler J, Hevko J. Analysis of nonvolatile lipids by mass spectrometry. *Chem Rev* 2001; 101: 479-526.
- 38 Raith K, Darius J, Neubert RH. Ceramide analysis utilizing gas chromatography-mass spectrometry. *J Chromatogr A* 2000; 876: 229-33.
- 39 van Smeden J, Hoppel L, van der Heijden R *et al.* LC/MS analysis of stratum corneum lipids: ceramide profiling and discovery. *J Lipid Res* 2011; 52: 1211-21.
- 40 Sugita M, Iwamori M, Evans J *et al.* High performance liquid chromatography of ceramides: application to analysis in human tissues and demonstration of ceramide excess in Farber's disease. *J Lipid Res* 1974; 15: 223-6.
- 41 Thakoersing VS, Gooris G, Mulder AA *et al.* Unravelling Barrier Properties of Three Different In-House Human Skin Equivalents. *Tissue Eng Part C Methods* 2012.

- 42 Nugroho AK, Li L, Dijkstra D *et al.* Transdermal iontophoresis of the dopamine agonist 5-OH-DPAT in human skin in vitro. *J Control Release* 2005; 103: 393-403.
- 43 Bligh EG, Dyer WJ. A rapid method of total lipid extraction and purification. *Can J Biochem Physiol* 1959; 37: 911-7.
- 44 Thakoersing VS, Ponec M, Bouwstra JA. Generation of human skin equivalents under submerged conditions-mimicking the in utero environment. *Tissue Eng Part A* 2010; 16: 1433-41.
- 45 Nagy K, Jakab A, Fekete J *et al.* An HPLC-MS approach for analysis of very long chain fatty acids and other apolar compounds on octadecyl-silica phase using partly miscible solvents. *Anal Chem* 2004; 76: 1935-41.
- 46 Williams J, Pandarinathan L, Wood J *et al.* Endocannabinoid metabolomics: a novel liquid chromatography-mass spectrometry reagent for fatty acid analysis. *AAPS J* 2006; 8: E655-60.
- 47 Masukawa Y, Narita H, Shimizu E *et al.* Characterization of overall ceramide species in human stratum corneum. *J Lipid Res* 2008; 49: 1466-76.
- 48 Farwanah H, Wohlrab J, Neubert RH *et al.* Profiling of human stratum corneum ceramides by means of normal phase LC/APCI-MS. *Anal Bioanal Chem* 2005; 383: 632-7.
- 49 Vekey K. Mass spectrometry and mass-selective detection in chromatography. *J Chromatogr A* 2001; 921: 227-36.
- 50 Zhao JJ, Yang AY, Rogers JD. Effects of liquid chromatography mobile phase buffer contents on the ionization and fragmentation of analytes in liquid chromatographic/ion spray tandem mass spectrometric determination. *J Mass Spectrom* 2002; 37: 421-33.
- 51 Bruins CHP, Jeronimus-Stratingh CM, Ensing K *et al.* On-line coupling of solid-phase extraction with mass spectrometry for the analysis of biological samples I. Determination of clenbuterol in urine. *Journal of Chromatography A* 1999; 863: 115-22.
- 52 Hoffmann Ed, Stroobant V. *Mass spectrometry: principles and applications*, 3rd edn. Chichester, West Sussex, England; Hoboken, NJ: J. Wiley. 2007.
- 53 Jessome LL, Volmer DA. Ion suppression: A major concern in mass spectrometry. *Lc Gc North America* 2006; 83-9.
- 54 Matuszewski BK, Constanzer ML, Chavez-Eng CM. Matrix effect in quantitative LC/MS/MS analyses of biological fluids: A method for determination of finasteride in human plasma at picogram per milliliter concentrations. *Analytical Chemistry* 1998; 70: 882-9.
- 55 Sommer U, Herscovitz H, Welty FK *et al.* LC-MS-based method for the qualitative and quantitative analysis of complex lipid mixtures. *J Lipid Res* 2006; 47: 804-14.
- 56 Cai SS, Hanold KA, Syage JA. Comparison of atmospheric pressure photoionization and atmospheric pressure chemical ionization for normal-phase LC/MS chiral analysis of pharmaceuticals. *Anal Chem* 2007; 79: 2491-8.
- 57 Vreeken RJ, Brinkman UAT, De Jong GJ *et al.* Chloroacetonitrile as eluent additive in thermospray liquid chromatography/negative ion mass spectrometry for the characterization of chlorinated organic pollutants. *Biological Mass Spectrometry* 1990; 19: 481-92.
- 58 Kato Y, Numajiri Y. Chloride attachment negative-ion mass spectra of sugars by combined liquid chromatography and atmospheric pressure chemical ionization mass spectrometry. *J Chromatogr* 1991; 562: 81-97.
- 59 Badjagbo K, Sauve S. High-throughput trace analysis of explosives in water by laser diode thermal desorption/atmospheric pressure chemical ionization-tandem mass spectrometry. *Anal Chem* 2012; 84: 5731-6.
- 60 Kanicky JR, Shah DO. Effect of degree, type, and position of unsaturation on the pKa of long-chain fatty acids. *J Colloid Interface Sci* 2002; 256: 201-7.
- 61 Norlen L, Nicander I, Lundsjo A *et al.* A new HPLC-based method for the quantitative analysis of inner stratum corneum lipids with special reference to the free fatty acid fraction. *Arch Dermatol Res* 1998; 290: 508-16.
- 62 Ansari MN, Nicolaides N, Fu HC. Fatty acid composition of the living layer and stratum corneum lipids of human sole skin epidermis. *Lipids* 1970; 5: 838-45.
- 63 Lampe MA, Burlingame AL, Whitney J *et al.* Human stratum corneum lipids: characterization and regional variations. *J Lipid Res* 1983; 24: 120-30.
- 64 Michael-Jubeli R, Bleton J, Baillet-Guffroy A. High-temperature gas chromatography-mass spectrometry for skin surface lipids profiling. *J Lipid Res* 2011; 52: 143-51.
- 65 Bonte F, Sauniois A, Pinguet P *et al.* Existence of a lipid gradient in the upper stratum corneum and its possible biological significance. *Arch Dermatol Res* 1997; 289: 78-82.
- 66 Masukawa Y, Narita H, Sato H *et al.* Comprehensive quantification of ceramide species in human stratum corneum. *J Lipid Res* 2009; 50: 1708-19.
- 67 Thakoersing VS, van Smeden J, Mulder AA *et al.* Increased Presence of Monounsaturated Fatty Acids in the Stratum Corneum of Human Skin Equivalents. *J Invest Dermatol* 2012.
- 68 Abraham W, Wertz PW, Downing DT. Linoleate-rich acylglucosylceramides of pig epidermis: structure determination by proton magnetic resonance. *J Lipid Res* 1985; 26: 761-6.
- 69 Law S, Wertz PW, Swartzendruber DC *et al.* Regional variation in content, composition and organization of porcine epithelial barrier lipids revealed by thin-layer chromatography and transmission electron microscopy. *Arch Oral Biol* 1995; 40: 1085-91.
- 70 Wertz PW, Downing DT. Ceramides of pig epidermis: structure determination. *J Lipid Res* 1983; 24: 759-65.
- 71 European Union. *Official journal of the European Union. Legislation 342. Regulation (EC) No 1223/2009*, English edition. edn., Vol. 52. Luxembourg: Office for official publications of the European Communities. 2009.

Supplementary Materials and Methods

Chemicals

HPLC grade (or higher) methanol (MeOH), n-heptane, isopropanol (IPA), acetonitrile (ACN), ethanol (EtOH) and acetic acid (HAc) were purchased from Biosolve (Valkenswaard, The Netherlands). HPLC grade chloroform (CHCl₃) was attained from Lab-Scan (Dublin, Ireland). Ultra purified water was prepared using a Purelab Ultra purification system (Elga Labwater, High Wycombe, UK). Potassium chloride was obtained from Merck (Darmstadt, Germany). 2-Hydroxydocosanoic (C_{22:0}-OH) and deuterated CHOL-D7 and were obtained from Larodan AB (Malmö, Sweden). Trypsin and trypsin inhibitor as well as CHOL, hexadecanoic (C_{16:0}), 9-hexadecenoic (C_{16:1}), octadecanoic (C_{18:0}), 9-octadecenoic (C_{18:1}), 9,12-octadecadienoic (C_{18:2}), eicosanoic (20:0), docosanoic (C_{22:0}), 13-docosenoic (C_{22:1}), tetracosanoic (C_{24:0}), 15-tetracosenoic (C_{24:1}) and octacosanoic (C_{28:0}) acids were obtained from Sigma-Aldrich GmbH (Steinheim, Germany). Deuterated octadecanoic (C_{18:0}-D₃₅) and deuterated tetracosanoic (C_{24:0}-D₄₇) acids were purchased from Cambridge Isotope Laboratories (Andover, MA, USA). Synthetic CER [N(24)DS(18)] was purchased from Avanti Polar Lipids (Alabaster, AL). All other synthetic CERs were kindly provided by Evonik (Essen, Germany): CER [EOS] (E(18:2)O(30)S(18)), CER [NS] (N(24)S(18)), CER [NP] (N(24)P(18)), CER [AS] (A(24)S(18)), CER [AP] (A(24)P(18)), CER [EOP] (E(18:2)O(30)P(18)), deuterated CER [E(18:2)O(30)S(18)]-D₃₁ and deuterated CER [N(24)S(18)]-D₄₇.

SC sample collection

Synthetic lipids as well as SC lipids from human *ex vivo* surgical skin were used to develop and validate the LC/MS method. To study the applicability of the developed method, 3 different sources were analyzed and compared to human *ex vivo* SC. The collection and processing of skin samples is in accordance to the Declaration of Helsinki. SC of healthy human volunteers was obtained by tape stripping using poly(phenylene sulfide) tape strips (Nichiban, Tokyo, Japan): 9 Tapes were successively applied on a single area (4½ cm²) of the ventral forearm, and afterwards peeled off with tweezers. Tape strips 1 to 5 were discarded to avoid contamination of superficial substances (e.g. sebum). Tapes 6 to 9 were punched to an area of 2 cm² and put separately in a glass vial containing 1 ml of lipid extraction solution chloroform/methanol/water (CHCl₃/MeOH/H₂O, 1:2:½, v/v); In addition to the tape-strip samples, 3 other epidermal skin sources were harvested: HSEs, human *ex vivo* skin and porcine skin. HSEs were cultured as described previously². Freshly excised *ex vivo* skin was obtained from surgeries performed at local hospitals and porcine skin was obtained from an accredited abattoir. Both skin samples were dermatomed to

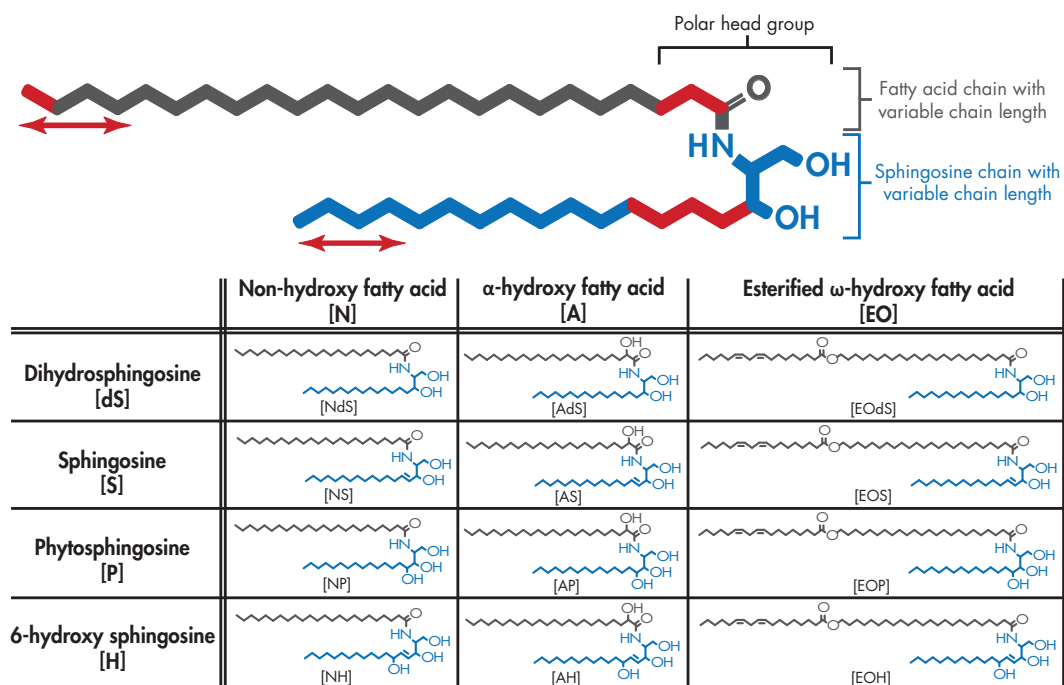
obtain an epidermal sheet with 0.6 mm thickness.

Successively, SC from all epidermal skin sources was isolated by trypsin digestion according to the procedure described in detail elsewhere³. Briefly, the skin was put in a Petri dish on Whatman filter soaked in a 0.1% trypsin in PBS solution pH 7.4 (8 g/L NaCl, 2.86 g/L Na₂HPO₄, 0.2 g/L KH₂PO₄, 0.19 g/L KCl) and stored overnight at 4°C. The skin was then incubated at 37°C for 1 hour and subsequently the SC layer was peeled off. The SC was washed once in 0.1% trypsin inhibitor in PBS solution, twice in demi water and stored in a dark, dry argon containing atmosphere to avoid lipid oxidation. To human SC samples, an internal standard solution was added containing equimolar concentrations of the deuterated lipids (FFA C18-D35, FFA C24-D47, CER [EOS]-D31, CER [NS]-D47).

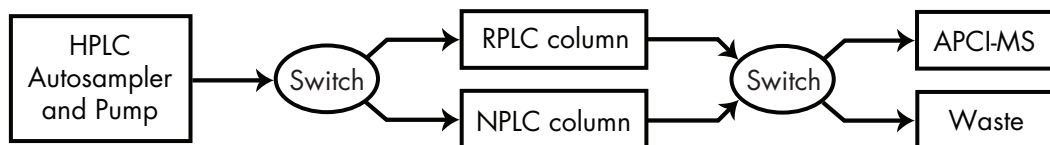
Lipid extraction

All sources of SC were then treated similarly according to the following procedure: Lipids were extracted according to an extended method of Bligh and Dyer⁴, described by Thakoersing *et al.*^{4,5}: Basically, a three step liquid-liquid extraction was performed using (sequentially) 3 different ratios of CHCl₃/MeOH/H₂O (1:2:½ ; 1:1:0 ; 2:1:0). The combined organic fractions were evaporated under N₂ gas at 40°C and reconstituted in heptane/CHCl₃/MeOH (95:2½:2½) to a final concentration of ~1.0 mg/ml (determined by weighing). This single solution was suitable for lipid analysis by both reverse phase chromatography (RPLC) regarding FFAs, and normal phase chromatography (NPLC) for analysis of CERs and CHOL. When sample storage was necessary, samples were stored under argon atmosphere, at -20°C in a dark environment.

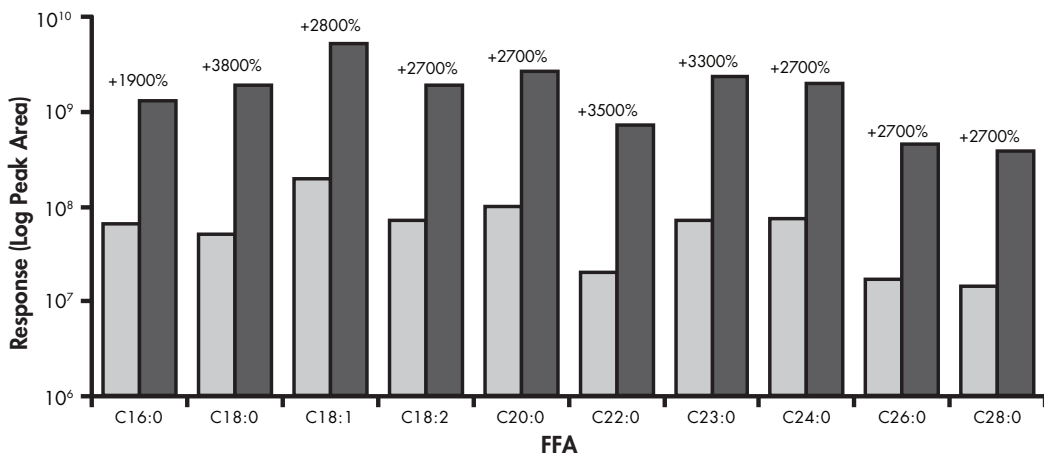
Supplementary Figures



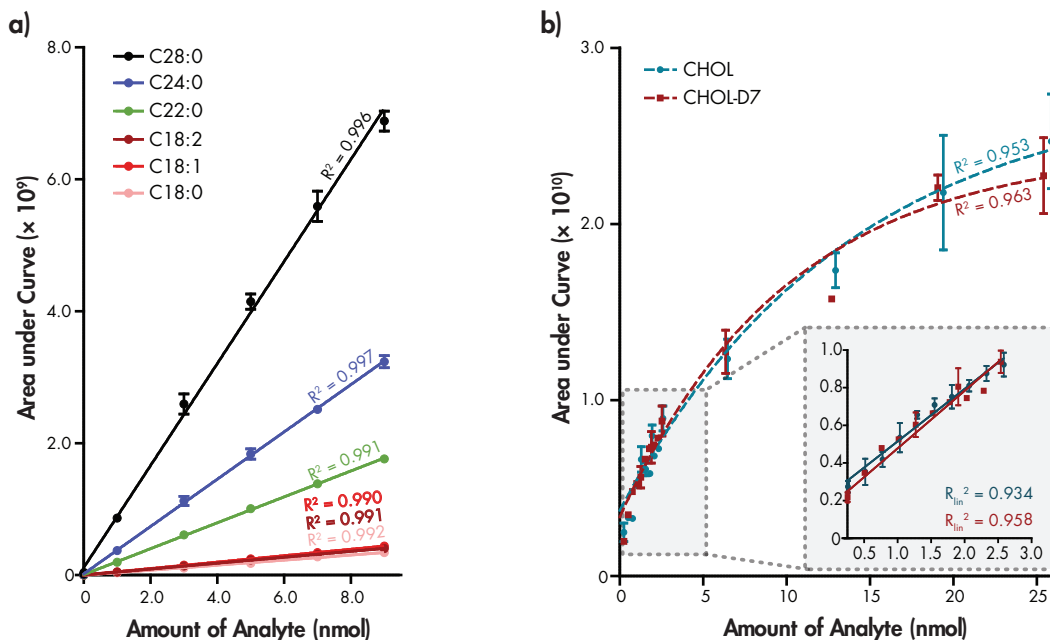
Supplementary Figure 1: Molecular structure of all CER subclasses and nomenclature according to Motta et al.⁶ All CERs bear a polar head group and two long carbon chains. Both chains may vary in molecular architecture (at the carbon positions marked in red) and each CER subclass is denoted by its sphingoid base (blue) and fatty acid chain (gray) resulting in the 12 CER subclasses in human SC. In addition, all CER subclasses show a varying carbon chain lengths (marked by red arrows). The number of total carbon atoms in the CERs is the number of carbon atoms in the fatty acid chain plus the number of carbon atoms in the sphingoid base.



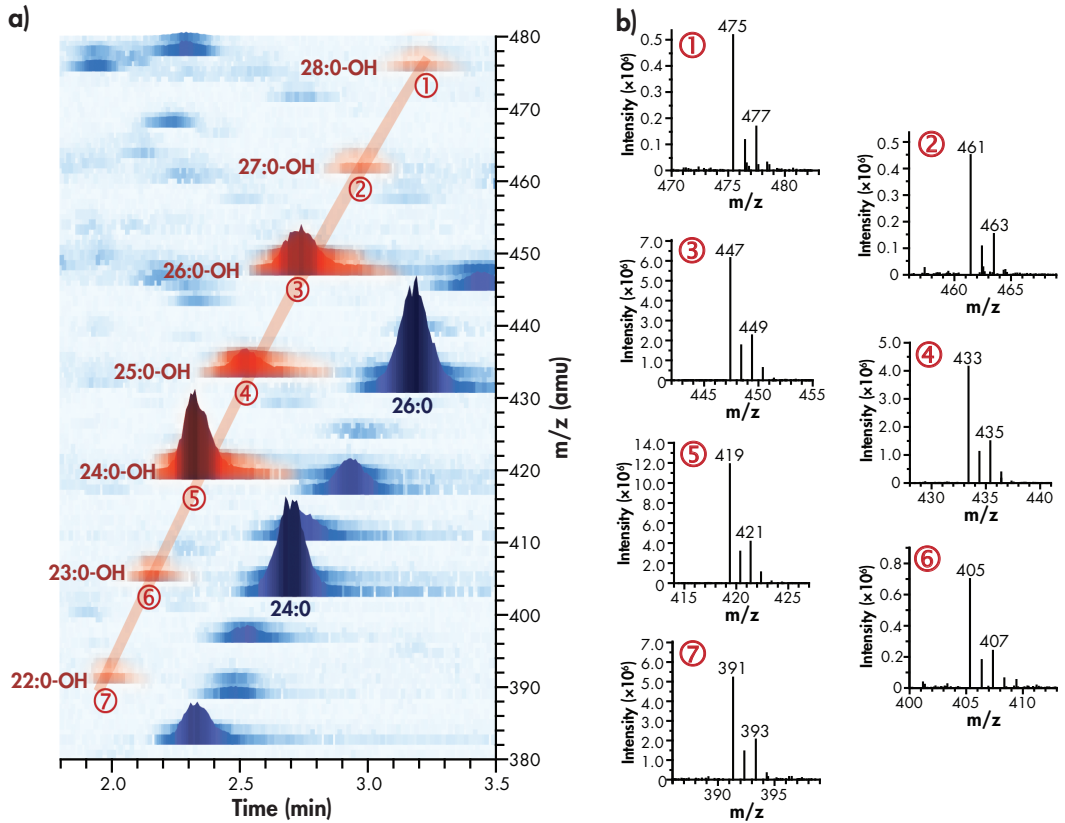
Supplementary Figure 2: Schematic setup of the LC/MS to analyze all 3 main lipid classes by either NPLC (CERs and CHOL) or RPLC (FFAs).



Supplementary Figure 3: Log-scaled bar plot of the response of various FFAs with and without post column addition of chloroform (20 $\mu\text{l}/\text{min}$), in dark blue and light blue, respectively. Numbers above the bars indicate the relative increase in peak area when chloroform is added, which is on average $\sim 2900\%$. Peak integration was performed on the main peaks, being the $[\text{M}+\text{Cl}]^-$ and $[\text{M}-\text{H}]^-$ for analysis with and without chloroform addition, respectively.



Supplementary Figure 4: Calibration curves of **a)** Synthetic FFAs and **b)** CHOL and deuterated CHOL (CHOL-D7). The inset shows a magnification from the range where a linear fit could be applied. Depicted R^2 values correspond to a linear fit, except for the full range CHOL and CHOL-D7 curves.



Supplementary Figure 5: **a)** 3D multi-mass chromatogram of the unknown lipid species marked in red and labeled 1-7, corresponding to the hypothesized OH-FFAs with a carbon chain length range between 22 and 28 carbon atoms. The individual mass spectra of each labeled peak is shown in **b)**, showing the main ion mass $[M+Cl]^+$ and its ^{37}Cl isotope peak at +2 amu of ~30% intensity.

Supplementary Tables

Supplementary Table I: Overview of chromatographic and mass spectrometric parameters used for analysis of FFAs, CERS and CHOL.

Parameter	FFA analysis*	CER + CHOL analysis ¹																																
Column type	Purospher Star LiChroCART 5 µm particle size, 55 × 2 mm i.d. Merck, Darmstadt, Germany	(PVA)-Sil 5 µm particle size, 100 × 2.1 mm i.d. YMC, Kyoto, Japan																																
LC-mode	RPLC	NPLC																																
Flow rate	500 (µl/min)	800 (µl/min)																																
Injection volume	10 (µl)	10 (µl)																																
Mobile phase ①	ACN/H ₂ O/CHCl ₃ /HAc (90/10/1/0.1)	Heptane																																
Mobile phase ②	MeOH/Heptane/CHCl ₃ /HAc (90/10/1/0.1)	Heptane/IPA/EtOH (50/25/25)																																
HPLC related parameters	<table border="1"> <thead> <tr> <th>Time (min)</th> <th>Mobile phase ratio (① : ②, %)</th> <th>Time (min)</th> <th>Mobile phase ratio (① : ②, %)**</th> </tr> </thead> <tbody> <tr> <td>0.0</td> <td>97:3</td> <td>0.0</td> <td>98:2</td> </tr> <tr> <td>0.5</td> <td>97:3</td> <td>2.5</td> <td>96:4</td> </tr> <tr> <td>1.5</td> <td>20:80</td> <td>2.6</td> <td>93:7</td> </tr> <tr> <td>3.5</td> <td>0:100</td> <td>6.0</td> <td>88:12</td> </tr> <tr> <td>6.5</td> <td>0:100</td> <td>11.0</td> <td>50:50</td> </tr> <tr> <td>9.5</td> <td>97:3</td> <td>12.5</td> <td>98:2</td> </tr> <tr> <td>13.0</td> <td>97:3</td> <td>19.0</td> <td>98:2</td> </tr> </tbody> </table>		Time (min)	Mobile phase ratio (① : ②, %)	Time (min)	Mobile phase ratio (① : ②, %)**	0.0	97:3	0.0	98:2	0.5	97:3	2.5	96:4	1.5	20:80	2.6	93:7	3.5	0:100	6.0	88:12	6.5	0:100	11.0	50:50	9.5	97:3	12.5	98:2	13.0	97:3	19.0	98:2
	Time (min)	Mobile phase ratio (① : ②, %)	Time (min)	Mobile phase ratio (① : ②, %)**																														
	0.0	97:3	0.0	98:2																														
	0.5	97:3	2.5	96:4																														
	1.5	20:80	2.6	93:7																														
	3.5	0:100	6.0	88:12																														
	6.5	0:100	11.0	50:50																														
	9.5	97:3	12.5	98:2																														
	13.0	97:3	19.0	98:2																														
System	Thermo Finnigan Surveyor Plus	Thermo Finnigan Surveyor Plus																																
Sample solvent	Heptane/CHCl ₃ /MeOH (95/2½/2½)	Heptane/CHCl ₃ /MeOH (95/2½/2½)																																
Sample tray temperature	21°C	21°C																																
MS related parameters	Vaporizer temperature	450°C	450°C																															
	Capillary temperature	250°C	250°C																															
	Capillary voltage	2 kV	3 kV																															
	Sheath gas, flow rate	Nitrogen, 0.8 L/min	Nitrogen, 0.6 L/min																															
	Auxiliary gas flow rate	Nitrogen, 3 L/min	Nitrogen, 2.4 L/min																															
	Discharge current	6 µA	6 µA																															
	Scan range	200 - 600 amu	360 - 1200 amu																															
	Ionization mode	APCI, negative	APCI, positive																															
	Resolution (FWHM)	0.7	0.7																															
	System	TS Quantum	TS Quantum																															

*: the final method is displayed here. An explanation of the choices made from the initial method to this final method is reported in the 'FFA method development' section. **: adaptations made to the method described previously¹.

Supplementary Table II: Basic parameters of CHOL and CER analysis. LOD and LOQ values are adapted from the previous report¹.

CERs/CHOL	Base peak (amu)	Rt (min)	k'	LOD (nM)	LOQ (nM)
E(18:2)O(30)S(18)	995.0	5.0	12.2	9	29
E(18:2)O(30)P(18)	1031.0	5.7	13.9	1	5
N(24)S(18)	632.6	5.2	12.7	13	45
N(24)dS(18)	652.7	4.9	11.9	6	21
N(24)P(18)	668.7	5.9	14.5	18	60
A(24)S(18)	648.6	6.4	15.7	28	94
A(24)P(18)	684.7	7.5	18.6	19	64
CHOL	369.4	1.87 ± 0.06	3.9	280	940
CHOLD7	376.4	1.93 ± 0.05	4.1	150	490

Supplementary Table III: Relative abundance of the 3 main ions observed (viz. [M-H]⁻, [M+Cl]⁻ and [M+HAc-H]⁻) when either 0% or 1% CHCl₃ (v/v) was added to the mobile phase, illustrated for 6 FFAs.

FFA chain length	Relative abundance (%) - No CHCl ₃ addition			Relative abundance (%) - 1% CHCl ₃ addition		
	[M-H] ⁻	[M+Cl] ⁻	[M+HAc-H] ⁻	[M-H] ⁻	[M+Cl] ⁻	[M+HAc-H] ⁻
C18:0	33 ± 12	52 ± 13	15 ± 1	<1	>99 ± 1	<1
C20:0	46 ± 12	37 ± 12	17 ± 1	<1	>99 ± 0	<1
C22:0	56 ± 9	26 ± 11	18 ± 3	<1	>99 ± 0	<1
C24:0	66 ± 9	18 ± 8	16 ± 1	<1	>99 ± 0	<1
C26:0	71 ± 9	14 ± 7	15 ± 2	<1	>99 ± 0	<1
C28:0	75 ± 6	9 ± 3	17 ± 4	<1	>99 ± 0	<1

Values are calculated by the AUC of each ion. Addition of CHCl₃ greatly favors the [M+Cl]⁻ adduct formation (≥99%), resulting in increased peak intensities (Supplementary Figure III).

Supplementary Reference

- van Smeden J, Hoppel L, van der Heijden R *et al.* LC/MS analysis of stratum corneum lipids: ceramide profiling and discovery. *J Lipid Res* 2011; 52: 1211-21.
- Thakoersing VS, Gooris G, Mulder AA *et al.* Unravelling Barrier Properties of Three Different In-House Human Skin Equivalents. *Tissue Eng Part C Methods* 2012.
- Nugroho AK, Li L, Dijkstra D *et al.* Transdermal iontophoresis of the dopamine agonist 5-OH-DPAT in human skin *in vitro*. *J Control Release* 2005; 103: 393-403.
- Bligh EG, Dyer WJ. A rapid method of total lipid extraction and purification. *Can J Biochem Physiol* 1959; 37: 911-7.
- Thakoersing VS, Ponc M, Bouwstra JA. Generation of human skin equivalents under submerged conditions-mimicking the *in utero* environment. *Tissue Eng Part A* 2010; 16: 1433-41.
- Motta S, Monti M, Sesana S *et al.* Ceramide composition of the psoriatic scale. *Biochim Biophys Acta* 1993; 1182: 147-51.



STRATUM CORNEUM LIPID
COMPOSITION IN ATOPIC
ECZEMA AND ITS ROLE IN THE
SKIN BARRIER FUNCTION

PART III

CHAPTER 5

LAMELLAR LIPID ORGANIZATION AND CERAMIDE COMPOSITION IN STRATUM CORNEUM OF PATIENTS WITH ATOPIC ECZEMA

J. van Smeden^{1*}, M. Janssens^{1*}, G.S. Gooris¹, W. Bras², G. Portales², P.J. Caspers³, R.J. Vreeken^{4,5}, S. Kezic⁶, A.P.M. Lavrijsen⁷ and J.A. Bouwstra¹

¹ Division of Drug Delivery Technology, Leiden Academic Centre for Drug Research, Leiden University, Leiden, The Netherlands

² Netherlands Organization for Scientific Research, DUBBLE CRG/ESRF, Grenoble, France

³ Center for Optical Diagnostics and Therapy, Department of Dermatology, Erasmus MC, Rotterdam, The Netherlands

⁴ Division of Analytical Biosciences, Leiden Academic Centre for Drug Research, Leiden University, Leiden, The Netherlands

⁵ Netherlands Metabolomics Centre, Leiden Academic Centre for Drug Research, Leiden University, Leiden, The Netherlands

⁶ Coronel Institute of Occupational Health, Academic Medical Center, University of Amsterdam, Amsterdam, The Netherlands

⁷ Department of Dermatology, Leiden University Medical Center, Leiden, The Netherlands

* Both authors contributed equally to this work

Adapted from Journal of Investigative Dermatology. 2011. 131:2136-2138.

The existence of an impaired skin barrier function in atopic eczema (AE, also referred to as atopic dermatitis) has been demonstrated previously, revealing the importance of the skin barrier in the pathophysiology of AE¹. Loss-of-function mutations in the filaggrin gene (*FLG*) are known to be major risk factors for developing AE². However, recent findings report a reduced skin barrier function irrespective of filaggrin genotype, suggesting the importance of additional factors for an impaired skin barrier in AE¹.

The skin barrier is primarily provided by the stratum corneum (SC), consisting of enucleated cells surrounded by lipid regions. SC lipids (primarily ceramides (CERs), cholesterol, and free fatty acids) form two lamellar phases: the short- and long periodicity phase (respectively SPP and LPP) with periodicities of ~6 nm and ~13 nm, respectively. These periodicities were determined by small angle X-ray diffraction (SAXD)³. Barrier properties of the skin may also depend on the lipid organization of the SC lipids and an altered lipid composition or organization may cause a reduced skin barrier in AE. Several studies have reported on the CER composition in AE patients^{4,5}. In the present study, the CER composition and lamellar lipid organization in the SC of AE skin have been simultaneously examined. For AE patients, we observe drastic changes in lipid organization which correlate with changes in CER composition, as compared with control subjects.

The study was conducted in accordance with the Declaration of Helsinki Principles and approved by the Ethical Committee of the Leiden University Medical Center. Subjects gave written informed consent. 6 Caucasian AE patients (23.3 ± 5.2 years; 2 males) and 6 Caucasian subjects without (history of) dermatological disorders (24.7 ± 7.6 years; 1 male)

were included. The subjects did not apply any dermatological products to their forearms for at least one week before the studies. To study the lipid properties irrespective of FLG mutations, we excluded subjects with any of the four most prevalent mutations found in European Caucasians: *2282del4*, *R501X*, *S3247X*, and *R2447X*, analyzed by genotyping⁶.

The lamellar lipid organization was studied using 4 mm biopsies harvested from the ventral forearm of non-lesional skin. The local severity of non-lesional AE skin was evaluated by local SCORing Atopic Dermatitis (SCORAD)⁷, and was 0 for all patients. SC was isolated by trypsin digestion⁸ and analyzed by SAXD using a microfocus beam (European Synchrotron Radiation Facility, Grenoble, France) similarly as described elsewhere⁹. The CER composition was examined in SC harvested by tape stripping non-lesional regions from the ventral forearm (PPS tape, Nichiban, Tokyo, Japan) close to the region of the biopsy. Tape strip numbers 6-9 were extracted, pooled and analyzed by liquid-chromatography (LC) (Alliance 2695, Waters Milford, MA) coupled to mass spectrometry (MS) (TSQ-Quantum, Thermo Finnigan, San Jose, CA)^{10,11}. The nomenclature of used

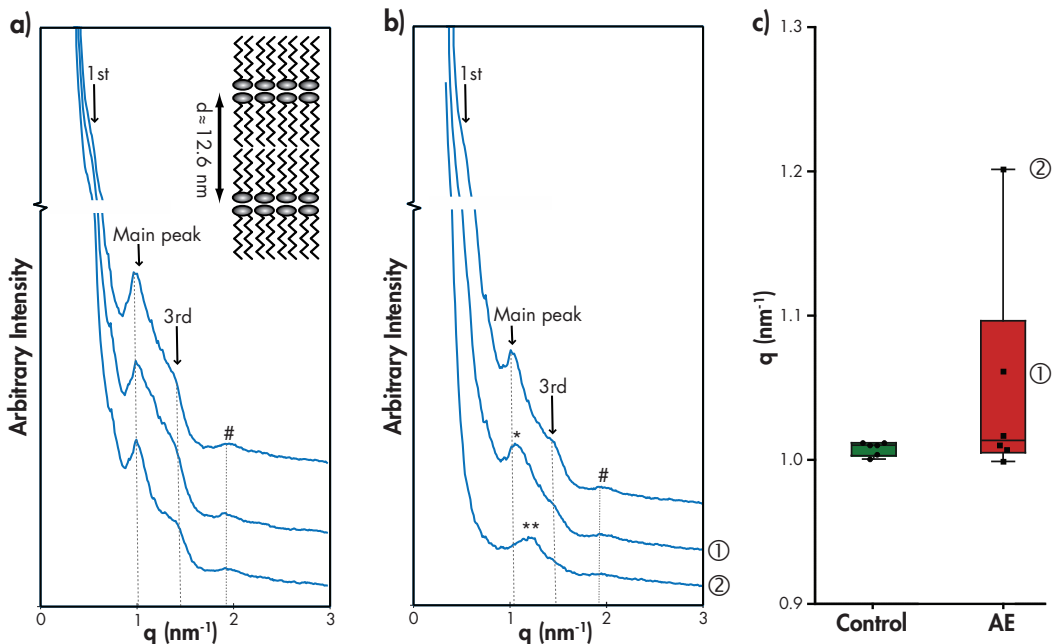


Figure 1: Diffraction patterns of **a)** control subjects, **b)** AE patients and **c)** boxplots showing the variance of the main peak position in both groups. The inset in the upper right corner of **a)** schematically represents the lipid organization and shows the periodicity of the LPP ($d \sim 12.6$ nm). 1 And 2 indicate patients with an altered SAXD profile (indicated by * and **). # Indicates phase separated cholesterol. From the positions of the peaks (q) the repeat distance of the LPP was calculated using the equation $d = n \cdot 2\pi/q_n$ (n = order of diffraction peak). The main peak is also caused by the 1st order diffraction peak of the SPP located at a slightly higher q -value than the 2nd order of the LPP.

CERs is described previously^{1,2}. Briefly, CERs contain a fatty acid chain (either an esterified ω -hydroxy (EO), α -hydroxy (A), or non-hydroxy (N) fatty acid) linked via an amide to a sphingosine chain (either a sphingosine (s), dihydrosphingosine (ds) phytosphingosine (P), or 6-hydroxysphingosine (H)), resulting in 12 CER subclasses.

Figure 1a shows three SC diffraction patterns representative for control subjects. The periodicity of the LPP was obtained from the peak positions³. All control subjects show three LPP peak positions (1st, 2nd and 3rd order) at scattering vector values (q) 0.50, 1.00 (main peak) and 1.45 nm⁻¹ respectively, corresponding to a periodicity of 12.6 nm. The 1st order peak of the SPP also contributes to the main peak, which is located at a slightly higher q -value. Figure 1b shows diffraction patterns of AE patients. The top diffraction pattern closely resembles those of control subjects and is representative for 4 patients. However, two patients (marked 1 and 2) show a different pattern: the central curve shows a shift in the main diffraction peak to a q -value of 1.06 nm⁻¹ (labeled *). The lower curve shows only a single reflection at $q = 1.20$ nm⁻¹ (labeled **). Increased q -values of the peak positions signify shorter periodicities of the lamellar phases in the SC of those patients. The boxplots (Figure 1c) show a small variance between the 6 control subjects, but a large variance within the group of patients.

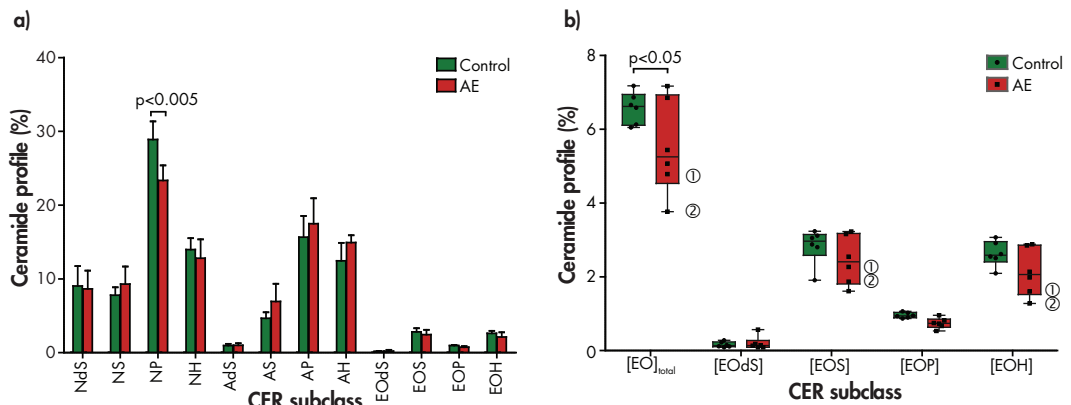


Figure 2: LC/MS analysis on human stratum corneum ceramides obtained from tape strips taken from the ventral forearm. To permit semi-quantitative analysis, two deuterated ceramides (CER [E(18:2)O(30)S(18)]) and CER [N(24)S(18)]) were used as internal standards. **a)** Bar graph of the relative ceramide abundance (in percentages) of every ceramide subclass of control subjects (black bars) and AE patients (grey bars) (mean \pm SD, $n=12$). An unpaired student's t -test showed a significant difference in CER [NP] content between control and AE subjects ($p < 0.005$). **b)** Boxplot of the relative ceramide abundance (in percentages) of the ceramide [EO] subclasses, as well showing the individual data points ($n=12$). White and grey boxes represent respectively control subjects and AE patients. ANOVA showed a significant difference in the total CER [EO] content ($[EOds] + [EOS] + [EOP] + [EOH]$): $p < 0.05$). Individual AE patients marked as 1 and 2 correspond to the same patients labeled in Figure 1.

Figure 2a shows the CER composition analyzed by LC/MS. All 12 CER subclasses were observed, including the newly identified CER [EODs]¹¹. The observed CER profile is very similar to that observed in previous studies using a fully quantitative method^{4,13}. AE skin showed a significant decrease in the abundance of CER [NP] content ($P < 0.005$, student's t-test) and in the content of long chain CERs (i.e. subclass [EO], Figure 2b, $p < 0.05$, two-way ANOVA), which is in accordance to recent findings⁴. The highest reduction in abundance of CER [EO]-subclasses was observed in patients showing an altered x-ray diffraction pattern: 1 and in particular 2 (Figures 1 and 2). Previous studies have shown that the LPP may be important for the skin barrier function¹⁴: isolated human CERs with a decreased CER [EO] level showed a strong reduction in formation of the LPP¹⁵. This variation in structure results in a more dominant influence of the 1st order SAXD peak of the SPP on the main SAXD peak, which explains the shift in peak position in the diffraction patterns of the two AE patients.

To our knowledge, our studies demonstrate for the first time that a change in CER composition can be associated with a change in the lamellar lipid organization in AE patients compared with control subjects. This association may lead to a better understanding of the altered SC lipid barrier in AE.

Acknowledgements

This research is supported by the Dutch Technology Foundation STW, which is part of the Netherlands Organisation for Scientific Research (NWO), and which is partly funded by the Ministry of Economic Affairs.

References

- 1 Jakasa I, Koster ES, Calkoen F *et al.* Skin barrier function in healthy subjects and patients with atopic dermatitis in relation to filaggrin loss-of-function mutations. *J Invest Dermatol* 2011; 131: 540-2.
- 2 Palmer CN, Irvine AD, Terron-Kwiatkowski A *et al.* Common loss-of-function variants of the epidermal barrier protein filaggrin are a major predisposing factor for atopic dermatitis. *Nature Genetics* 2006; 38: 441-6.
- 3 Bouwstra JA, Gooris GS, van der Spek JA *et al.* Structural investigations of human stratum corneum by small-angle X-ray scattering. *The Journal of investigative dermatology* 1991; 97: 1005-12.
- 4 Ishikawa J, Narita H, Kondo N *et al.* Changes in the ceramide profile of atopic dermatitis patients. *J Invest Dermatol* 2010; 130: 2511-4.
- 5 Jungersted JM, Scheer H, Mempel M *et al.* Stratum corneum lipids, skin barrier function and filaggrin mutations in patients with atopic eczema. *Allergy* 2010; 65: 911-8.
- 6 Sandilands A, Terron-Kwiatkowski A, Hull PR *et al.* Comprehensive analysis of the gene encoding filaggrin uncovers prevalent and rare mutations in ichthyosis vulgaris and atopic eczema. *Nature Genetics* 2007; 39: 650-4.
- 7 Stalder JF, Taieb A. Severity scoring of atopic dermatitis: the scorad index. Consensus Report of the European Task Force on Atopic Dermatitis. *Dermatology* 1993; 186: 23-31.
- 8 Tanojo H, Bouwstra JA, Junginger HE *et al.* In vitro human skin barrier modulation by fatty acids: Skin permeation and thermal analysis studies. *Pharmaceutical Research* 1997; 14: 42-9.
- 9 Bras W, Dolbnya IP, Detollenaere D *et al.* Recent experiments on a combined small-angle/wide-angle X-ray scattering beam line at the ESRF. *Journal of Applied Crystallography* 2003; 36: 791-4.
- 10 Thakoersing VS, Ponec M, Bouwstra JA. Generation of human skin equivalents under submerged conditions-mimicking the in utero environment. *Tissue Eng Part A* 2010; 16: 1433-41.
- 11 van Smeden J, Hoppel L, van der Heijden R *et al.* LC/MS analysis of stratum corneum lipids: ceramide profiling and discovery. *J Lipid Res* 2011; 52: 1211-21.
- 12 Motta S, Monti M, Sesana S *et al.* Ceramide composition of the psoriatic scale. *Biochim Biophys Acta* 1993; 1182: 147-51.
- 13 Masukawa Y, Narita H, Sato H *et al.* Comprehensive quantification of ceramide species in human stratum corneum. *J Lipid Res* 2009; 50: 1708-19.
- 14 de Jager MW, Gooris GS, Ponec M *et al.* Lipid mixtures prepared with well-defined synthetic ceramides closely mimic the unique stratum corneum lipid phase behavior. *J Lipid Res* 2005; 46: 2649-56.
- 15 Bouwstra JA, Gooris GS, Dubbelaar FE *et al.* Phase behavior of lipid mixtures based on human ceramides: coexistence of crystalline and liquid phases. *Journal of lipid research* 2001; 42: 1759-70.

CHAPTER 6

INCREASE IN SHORT-CHAIN CERAMIDES CORRELATES WITH AN ALTERED LIPID ORGANIZATION AND DECREASED BARRIER FUNCTION IN ATOPIC ECZEMA PATIENTS

Jeroen van Smeden^{1,*}, Michelle Janssens^{1,*}, Gert S. Gooris¹, Wim Bras², Giuseppe Portale², Peter J. Caspers^{3,4}, Rob J. Vreeken^{5,6}, Thomas Hankemeier^{5,6}, Sanja Kezic⁷, Ron Wolterbeek⁸, Adriana P.M. Lavrijsen⁹, and Joke A. Bouwstra¹

¹Division of Drug Delivery Technology, Leiden Academic Centre for Drug Research, Leiden University, Leiden, The Netherlands.

²Netherlands Organization for Scientific Research, DUBBLE CRG/ESRF, Grenoble, France.

³Center for Optical Diagnostics and Therapy, Department of Dermatology, Erasmus MC, Rotterdam, The Netherlands.

⁴River Diagnostics BV, Rotterdam, The Netherlands.

⁵Division of Analytical Biosciences, Leiden Academic Centre for Drug Research, Leiden University, Leiden, The Netherlands.

⁶Netherlands Metabolomics Centre, Leiden Academic Centre for Drug Research, Leiden University, Leiden, The Netherlands.

⁷Coronel Institute of Occupational Health, Academic Medical Center, University of Amsterdam, Amsterdam, The Netherlands.

⁸Department of Medical Statistics and Bioinformatics, Leiden University Medical Center, Leiden, The Netherlands.

⁹Department of Dermatology, Leiden University Medical Center, Leiden, The Netherlands.

*Both authors contributed equally to this work

Adapted from *Journal of Lipid Research*. 2012. 53:2755-2766.

Abstract

A hallmark of atopic eczema (AE) is skin barrier dysfunction. Lipids in the stratum corneum (SC), primarily ceramides, free fatty acids and cholesterol, are crucial for the barrier function, but their role in relation to AE is indistinct. Filaggrin is an epithelial barrier protein with a central role in the pathogenesis of AE. Nevertheless, the precise causes of AE-associated barrier dysfunction are largely unknown. In this study, a comprehensive analysis of ceramide composition and lipid organization in non-lesional SC of AE patients and control subjects was performed by means of mass spectrometry, infrared spectroscopy, and X-ray diffraction. In addition, the skin barrier and clinical state of the disease were examined. The level of ceramides with an extreme short chain length is drastically increased in SC of AE patients, which leads to an aberrant lipid organization and a decreased skin barrier function. Changes in SC lipid properties correlate with disease severity but are independent of filaggrin mutations. We demonstrate for the first time that changes in ceramide chain length and lipid organization are directly correlated with the skin barrier defects in non-lesional skin of AE patients. We envisage that these insights will provide a new therapeutic entry in therapy and prevention of AE.

Introduction

The skin offers a protective barrier against allergens, irritants, and microorganisms and prevents excessive transepidermal water loss (TEWL). The barrier function strongly relies on the outermost layer of the skin, the stratum corneum (SC), which consists of corneocytes embedded in a highly organized lipid matrix^{1,2}. This lipid matrix is

considered to be important for a proper skin barrier function.

Ceramides (CERs), cholesterol, and free fatty acids are the main lipid classes in SC. To date, 12 CER subclasses in human SC have been identified with a wide chain length distribution^{3,4}. An explanation of the CER nomenclature is given in Figure 1. The aim of the present study was to determine the chain lengths of each CER subclass in non-lesional skin of atopic eczema (AE) patients and to correlate these with lipid organization, skin barrier function and disease severity, see Figure 2.

AE is a chronic relapsing inflammatory skin disease characterized by a broad spectrum of clinical manifestations, such as erythema, dryness, and intense pruritus^{5,6}. AE affects over 15% of Caucasian children and 2-10% of adults, and its prevalence is increasing rapidly, especially in developed countries⁷⁻¹¹. Patients have a decreased skin barrier

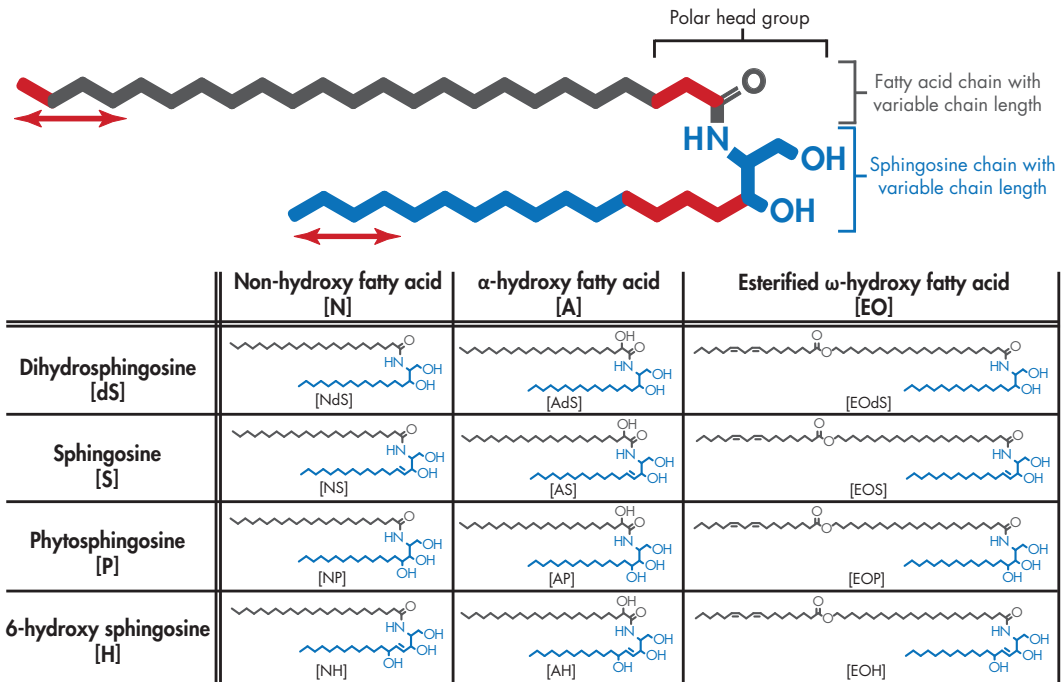


Figure 1: Structure and nomenclature of CERs. All CERs bear a polar head group and two long carbon chains. The polar head group may vary in molecular architecture (at the carbon positions marked in red), resulting in 12 different subclasses in human SC. Both chains in every CER subclass show varying carbon chain lengths (marked by red arrows). Each CER subclass is denoted by its sphingoid base (blue) and fatty acid chain (gray), resulting in the 12 CER subclasses. The abbreviations are as follows: For the sphingoid base: dihydrosphingosine (ds), sphingosine (s), phytosphingosine (p), 6-hydroxy sphingosine (h). The various acyl chains are denoted by: Non-hydroxy fatty acid (N), α -hydroxy fatty acid (A) and esterified ω -hydroxy fatty acid (EO). This results in the 12 CER subclass notations: [NdS], [AdS], [EOdS], [NS], [AS], [EOS], [NP], [AP], [EOP], [NH], [AH], [EOH]. The number of total carbon atoms in the CERs (e.g. C₃₄ CERs) is the number of carbon atoms in the fatty acid chain plus the number of carbon atoms in the sphingoid base.

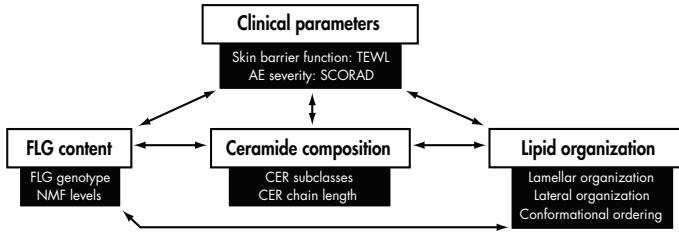


Figure 2: Schematic overview of the SC lipid parameters, clinical parameters, and the determinants of the filaggrin content discussed in this article. These different parameters may all affect the skin barrier and are therefore investigated in this study. Arrows indicate possible correlations that are studied throughout the manuscript.

function in lesional and non-lesional skin¹²⁻¹⁶.

In previous studies, it has been shown that AE is strongly associated with mutations in the filaggrin gene (*FLG*)¹⁷⁻¹⁹, but the role of *FLG* mutations for the barrier dysfunction is yet inconclusive²⁰⁻²⁵. Other factors, such as aberrations in the SC lipids, may play a role in the decreased skin barrier in AE^{12,26,27}. In healthy SC, lipids form two lamellar phases with repeat distances of approximately 6 and 13 nm. These are referred to as the short periodicity phase (SPP) and long periodicity phase (LPP), respectively^{28,29}. A schematic presentation of the lipid organization is provided in Figure 3. Within the lipid lamellae, the lipids have a dense (orthorhombic) lateral organization, although a subpopulation of the lipids can be less densely packed in a hexagonal organization³⁰⁻³².

CERs play a crucial role in the lipid organization³³, and they have a characteristic molecular architecture. Several studies have reported significant changes in CER subclasses in non-lesional SC of AE patients: reduced CER [NP], increased CER [AS], and reduced long chain CERs [EOH] and [EOS]^{12,23,34-36}. Some of these changes could be correlated with changes in skin barrier function. However, no information was reported on the effect of chain length distribution of CERs on the skin barrier until recently: Ishikawa *et al.* showed that lesional skin has a significantly increased level of short-chain CERs (with a total chain length of 34 carbon atoms) in one specific CER subclass, which correlates with the impaired skin barrier function³⁷. These results suggest that CER chain length may be an important factor in skin barrier dysfunction of AE patients. These findings were the starting point of the present study, in which we performed a detailed analysis on CER composition, focusing in particular on the CER chain length distribution in non-lesional SC of AE patients in relation to lipid organization and skin barrier dysfunction. We studied SC of non-lesional skin, as we aimed to monitor the changes in lipid properties in the absence of inflammation. We have identified several CER subclasses that exhibit an increased level of extremely short C₃₄ chains in AE, and we demonstrate that the overall level of C₃₄ is increased in AE. The changes in CER chain length distribution correlated with changes in lipid organization, skin barrier function, disease severity, and levels

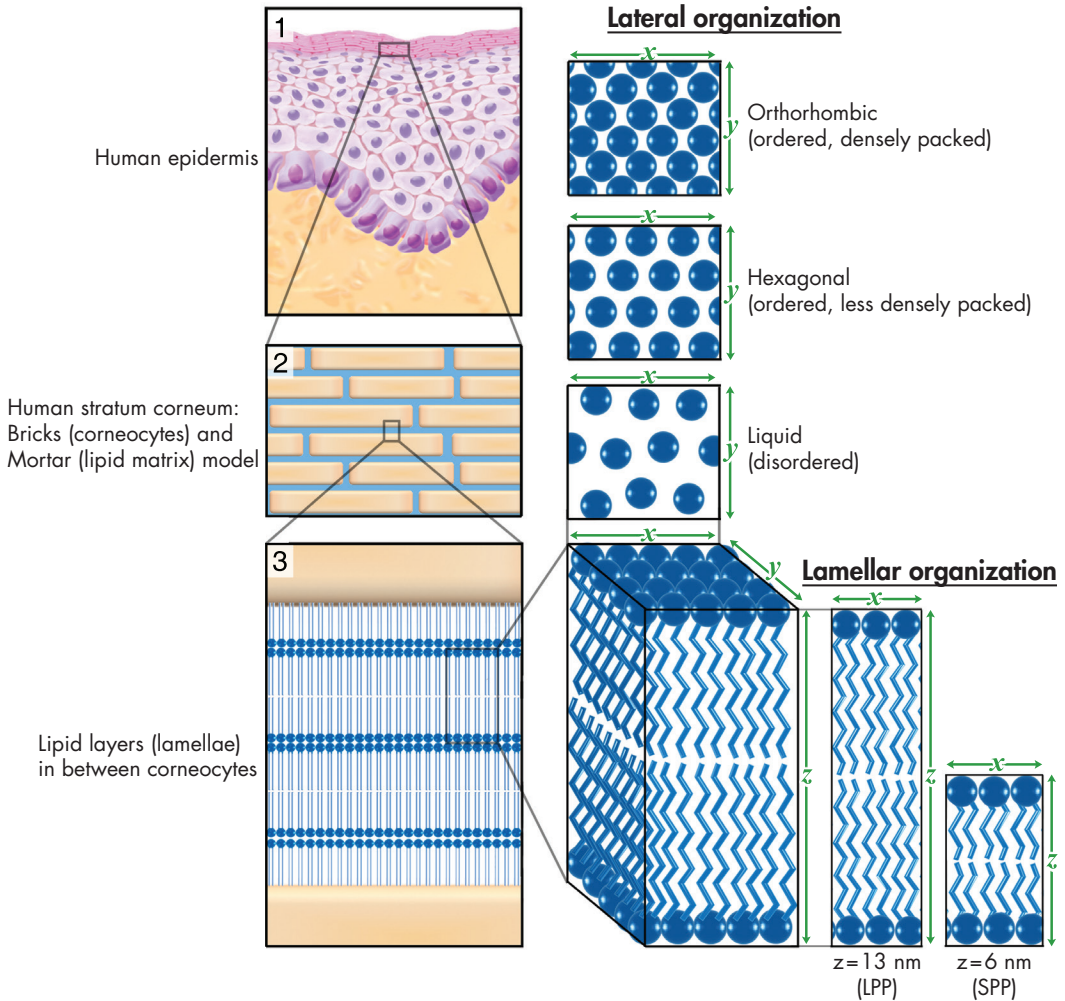


Figure 3: Lamellar and lateral organization in human stratum corneum. **a)** The outermost layer of the epidermis, the stratum corneum (SC), consists of dead cells (corneocytes) embedded in a lipid matrix, also referred to as the brick (corneocytes) and mortar (lipids) structure **b)**. The intercellular lipids are arranged in layers (lamellae) **c)**, with two coexisting lamellar phases. These lamellar phases have a repeat distance of 6 nm (referred to as the short periodicity phase (SPP)) or 13 nm (referred to as the long periodicity phase (LPP)). The lateral organization is the plane perpendicular to the direction of the lamellar organization. There are three possible arrangements of the lipids: a very dense, ordered, orthorhombic organization; a less dense, ordered, hexagonal organization; or a disordered, liquid organization.

of natural moisturizing factor (NMF, composed of filaggrin-derived amino acids, their metabolites, specific sugars, and salts). Changes in CER chain length distribution did not correlate with *FLG* genotype. These results demonstrate for the first time that CER chain length is an important factor in skin barrier dysfunction in non-lesional skin of AE.

Material and Methods

Study population and general study setup

The study was conducted in accordance with the Declaration of Helsinki Principles, and was approved by the Ethical Committee of the Leiden University Medical Center. All subjects gave written informed consent. 15 Caucasian subjects without (history of) dermatological disorders (25.0 ± 5.2 years; 5 males) and 28 Caucasian AE patients (25.6 ± 5.6 years; 11 males) were included. The group of AE patients consists of 14 patients with and 14 patients without the presence of common *FLG* genotype mutations (see *FLG* mutation analysis below). Subjects did not apply any dermatological products to their forearms for at least one week prior to the study. The study itself was performed in a temperature and humidity controlled room, and subjects were acclimatized for 45 min prior to the measurements. Per subject, all measurements were performed on a single day on one of the ventral forearms, which was observed by a dermatologist at the start of the study to carefully depict an area of non-lesional skin, which was marked accordingly. At this area, NMF levels were determined with Raman spectroscopy, followed by subsequent tape stripping, TEWL, and Fourier transform infrared spectroscopy (FTIR) measurements, as described below. At the end of the study day, buccal mucosa cells were collected with a cotton swab, and SCORing Atopic Dermatitis (SCORAD) was performed by a dermatologist to determine the severity of the disease. Finally, a 4 mm biopsy was harvested close to the area where all measurements were performed.

FLG mutation analysis

The influence of *FLG* mutations on lipid properties was studied. We screened all subjects on the four most prevalent mutations found in European Caucasians (*2282del4*, *R501X*, *S3247X* and *R2447X*), covering around 93% of all *FLG* mutations known to date³⁸. Buccal mucosa cells were collected by rubbing the inside of the cheeks with a cotton swab on a plastic stick after rinsing the mouth with water. Mutations were determined by genotyping after DNA extraction³⁹.

Skin barrier function assessment by TEWL

A Tewameter 210 (Courage+Khazaka, Köln, Germany) was used to measure TEWL on the marked area on the ventral forearm of the subject. The forearm was placed in an open chamber, and TEWL values were recorded for 2 minutes, after which an average reading during the last 10 seconds of the measurement was calculated. This procedure was performed before tape stripping (baseline TEWL) and after every two tape strips to have an indication of the amount of removed SC.

SCORAD

SCORAD was performed by the dermatologist to determine the severity of the disease⁴⁰.

Determination of NMF levels in SC

Confocal Raman microspectroscopy (3510 Skin Composition Analyzer, River Diagnostics, Rotterdam, The Netherlands) was used to measure NMF in the SC of the ventral forearm. The principles and experimental details of this method and the procedure have been described elsewhere^{41,42}. Depth profiles of Raman spectra were measured at 2 μm intervals from the skin surface to 20 μm below the skin surface. In each subject, 15 profiles were measured at different spots within the marked area on the ventral forearm. Raman spectra were recorded between 400 and 1800 cm^{-1} with a 785 nm laser. Laser power on the skin was 25 mW. NMF levels relative to keratin were determined from the Raman spectra measured between 4 and 8 μm by means of classical least-squares fitting. Relative NMF to keratin levels were calculated from the recorded Raman spectra by using SkinTools 2.0 (River Diagnostics, Rotterdam, The Netherlands).

Tape stripping procedure

To harvest SC lipids, the following tape stripping procedure was performed on both control subjects and non-lesional regions of AE patients: multiple poly(phenylene sulfide) tape strips (Nichiban, Tokyo, Japan) were successively applied at the same area (4.5 cm^2) on the ventral forearm. All tapes were pressed to the targeted skin with a pressure of 450 g/cm^2 using a D-Squame pressure instrument (Cuderm Corp., Dallas, TX). Tweezers were used to remove the tape in a fluent stroke, using alternating directions for each successive tape strip. The Squamescan 850A (Heiland Electronic, Wetzlar, Germany) was used to determine the amount of SC removed to obtain a good indication of the depth of each tape strip taken^{43,44}. Calibration was performed by a bicinchoninic acid (BCA) assay using bovine serum albumin (BSA). The predicted total amount of protein in the SC was calculated by plotting $1/\text{TEWL}$ against the cumulative amount of protein removed. The intercept with the x-axis is indicative for the total amount of protein in the SC according to Kalia *et al.*⁴³. Tapes 6 to 9 were selected for lipid composition analysis, as these tapes do not show surface contamination (observed when analyzing tape strips from the surface of the SC). All tapes were punched to a circular area of 2 cm^2 , put individually into glass vials containing 1 mL chloroform/methanol/water (1:2:½) and stored at -20°C under argon atmosphere prior to lipid extraction.

Lipid extraction and ceramide analysis by LC/MS

Lipid extraction was performed on 4 tape strips (numbers 6 to 9) of each subject. Before lipids were extracted from tape strips by liquid-liquid extraction, 2 deuterated internal ceramide standards (CER [NS] C₂₄ and, CER [EOS] C₃₀ linoleate) were added to compare CER levels between control group and non-lesional skin of AE patients. Then, a slightly enhanced extraction procedure of the commonly used Bligh and Dyer method was performed on all 4 selected tape strips individually: 3 different ratios of solvent mixtures chloroform/methanol/water (1:2:½; 1:1:0; 2:1:0) were used sequentially to extract all lipids. A detailed procedure is described elsewhere^{45,46}. Afterwards, lipid extracts from all 4 individual tapes were pooled, dried under N₂ gas and reconstituted in 100 µl chloroform/methanol/heptane (2½:2½:95) to obtain a total lipid concentration around 1.0 mg/mL. Samples were stored at -20°C until use. The analysis was performed by LC/MS using a recently developed LC/MS method described in detail elsewhere⁴. Briefly, 10 µl of each lipid sample was automatically injected and separated onto an analytical normal phase column (PVA-bonded column; 100 × 2.1 mm i.d., 5 µm particle size, YMC (Kyoto, Japan)) by a gradient solvent system from heptane to heptane/IPA/ethanol at a flow rate of 0.8 mL/min using an Alliance 2695 HPLC system (Waters Milford, MA). The HPLC was coupled to a mass spectrometer (TSQ Quantum, Thermo Finnigan, San Jose, CA) in atmospheric pressure chemical ionization (APCI), positive scan mode with a scan range set at 360-1200 amu. The temperature of the source heater and heated capillary were set to 450°C and 250°C, respectively, and the discharge current was set to 5 µA. The ceramide analysis was performed using Xcalibur software version 2.0, and its nomenclature used throughout this article is according to Motta *et al.*⁴⁷ in which ceramide subclasses are classified by letter abbreviations according to their two individual chains: the sphingoid base (either dihydrosphingosine (ds), sphingosine (s), 6-hydroxy sphingosine (H) or phyto-sphingosine (P)), chemically linked to the fatty acid chain (either an α-hydroxy fatty acid (A), an esterified ω-hydroxy fatty acid (EO) or a non-hydroxy fatty acid (N)). This results in 12 different CER subclasses, namely [AdS], [AS], [AH], [AP], [EODs], [EOS], [EOH], [EOP], [NDS], [NS], [NH], and [NP]. The CER nomenclature and its molecular structure are explained in Figure 1.

Lateral organization and conformational ordering of the lipids

To obtain information on the lateral organization and conformational ordering of the lipids, FTIR spectra were recorded in the same skin region also used for lipid analysis. FTIR spectra of the SC were collected after each 2 tape strips using a Varian 670-IR spectrometer (Varian Inc., Santa Clara, CA) equipped with a broad band mercury-

cadmium-telluride (MCT) detector and an external sample compartment containing a GladiATR (Pike, Madison, WI) attenuated total reflection (ATR) accessory with a single reflection diamond. The spectral resolution was 2 cm^{-1} . The instrument was continuously purged with dry N_2 . Each spectrum was an average of 150 scans. For data treatment the instrument software Resolutions Pro 4.1 (Varian Inc.) was used. We calculated positions of the CH_2 symmetric stretching vibration and second derivatives of the scissoring bandwidth as described previously^{48,49}. Shortly, the second derivative was calculated and it was baseline-corrected between the endpoints of the scissoring region ($\sim 1460\text{--}1480\text{ cm}^{-1}$). We calculated the bandwidth at 50% of the peak height (full width half maximum, FWHM) and determined CH_2 symmetric stretching vibration positions of spectra recorded between the removal of 2 to 10 tape strips.

Biopsy and small angle X-ray diffraction measurements

After tape stripping, 4 mm biopsies were taken from the ventral forearm close to the region of the tape stripping. SC was isolated by trypsin digestion as described earlier⁵⁰. This procedure does not affect the lipid organization in SC⁵¹. The SC sheets were measured by small angle X-ray diffraction (SAXD) performed at the European Synchrotron Radiation Facility (ESRF, Grenoble, France) using station BM26B. Prior to the measurements, SC was hydrated over a 27% NaBr solution during 24h. To obtain high quality diffraction patterns SC was carefully oriented parallel to the primary X-ray beam. SAXD patterns were detected with a Frelon 2000 charge-coupled device (CCD) detector at room temperature for a period of 10 minutes using a microfocus beam, similarly as described elsewhere⁵². Samples were checked for evidence of radiation damage, and exposure time to X-rays was kept to a minimum. From the scattering angle, the scattering vector (q) was calculated by $q = 4\pi \sin \theta / \lambda$, in which λ is the wavelength of the X-rays at the sample position and θ the scattering angle.

Statistical analysis

Statistical analysis was performed using SPSS Statistics. Non-parametric Mann-Whitney tests were performed when comparing 2 groups and stated significant when $P < 0.05$. When the effect of *FLG* was taken into account and trends were observed, Kruskal-Wallis tests, and eventually, additional Mann-Whitney tests were performed. Bivariate analysis was performed to analyze which parameters showed a significant correlation, and their respective Spearman's ρ correlation coefficients were calculated. Univariate general linear model analysis was performed to correlate the biologically and clinically relevant parameters to 2 independent lipid parameters, as well as to the predicted and the observed average chain length.

Results

Description of study population

Fourteen out of 28 AE patients were carriers of at least one of the four most common *FLG* mutations (details in Supplementary Table I). Patient and control subject characteristics are provided in Supplementary Table II. Two control subjects were heterozygous for *FLG* mutations. Severity of the disease was scored by an experienced dermatologist using SCORAD (Figure 4a). AE patients showed an elevated TEWL in non-lesional skin compared with control subjects (12.2 ± 6.5 g/m²/h and 6.5 ± 1.7 g/m²/h, respectively; $P < 0.0005$, Figure 4b) and lower NMF levels compared with control subjects (0.66 ± 0.39 and 1.05 ± 0.20 , respectively; $P < 0.01$, Figure 4c).

Reduced CER chain length correlates with a decreased barrier function

From the LC/MS data, lipid profiles were constructed and examples are shown in Supplementary Figure 1. From manual integration of these lipid profiles, the relative abundance of all CER subclasses could be calculated (Supplementary Figure 2). Statistical differences between control subjects and AE patients were observed in 7 subclasses: CERS [EOP], [EOH], [NS], [NP], [NH], [AS] and [AH] ($P < 0.05$). No difference was observed between carriers and non-carriers of *FLG* mutations. The total CER level in the control group and in non-lesional skin of AE patients was not significantly different 37.0 ± 3.6 and $38.5.4 \pm 2.4$ ng/ μ g protein, respectively ($P > 0.1$).

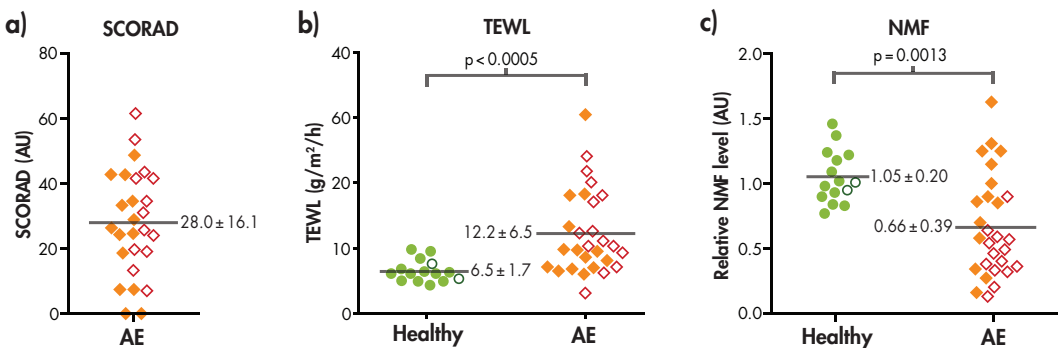


Figure 4: SCORAD, TEWL and NMF levels in control subjects and AE patients. Dot plots showing individual control subjects (○ and ●) and AE patients (◇ and ◆) of the measured parameters (a) SCORAD, (b) TEWL and (c) NMF levels. Open and filled data points indicate carriers and non-carriers of *FLG* mutations, respectively. Means are indicated by gray horizontal lines and their corresponding values (\pm SD). Significant differences were observed between control subjects and AE patients for both TEWL and NMF. *FLG* mutations were associated with reduced NMF levels in AE patients ($P < 0.005$) but not with SCORAD and TEWL.

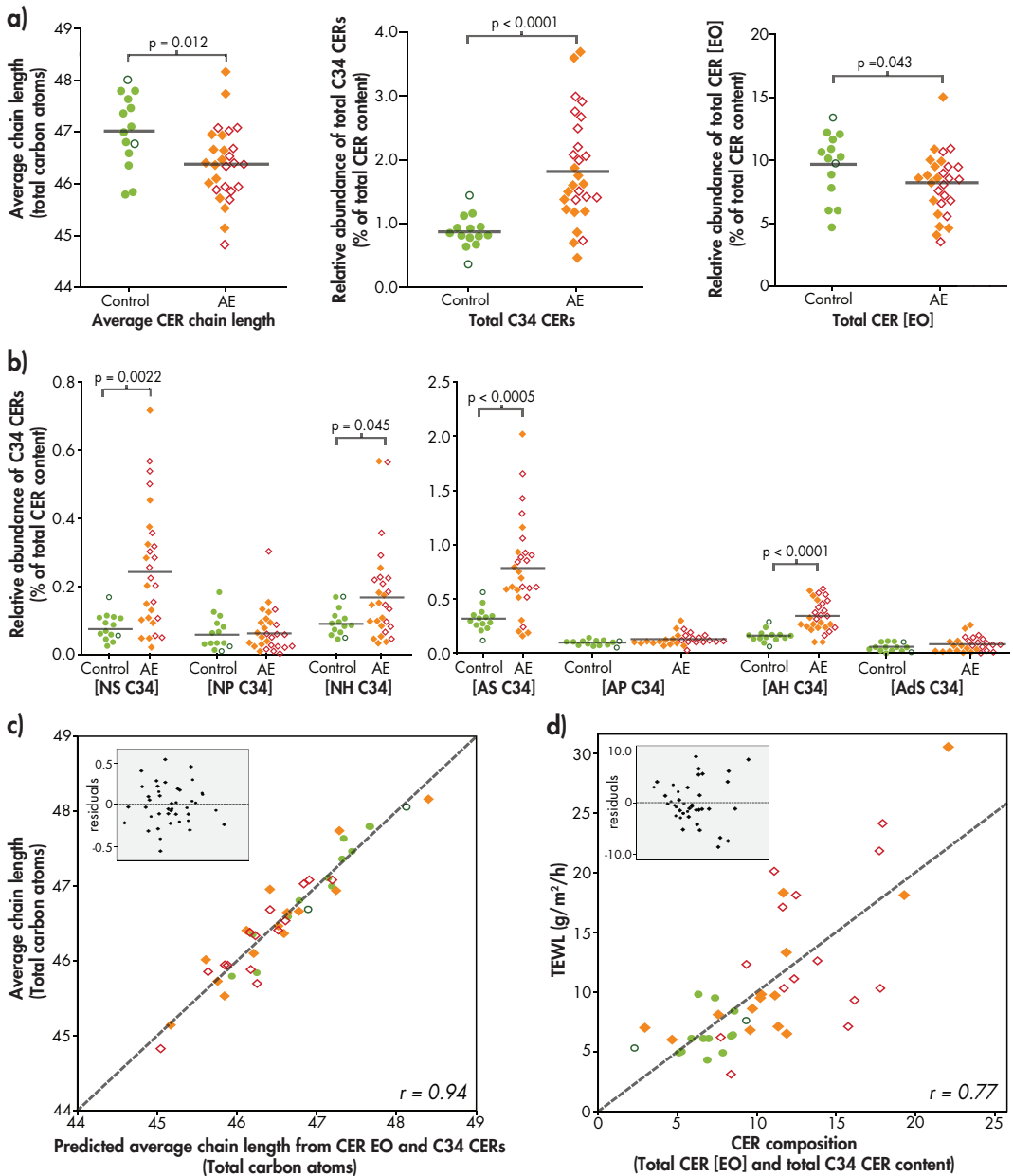


Figure 5: CER composition in control subjects and AE patients. **a)** Dot plot showing the average chain length of all CERs in total; the relative abundance of total C34 CERs; and the relative abundance of total [EO] CERs. **b)** Dot plots indicating the relative abundance of C34 CER species for each subclass. **c)** Scatter plot of univariate analysis of the predicted average chain length (by the abundance of C34 CERs and [EO] CERs) versus the observed average chain length. Gray dotted lines represents the optimal fit ($r=0.94$). **d)** Scatter plot of univariate analysis of C34 CER and CER [EO] versus the TEWL. Insets show the residuals of the respective plots. Gray dotted lines represents the optimal fit ($r=0.77$). Control subjects are indicated by \circ and \bullet . AE patients with are indicated by \diamond and \blacklozenge . Open and filled data points indicate carriers and non-carriers of FLG mutations, respectively.

The average CER chain length was significantly decreased by 0.64 ± 0.23 total carbon atoms in AE patients (mean \pm SEM; $P=0.012$, Figure 5a). No difference was observed between carriers and non-carriers of *FLG* mutations ($P>0.1$). Figure 5a shows that in non-lesional skin of AE patients, extremely short C₃₄ CERs were increased within several CER subclasses. This was primarily observed in CER subclasses [AS], [AH], [NS] and [NH] (Figure 5b, $P<0.05$). The increase in total C₃₄ CERs in AE ($P<0.0001$) contributes to a reduction in overall chain length. In addition, the very long chain CERs belonging to the [EO] subclass are significantly reduced, which is primarily caused by significantly decreased levels of CER [EOH] and [EOP] ($P=0.019$ and $P=0.040$, respectively, Figure 5a and Supplementary Figure 2b). Univariate analysis shows that an increased level of C₃₄ CERs and decreased level of CERs [EO] largely contribute to a reduction in average CER chain length, as can be observed from Figure 5c. The influence of *FLG* mutations on any of the CER chain length parameters was not significant ($P>0.1$; detailed overview in Supplementary Tables III-V).

The observed changes in CER chain length were compared with changes in barrier function as assessed by TEWL. The results in Figure 5d show a strong correlation between TEWL and the levels of C₃₄ CERs and CER [EO]: univariate analysis of TEWL versus the total C₃₄ CERs and total CER [EO] levels shows a correlation coefficient of 0.77 ($P<0.0001$). Correlations between the relative abundances of the various CER subclasses with TEWL are shown in Table I. CER [EOH] and CER [AS] are the two subclasses which are most significantly associated with TEWL. This again indicates the importance of the chain length for the skin barrier in AE: the exceptional long CER [EOH] is decreased, whereas CER [AS] (the CER subclass with the highest abundance of exceptionally short C₃₄ CERs) is increased. The changes in CER composition are irrespective of *FLG* mutation status ($P=0.58$).

CER subclass	TEWL
CER [EOdS]	-0.245
CER [EOS]	-0.177
CER [EOP]	-0.434**
CER [EOH]	-0.617***
CER [NdS]	-0.226
CER [NS]	0.407**
CER [NP]	-0.483**
CER [NH]	-0.420**
CER [AdS]	0.214
CER [AS]	0.650***
CER [AP]	0.255
CER [AH]	0.195
Total CER [EO]	-0.441**
Total C₃₄ CERs	0.738***
Average CER chain length	0.528***

Table I: Correlation coefficients of the various CER subclasses versus TEWL. The table contains all 12 CER subclasses as well as the CERs that strongly influence the chain length (i.e. total CER [EO] and total C₃₄ CERs).

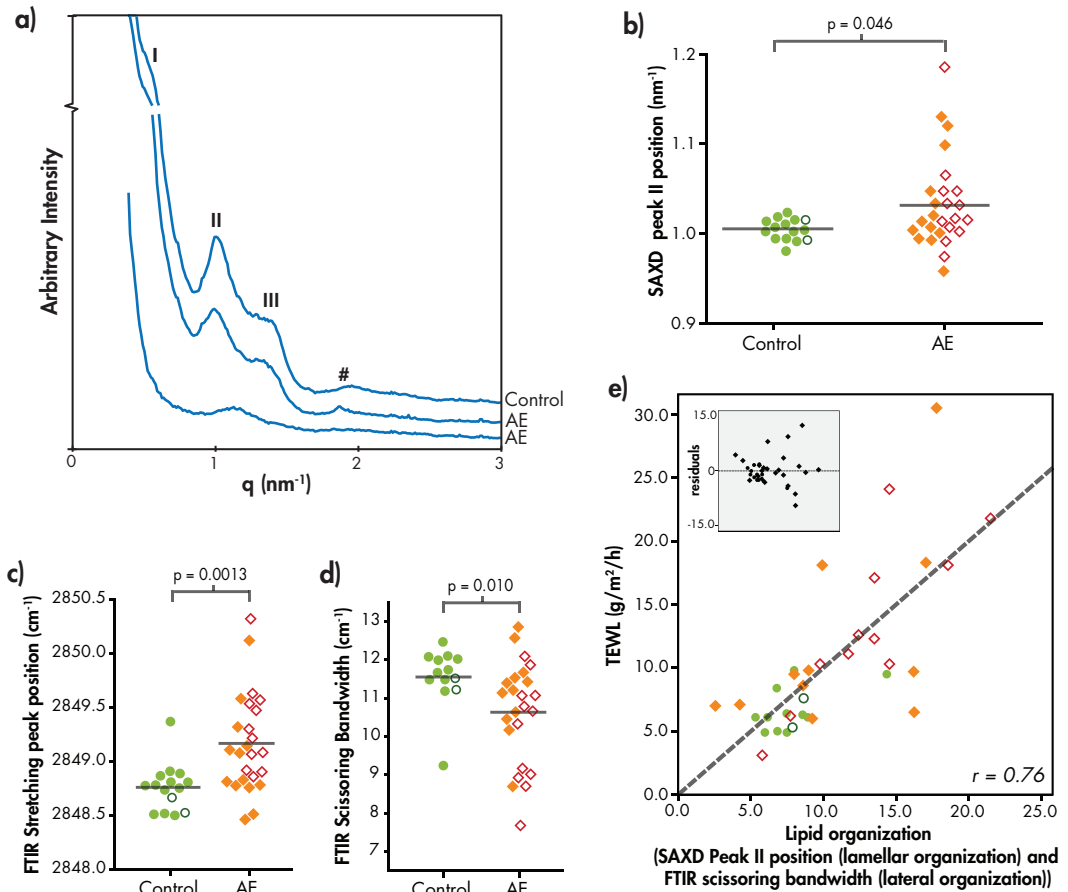


Figure 6: Lipid organization in control subjects and AE patients. **a)** The upper SAXD curve of a control subject shows the 1st (I), 2nd (II) and 3rd (III) order peak positions of the LPP. # indicates phase separated cholesterol. The middle diffraction curve is from an AE patient and resembles the pattern of SC of the control subject. The bottom curve of an AE patient shows only the presence of peak II. **b)** Position of peak II in SAXD curves. **c)** Position of the stretching vibrations in the FTIR spectrum. **d)** Scissoring bandwidth in the FTIR spectrum. **e)** Correlation between lipid organization and TEWL. Scatter plot of univariate analysis of SAXD peak II position + bandwidth of scissoring vibrations versus the TEWL. The inset shows the residuals of this plot. The gray dotted line represents the optimal fit ($r=0.76$). Control subjects are indicated by \circ and \bullet . AE patients with are indicated by \diamond and \blacklozenge . Open and filled data points indicate carriers and non-carriers of FLG mutations, respectively.

Altered lamellar and lateral lipid organization correlates with a decreased barrier function

SAXD gives information about the lamellar organization of intercellular lipids in SC²⁸ (explanation in Supplementary Figure 3). The lipids form two lamellar phases, the SPP and LPP. Figure 6a shows three examples of SAXD curves from SC. The upper curve is a typical example of a control subject. The central curve is typical for AE. The bottom curve

is representative for a subgroup of AE patients with an aberrant SAXD profile. The upper two curves show lipid-based features as two weak diffraction peaks (labeled I and III) and a strong peak (labeled II). The LPP contributes to all three peaks, whereas the SPP contributes only to peak II (Supplementary Figure 3). In the bottom curve, both peaks I and III are absent, and peak II is shifted to higher q -values. Peaks I and III were not present in 5 out of 28 patients. As peak I and peak III are attributed to the LPP, this indicates that there is a drastic reduction in the presence of the LPP in those patients.

Figure 6b shows the position of the strong peak (II) in the SAXD curves from control subjects (left) and AE patients (right). The peak position shows a larger variance within the group of AE patients compared with the group of control subjects. The average position of the strong peak is located at significantly higher q -values for AE patients compared with control subjects (1.03 nm^{-1} and 1.00 nm^{-1} , respectively, $P=0.046$). The position of peak II showed no difference between AE patients with and patients without *FLG* mutations ($P=0.76$).

FTIR was used to obtain information on the lateral lipid organization. Two types of vibrations were monitored, the CH_2 symmetric stretching vibrations and the CH_2 scissoring vibrations (Supplementary Figure 4). A low ($\sim 2848 \text{ cm}^{-1}$) wavenumber of the CH_2 symmetric stretching vibrations indicates the presence of a highly ordered lipid organization (either hexagonal or orthorhombic), whereas a high (2853 cm^{-1}) wavenumber indicates a liquid disordered phase⁵³. The mean value of the position of the CH_2 symmetric stretching vibrations of AE patients shows a small but significant shift to higher values compared with control subjects (2849.2 cm^{-1} versus 2848.8 cm^{-1} , respectively, $P=0.0013$, Figure 6c). In addition, the variance in the group of AE patients is larger than in control subjects. To distinguish between an orthorhombic (dense) or hexagonal (less dense) lateral organization, the bandwidth of the CH_2 scissoring vibrations was monitored. A narrow bandwidth (typically 8 cm^{-1}) indicates the presence of only a hexagonal lipid organization, whereas a large bandwidth of typically 11 cm^{-1} is indicative for the presence of mainly an orthorhombic organization⁴⁹. The average bandwidth of the scissoring vibrations was significantly lower in AE patients compared with control subjects (10.6 cm^{-1} versus 11.6 cm^{-1} , respectively, $P=0.010$, Figure 6d), demonstrating a reduction of lipids in an orthorhombic organization and thus a less dense lipid organization. No significant influence of *FLG* mutations on the lipid organization in AE patients was found ($P>0.05$, Figures 6b-d).

Univariate analysis was performed between TEWL and two independent lipid organization parameters: a lamellar organization component (SAXD peak II position) and a lateral organization component (FTIR scissoring bandwidth). The correlation coefficient

Lipid organization / CER composition parameters	Correlation coefficients (r)
SAXD peak II position vs total C34 CER content	0.432**
SAXD peak II position vs total CER [EO] content	-0.393**
SAXD peak II position vs average CER chain length	-0.370*
FTIR scissoring bandwidth vs total C34 CER content	-0.669***
FTIR scissoring bandwidth vs total CER [EO] content	0.267
FTIR scissoring bandwidth vs average CER chain length	0.386*
FTIR stretching vs total C34 CER content	0.607***
FTIR stretching vs total CER [EO] content	-0.399*
FTIR stretching vs average CER chain length	-0.471**

Table II: Correlation coefficients of lipid composition and lipid organization parameters.

Correlated parameters	Correlation coefficients (r)
TEWL vs SCORAD	0.560**
TEWL vs SAXD peak II position	0.450**
TEWL vs FTIR scissoring bandwidth	-0.735**
TEWL vs FTIR stretching	0.645**
TEWL vs total C34 CER content	0.738**
TEWL vs total CER [EO] content	-0.441**
TEWL vs average CER chain length	-0.528**
TEWL vs NMF	-0.643**
SCORAD vs SAXD peak II position	0.164
SCORAD vs FTIR scissoring bandwidth	-0.474*
SCORAD vs FTIR stretching	0.534**
SCORAD vs total C34 CER content	-0.470*
SCORAD vs total CER [EO] content	-0.238
SCORAD vs average CER chain length	-0.265
SCORAD vs NMF	-0.362*
NMF vs SAXD peak II position	-0.501**
NMF vs FTIR scissoring bandwidth	0.697**
NMF vs FTIR stretching	-0.778**
NMF vs total C34 CER content	-0.611**
NMF vs total CER [EO] content	0.416**
NMF vs average CER chain length	0.456**

Table III: Correlations between the various parameters.

was $r=0.76$ ($P<0.0001$, Figure 6e), which demonstrates that skin barrier function as measured by TEWL is significantly influenced by lipid organization.

Altered CER composition correlates with aberrant lipid organization.

As the CER composition and lipid organization both show a relationship with a reduced skin barrier (TEWL), the relation between the lipid parameters is summarized in Table II. The levels of C34 CERs and CER [EO] associate with both the lamellar organization (SAXD) and lateral lipid organization (FTIR scissoring bandwidth and stretching vibrations position). A powerful correlation of 0.71 was observed when both the lamellar and lateral organization components (SAXD and CH₂ scissoring) were plotted versus the two components of the CER composition ([EO] CERs and C34 CERs). Supplementary Figure 5 illustrates this correlation.

Altered CER composition and aberrant lipid organization correlate with NMF levels and SCORAD

A detailed overview of correlation coefficients between different parameters is presented in Table III. NMF levels correlate ($r > 0.4$, $P < 0.01$) with both lamellar and lateral lipid organization as well as with chain length of the CERS. SCORAD (disease severity) was associated with CER composition (i.e. total C₃₄ CERS and total CER [EO] content) and lipid organization (i.e. SAXD peak II position and FTIR scissoring bandwidth), with correlation coefficients of 0.56 ($P < 0.01$) and 0.58 ($P < 0.01$), respectively.

FLG mutations correlate with NMF levels, but not with SCORAD and TEWL levels.

NMF levels were significantly lower in FLG carriers than in non-carriers (0.45 ± 0.19 and 0.87 ± 0.43 , respectively, $P < 0.005$). Both SCORAD and TEWL values were independent of FLG genotype ($P = 0.34$ and $P = 0.23$), respectively.

Discussion

We performed an integral analysis of CER composition, focusing on the chain length distribution of each of the CER subclasses in relation to lipid organization and their correlation with skin barrier function (TEWL), disease severity (SCORAD), FLG mutations and NMF levels. This study provides detailed information about the role of lipids in the impaired skin barrier function of non-lesional AE skin.

The results show a reduced average CER chain length in non-lesional skin of AE patients. This reduction in chain length can be attributed to an increase in extremely short C₃₄ CERS as well as a reduction in very long CER [EO] subclasses. The increment in C₃₄ CERS has recently been reported by Ishikawa *et al.* for a single subclass (CER [NS]) in lesional skin of AE patients³⁷. Here we show in non-lesional skin a largely increased level of C₃₄ CERS in four CER subclasses: CER [NS], [NH], [AS] and [AH]. In addition, the results show changed levels in some of the CER subclasses consistent with previous reports: a decrease in CER [NP] level and an increase in CER [AS] level^{12,34-37,54,55}. We did not observe a change in CER/protein levels between AE patients and controls. Interestingly, the reduction in CER chain length found in the present study had a much stronger impact on the skin barrier function than did the changes in CER subclass levels: the TEWL increases proportionally with decreasing chain length. These findings are in excellent agreement with earlier *in vitro* studies showing that a reduction in chain length of CERS has a stronger impact on the lipid organization and permeability than a change in the ratio between CER subclasses keeping the chain length approximately equal⁵⁶⁻⁵⁸, unpublished results M. Oguri, G.S. Gooris, J.A. Bouwstra). Di Nardo *et al.* observed a reduction in CER/CHOL ratio in non-

lesional skin of AE patients, whereas other studies do not report a decrease in CER content in non-lesional AE skin^{20,35-37,54}. Groen *et al.*⁵⁸ observed that when increasing the CER or FFA level while keeping the level of the other two main lipid classes equal, did not affect the permeability *in vitro*. Therefore these studies suggest that the CER composition and chain length rather than the ratio between lipid classes does play a major role in the increased TEWL in non-lesional skin in patients with AE. The increment in C₃₄ CERs and decrement in CER [EO] suggest that elongation of the acyl chains is reduced. As the elongase family plays an important role in the elongation of fatty acids in the viable epidermis, we hypothesize that the higher abundance of C₃₄ CERs may be due to a misbalance in the activity of some of the members of the elongase family^{59,60}.

Several publications report on the lipid organization in AE patients: Pilgram *et al.* reported changes in the lateral packing when comparing three AE patients with three controls³². In a very recent study, we reported the first results on a very limited number of subjects focusing on the lamellar phases and ceramide subclasses without examining the CER chain lengths⁶¹. In addition, several studies focused on the (delayed or incomplete) lamellar body extrusion process in AE⁶²⁻⁶⁴, possibly caused by a reduced peroxisome proliferator-activated receptor activation⁶⁵. In the present study we were particularly interested in the influence of CER chain length on the lipid organization in AE patients.

With respect to the lamellar lipid organization, we observed a shift in the peak II position of SAXD curves of SC in AE patients. This observation indicates a reduced value of the repeat distances of the lamellar phases and/or a reduced formation of the LPP²⁸. The correlation between SAXD peak II position with CER [EO] and C₃₄ CER levels indicates that changes in these CER levels affect the lamellar organization. When focusing on the lateral organization, AE patients show a less dense lipid packing compared with controls that correlates strongly with a higher level of C₃₄ CERs. This finding shows that CER chain length is also an important determinant of the lateral lipid organization in SC. The observed changes in lamellar and lateral organization correlate with the increased TEWL levels and thus with an abnormal skin barrier function in patients with AE. The findings in this study strongly support the hypothesis that in AE patients a reduction in CER chain length leads to a change in lipid organization, which in turn leads to an impaired barrier function. In addition, the present study shows that this impaired barrier function is correlated with the disease severity as determined by SCORAD, which is supported by literature^{66,67}. This may indicate that as a result of inflammation, lipid synthesis is influenced (even at non-lesional sites), and subsequently the barrier function is decreased.

As *FLG* mutations are known to be predisposing factors for AE¹⁷, an interesting question is whether lipid changes are associated with the presence of *FLG* mutations. We

screened our subjects for four of the most prevalent *FLG* mutations accounting for 93% of the European *FLG* mutation spectrum³⁸. In our study cohort, there is no evidence that *FLG* mutations have an effect on CER composition and lipid organization. In contrast, in a recent study in ichthyosis vulgaris patients⁶⁸, changes in the lamellar organization were observed between the patients and controls. In that investigation, however, the majority of the patients were homozygote or compound heterozygote with respect to *FLG* mutations, and no inflammation was observed in these patients.

In previous studies, as well as in the current study, AE patients with *FLG* mutations showed significantly reduced NMF levels^{22,69}. Remarkably, in this study changes in lipids correlated with NMF levels but not with the presence or absence of *FLG* mutations. This suggests that between *FLG* gene (genotype) and NMF (phenotype), other (translational and environmental) factors may also influence NMF levels. These factors may include *FLG* copy numbers (repeat alleles on the *FLG* gene)⁷⁰ and interleukin levels, which can downregulate flaggrin expression⁷¹. Changes in NMF levels are suggested to lead to a change in pH, and together with altered interleukin levels and protease activity this may affect enzymes involved in CER biosynthesis^{5,68,72-74} and therefore change the CER composition and lipid organization. Thus, despite the fact that we did not find a correlation between the lipids and *FLG* mutation status, flaggrin might play an indirect role in the decreased barrier function of AE patients, although the underlying mechanism remains unclear. Besides, other barrier proteins may be involved. This will be subject of future studies by our group. In conclusion, in this study we have shown that the CER chain length is altered in AE patients by elevated C₃₄ CERS levels and reduced CER [EO] levels. These changes correlate with an altered lipid organization and a decreased barrier function in AE patients. In addition, a significant correlation was observed between disease severity and change in lipid composition and organization. Our results suggest a novel therapeutic entry to repair skin barrier defects in AE patients, aimed at normalizing CER chain length distribution. Such a treatment could improve the SC lipid organization and restore the skin barrier function of AE patients.

Acknowledgements

This research is supported by the European Cooperation in Science and Technology (COST) and the Dutch Technology Foundation STW, which is part of the Netherlands Organisation for Scientific Research (NWO), and which is partly funded by the Ministry of Economic Affairs. The authors thank Cosmoferm for provision of the synthetic CERS and the Netherlands Organization for Scientific Research (NWO) for provision of beam time.

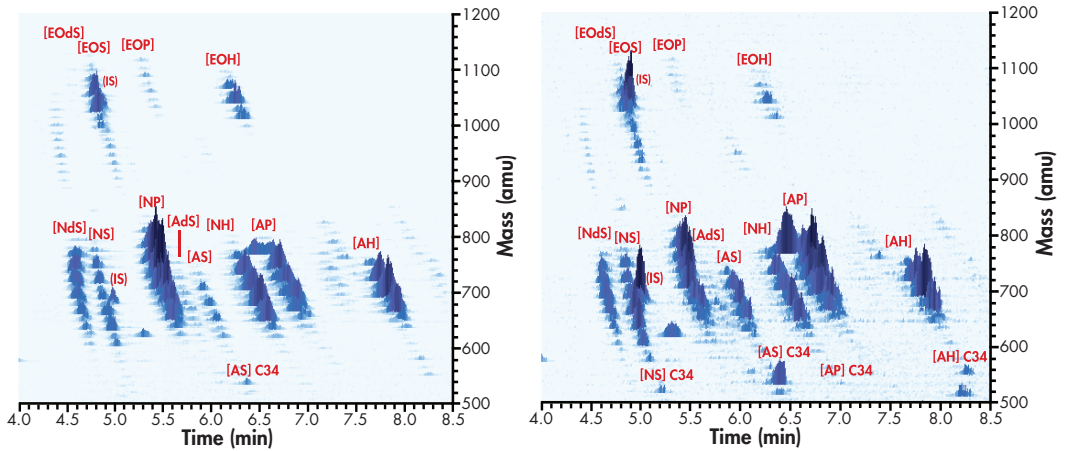
References

- 1 Proksch E, Folster-Holst R, Jensen JM. Skin barrier function, epidermal proliferation and differentiation in eczema. *J Dermatol Sci* 2006; 43: 159-69.
- 2 Elias PM, Menon GK. Structural and lipid biochemical correlates of the epidermal permeability barrier. *Adv Lipid Res* 1991; 24: 1-26.
- 3 Masukawa Y, Narita H, Sato H *et al*. Comprehensive quantification of ceramide species in human stratum corneum. *J Lipid Res* 2009; 50: 1708-19.
- 4 van Smeden J, Hoppel L, van der Heijden R *et al*. LC/MS analysis of stratum corneum lipids: ceramide profiling and discovery. *J Lipid Res* 2011; 52: 1211-21.
- 5 Cork MJ, Robinson DA, Vasilopoulos Y *et al*. New perspectives on epidermal barrier dysfunction in atopic dermatitis: gene-environment interactions. *J Allergy Clin Immunol* 2006; 118: 3-21; quiz 2-3.
- 6 Leung DY, Bieber T. Atopic dermatitis. *Lancet* 2003; 361: 151-60.
- 7 Alanne S, Nermes M, Soderlund R *et al*. Quality of life in infants with atopic dermatitis and healthy infants: a follow-up from birth to 24 months. *Acta Paediatr* 2011; 100: e65-70.
- 8 Mozaffari H, Pourpak Z, Poursayed S *et al*. Quality of life in atopic dermatitis patients. *J Microbiol Immunol Infect* 2007; 40: 260-4.
- 9 Slattery MJ, Essex MJ, Paletz EM *et al*. Depression, anxiety, and dermatologic quality of life in adolescents with atopic dermatitis. *J Allergy Clin Immunol* 2011; 128: 668-71 e3.
- 10 van Valburg RW, Willemsen MG, Dirven-Meijer PC *et al*. Quality of life measurement and its relationship to disease severity in children with atopic dermatitis in general practice. *Acta Derm Venereol* 2011; 91: 147-51.
- 11 Williams H, Flohr C. How epidemiology has challenged 3 prevailing concepts about atopic dermatitis. *Journal of Allergy and Clinical Immunology* 2006; 118: 209-13.
- 12 Di Nardo A, Wertz P, Giannetti A *et al*. Ceramide and cholesterol composition of the skin of patients with atopic dermatitis. *Acta Derm Venereol* 1998; 78: 27-30.
- 13 Yoshiike T, Aikawa Y, Sindhvananda J *et al*. Skin barrier defect in atopic dermatitis: increased permeability of the stratum corneum using dimethyl sulfoxide and theophylline. *J Dermatol Sci* 1993; 5: 92-6.
- 14 Werner Y, Lindberg M. Transepidermal water loss in dry and clinically normal skin in patients with atopic dermatitis. *Acta Derm Venereol* 1985; 65: 102-5.
- 15 Seidenari S, Giusti G. Objective assessment of the skin of children affected by atopic dermatitis: A study of pH, capacitance and TEWL in eczematous and clinically uninvolved skin. *Acta Dermato-Venereologica* 1995; 75: 429-33.
- 16 Elias PM, Schmuth M. Abnormal skin barrier in the etiopathogenesis of atopic dermatitis. *Current Opinion in Allergy and Clinical Immunology* 2009; 9: 437-46.
- 17 Palmer CN, Irvine AD, Terron-Kwiatkowski A *et al*. Common loss-of-function variants of the epidermal barrier protein filaggrin are a major predisposing factor for atopic dermatitis. *Nat Genet* 2006; 38: 441-6.
- 18 Hudson TJ. Skin barrier function and allergic risk. *Nature Genetics* 2006; 38: 399-400.
- 19 Seguchi T, Chang Yi C, Kusuda S *et al*. Decreased expression of filaggrin in atopic skin. *Archives of Dermatological Research* 1996; 288: 442-6.
- 20 Angelova-Fischer I, Mannheimer AC, Hinder A *et al*. Distinct barrier integrity phenotypes in filaggrin-related atopic eczema following sequential tape stripping and lipid profiling. *Exp Dermatol* 2011; 20: 351-6.
- 21 Jakasa I, Koster ES, Calkoen F *et al*. Skin barrier function in healthy subjects and patients with atopic dermatitis in relation to filaggrin loss-of-function mutations. *J Invest Dermatol* 2011; 131: 540-2.
- 22 O'Regan GM, Kemperman PM, Sandilands A *et al*. Raman profiles of the stratum corneum define 3 filaggrin genotype-determined atopic dermatitis endophenotypes. *J Allergy Clin Immunol* 2010; 126: 574-80 e1.
- 23 Jungersted JM, Scheer H, Mempel M *et al*. Stratum corneum lipids, skin barrier function and filaggrin mutations in patients with atopic eczema. *Allergy* 2010; 65: 911-8.
- 24 Flohr C, England K, Radulovic S *et al*. Filaggrin loss-of-function mutations are associated with early-onset eczema, eczema severity and transepidermal water loss at 3 months of age. *Br J Dermatol* 2010; 163: 1333-6.
- 25 Landstad BJ, Ekholm J, Broman L *et al*. Working environmental conditions as experienced by women working despite pain. *Work* 2000; 15: 141-52.
- 26 Elias PM. Stratum corneum defensive functions: An integrated view. *Journal of Investigative Dermatology* 2005; 125: 183-200.
- 27 Elias PM, Steinhoff M. "Outside-to-Inside" (and now back to "Outside") pathogenic mechanisms in atopic dermatitis. *Journal of Investigative Dermatology* 2008; 128: 1067-70.
- 28 Bouwstra JA, Gooris GS, van der Spek JA *et al*. Structural investigations of human stratum corneum by small-angle X-ray scattering. *J Invest Dermatol* 1991; 97: 1005-12.
- 29 Madison KC, Swartzendruber DC, Wertz PW *et al*. Presence of intact intercellular lipid lamellae in the upper layers of the stratum corneum. *J Invest Dermatol* 1987; 88: 714-8.
- 30 Ongpipattanakul B, Francoeur ML, Potts RO. Polymorphism in stratum corneum lipids. *Biochim Biophys Acta* 1994; 1190: 115-22.
- 31 Bommannan D, Potts RO, Guy RH. Examination of stratum corneum barrier function in vivo by infrared spectroscopy. *J Invest Dermatol* 1990; 95: 403-8.
- 32 Pilgram GS, Vissers DC, van der Meulen H *et al*. Aberrant lipid organization in stratum corneum of patients with atopic dermatitis and lamellar ichthyosis. *J Invest Dermatol* 2001; 117: 710-7.
- 33 Bouwstra JA, Ponc M. The skin barrier in healthy and diseased state. *Biochim Biophys Acta* 2006; 1758: 2080-95.
- 34 Bleck O, Abeck D, Ring J *et al*. Two ceramide subfractions detectable in Cer(AS) position by HPTLC in skin surface lipids of non-lesional skin of atopic eczema. *J Invest Dermatol* 1999; 113: 894-900.
- 35 Farwanah H, Raith K, Neubert RH *et al*. Ceramide profiles

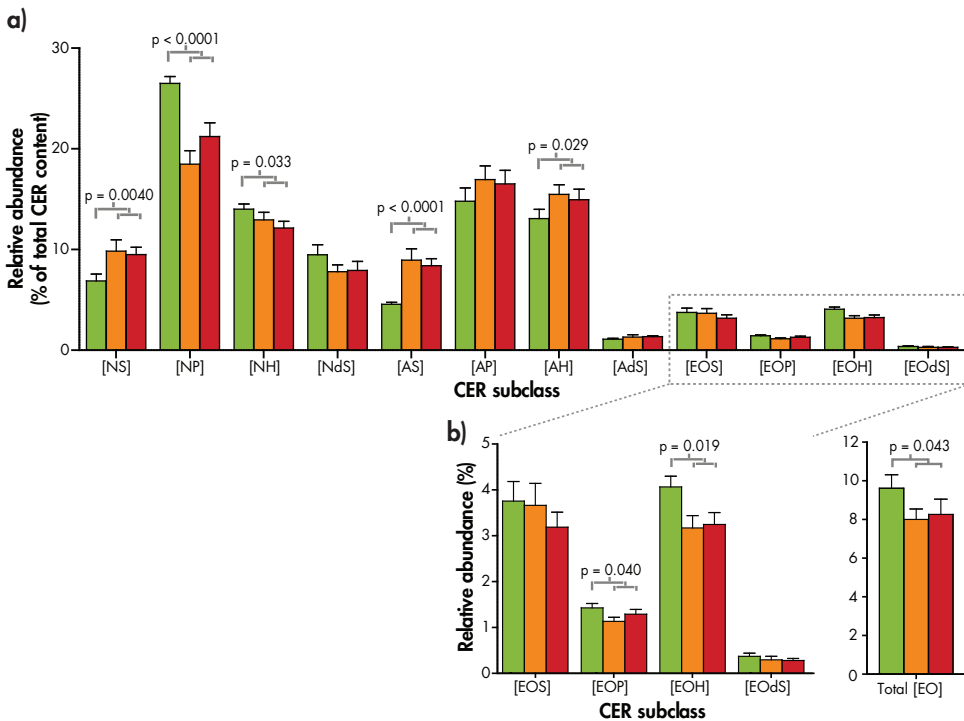
- of the uninvolved skin in atopic dermatitis and psoriasis are comparable to those of healthy skin. *Arch Dermatol Res* 2005; 296: 514-21.
- 36 Imokawa G, Abe A, Jin K *et al.* Decreased level of ceramides in stratum corneum of atopic dermatitis: an etiologic factor in atopic dry skin? *J Invest Dermatol* 1991; 96: 523-6.
- 37 Ishikawa J, Narita H, Kondo N *et al.* Changes in the ceramide profile of atopic dermatitis patients. *J Invest Dermatol* 2010; 130: 2511-4.
- 38 Chen H, Common JE, Haines RL *et al.* Wide spectrum of filaggrin-null mutations in atopic dermatitis highlights differences between Singaporean Chinese and European populations. *Br J Dermatol* 2011; 165: 106-14.
- 39 Sandilands A, Terron-Kwiatkowski A, Hull PR *et al.* Comprehensive analysis of the gene encoding filaggrin uncovers prevalent and rare mutations in ichthyosis vulgaris and atopic eczema. *Nat Genet* 2007; 39: 650-4.
- 40 Stalder JF, Taieb A. Severity scoring of atopic dermatitis: the SCORAD index. Consensus Report of the European Task Force on Atopic Dermatitis. *Dermatology* 1993; 186: 23-31.
- 41 Caspers PJ, Lucassen GW, Carter EA *et al.* In vivo confocal Raman microspectroscopy of the skin: noninvasive determination of molecular concentration profiles. *J Invest Dermatol* 2001; 116: 434-42.
- 42 Caspers PJ, Lucassen GW, Puppels GJ. Combined in vivo confocal Raman spectroscopy and confocal microscopy of human skin. *Biophys J* 2003; 85: 572-80.
- 43 Kalia YN, Alberti I, Naik A *et al.* Assessment of topical bioavailability in vivo: the importance of stratum corneum thickness. *Skin Pharmacol Appl Skin Physiol* 2001; 14 Suppl 1: 82-6.
- 44 Voegeli R, Heiland J, Doppler S *et al.* Efficient and simple quantification of stratum corneum proteins on tape strippings by infrared densitometry. *Skin Res Technol* 2007; 13: 242-51.
- 45 Bligh EG, Dyer WJ. A rapid method of total lipid extraction and purification. *Can J Biochem Physiol* 1959; 37: 911-7.
- 46 Thakoersing VS, Ponc M, Bouwstra JA. Generation of human skin equivalents under submerged conditions-mimicking the in utero environment. *Tissue Eng Part A* 2010; 16: 1433-41.
- 47 Motta S, Monti M, Sesana S *et al.* Ceramide composition of the psoriatic scale. *Biochim Biophys Acta* 1993; 1182: 147-51.
- 48 Boncheva M, Damien F, Normand V. Molecular organization of the lipid matrix in intact Stratum corneum using ATR-FTIR spectroscopy. *Biochim Biophys Acta* 2008; 1778: 1344-55.
- 49 Damien F, Boncheva M. The extent of orthorhombic lipid phases in the stratum corneum determines the barrier efficiency of human skin in vivo. *J Invest Dermatol* 2010; 130: 611-4.
- 50 Tanojo H, BosvanGeest A, Bouwstra JA *et al.* In vitro human skin barrier perturbation by oleic acid: Thermal analysis and freeze fracture electron microscopy studies. *Thermochimica Acta* 1997; 293: 77-85.
- 51 Schreiner V, Gooris GS, Pfeiffer S *et al.* Barrier characteristics of different human skin types investigated with X-ray diffraction, lipid analysis, and electron microscopy imaging. *J Invest Dermatol* 2000; 114: 654-60.
- 52 Bras W, Dolbnya IP, Detolenaere D *et al.* Recent experiments on a combined small-angle/wide-angle X-ray scattering beam line at the ESRF. *Journal of Applied Crystallography* 2003; 36: 791-4.
- 53 Moore DJ, Rerek ME, Mendelsohn R. FTIR spectroscopy studies of the conformational order and phase behavior of ceramides. *Journal of Physical Chemistry B* 1997; 101: 8933-40.
- 54 Yamamoto A, Serizawa S, Ito M *et al.* Stratum corneum lipid abnormalities in atopic dermatitis. *Arch Dermatol Res* 1991; 283: 219-23.
- 55 Matsumoto M, Umemoto N, Sugiura H *et al.* Difference in ceramide composition between "dry" and "normal" skin in patients with atopic dermatitis. *Acta Derm Venereol* 1999; 79: 246-7.
- 56 de Jager M, Groenink W, Bielsa i Guivernau R *et al.* A novel in vitro percutaneous penetration model: evaluation of barrier properties with p-aminobenzoic acid and two of its derivatives. *Pharm Res* 2006; 23: 951-60.
- 57 de Sousa Neto D, Gooris G, Bouwstra J. Effect of the omega-acylceramides on the lipid organization of stratum corneum model membranes evaluated by X-ray diffraction and FTIR studies (Part I). *Chem Phys Lipids* 2011; 164: 184-95.
- 58 Groen D, Poole DS, Gooris GS *et al.* Is an orthorhombic lateral packing and a proper lamellar organization important for the skin barrier function? *Biochim Biophys Acta* 2011; 1808: 1529-37.
- 59 Ohno Y, Suto S, Yamanaka M *et al.* ELOVL1 production of C24 acyl-CoAs is linked to C24 sphingolipid synthesis. *Proc Natl Acad Sci U S A* 2010; 107: 18439-44.
- 60 Park YH, Jang WH, Seo JA *et al.* Decrease of ceramides with very long-chain fatty acids and downregulation of elongases in a murine atopic dermatitis model. *J Invest Dermatol* 2012; 132: 476-9.
- 61 Janssens M, van Smeden J, Gooris GS *et al.* Lamellar lipid organization and ceramide composition in the stratum corneum of patients with atopic eczema. *J Invest Dermatol* 2011; 131: 2136-8.
- 62 Fartasch M, Bassukas ID, Diepgen TL. Disturbed extruding mechanism of lamellar bodies in dry non-eczematous skin of atopics. *Br J Dermatol* 1992; 127: 221-7.
- 63 Marsella R, Samuelson D, Doerr K. Transmission electron microscopy studies in an experimental model of canine atopic dermatitis. *Vet Dermatol* 2010; 21: 81-8.
- 64 Scharschmidt TC, Man MQ, Hatano Y *et al.* Filaggrin deficiency confers a paracellular barrier abnormality that reduces inflammatory thresholds to irritants and haptens. *J Allergy Clin Immunol* 2009; 124: 496-506, e1-6.
- 65 Man MQ, Barish GD, Schmutz M *et al.* Deficiency of PPARbeta/delta in the epidermis results in defective cutaneous permeability barrier homeostasis and increased inflammation. *J Invest Dermatol* 2008; 128: 370-7.
- 66 Chamlin SL, Kao J, Frieden IJ *et al.* Ceramide-dominant barrier repair lipids alleviate childhood atopic dermatitis: changes in barrier function provide a sensitive indicator of disease activity. *J Am Acad Dermatol* 2002; 47: 198-208.
- 67 Nemoto-Hasebe I, Akiyama M, Nomura T *et al.* Clinical

- severity correlates with impaired barrier in filaggrin-related eczema. *J Invest Dermatol* 2009; 129: 682-9.
- 68 Gruber R, Elias PM, Crumrine D *et al*. Filaggrin genotype in ichthyosis vulgaris predicts abnormalities in epidermal structure and function. *Am J Pathol* 2011; 178: 2252-63.
- 69 Kezic S, Kemperman PM, Koster ES *et al*. Loss-of-function mutations in the filaggrin gene lead to reduced level of natural moisturizing factor in the stratum corneum. *J Invest Dermatol* 2008; 128: 2117-9.
- 70 Irvine AD, McLean WHI, Leung DYM. MECHANISMS OF DISEASE Filaggrin Mutations Associated with Skin and Allergic Diseases. *New England Journal of Medicine* 2011; 365: 1315-27.
- 71 Howell MD, Kim BE, Gao P *et al*. Cytokine modulation of atopic dermatitis filaggrin skin expression. *J Allergy Clin Immunol* 2007; 120: 150-5.
- 72 Hachem JP, Man MQ, Crumrine D *et al*. Sustained serine proteases activity by prolonged increase in pH leads to degradation of lipid processing enzymes and profound alterations of barrier function and stratum corneum integrity. *J Invest Dermatol* 2005; 125: 510-20.
- 73 Nakagawa N, Sakai S, Matsumoto M *et al*. Relationship between NMF (lactate and potassium) content and the physical properties of the stratum corneum in healthy subjects. *J Invest Dermatol* 2004; 122: 755-63.
- 74 Schmid-Wendtner MH, Korting HC. The pH of the skin surface and its impact on the barrier function. *Skin Pharmacol Physiol* 2006; 19: 296-302.

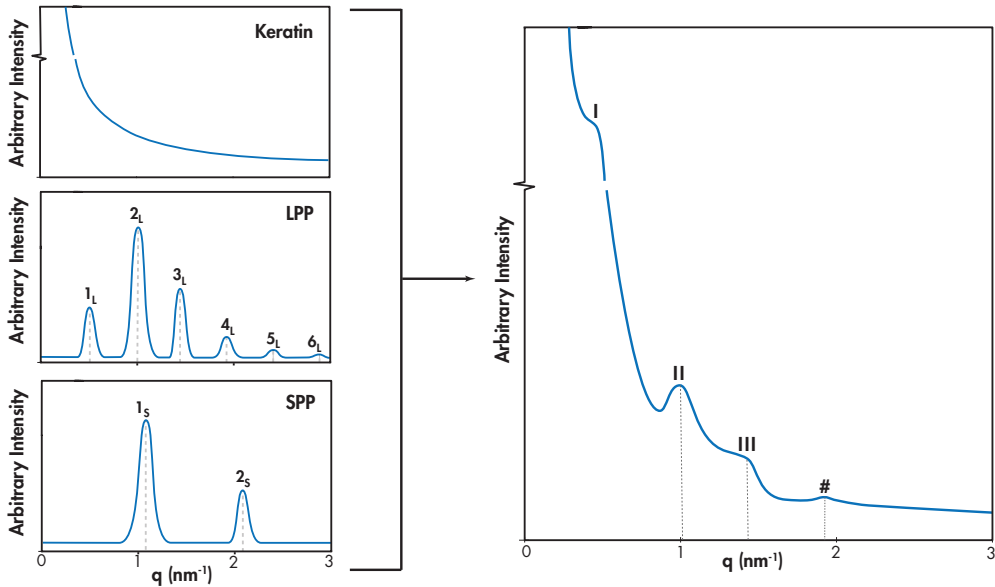
Supplementary Material



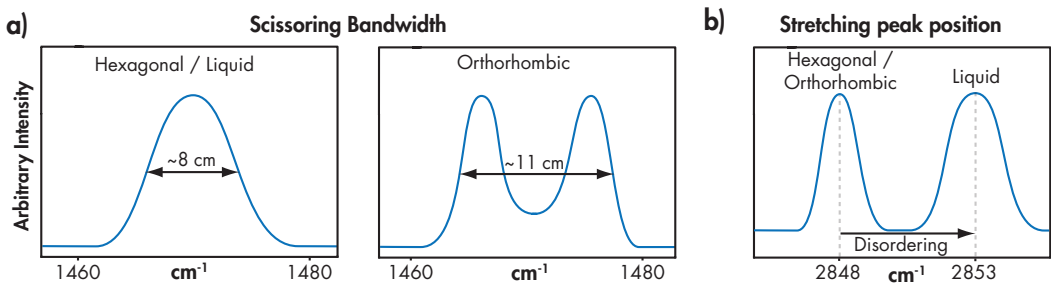
Supplementary Figure 1: Representative 3D multi-mass chromatograms of SC ceramides of a healthy subject (left) and an AE patient (right). All subclasses are indicated by their abbreviation. IS indicates one of the deuterated internal standards (CER classes [EOS] and [NS]) which were added to every sample to enable semi-quantitative analysis.



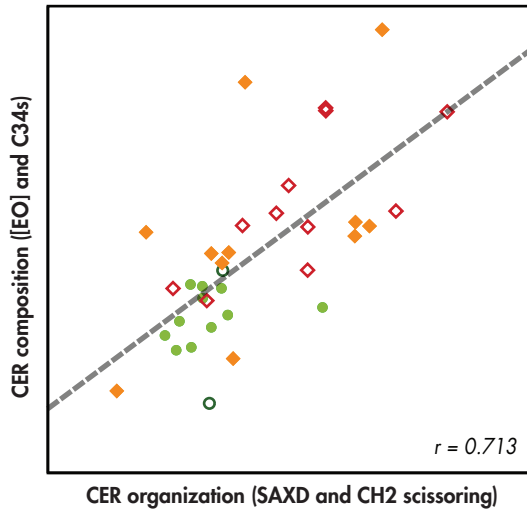
Supplementary Figure 2: Bar plot showing the relative abundances of all CER subclasses (a) and only the very long [EO] CER subclasses (b) (Mean \pm SEM). Green bars correspond to the control group, while orange and red bars correspond to AE patients who do not and do carry FLG mutations, respectively.



Supplementary Figure 3: Lamellar organization in human stratum corneum. The right graph shows a typical SAXD profile of human SC. The scattering intensity (I) is plotted as a function of q , which is defined by $q = 2\pi \sin \theta / \lambda$, in which λ is the wavelength of the X-rays and θ the angle of the scattered X-rays. The X-ray diffraction graph of human stratum corneum is characterized by a high intensity at low q values due to keratin in the corneocytes and a series of peaks. The peaks indicated by I (weak peak), II (strong peak) and III (weak peak) are attributed to the LPP. Peak II is also attributed to the SPP. The peak indicated by # is due to cholesterol. A schematic drawing of the X-ray curves of the keratin, LPP and SPP is also shown on the left. The 1st, 2nd, 3rd, 4th, 5th and 6th order of the LPP (indicated by 1L-6L) and 1st and 2nd order of the SPP (indicated by 1S and 2S). From the positions of the peaks (q) the repeat distance of the LPP and SPP can be calculated using the equation $d = n \cdot 2\pi / q_n$ (n = order of diffraction peak). When comparing the positions of the LPP and SPP to that in the diffraction pattern of the SC, peak I and III are only attributed to the LPP, while II is attributed to the LPP (2L) and SPP (1S). Higher order reflections cannot be detected due to the low intensities of these peaks.



Supplementary Figure 4: The lateral organization can be measured by Fourier transform infrared spectroscopy (FTIR) by focusing on the CH_2 scissoring vibrations ($1460\text{--}1480\text{ cm}^{-1}$) and the CH_2 symmetric stretching vibrations ($2848\text{--}2053\text{ cm}^{-1}$). **a)** An orthorhombic organization results in a splitting of the scissoring vibrations, while a hexagonal packing results in a single vibration. Therefore, an increased bandwidth of the scissoring vibrations is indicative for an increased fraction of lipids forming orthorhombic lipid domains. In addition, the CH_2 symmetric stretching vibration provides information about the conformational ordering of the lipids **b)**; a lower frequency ($\sim 2848\text{ cm}^{-1}$) indicates a fully extended chains (high degree of conformational ordering) of the lipids, whereas a high wavenumber (2853 cm^{-1}) is indicative for a liquid organization (low degree of conformational ordering).



Supplementary Figure 5: Scatter plot of univariate analysis of the predicted correlation between the CER organization (lamellar organization (SAXD) and lateral organization (CH₂ scissoring) versus the CER organization (the abundance of [EO] CERS and C₃₄ CERS). Gray dotted line represents the optimal fit ($r=0.713$). Control subjects are indicated by ●/○. Non-lesional skin and lesional skin of AE patients are indicated by ◆/◇ and ■/□. Open and filled data points indicate carriers and non-carriers of FLG mutations, respectively.

Supplementary Table I. Mutations in the cohort of AE patients.

Loss-of-function mutation	2282del4	R501X	R2447X	S3247X
Heterozygous: 10	4	4	1	1
Homozygous: 3	2	1	-	-
Compound heterozygous: 1	1	1	-	-

Supplementary Table II. Characteristics of the subjects

Parameter	Control (n=15)	AE (n=28)
Age (years)	25.0 ± 5.2	25.6 ± 5.6
Female gender	10	17
Total SCORAD	-	28.0 ± 16.1
TEWL (g/m ² /h)	6.5 ± 1.7	12.2 ± 6.5
NMF (AU)	1.05 ± 0.2	0.66 ± 0.39
FLG mutation	2	14

Supplementary Table III. Statistical data of the relative abundance of the 12 CER subclasses in control subjects versus AE patients and AE patients that carry and do not carry FLG mutations.

CER subclass	Control (%, mean \pm SD)	AE (%, mean \pm SD)	Statistical significance (P-value)	FLG mutation in patients (%, mean \pm SD)	No FLG mutation in patients (%, mean \pm SD)	Statistical significance (P-value)
[EOS]	3.76 \pm 0.59	3.43 \pm 1.52	0.191	3.66 \pm 1.79	3.19 \pm 1.22	0.550
[EOP]	1.43 \pm 0.36	1.21 \pm 0.36	0.040	1.13 \pm 0.33	1.29 \pm 0.38	0.270
[EOH]	4.06 \pm 0.87	3.21 \pm 0.97	0.019	3.17 \pm 1.01	3.25 \pm 0.97	0.783
[EOdS]	0.37 \pm 0.26	0.29 \pm 0.23	0.286	0.30 \pm 0.28	0.28 \pm 0.17	0.713
[NS]	6.88 \pm 2.57	9.67 \pm 3.44	0.003	9.84 \pm 4.20	9.51 \pm 2.64	0.646
[NP]	26.5 \pm 2.57	19.85 \pm 5.16	<0.001	18.49 \pm 4.99	21.21 \pm 5.14	0.183
[NH]	14.01 \pm 1.94	12.54 \pm 2.63	0.033	12.94 \pm 2.83	12.14 \pm 2.45	0.462
[NdS]	9.48 \pm 3.75	7.86 \pm 2.92	0.063	7.80 \pm 2.59	7.92 \pm 3.32	0.783
[AS]	4.57 \pm 0.68	8.67 \pm 3.48	<0.001	8.95 \pm 4.24	8.39 \pm 2.65	0.963
[AP]	14.79 \pm 4.96	16.73 \pm 4.94	0.308	16.95 \pm 5.05	16.52 \pm 5.02	0.890
[AH]	13.07 \pm 3.46	15.21 \pm 3.66	0.028	15.47 \pm 3.59	14.96 \pm 3.84	0.462
[AdS]	1.09 \pm 0.32	1.32 \pm 0.66	0.272	1.30 \pm 0.88	1.35 \pm 0.36	0.141

Supplementary Table IV. Data of the relative abundance of all C₃₄ CERs between control versus AE and AE patients that carry and do not carry FLG mutations. CA is the total number of carbon atoms.

CER	Control (%, mean \pm SD)	AE (%, mean \pm SD)	Statistical significance (P-value)	FLG mutation in patients (%, mean \pm SD)	No FLG mutation in patients (%, mean \pm SD)	Statistical significance (P-value)
[AS] C34	0.32 \pm 0.11	0.78 \pm 0.44	<0.001	0.68 \pm 0.48	0.89 \pm 0.38	0.089
[AP] C34	0.10 \pm 0.02	0.13 \pm 0.06	0.058	0.13 \pm 0.07	0.13 \pm 0.05	0.232
[AH] C34	0.16 \pm 0.06	0.34 \pm 0.14	<0.001	0.30 \pm 0.14	0.39 \pm 0.13	0.089
[AdS] C34	0.06 \pm 0.04	0.08 \pm 0.07	0.337	0.07 \pm 0.08	0.09 \pm 0.05	0.251
[NS] C34	0.08 \pm 0.04	0.25 \pm 0.18	0.002	0.22 \pm 0.20	0.28 \pm 0.17	0.198
[NP] C34	0.06 \pm 0.05	0.07 \pm 0.06	0.936	0.07 \pm 0.04	0.06 \pm 0.08	0.141
[NH] C34	0.10 \pm 0.04	0.17 \pm 0.14	0.045	0.14 \pm 0.14	0.20 \pm 0.14	0.118

Supplementary Table V. Statistical overview of the relative abundance regarding CER [EO] and CERs C₃₄ for control subjects and AE patients. The effect of FLG mutations in patients is shown as well.

Parameter	Control (mean \pm SD)	AE (mean \pm SD)	Statistical significance (P-value)	FLG mutation in patients (mean \pm SD)	No FLG mutation in patients (mean \pm SD)	Statistical significance (P-value)
CER [EO] (%)	9.62 \pm 2.62	8.13 \pm 2.47	0.079*	8.26 \pm 2.94	8.00 \pm 2.00	0.788*
CERs C ₃₄ (%)	0.87 \pm 0.26	1.83 \pm 0.83	0.00017*	1.62 \pm 0.95	2.04 \pm 0.68	0.185*
Mean chain length (CA)	47.0 \pm 0.72	46.4 \pm 0.72	0.012**	46.7 \pm 0.78	46.4 \pm 0.74	0.277**

CHAPTER 7

THE ESSENCE OF FREE FATTY ACIDS AND LIPID CHAIN LENGTH FOR THE SKIN BARRIER FUNCTION IN PATIENTS WITH ATOPIC ECZEMA

Jeroen van Smeden^{1,*}, Michelle Janssens^{1,*},
Edward C.J. Kaye¹, Peter J. Caspers^{2,3},
Adriana P. Lavrijsen⁴, Rob J. Vreeken^{5,6} and
Joke A. Bouwsira¹

¹ Division of Drug Delivery Technology,
Leiden Academic Centre for Drug Research,
Leiden University, Leiden, The Netherlands.

² Center for Optical Diagnostics and
Therapy, Department of Dermatology,
Erasmus MC, Rotterdam, The Netherlands.

³ RiverD International BV, Rotterdam,
The Netherlands.

⁴ Department of Dermatology, Leiden
University Medical Center, Leiden,
The Netherlands.

⁵ Division of Analytical Biosciences, Leiden
Academic Centre for Drug Research,
Leiden University, Leiden, The Netherlands.

⁶ Netherlands Metabolomics Centre, Leiden
Academic Centre for Drug Research,
Leiden University, Leiden, The Netherlands.

*Both authors contributed equally to this work

Manuscript in preparation to this work

Adapted from Journal of Lipid Research.
2012. 53:2755-2766.

Abstract

One of the features of atopic eczema (AE) is a decreased skin barrier function. The stratum corneum (SC) lipids – comprised of ceramides (CERs), free fatty acids (FFAs), and cholesterol – form a highly ordered lipid organization that fulfill a predominant role in this barrier function. Recently, the detailed CER composition in non-lesional skin has been investigated in AE patients. In the present study, we report for the first time *i)* the extracellular SC FFA composition, including chain length and degree of unsaturation, in both lesional and non-lesional skin; and *ii)* how these factors associate with the examined CER composition and the impaired skin barrier in AE.

The results show a clearly distinguishable lipid profile between control skin, non-lesional and lesional AE skin. In particular the FFA chain lengths are clearly reduced in AE SC, and the changes are much more pronounced in lesional skin than in non-lesional skin. The CER composition and lipid organization were also examined in lesional skin and compared to data on non-lesional skin, previously reported. We noticed a strong reduction in CER chain length and a reduced density in the lipid organization. Changes in the chain length distribution of FFAs and CERs were strongly associated. In addition, we encountered a strong association between a reduction in chain length of both lipid classes and the increased presence of a less dense lipid organization. The changes in lipid organization did also associate with a reduced skin barrier function and were more pronounced in lesional skin.

These changes in composition, organization and barrier function were strongly observed in lesional skin, but already present in non-lesional skin, and demonstrate the importance of the FFAs and the

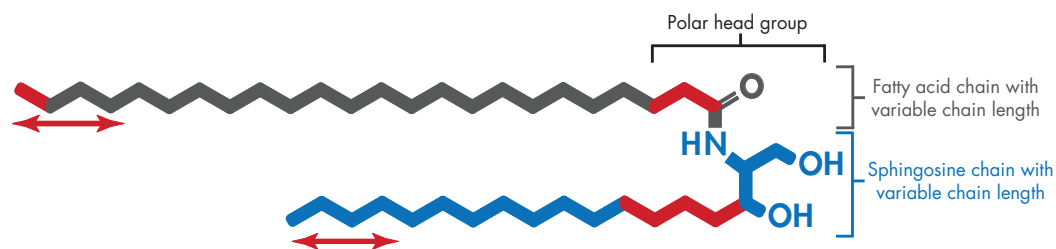
lipid chain length for a proper lipid organization and skin barrier function.

Introduction

Atopic eczema (AE) is a very common skin disease with a current prevalence of 10-15% in developed countries¹⁻⁵. AE has multiple manifestations, such as erythema, skin dryness, and pruritic skin lesions. The etiology of AE is complex: it is a multifactorial disease in which genetics, environmental factors, and an immune dysregulation all interplay. Although the immunological dysregulation is characteristic for AE patients, the skin barrier dysfunction also plays an important role⁶⁻¹⁰. A reduced skin barrier may result in an increased penetration of allergens and irritants, thereby provoking an immune response¹¹. A commonly used parameter to indicate a (reduced) skin barrier function is transepidermal water loss (TEWL). Patients show increased TEWL values at both lesional and non-lesional sites, indicating that the skin barrier is affected in both inflamed and non-inflamed regions^{8,12,13}.

In 2006 it was reported – and since then replicated in many studies – that loss-of-function mutations in the filaggrin gene (*FLG*) are a major predisposing factor for developing AE¹⁴⁻¹⁷. Filaggrin is a well-known skin barrier protein responsible for proper keratin filament alignment¹⁸. In addition, filaggrin degradation products – i.e. the natural moisturizing factor (NMF) – are important to retain the moist and acidic nature of the stratum corneum (SC), which is the uppermost layer of the skin where the main barrier of the skin is located¹⁹. However, the reduced skin barrier in AE cannot fully be explained by *FLG* mutations, as i) 50-70% of all AE patients are non-carriers of such a mutation¹⁹ and ii) in a number of studies no relation was observed between *FLG* mutations and the impaired skin barrier in AE²⁰⁻²³.

Because the lipids play an important role in the skin barrier – also with respect to AE^{7,24-27} – the aim of this study is to determine the lipid chain length distribution and in particular free fatty acid composition in AE, and their relation with the skin barrier function. The SC consists of corneocytes with a lipid matrix in the intercellular regions. The lipids are composed of an approximately equimolar ratio of cholesterol, free fatty acids (FFAs) and ceramides (CERS, molecular architecture is explained in Figure 1)²⁸⁻³¹. These lipids are organized in regularly stacked lipid layers^{24,25,32,33}. Within these layers, the lipids form a very dense, highly ordered packing – the so-called orthorhombic organization – but a subpopulation is also present in a less dense – hexagonal – or even liquid organization (Figure 2)³⁴⁻³⁶. In a recent study we examined the CER composition and lipid organization in non-lesional skin of AE patients, from which it was concluded that a reduction in the average chain length of SC CERS coincided with an increase in



	Non-hydroxy fatty acid, [N]	α -hydroxy fatty acid, [A]	Esterified ω -hydroxy fatty acid, [EO]
Dihydrosphingosine, [dS]	[NdS]	[AdS]	[EOdS]
Sphingosine, [S]	[NS]	[AS]	[EOS]
Phytosphingosine, [P]	[NP]	[AP]	[EOP]
6-hydroxy sphingosine, [H]	[NH]	[AH]	[EOH]

Figure 1: Explanation of CER subclasses and CER chain length. CERs are composed of a fatty acid chain linked to a sphingosine base. Both chains show a wide distribution in their carbon chains length (indicated by the arrows, the numbers represent the general distribution). This results in a wide range of the total carbon chain length of CERs, that is, the carbon atoms of the two chains combined. In addition, CERs can have an additional functional group at the carbon positions labeled in red, which results in the presence of 12 subclasses, denoted as: [NdS], [AdS], [EOdS], [NS], [AS], [EOS], [NP], [AP], [EOP], [NH], [AH], [EOH].

the hexagonal organization. These changes in CER composition and lipid organization strongly correlated to the degree of skin barrier dysfunction, suggesting that CER chain length may be a key factor for a proper lipid organization and impaired skin barrier function in non-lesional AE skin³⁷.

Building on these recent findings in non-lesional skin, this study presents for the first time a detailed analysis of the FFAs chain length distribution in lesional as well as in non-lesional AE skin. We focused on the chain length distribution as well as on the presence of mono-unsaturated FFAs (MUFAs) and the very sparsely studied hydroxy-FFAs. Previously, a wide chain length distribution has been observed in healthy subjects ranging from mainly 16 to 36 carbon atoms³⁸⁻⁴⁰. To the best of our knowledge, only one study reports on the FFA chain length in AE patients, mentioning the very long chain fatty acids only.

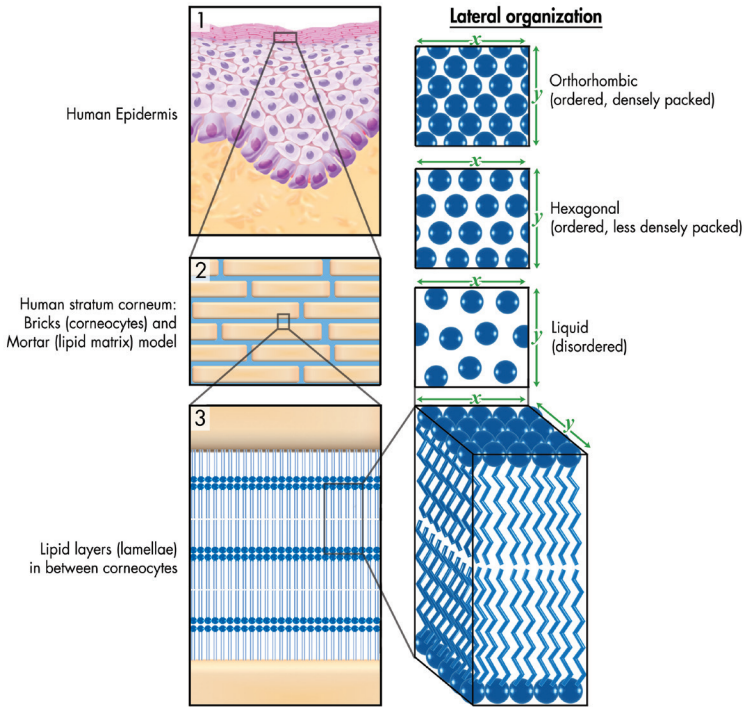


Figure 2: Lateral organization in human stratum corneum. (1) The outermost layer of the epidermis, the stratum corneum (SC), consists of dead cells (corneocytes) embedded in a lipid matrix, also referred to as the brick (corneocytes) and mortar (lipids) structure (2). The intercellular lipids are arranged in layers (lamellae). The lateral organization is the plane perpendicular to the direction of the lamellar organization. There are three possible arrangements of the lipids: a very dense, ordered, orthorhombic organization; a less dense, ordered, hexagonal organization; or a disordered, liquid organization.

They observed a decreased presence of FFAs longer than 24 carbon atoms⁴¹. Based on our detailed FFA analysis, we studied the association of changes in chain length distribution of the FFAs with the chain length distribution of the CERS, as literature reports a common synthetic pathway for both lipid classes^{42,43}. It was found that the average FFA chain length in AE patients is shortened, which is in conjunction with a reduced CER chain length. In addition, we examined possible correlations between changes in chain length profiles of the FFAs (and CERS) versus *i*) a modulation in lipid organization, *ii*) a reduction in skin barrier function monitored by TEWL and *iii*) *FLG* mutations.

Materials and Methods

General study setup

The study is in accordance to declaration of Helsinki and consists of 15 Caucasian control subjects (25.0±5.2 years; 5 males) and 28 Caucasian AE patients (25.6±5.6 years; 11 males), of which 11 did show lesional skin sites at the day in which all measurements were performed. Patients were screened by the four most prevalent mutations found in the European population (*2282del4*, *R501X*, *S3247X* and *R2447X*): 14 patients and 2 control subjects appeared as carriers for a *FLG* mutation. No dermatologic products were

applied on the forearms of any of the subjects at least one week prior to the study. Various techniques to study the lipid composition and organization are described in more detail below. All measurements were performed on both non-lesional skin and lesional skin (if present) of the ventral forearms. A dermatologist marked an area of 4.5 cm² on the ventral forearm of the control subjects and AE patients. On this area, the TEWL was measured using an open chamber Tewameter TM 210 (Courage+Khazaka, Köln, Germany) device. Values were recorded for a period of two minutes after which an average reading during the last 10 seconds of the measurement was calculated. This procedure was performed before tape stripping (baseline TEWL) and after each two tape strips.

SC lipids were obtained by tape stripping. In between each 2 tape strips, FTIR measurements were performed to study the lipid organization. In order to determine *FLG* mutations, buccal mucosa cells were collected by rubbing the inside of the cheeks with a cotton swab on a plastic stick after rinsing the mouth with water. Mutations were determined by genotyping after DNA extraction¹⁵.

Tape stripping procedure and LC/MS analysis

SC lipids were harvested using multiple poly(phenylene sulfide) tape strips (Nichiban, Tokyo, Japan). Successive tapes were pressed on the marked area using a pressure device, and were removed in one fluent stroke using tweezers. To avoid contamination of surface lipids (e.g. sebum), tape strips 1-5 were discarded and only tapes 6 to 9 were used for lipid analysis of non-lesional skin and – if possible – from lesional skin. The tapes were punched to an area of 2 cm² and stored in chloroform/methanol/water (1:2:½) at a dark, cold (-20°C), and dry environment, under argon atmosphere. Afterwards, lipid extraction of all samples was performed using an adapted procedure of the Bligh and Dyer method described by Thakoersing *et al.*⁴⁴ Lipids were reconstituted in chloroform/methanol/heptane (2½:2½:95) and ready for analysis by LC/MS using a recently developed method for analysis of both CERS and FFAs^{45,46} (van Smeden, unpublished data). Figure 1 explains the nomenclature (according to Motta *et al.*⁴⁷) and variation in chemical structure for these CER subclasses.

Prior to the analysis of the FFA composition, a particular problem for the quantification of FFA C16:0, C17:0, C18:0 and C18:1 was encountered. These endogenous lipids are also present in the tape-strips used to harvest the SC, thereby interfering with the analysis of SC FFAs (van Smeden, unpublished data). However, it was possible to correct for the amount of these lipids on the tape. This procedure is explained in detail in the supplement (Supplementary Figure 1 and Supplementary Table I).

Lateral lipid organization by FTIR and its principles

Fourier transform infrared spectroscopy (FTIR) spectra were recorded after each two tape-strips in order to obtain information on the lateral organization and conformational ordering of the lipids. A Varian 670-IR spectrometer (Varian Inc., Santa Clara, CA) equipped with a broad band mercury-cadmium-telluride (MCT) detector and an external sample compartment containing a GladiATR (Pike, Madison, WI) attenuated total reflection (ATR) accessory with a single reflection diamond was used. The spectral resolution was 2 cm^{-1} . The instrument was continuously purged with dry N_2 . Each spectrum was an average of 150 scans. For data treatment, the instrument software Resolutions Pro 4.1 (Varian Inc.) was used. Positions of the CH_2 symmetric stretching vibrations and scissoring bandwidth were calculated as described previously^{48,49}. Shortly, the second derivative was calculated and it was baseline-corrected between the endpoints of the scissoring region ($\sim 1460\text{--}1480\text{ cm}^{-1}$). We calculated the bandwidth at 50% of the peak height (full width half maximum, FWHM) and determined CH_2 symmetric stretching vibration positions of spectra recorded between the removal of 2 to 10 tape strips. The width of the peak is indicative for the size and amount of orthorhombic lipid domains⁵⁰. The stretching peak position indicates whether lipids are present in either a highly ordered organization (low peak position at $\sim 2848\text{ cm}^{-1}$) or a disordered/liquid phase (high peak position $\sim 2853\text{ cm}^{-1}$).

Data analysis

All statistical outcomes were determined using SPSS Statistics 17.0. In general, data was not Gaussian distributed and therefore non-parametric Mann-Whitney tests are more appropriate when 2 groups were compared, and Spearman's ρ correlation coefficients are shown. Jonckheere trend tests were performed to assess significance of trends between control, non-lesional and lesional SC. Differences were considered significant when $P < 0.05$. For some subjects in some of the parameters, data could not be determined and therefore missing. These data points were not replaced but are left blank. For lesional skin it was in a few cases not possible to obtain 4 tape strips. In that case we used merely 2 or 3 tapes. This is one of the reasons why we do not report absolute data on the lipid composition, but rather relative values. Another important reason for presenting relative data is because the lipid composition is compared to the lipid organization. The latter is depending on the relative amounts of the former, rather than absolute amounts. We therefore chose for presenting relative data.

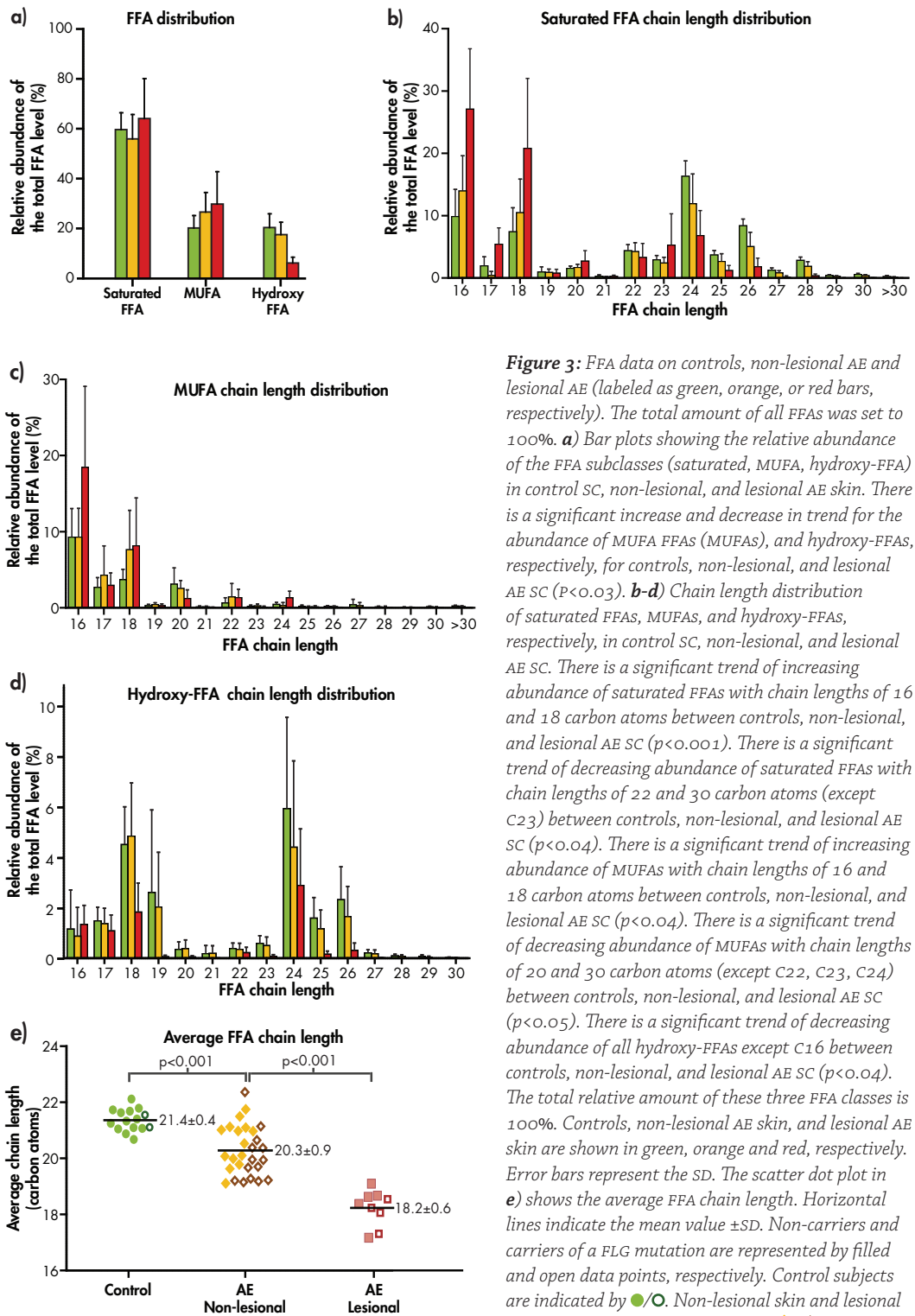


Figure 3: FFA data on controls, non-lesional AE and lesional AE (labeled as green, orange, or red bars, respectively). The total amount of all FFAs was set to 100%. **a)** Bar plots showing the relative abundance of the FFA subclasses (saturated, MUFA, hydroxy-FFA) in control SC, non-lesional, and lesional AE skin. There is a significant increase and decrease in trend for the abundance of MUFA FFAs (MUFAs), and hydroxy-FFAs, respectively, for controls, non-lesional, and lesional AE SC ($p < 0.03$). **b-d)** Chain length distribution of saturated FFAs, MUFAs, and hydroxy-FFAs, respectively, in control SC, non-lesional, and lesional AE SC. There is a significant trend of increasing abundance of saturated FFAs with chain lengths of 16 and 18 carbon atoms between controls, non-lesional, and lesional AE SC ($p < 0.001$). There is a significant trend of decreasing abundance of saturated FFAs with chain lengths of 22 and 30 carbon atoms (except C23) between controls, non-lesional, and lesional AE SC ($p < 0.04$). There is a significant trend of increasing abundance of MUFAs with chain lengths of 16 and 18 carbon atoms between controls, non-lesional, and lesional AE SC ($p < 0.04$). There is a significant trend of decreasing abundance of MUFAs with chain lengths of 20 and 30 carbon atoms (except C22, C23, C24) between controls, non-lesional, and lesional AE SC ($p < 0.05$). There is a significant trend of decreasing abundance of all hydroxy-FFAs except C16 between controls, non-lesional, and lesional AE SC ($p < 0.04$). The total relative amount of these three FFA classes is 100%. Controls, non-lesional AE skin, and lesional AE skin are shown in green, orange and red, respectively. Error bars represent the SD. The scatter dot plot in **e)** shows the average FFA chain length. Horizontal lines indicate the mean value \pm SD. Non-carriers and carriers of a FLG mutation are represented by filled and open data points, respectively. Control subjects are indicated by \bullet/\circ . Non-lesional skin and lesional skin of AE patients are indicated by \blacklozenge/\lozenge and \blacktriangle/\triangle .

Results

Altered FFA composition in SC of AE patients

AE patients showed – in both lesional and non-lesional skin – an increase in MUFAs at the expense of hydroxy-FFAs (Figure 3a), whereas the total level of saturated (non-hydroxy) FFAs was unchanged. In lesional skin, changes in levels of the various FFA subclasses are more pronounced than in non-lesional skin. For the saturated FFAs, the chain length distribution is notably changed: very long chain FFAs (≥ 24 carbon atoms) were strongly reduced whereas shorter FFAs – in particular C16:0 and C18:0 – were increased (Figure 3b). These changes in FFA chain length distribution were more pronounced in lesional SC, but already of significance in non-lesional skin. The MUFAs showed higher levels of short FFAs C16:1 and C18:1 in non-lesional and lesional skin compared to the control (Figure 3c). Hydroxy-FFAs ≥ 18 carbon atoms were decreased, predominantly in lesional skin (Figure 3d). All these changes resulted in a significantly decrease in average FFA chain length in non-lesional as well as lesional AE skin compared to controls (20.3 ± 0.9 , 18.2 ± 0.6 and 21.4 ± 0.4 carbon atoms, respectively, $P < 0.001$, Figure 3e). FFA profiles of AE patients from both lesional and non-lesional skin were compared per subject (pairing), and the

Parameters	Control		P-value
	Noncarriers (n=13)	FLG mutation (n=2)	
TEWL	6.5±1.7	6.5±1.6	0.933
FTIR Scissoring Bandwidth	11.6±0.9	11.4±0.2	0.410
FTIR Stretching peak position	2848.8±0.2	2848.6±0.1	0.305
NMF levels	1.064±0.217	0.98±0.042	0.800
Average CER chain length	47.0±0.7	47.4±1.0	0.549
Average FFA chain length	22.6±0.9	22.6±0.3	0.933
Abundance of MUFAs	0.129±0.081	0.123±0.055	0.933
Acyl-CERs total	9.3±2.6	11.6±2.6	0.361
C34 CERs total	0.87±0.16	0.90±0.76	>0.99

Table I: Influence of loss-of-function FLG mutations on several parameters related to lipid parameters or the skin barrier function.

Parameters	AE - Non-lesional			AE - Lesional		
	Noncarriers (n=14)	FLG mutation (n=14)	P-value	Noncarriers (n=6)	FLG mutation (n=5)	P-value
TEWL	11.4±6.8	13.1±6.2	0.246	25.7±12.1	29.8±12.0	0.662
FTIR Scissoring Bandwidth	11.1±1.1	10.1±1.4	0.089	10.5±0.8	7.8±1.8	0.016
FTIR Stretching peak position	2849.0±0.5	2849.3±0.4	0.052	2849.2±0.3	2849.8±0.6	0.151
NMF levels	0.875±0.431	0.451±0.195	0.008	0.454±0.18	0.37±0.168	0.662
Average CER chain length	46.5±0.8	46.3±0.6	0.603	45.0±2.1	43.4±2.4	0.413
Average FFA chain length	21.2±1.1	21.2±1.7	0.701	19.2±1.7	19.3±2.2	0.841
Abundance of MUFAs	0.184±0.091	0.203±0.081	0.329	0.205±0.087	0.225±0.144	0.841
Acyl-CERs total	8.3±2.9	8.0±2.0	0.713	4.0±0.9	5.8±3.4	0.556
C34 CERs total	1.62±0.95	2.04±0.68	0.066	6.38±2.55	7.11±1.82	>0.99

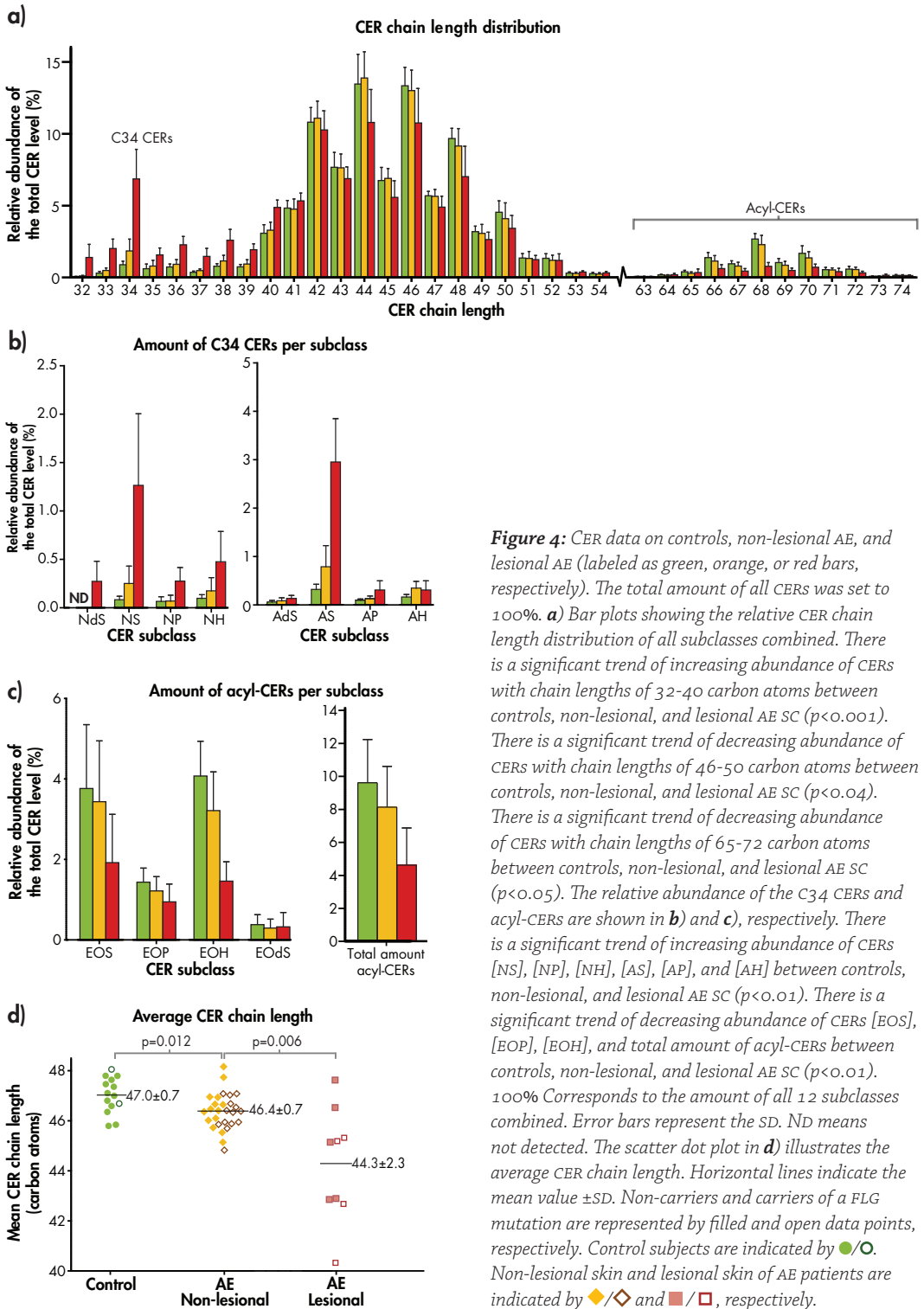
average FFA chain length was always lower in lesional skin compared to non-lesional skin (Supplementary Figure 2). No effects were observed of *FLG* mutation status on the FFA composition, neither in the FFA chain length, nor in the abundance of hydroxy-FFAs or MUFAs ($P > 0.1$, Table I).

Altered CER chain length in SC of AE patients

We compared changes in the FFA composition of AE patients in both lesional and non-lesional sites to changes in CER composition. Of all CER subclasses, the overall CER chain length distribution was determined in non-lesional and lesional skin (Figure 4a). Chain lengths of all CER subclasses showed a broad distribution mainly between 32 and 54 carbon atoms. The only exceptions were the acyl-CERs, which showed a range between 64 and 74 carbon atoms. This is mainly due to the additional fatty acid moiety attached to the CER. In AE patients, the level of long chain CERs (>42 carbon atoms) was reduced and the level of short chain CERs (<42 carbon atoms) was increased. Differences are most pronounced for lesional skin, but were also significantly altered in non-lesional skin. Among the short CERs, in particular the CERs with 34 carbon atoms (C₃₄ CERs) are increased in AE (Figure 4b). To obtain more information on which CER subclasses were involved in this strong increase in C₃₄ CERs, we also analyzed the level of all CER subclasses. The relative abundance of the 12 individual CER subclasses (see Figure 1) in lesional skin were combined with those in non-lesional skin previously reported³⁷. The most prominent changes in lesional skin are an increase in CER [NS] and CER [AS], and a decrease in CER [NP] (Supplementary Figure 3). The CER chain length distribution shows a progressive increase in C₃₄ CERs, predominantly in the CER [NS] and CER [AS] subclasses, and a reduction of almost 50% was observed for the long chain acyl-CERs in lesional AE SC (see Figures 4b and 4c). Together, this results in a significant reduction of the average CER chain length in both in non-lesional and lesional AE SC, compared to controls ($P < 0.012$, Figure 4d).

A direct intra-subject comparison (paired statistics) between lesional and non-lesional skin from the same patient showed a lower average CER chain length in lesional skin as compared to the non-lesional skin sites (Supplementary Figure 2). Since we also observed this trend for the FFAs, we calculated the total lipid chain length and compared lesional skin with non-lesional skin sites (Figure 5). From these paired observations we noticed for each individual a reduction in total lipid chain length at lesional skin sites compared to non-lesional skin sites.

No indications were found that *FLG* mutations have an effect on the lipid composition in AE patients (Table I). No significant changes were observed between subjects with and



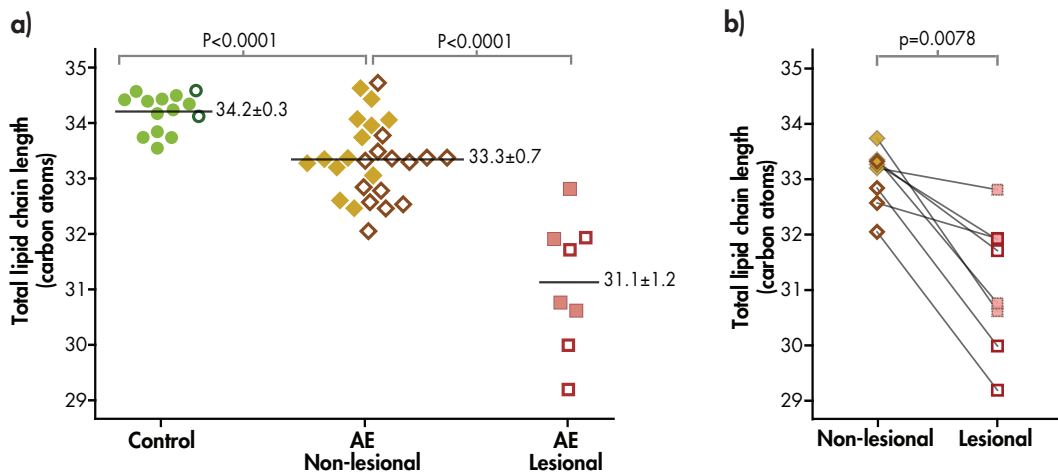


Figure 5: a) Dot plots of the calculated total lipid chain length (FFAs + CERS) for all three groups: control, AE – non-lesional, and AE – lesional. Non-carriers and carriers of a *FLG* mutation are represented by filled and open data points, respectively. Control subjects are indicated by ●/○. Non-lesional skin and lesional skin of AE patients are indicated by ◆/◇ and ■/□, respectively. **b)** Paired plot of the calculated total lipid chain length of a selected subset of patients from which both non-lesional and lesional skin was analyzed.

without a *FLG* mutation for either lesional and non-lesional skin: neither in the level of acyl-CERS ($P > 0.1$), nor in the average CER chain length ($P > 0.1$), nor in the total level of C34 CERS ($P > 0.1$).

Relationship between FFA and CER composition

As presented in Table II, the average CER chain length correlated to the average FFA chain length ($r = 0.60$, $P < 0.001$). More precisely, a high abundance of short chain FFAs (<23 carbon atoms) is accompanied by a high abundance of short chain CERS (<42 carbon atoms), whereas an increased presence of long chain FFAs (>23 carbon atoms) correlates to an increase in long chain CERS (>42 carbon atoms), as illustrated by the correlation map in Supplementary Figure 4 and in Supplementary Table II.

Correlated Parameters	Correlation coefficient
Average CER chain length versus average FFA chain length	0.596*
Average CER chain length versus stretching peak position	-0.567*
Average CER chain length versus scissoring bandwidth	0.517*
Average FFA chain length versus stretching peak position	-0.683*
Average FFA chain length versus scissoring bandwidth	0.727*

Table II: Spearman correlation coefficients of lipid composition and lipid organization parameters.

Altered lipid composition in AE patients corresponds to a less ordered lipid organization

We investigated whether the observed changes in SC lipid composition in AE affect the lipid organization in these patients. The lateral lipid organization was assessed by attenuated total reflectance (ATR) FTIR spectroscopy, primarily focusing on lesional skin of AE patients. Principles of ATR-FTIR measurements are explained in the materials and methods section. The stretching peak position in AE patients was located at a higher wavenumber compared to control subjects in both non-lesional as well as lesional AE SC ($P < 0.001$; Figure 6a). This indicates that the organization of SC lipids in AE patients is less ordered compared to control subjects. The difference in stretching peak position between lesional and non-lesional skin was not significant ($P = 0.083$).

To obtain information about the hexagonal or orthorhombic organization of SC lipids, the scissoring bandwidth was determined. Lesional SC of AE patients shows a scissoring bandwidth of $9.1 \pm 1.9 \text{ cm}^{-1}$, which is significantly lower than the bandwidth in non-lesional skin of AE patients ($10.6 \pm 1.3 \text{ cm}^{-1}$) and in control skin ($11.6 \pm 0.8 \text{ cm}^{-1}$; $P < 0.001$; Figure 6b). This indicates that the subpopulations of lipids in a highly ordered orthorhombic phase are less dominantly present in lesional skin in AE compared to non-lesional skin of AE patients and control subjects.

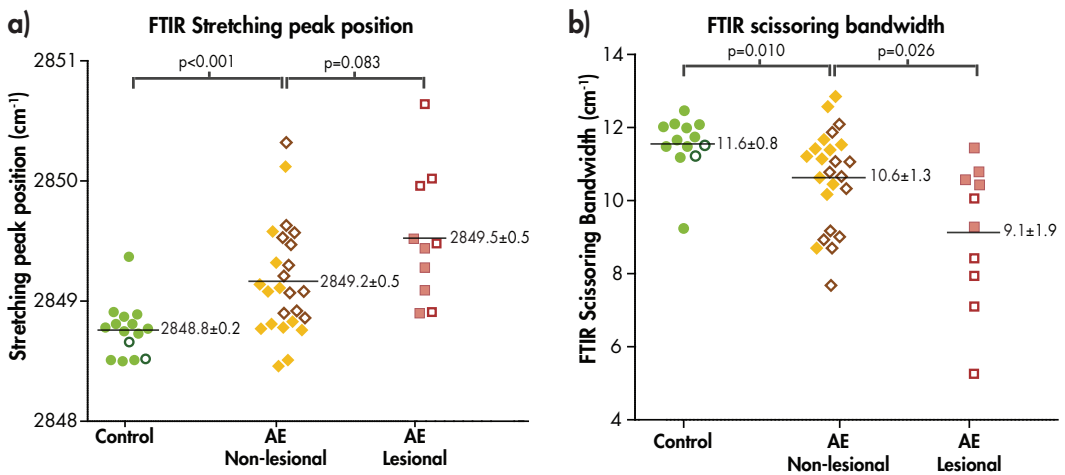


Figure 6: Scatter dot plots of **a)** the FTIR CH₂ stretching peak position and **b)** the FTIR CH₂ scissoring bandwidth for all three groups: control, AE – non-lesional, and AE – lesional. Non-carriers and carriers of a FLG mutation are represented by filled and open data points, respectively. Control subjects are indicated by ●/○. Non-lesional skin and lesional skin of AE patients are indicated by ◆/◇ and ■/□, respectively.

Regarding the influence of *FLG* mutations, a significant difference was observed for the scissoring bandwidth in lesional skin between AE patients with and without a *FLG* mutation: $P=0.016$. This was not found for the stretching peak position ($P>0.05$).

Table II shows that the average CER chain lengths correlate to a high extent with the change in lateral lipid ordering ($|r|>0.51$; $P<0.001$), and the correlation of FFA chain length with the change in lateral lipid ordering is even stronger ($|r|>0.68$; $P<0.001$). Supplemental Figures 5a and b show this correlation between FFA chain length and FTIR bandwidth in more detail ($r=0.73$; $P<0.001$): It becomes clear that FFAs with chain lengths ≤ 20 relate to a lower FTIR bandwidth (more hexagonal lipid organization) whereas FFAs with chain lengths ≥ 24 associates with a higher FTIR bandwidth and therefore more orthorhombic lipid organization.

Skin barrier function shows a high affinity with lipid chain length and lipid ordering

Supplemental Figure 6 shows that the TEWL is significantly increased in non-lesional as well as lesional AE SC compared to controls (12.2 ± 6.5 g/m²/h, 27.6 ± 11.6 g/m²/h, 6.5 ± 1.7 g/m²/h, respectively, $P<0.0005$). Figure 7a shows that the increase in TEWL associates very well with the average lipid chain length: a reduction in average chain length corresponds to an increase in TEWL ($r=-0.80$, $P<<0.001$). Short lipid chain FFAs and CERs (<20 and <41 carbon atoms, respectively) correlate positively with TEWL, whereas long lipid chains (>23 and >42 carbon atoms for FFAs and CERs, respectively) are negatively correlated (Figures 7b and c). Also for the lipid organization a high correlation with TEWL was observed for both the scissoring bandwidth and the stretching peak position (Figure 7d and e): a decrease in lipid ordering corresponds to an increase in TEWL.

Discussion

As there is increasing evidence that SC lipids play a role in the impaired barrier function of AE^{7,27}, we investigated the lipid chain length distribution in SC of AE patients, focusing on FFAs. In addition, we examined the CER composition in lesional skin in these patients. A clear shift to shorter SC lipid chain lengths was observed in AE patients for both CERs and FFAs. Short chain FFAs (≤ 20 carbon atoms) showed a negative correlation with FTIR bandwidth and long chain FFAs (≥ 24 carbon atoms) showed a positive correlation with FTIR bandwidth. Previous *in vitro* studies with lipid model systems have shown that the formation of the hexagonal organization is strongly enhanced by a decreased FFA chain length⁵⁴. This leads to the conclusion that the FFA chain length is an important determinant for the lipid organization in AE: short chain FFAs enhance the formation of a hexagonal lipid organization whereas long chain FFAs enhance the formation of an

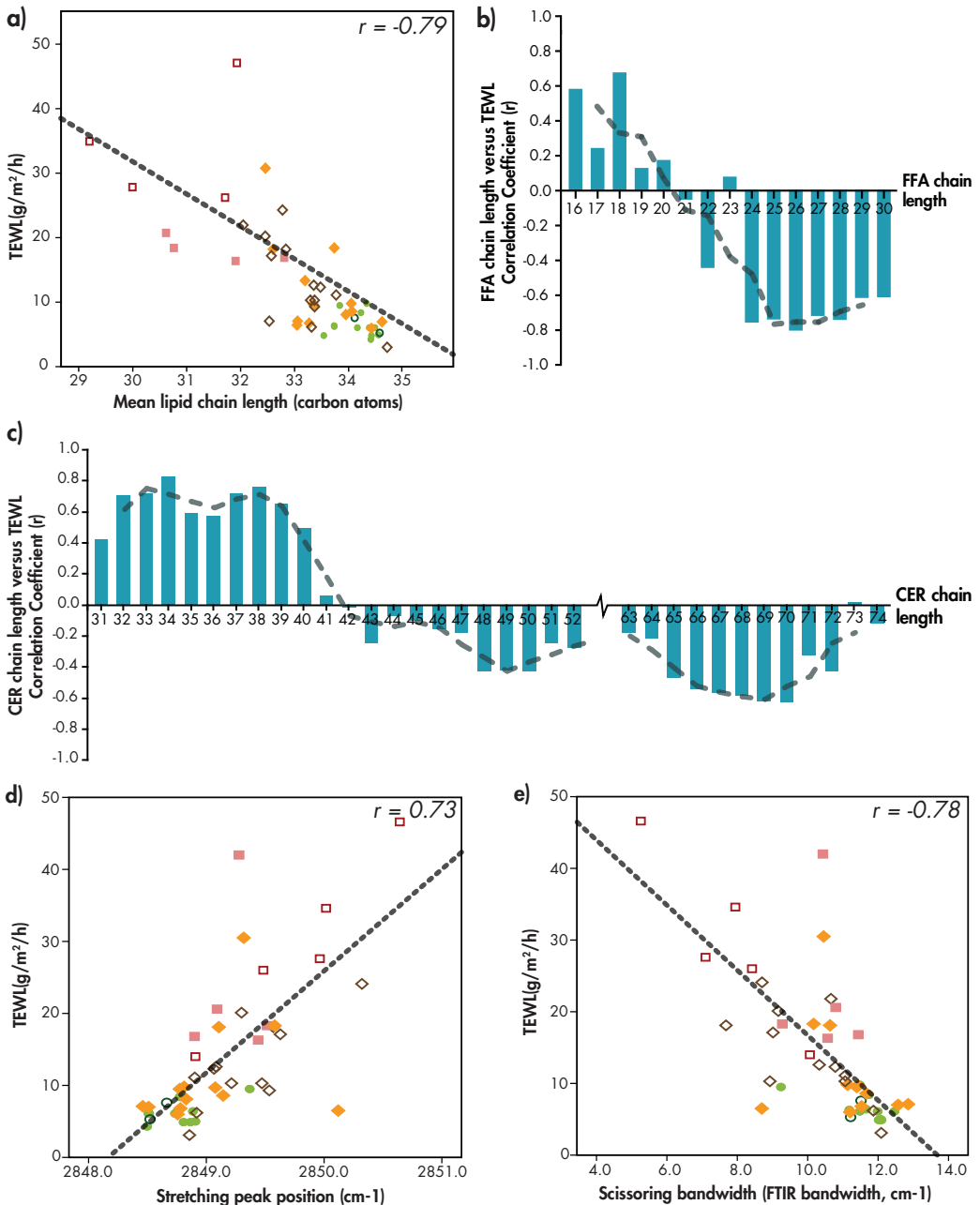


Figure 7: **a)** Correlation plot in which the lipid chain length of all individual subjects is plotted versus the TEWL. The dashed line indicates the optimal fit through the data. **b)** and **c)** present bar plots in which each individual chain length of respectively FFAs and CERs is plotted versus their respective spearman correlation coefficients with TEWL. The dashed line indicates the moving average (period = 3). **d)** and **e)** are correlation plots of the TEWL vs either the stretching peak position or the scissoring bandwidth, respectively. The dashed lines indicate the optimal fit through the data. Non-carriers and carriers of a FLG mutation are represented by filled and open data points, respectively. Control subjects are indicated by \bullet/\circ . Non-lesional skin and lesional skin of AE patients are indicated by \blacklozenge/\lozenge and \blacksquare/\square , respectively. Concerning the correlation plots, spearman correlation coefficients are plotted in the upper right corner.

orthorhombic lipid organization. Furthermore, we observed an increased level of MUFAs in SC of AE patients, which also correlated to the presence of a hexagonal lipid organization in *in vitro* studies (unpublished results).

The reduction in FFA chain length matches the presence of shorter CERS: AE patients showed a shift from long chain CERS (≥ 43 carbon atoms) towards short chain CERS (≤ 42 carbon atoms). It has been reported that the sphingosine base in CERS is on average about 18-20 carbon atoms long⁵². Using these numbers in estimating the acyl chain length in the CERS, our results suggest that CERS having an approximate acyl chain length of ≥ 23 carbon atoms (42 minus 18-20 carbon atoms) are decreased in SC of AE patients. This matches our observations in the decreased levels of FFAs > 23 carbon atoms. In addition, the high levels of C₃₄ CERS in AE patients correspond to an acyl chain length similar to the 16 carbon atoms of the FFAs. The level of this particular FFA is also highly elevated in these patients. These correlations between CERS and FFAs demonstrate for the first time that the acyl chain length in CERS correlates with the FFA chain length, which is a strong argument for a common synthetic pathway^{42,43}.

The reduction in long chain FFAs corresponds to a reduction in long-chain acyl-CER levels in AE. These acyl-CERS are also crucial for a proper organization of the lipids: *in vitro* studies have shown that a reduced level of acyl-CERS results in a less thermostable orthorhombic organization⁵³. The decreased amount of acyl-CERS in AE patients could also play an important role in the reduced skin barrier function, as permeability studies have shown that lower levels of acyl-CERS results in increased permeation⁵⁴, or could even lead to neonatal death by epidermal dehydration in mice completely lacking acyl-CERS⁴⁰. Therefore, not only the changes in FFA composition, but also reduced levels of acyl-CERS may contribute to the increased hexagonal organization and impaired skin barrier function in AE.

TEWL is a commonly accepted measure of skin barrier integrity. The results demonstrate that the increase in TEWL is strongly associated with the decreased lipid chain length. In other words, an increased abundance of short lipid chains contributes to an increased TEWL in AE, whereas an increased presence of long chain lipids correspond to lower TEWL values. In addition, the increased TEWL values observed in AE patients show a strong association with the altered lipid organization in AE. This raises the question whether the changes in lipid chain length are causative for the changes in lipid organization and increased TEWL. Previous *in vitro* studies by Groen *et al.* with model lipid membranes demonstrate that a shorter FFA chain length leads to an increased permeability of benzoic acid⁵¹.

These findings provide new fundamental insights for possible barrier repair: the

presence of long-chain lipids may be crucial for the lipid organization and therefore a proper skin barrier function. A possible treatment to compensate for the reduced long chain lipids may therefore focus on topical application of long-chain lipids. Our observed relation between the FFAs and CERs also imply that normalization of the FFA chain length distribution in AE skin will also contribute to normalization of the CER chain length distribution in these patients. As discussed below, most probably the elongase enzyme family will play an important role here.

One of the challenges is to unravel the changes in the biochemical synthesis of the lipids that are responsible for the altered SC lipid composition in AE, as this may result in new targets for normalizing the skin barrier function. The shift to a shorter FFA chain length distribution suggests that FFA elongation is hampered to some extent. It is known that elongation of FFAs $\geq C16$ occurs by a series of elongases, ELOVL 1-7⁵⁵, all having a certain selection towards a specific FFA chain length⁴³. Currently, little is known about these elongases in the epidermis. It has been reported that ELOVL 1, 3, 4 and 6 are expressed in mammalian skin⁵⁶. Only ELOVL4 is identified in the epidermis on a protein level and plays a crucial role in the elongation of FFAs $\geq C24$ ^{40,57}. Our data on AE shows a decrease in FFAs $\geq C24$, from which we hypothesize that the ELOVL4 protein level and/or activity may be decreased in AE patients. Although no information has been reported on humans with respect to AE, two studies in ELOVL4 knockout mice demonstrate a strong reduction in very long chain FFAs, supporting our hypothesis^{40,58}. In addition, the loss of functional ELOVL4 in mice has been related to a reduced level of hydroxy-FFAs, in particular long chain hydroxy-FFAs⁴⁰. Interestingly, in our study a reduced level of hydroxy-FFAs is also observed. As we also observed increased levels in FFAs with 16 and 18 carbons, ELOVL6 and ELOVL1 – which are the major enzymes involved in elongation of respectively FFAs $> C16$ and FFAs $> C18$ – may also be reduced in activity in the epidermis of patients with AE. Furthermore, if the elongation of these short chain FFAs is hampered, an alternative metabolic pathway may also become more important. This pathway involves the synthesis of MUFAs by stearoyl-CoA desaturases (SCDs)⁵⁹. Indeed an increased level of MUFAs with chain lengths of 16 and 18 carbon atoms is observed in SC of AE patients that may be caused by an increased activity of SCD. Another aspect that should be considered is the importance of the sebaceous lipids in relationship to the SC barrier. Previous studies have reported an altered level of sebaceous lipids in AE, which may affect the SC barrier function in these patients⁶⁰⁻⁶².

Eleven AE patients had both lesional and non-lesional sites at their ventral forearms. We could therefore perform an intra-subject comparison of non-lesional and lesional skin. The shift to shorter FFA and CER chain lengths was more pronounced in lesional

skin compared to non-lesional skin. These changes in lipid composition can mainly be attributed to inflammation, although increased levels of cutaneous microbes (e.g. *Staphylococcus aureus*), genetic mosaicism¹⁸ or environmental factors could also play a role. Cytokines, which play a role in inflammation, are capable of interfering to a large extent with the lipid synthesis in multiple ways: they have shown to be involved in i) reduced levels of enzymes involved in CER synthesis (e.g. β -glucocerebrosidase and acid sphingomyelinase), thereby affecting the CER composition⁶³; ii) peroxisome proliferator-activated receptors (PPARs), which are closely related to the skin lipid metabolic pathway and show a relation to AE⁶⁴: PPAR- α and PPAR- β/δ are respectively down- and upregulated in AE patients^{65,66}. These nuclear receptors promote SC barrier formation and are suggested to have anti-inflammatory properties in skin⁶⁷⁻⁷⁰; iii) TNF- α and several other cytokines, which downregulate filaggrin expression⁷¹⁻⁷³. This may result in lower NMF levels thereby affecting the local pH. It has been suggested that such a pH change may alter the lipid synthesis in the epidermis⁷⁴. This is emphasized by the importance of environmental factors that can also raise the pH of the skin, of which washing the skin with soap and other detergents may be the most important one^{75,76}.

Downregulation of filaggrin expression may be a factor interfering with *FLG* mutations and lipid parameters. This can explain the absence of a correlation between *FLG* mutations and lipid parameters. This suggests that mutations in the *FLG* genotype have no direct effect on the metabolic skin lipid pathways, but can indirectly affect these pathways via the filaggrin breakdown products (NMF)³⁷³⁷. Most enzymes involved in lipid synthesis are pH dependent, and changes in NMF levels caused by *FLG* mutations may therefore indirectly lead to a dysfunction in lipid synthesis and skin barrier function.

Summarizing, we analyzed the SC lipid chain length distribution in non-lesional and lesional skin of AE patients. The results demonstrate an increased presence of short chain FFAs and a decreased presence of long-chain FFAs in SC of AE patients. These changes are in line with the changes observed for the CERs, and lead to an altered lipid organization and decreased skin barrier function in AE. The outcomes of this study do not only give more insights in fundamental SC lipid knowledge, but also suggest possible new targets for future drug therapy for both lesional and non-lesional AE skin.

Acknowledgements

This research is supported by the Dutch Technology Foundation STW, which is part of the Netherlands Organisation for Scientific Research (NWO), and which is partly funded by the Ministry of Economic Affairs. The authors acknowledge Evonik for provision of the synthetic CERs.

References

- 1 Alanne S, Nermes M, Soderlund R *et al*. Quality of life in infants with atopic dermatitis and healthy infants: a follow-up from birth to 24 months. *Acta Paediatr* 2011; 100: e65-70.
- 2 Mozaffari H, Pourpak Z, Poursayed S *et al*. Quality of life in atopic dermatitis patients. *J Microbiol Immunol Infect* 2007; 40: 260-4.
- 3 Slattery MJ, Essex MJ, Paletz EM *et al*. Depression, anxiety, and dermatologic quality of life in adolescents with atopic dermatitis. *J Allergy Clin Immunol* 2011; 128: 668-71 e3.
- 4 van Valburg RW, Willemsen MG, Dirven-Meijer PC *et al*. Quality of life measurement and its relationship to disease severity in children with atopic dermatitis in general practice. *Acta Derm Venereol* 2011; 91: 147-51.
- 5 Williams H, Flohr C. How epidemiology has challenged 3 prevailing concepts about atopic dermatitis. *Journal of Allergy and Clinical Immunology* 2006; 118: 209-13.
- 6 Di Nardo A, Wertz P, Giannetti A *et al*. Ceramide and cholesterol composition of the skin of patients with atopic dermatitis. *Acta Derm Venereol* 1998; 78: 27-30.
- 7 Elias PM, Schmutz M. Abnormal skin barrier in the etiopathogenesis of atopic dermatitis. *Current Opinion in Allergy and Clinical Immunology* 2009; 9: 437-46.
- 8 Seidenari S, Giusti G. Objective assessment of the skin of children affected by atopic dermatitis: A study of pH, capacitance and TEWL in eczematous and clinically uninvolved skin. *Acta Dermato-Venereol* 1995; 75: 429-33.
- 9 Werner Y, Lindberg M. Transepidermal water loss in dry and clinically normal skin in patients with atopic dermatitis. *Acta Derm Venereol* 1985; 65: 102-5.
- 10 Yoshiike T, Aikawa Y, Sindhvananda J *et al*. Skin barrier defect in atopic dermatitis: increased permeability of the stratum corneum using dimethyl sulfoxide and theophylline. *J Dermatol Sci* 1993; 5: 92-6.
- 11 Feingold KR, Jiang YJ. The mechanisms by which lipids coordinately regulate the formation of the protein and lipid domains of the stratum corneum: Role of fatty acids, oxysterols, cholesterol sulfate and ceramides as signaling molecules. *Dermato-endocrinology* 2011; 3: 113-8.
- 12 Addor FA, Aoki V. Skin barrier in atopic dermatitis. *An Bras Dermatol* 2010; 85: 184-94.
- 13 Elias PM, Schmutz M. Abnormal skin barrier in the etiopathogenesis of atopic dermatitis. *Current Allergy and Asthma Reports* 2009; 9: 265-72.
- 14 Palmer CN, Irvine AD, Terron-Kwiatkowski A *et al*. Common loss-of-function variants of the epidermal barrier protein filaggrin are a major predisposing factor for atopic dermatitis. *Nat Genet* 2006; 38: 441-6.
- 15 Sandilands A, Terron-Kwiatkowski A, Hull PR *et al*. Comprehensive analysis of the gene encoding filaggrin uncovers prevalent and rare mutations in ichthyosis vulgaris and atopic eczema. *Nat Genet* 2007; 39: 650-4.
- 16 Brown SJ, McLean WH. One remarkable molecule: filaggrin. *The Journal of investigative dermatology* 2012; 132: 751-62.
- 17 Sandilands A, Sutherland C, Irvine AD *et al*. Filaggrin in the frontline: role in skin barrier function and disease. *Journal of cell science* 2009; 122: 1285-94.
- 18 Brown SJ, Irvine AD. Atopic eczema and the filaggrin story. *Seminars in Cutaneous Medicine and Surgery* 2008; 27: 128-37.
- 19 Mao-Qiang M, Fowler AJ, Schmutz M *et al*. Peroxisome-proliferator-activated receptor (PPAR)-gamma activation stimulates keratinocyte differentiation. *The Journal of investigative dermatology* 2004; 123: 305-12.
- 20 Jakasa I, Koster ES, Calkoen F *et al*. Skin barrier function in healthy subjects and patients with atopic dermatitis in relation to filaggrin loss-of-function mutations. *J Invest Dermatol* 2011; 131: 540-2.
- 21 Angelova-Fischer I, Mannheimer AC, Hinder A *et al*. Distinct barrier integrity phenotypes in filaggrin-related atopic eczema following sequential tape stripping and lipid profiling. *Exp Dermatol* 2011; 20: 351-6.
- 22 Jungersted JM, Scheer H, Mempel M *et al*. Stratum corneum lipids, skin barrier function and filaggrin mutations in patients with atopic eczema. *Allergy* 2010; 65: 911-8.
- 23 Flohr C, England K, Radulovic S *et al*. Filaggrin loss-of-function mutations are associated with early-onset eczema, eczema severity and transepidermal water loss at 3 months of age. *Br J Dermatol* 2010; 163: 1333-6.
- 24 Proksch E, Folster-Holst R, Jensen JM. Skin barrier function, epidermal proliferation and differentiation in eczema. *J Dermatol Sci* 2006; 43: 159-69.
- 25 Elias PM, Menon GK. Structural and lipid biochemical correlates of the epidermal permeability barrier. *Adv Lipid Res* 1991; 24: 1-26.
- 26 Jiang YJ, Lu B, Kim P *et al*. PPAR and LXR activators regulate ABCA12 expression in human keratinocytes. *The Journal of investigative dermatology* 2008; 128: 104-9.
- 27 Proksch E, Jensen JM, Elias PM. Skin lipids and epidermal differentiation in atopic dermatitis. *Clin Dermatol* 2003; 21: 134-44.
- 28 Wertz PW. Lipids and barrier function of the skin. *Acta Derm Venereol Suppl* (Stockh) 2000; 208: 7-11.
- 29 van Smeden J, Hoppel L, van der Heijden R *et al*. LC/MS analysis of stratum corneum lipids: ceramide profiling and discovery. *J Lipid Res* 2011; 52: 1211-21.
- 30 Coderch L, Lopez O, de la Maza A *et al*. Ceramides and skin function. *Am J Clin Dermatol* 2003; 4: 107-29.
- 31 Downing DT, Stewart ME, Wertz PW *et al*. Skin lipids: an update. *J Invest Dermatol* 1987; 88: 28-68.
- 32 Bouwstra JA, Gooris GS, van der Spek JA *et al*. Structural investigations of human stratum corneum by small-angle X-ray scattering. *J Invest Dermatol* 1991; 97: 1005-12.
- 33 Madison KC, Swartzendruber DC, Wertz PW *et al*. Presence of intact intercellular lipid lamellae in the upper layers of the stratum corneum. *J Invest Dermatol* 1987; 88: 714-8.
- 34 Bommannan D, Potts RO, Guy RH. Examination of stratum corneum barrier function in vivo by infrared spectroscopy. *J Invest Dermatol* 1990; 95: 403-8.
- 35 Ongpipattanakul B, Francoeur ML, Potts RO. Polymorphism in stratum corneum lipids. *Biochim Biophys Acta* 1994; 1190: 115-22.
- 36 Pilgram GS, Vissers DC, van der Meulen H *et al*. Aberrant lipid organization in stratum corneum of patients with atopic

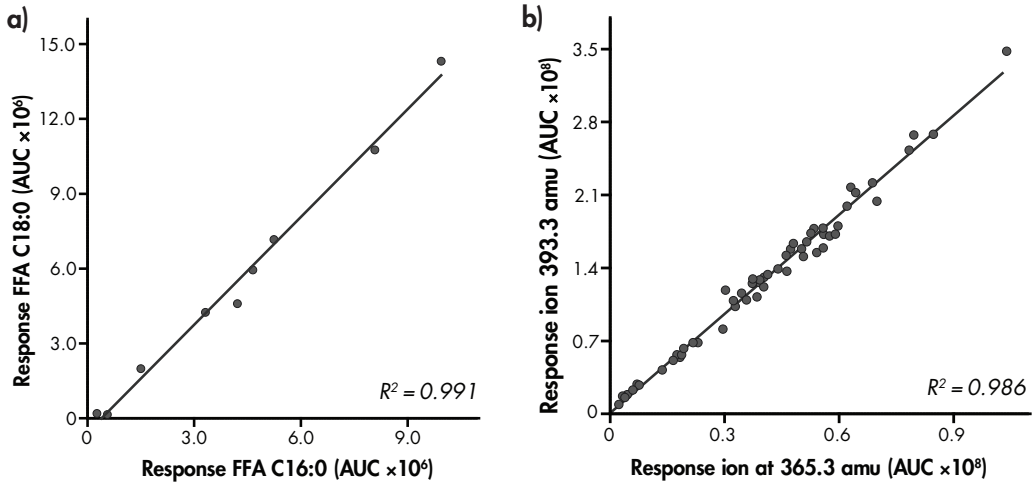
- dermatitis and lamellar ichthyosis. *J Invest Dermatol* 2001; 117: 710-7.
- 37 Janssens M, van Smeden J, Gooris GS *et al*. Increase in short-chain ceramides correlates with an altered lipid organization and decreased barrier function in atopic eczema patients. *J Lipid Res* 2012; 53: 2755-66.
- 38 Ansari MN, Nicolaidis N, Fu HC. Fatty acid composition of the living layer and stratum corneum lipids of human sole skin epidermis. *Lipids* 1970; 5: 838-45.
- 39 Norlen L, Nicander I, Lundsjo A *et al*. A new HPLC-based method for the quantitative analysis of inner stratum corneum lipids with special reference to the free fatty acid fraction. *Arch Dermatol Res* 1998; 290: 508-16.
- 40 Vasireddy V, Uchida Y, Salem N, Jr. *et al*. Loss of functional ELOVL4 depletes very long-chain fatty acids (> =C28) and the unique omega-O-acylceramides in skin leading to neonatal death. *Hum Mol Genet* 2007; 16: 471-82.
- 41 Macheleidt O, Kaiser HW, Sandhoff K. Deficiency of epidermal protein-bound omega-hydroxyceramides in atopic dermatitis. *J Invest Dermatol* 2002; 119: 166-73.
- 42 Ohno Y, Suto S, Yamanaka M *et al*. ELOVL1 production of C24 acyl-CoAs is linked to C24 sphingolipid synthesis. *Proc Natl Acad Sci U S A* 2010; 107: 18439-44.
- 43 Uchida Y. The role of fatty acid elongation in epidermal structure and function. *Dermatoendocrinol* 2011; 3: 65-9.
- 44 Thakoersing VS, Ponec M, Bouwstra JA. Generation of human skin equivalents under submerged conditions-mimicking the in utero environment. *Tissue Eng Part A* 2010; 16: 1433-41.
- 45 Chang SS, Jiang WW, Smith I *et al*. Chronic cigarette smoke extract treatment selects for apoptotic dysfunction and mitochondrial mutations in minimally transformed oral keratinocytes. *International journal of cancer. Journal international du cancer* 2010; 126: 19-27.
- 46 Rivier M, Castiel I, Safonova I *et al*. Peroxisome proliferator-activated receptor-alpha enhances lipid metabolism in a skin equivalent model. *The Journal of investigative dermatology* 2000; 114: 681-7.
- 47 Motta S, Monti M, Sesana S *et al*. Ceramide composition of the psoriatic scale. *Biochim Biophys Acta* 1993; 1182: 147-51.
- 48 Boncheva M, Damien F, Normand V. Molecular organization of the lipid matrix in intact Stratum corneum using ATR-FTIR spectroscopy. *Biochim Biophys Acta* 2008; 1778: 1344-55.
- 49 Damien F, Boncheva M. The extent of orthorhombic lipid phases in the stratum corneum determines the barrier efficiency of human skin in vivo. *J Invest Dermatol* 2010; 130: 611-4.
- 50 Mendelsohn R, Liang GL, Strauss HL *et al*. IR spectroscopic determination of gel state miscibility in long-chain phosphatidylcholine mixtures. *Biophys J* 1995; 69: 1987-98.
- 51 Groen D, Poole DS, Gooris GS *et al*. Is an orthorhombic lateral packing and a proper lamellar organization important for the skin barrier function? *Biochim Biophys Acta* 2011; 1808: 1529-37.
- 52 Masukawa Y, Narita H, Sato H *et al*. Comprehensive quantification of ceramide species in human stratum corneum. *J Lipid Res* 2009; 50: 1708-19.
- 53 de Sousa Neto D, Gooris G, Bouwstra J. Effect of the omega-acylceramides on the lipid organization of stratum corneum model membranes evaluated by X-ray diffraction and FTIR studies (Part I). *Chem Phys Lipids* 2011; 164: 184-95.
- 54 de Jager M, Groenink W, Bielsa i Guivernau R *et al*. A novel in vitro percutaneous penetration model: evaluation of barrier properties with p-aminobenzoic acid and two of its derivatives. *Pharm Res* 2006; 23: 951-60.
- 55 Matsuzaka T, Shimano H, Yahagi N *et al*. Cloning and characterization of a mammalian fatty acyl-CoA elongase as a lipogenic enzyme regulated by SREBPs. *J Lipid Res* 2002; 43: 911-20.
- 56 Guillou H, Zdravec D, Martin PG *et al*. The key roles of elongases and desaturases in mammalian fatty acid metabolism: Insights from transgenic mice. *Prog Lipid Res* 2010; 49: 186-99.
- 57 Li W, Sandhoff R, Kono M *et al*. Depletion of ceramides with very long chain fatty acids causes defective skin permeability barrier function, and neonatal lethality in ELOVL4 deficient mice. *Int J Biol Sci* 2007; 3: 120-8.
- 58 Cameron DJ, Tong Z, Yang Z *et al*. Essential role of Elov14 in very long chain fatty acid synthesis, skin permeability barrier function, and neonatal survival. *Int J Biol Sci* 2007; 3: 111-9.
- 59 Miyazaki M, Ntambi JM. Chapter 7 - Fatty acid desaturation and chain elongation in mammals. In: *Biochemistry of Lipids, Lipoproteins and Membranes (Fifth Edition) (Dennis EV, Jean EV, eds)*. San Diego: Elsevier, 2008; 191-V.
- 60 Yamamoto A, Serizawa S, Ito M *et al*. Stratum corneum lipid abnormalities in atopic dermatitis. *Arch Dermatol Res* 1991; 283: 219-23.
- 61 Abe T, Ohkido M, Yamamoto K. Studies on skin surface barrier functions--skin surface lipids and transepidermal water loss in atopic skin during childhood. *The Journal of dermatology* 1978; 5: 223-9.
- 62 Rajka G. Transepidermal water loss on the hands in atopic dermatitis. *Arch Dermatol Forsch* 1974; 251: 111-5.
- 63 Briot A, Deraison C, Lacroix M *et al*. Kallikrein 5 induces atopic dermatitis-like lesions through PAR2-mediated thymic stromal lymphopoietin expression in Netherton syndrome. *J Exp Med* 2009; 206: 1135-47.
- 64 Sertznig P, Seifert M, Tilgen W *et al*. Peroxisome proliferator-activated receptors (PPARs) and the human skin: importance of PPARs in skin physiology and dermatologic diseases. *Am J Clin Dermatol* 2008; 9: 15-31.
- 65 Staumont-Salle D, Abboud G, Brenuchon C *et al*. Peroxisome proliferator-activated receptor alpha regulates skin inflammation and humoral response in atopic dermatitis. *J Allergy Clin Immunol* 2008; 121: 962-8 e6.
- 66 Plager DA, Leontovich AA, Henke SA *et al*. Early cutaneous gene transcription changes in adult atopic dermatitis and potential clinical implications. *Exp Dermatol* 2007; 16: 28-36.
- 67 Hanley K, Jiang Y, Crumrine D *et al*. Activators of the nuclear hormone receptors PPARalpha and FXR accelerate the development of the fetal epidermal permeability barrier. *J Clin Invest* 1997; 100: 705-12.
- 68 Jiang YJ, Barish G, Lu B *et al*. PPARdelta activation promotes stratum corneum formation and epidermal permeability barrier development during late gestation. *J Invest Dermatol* 2010; 130: 511-9.

- 69 Man MQ, Barish GD, Schmuth M *et al.* Deficiency of PPARbeta/delta in the epidermis results in defective cutaneous permeability barrier homeostasis and increased inflammation. *J Invest Dermatol* 2008; 128: 370-7.
- 70 Schmuth M, Jiang YJ, Dubrac S *et al.* Thematic review series: skin lipids. Peroxisome proliferator-activated receptors and liver X receptors in epidermal biology. *J Lipid Res* 2008; 49: 499-509.
- 71 Kim BE, Howell MD, Guttman-Yassky E *et al.* TNF-alpha downregulates filaggrin and loricrin through c-Jun N-terminal kinase: role for TNF-alpha antagonists to improve skin barrier. *J Invest Dermatol* 2011; 131: 1272-9.
- 72 Hvid M, Vestergaard C, Kemp K *et al.* IL-25 in atopic dermatitis: a possible link between inflammation and skin barrier dysfunction? *J Invest Dermatol* 2011; 131: 150-7.
- 73 Gutowska-Owsiak D, Schaupp AL, Salimi M *et al.* Interleukin-22 downregulates filaggrin expression and affects expression of profilaggrin processing enzymes. *Br J Dermatol* 2011; 165: 492-8.
- 74 Elias PM, Schmuth M. Abnormal skin barrier in the etiopathogenesis of atopic dermatitis. *Curr Opin Allergy Clin Immunol* 2009; 9: 437-46.
- 75 Cork MJ, Robinson D, Vasilopoulos Y *et al.* Predisposition to sensitive skin and atopic eczema. *Community practitioner : the journal of the Community Practitioners' & Health Visitors' Association* 2005; 78: 440-2.
- 76 Mucke H, Mohr KT, Rummeler A *et al.* [Skin pH value on hands after application of soap, cleaners and hand disinfectants]. *Die Pharmazie* 1993; 48: 468-9.

Supplementary data

Quantitative analysis of FFA C16:0 and C18:0, correcting for tape strip contamination
Recently, we developed a method that enables analysis of FFAs by LC/MS, and applied that method on tape-stripped SC. However, endogenous C16:0, C17:0, C18:0, and C18:1 FFAs are abundantly present on control tapes (blanks), thereby interfering with the results. To correct for the amount of these four endogenous lipids on tape, it was not possible to simply subtract a certain amount of these lipids as the tape appeared to be too inhomogeneous for a reliable correction: We observed that the amount could vary ~100 fold. Therefore, a more comprehensive correction method was needed that corrects for these 2 lipids for each individual tape strip.

Although the variation in absolute amounts of endogenous lipids is very high, we observed that the ratio of these lipids is always the same. In example, C16:0 is always linearly correlated to the amount of C18:0, which can be appreciated from Supplementary Figure 1a. We also analyzed two peaks which appear in blank tape strips but not in human SC, possibly exogenous lipids. Again, a very high correlation was observed between the amounts of the two unidentified peaks (Supplementary Figure 1b). The amount of these two lipid peaks also correlates very well (but not perfectly) to the amount of the four endogenous FFAs (Supplementary Table I). Hence, by quantifying the two exogenous lipids on tapes that do not interfere with SC from *in vivo* subjects, we could calculate the predicted amount of endogenous lipids C16:0, C17:0, C18:0, C18:1. Indeed, we were able to successfully correct for the amount of contamination of these lipids. However, we mention that the methodological error does increase since we did not observe perfect correlations: Since the R^2 -values of the correlations are around 0.85-0.95, the expected increment in error is around 10%. Nevertheless, either taking into account or completely leaving out the C16:0 and C18:0 data did not change any of the conclusions that could be drawn from the data.

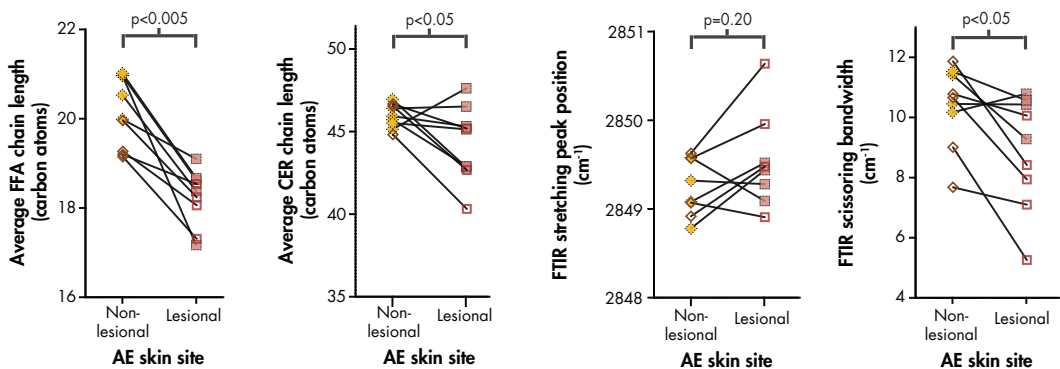


Supplementary Figure 1: Tape strips were analyzed to obtain information on the amount of endogenous lipids that interfere with data from SC lipids, and how to correct for this contamination. Data are presented as scatter dot plots and their correlations of **a)** endogenous FFAs C16:0 versus C18:0 ($R^2=0.991$) analyzed from control tape strips. **b)** Exogenous ions m/z 365.3 amu versus 393.3 amu. Data points include control tape strips as well as tapes from all subjects.

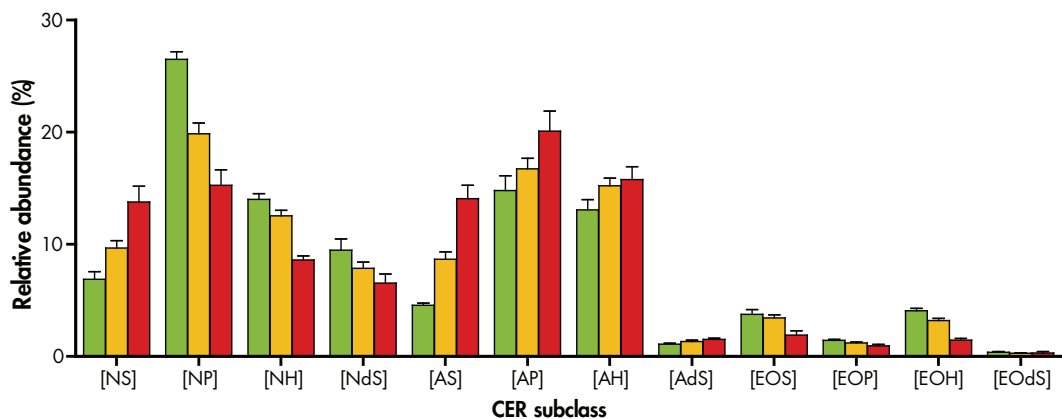
Supplementary Table I: Correlation coefficients (R^2) between the endogenous lipids and the two exogenous lipids.

Endogenous lipid	Correlation Coefficient	
	Exogenous ion 1 ($m/z = 365.3$ amu)	Exogenous ion 2 ($m/z = 393.3$ amu)
C16:0	0.917	0.852
C17:0	0.862	0.855
C18:0	0.942	0.903
C18:1	0.944	0.890

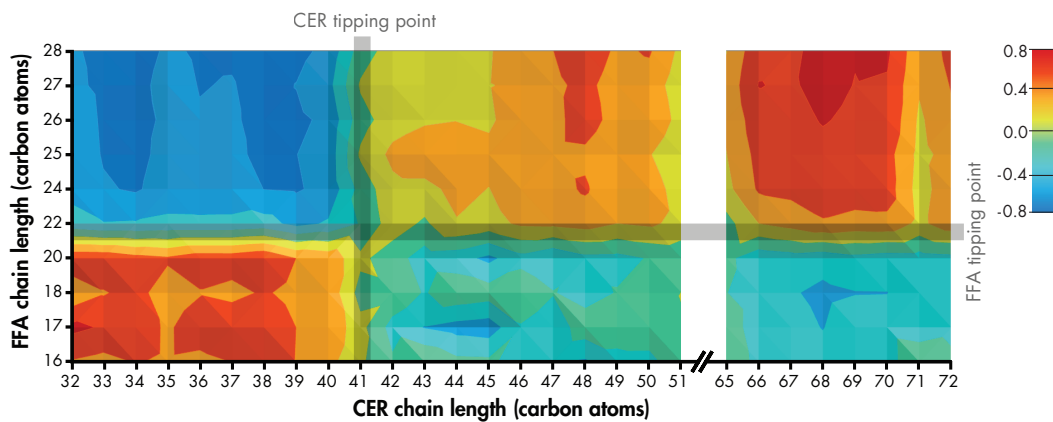
The correlation coefficients state the accuracy in which the amounts of the two exogenous ions (viz. m/z 365.3 and 393.3 amu) are correctly predicting the amount of endogenous lipids related to the tape. In general, exogenous ion 1 was chosen to predict the amount of endogenous lipids, as the correlation coefficient was higher compared to exogenous ion 2.



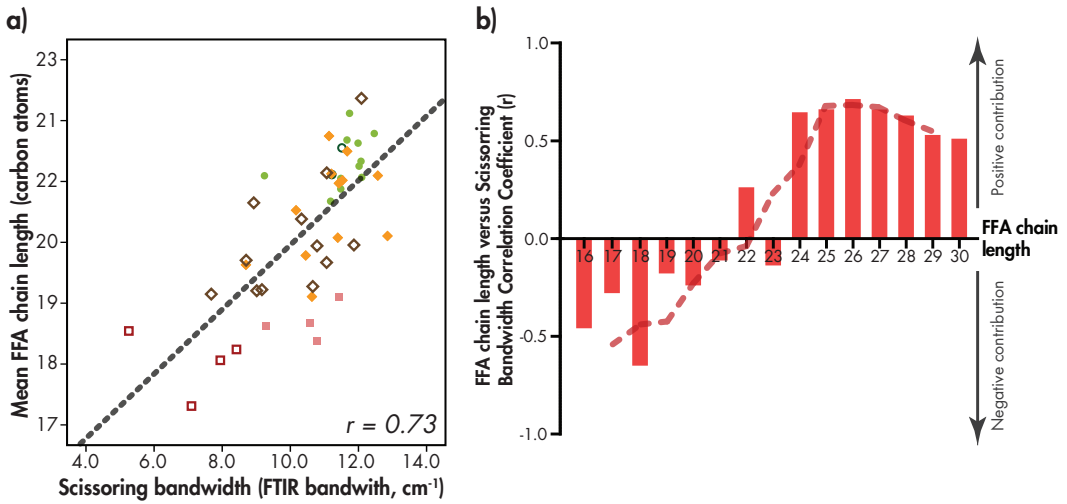
Supplementary Figure 2: Paired data of non-lesional and lesional AE skin for the FFA chain length, CER chain length, FTIR stretching peak position and FTIR bandwidth. P-values are calculated from the Wilcoxon signed rank test. Non-lesional skin and lesional skin of AE patients are indicated by $\blacklozenge/\blacklozenge$ and $\blacksquare/\blacksquare$, respectively. Open and filled data points indicate carriers and non-carriers of FLG mutations, respectively.



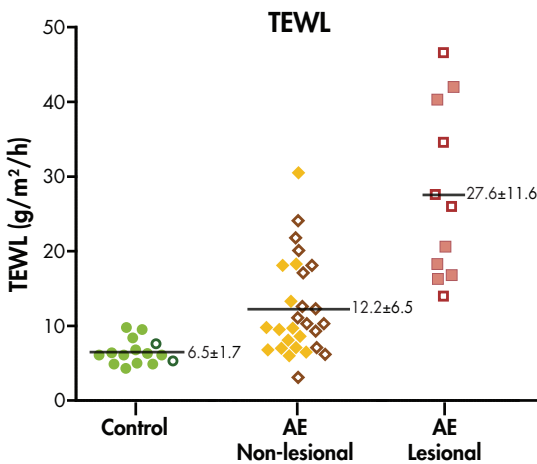
Supplementary Figure 3: Relative CER composition of each subclass for control (green), AE - non-lesional (orange), and AE - lesional (red).



Supplementary Figure 4: Correlation map. On the horizontal axis are the individual CER chain lengths, whereas on the vertical axis are the individual FFA chain lengths. Strong negative or positive correlations are depicted in blue or red, respectively. Gray strokes indicate the tipping point of the chain length correlations; in other words, where positive correlations turn into negative correlations and vice versa.



Supplementary Figure 5: **a)** Correlation plot in which the scissoring bandwidth of all individuals is plotted versus the mean FFA chain length. The gray dashed line indicates the optimal linear fit. Control subjects are indicated by \bullet/\circ . Non-lesional skin and lesional skin of AE patients are indicated by \blacklozenge/\lozenge and \blacksquare/\square , respectively. Open and filled data points indicate carriers and non-carriers of FLG mutations, respectively. **b)** Bar plots demonstrating the correlation between each individual FFA chain length (x-axis) versus the FTIR scissoring bandwidth. Positive correlation coefficients indicate that these FFAs contribute to a more ordered lateral lipid packing, whereas FFAs with negative correlation coefficients contribute to a less ordered packing of the lipids. The dashed line indicates the moving average (period = 3).



Supplementary Figure 6: TEWL levels in control subjects, non-lesional SC and lesional SC of AE patients. Control subjects are indicated by \bullet/\circ . Non-lesional skin and lesional skin of AE patients are indicated by \blacklozenge/\lozenge and \blacksquare/\square , respectively. Open and filled data points indicate carriers and non-carriers of FLG mutations, respectively. Means are indicated by gray horizontal lines and their corresponding values (\pm SD). Significant differences were observed between control subjects, non-lesional, and lesional SC of AE patients ($P < 0.0005$).

Supplementary Table II: Correlations between short/long CERS versus short/long FFAs.

	FFAs <C23	FFAs >C23
CERs <C42	0.496*	-0.541*
CERs >C42	-0.429*	-0.481*

Spearman correlations showing that short CERS correlate positively with short FFAs and negatively with long FFAs, and vice versa for long CERS. *: $P < 0.01$.

CHAPTER 8

LIPID TO PROTEIN RATIO PLAYS AN IMPORTANT ROLE IN THE SKIN BARRIER FUNCTION OF PATIENTS WITH ATOPIC ECZEMA

M. Janssens¹, J. van Smeden¹, G.J. Puppels^{2,3}, A.P.M. Lavrijsen⁴, P.J. Caspers^{2,3}, J.A. Bouwstra¹

¹ Division of Drug Delivery Technology, Leiden Academic Centre for Drug Research, Leiden University, Leiden, The Netherlands.

² Center for Optical Diagnostics and Therapy, Department of Dermatology, Erasmus MC, Rotterdam, The Netherlands.

³ River Diagnostics BV, Rotterdam, The Netherlands.

⁴ Department of Dermatology, Leiden University Medical Center, Leiden, The Netherlands.

Abstract

The barrier function of the skin is primarily provided by the stratum corneum (SC), the outermost layer of the skin. Skin barrier impairment is thought to be a primary factor in the pathogenesis of atopic eczema (AE). Filaggrin is an epidermal barrier protein and common mutations in the filaggrin gene strongly predispose for AE. However, there is no strong evidence that filaggrin mutations are related to the reduced skin barrier in AE. It was recently shown that the SC lipid composition and organization play a role in the reduced skin barrier in AE.

We determined the dry SC mass per surface area of controls and AE patients as well as the ratio between lipid and protein bands in the Raman spectra being a measure for the lipid/protein ratio in SC. The results show that the dry SC mass per skin area is altered only in lesional SC of AE patients compared to control subjects. Much more pronounced was the observed reduction in the lipid/protein ratio in SC of AE patients, both in lesional and non-lesional SC. These changes correlate with the barrier function and may indicate that the lipid/protein ratio plays a role in the reduced skin barrier function in AE.

Introduction

Atopic eczema (AE) is a chronic relapsing, inflammatory skin disease characterized by erythema, pruritus, and xerosis. AE is currently affecting over 15% of Caucasian children and 2-10% of adults, and its prevalence is increasing¹⁻⁴. Eczematous lesions have a red, flaky appearance and cause severe itching. There is increasing evidence that AE is related to an impaired skin barrier function^{5,6}. AE is strongly associated to mutations in the filaggrin gene (*FLG*), encoding the barrier protein filaggrin⁷. Filaggrin has

a role in the alignment of keratin filaments, facilitating the flattening of keratinocytes during terminal cornification⁸. In addition, flaggrin is metabolized into hygroscopic molecules, together with specific salts and sugars referred to as the natural moisturizing factor (NMF), which is important for SC hydration⁹. Despite the fact that an impaired barrier function has been demonstrated in adult AE patients, the precise role of flaggrin for the skin barrier function is not completely understood and compelling evidence that *FLG* mutations are the cause of the reduced barrier function in AE is missing¹⁰⁻¹².

The primary function of the skin is to reduce epidermal water loss and to prevent the penetration of harmful agents by acting as a permeability barrier to the environment. This barrier is provided by the stratum corneum (SC), the outermost layer of the skin. It contains nonviable corneocytes oriented parallel to the skin surface. The corneocytes are surrounded by a cornified cell envelope, consisting of a densely cross-linked layer of proteins. This envelope reduces the uptake of most substances into the corneocytes and therefore redirects the transport of most substances along the intercellular regions¹³. The intercellular regions are filled with highly organized lipids with a characteristic composition and organization. For this reason, lipid composition and organization are considered to be crucial for an adequate skin barrier function. The major lipid classes in the SC are ceramides (CERS), free fatty acids, and cholesterol.

In previous studies, changes have been observed in the CER composition of non-lesional as well as lesional SC of AE patients^{5,14-18}. Changes in several of the CER subclasses correlate with a reduced skin barrier function as measured by transepidermal water loss (TEWL). More recently, strong evidence was observed that besides changes in CER subclasses, the CER chain length plays a prominent role in the impaired barrier function of AE skin: in non-lesional SC of AE patients both CER chain length and skin barrier function were significantly reduced¹⁹.

Besides the lipid composition and organization, the lipid/protein ratio in the SC as well as the SC thickness may affect the skin barrier function. The aim of the present study was to determine the lipid/protein ratio in SC of control subjects and AE patients. In addition, the dry SC mass per surface area was determined, being a measure for the SC thickness. Subsequently, these parameters were related to the barrier function of the skin, as measured by TEWL. The results show that the dry SC mass per surface area is altered in lesional AE SC but not in non-lesional AE SC, as compared to controls. The lipid/protein ratio is lower in both non-lesional and lesional SC in AE compared to that in SC of control subjects. The lipid/protein ratio correlates strongly with TEWL values. Therefore, besides lipid composition and organization, the lipid/protein ratio may be an important factor in the impaired skin barrier function in AE patients.

Materials and Methods

Study population and study setup

The study was approved by the Medical Ethics Committee of the Leiden University Medical Center and conducted in accordance with the Declaration of Helsinki Principles. All subjects gave written informed consent. Twenty-eight Caucasian AE patients (25.6 ± 5.6 years; 11 males) and fifteen Caucasian control subjects without (history of) dermatological disorders (25.0 ± 5.2 years; 5 males) were included. In the AE group, 14 patients were carrier of at least one prevalent *FLG* null allele. At the time of the study, 11 out of 28 AE patients suffered from eczematous lesions on at least one of the ventral forearms. The subjects did not apply any dermatological products to their forearms for at least one week prior to the study. Measurements were performed in a temperature and humidity controlled room, in which the subjects were acclimatized for 45 minutes prior to the measurements. All measurements were performed on a single day. A dermatologist marked an area (~ 4.5 cm²) of non-lesional skin and, if applicable, an area (~ 4.5 cm²) of lesional skin on the forearm of each AE patient at the start of the study day. The Raman spectroscopy measurements were performed on these marked areas. After the Raman measurements, the same skin areas were tape stripped while TEWL was monitored after each two tape strips. At the end of the study day, buccal mucosa cells were collected with a cotton swab for *FLG* genotyping.

FLG mutation analysis

All subjects were screened for any of the four most prevalent mutations found in the European Caucasian population (*2282del4*, *R501X*, *R2447X*, *S3247X*), as described previously¹⁹.

Skin barrier function assessment

TEWL was monitored using a Tewameter TM 210 (Courage+Khazaka, Köln, Germany). The marked area on the subjects' ventral forearm was placed in an open chamber, and TEWL values were recorded for a period of at least two minutes after which an average reading was calculated from the last 10 seconds of the measurement. Recordings were performed prior to tape stripping (baseline TEWL) and after each second tape strip, to assure proper monitoring of the changes in skin barrier function.

Confocal Raman microspectroscopy

Confocal Raman microspectroscopy (3510 Skin Composition Analyzer, River Diagnostics, Rotterdam, The Netherlands) was used to determine the lipid/protein ratio

of the ventral forearm. The principles of Raman spectroscopy and the procedures have been described elsewhere^{20,21}.

Spectra were recorded in the high wavenumber spectral region (2500-4000 cm^{-1}) using a 671 nm laser. The spatial resolution was 5 cm^{-1} . Laser power on the skin was 20 mW. Spectra were obtained from the skin surface to a depth of 40 μm with 2 μm steps. This was repeated on 15 different locations within the marked area. In order to avoid interfering Raman signals from skin surface contamination, such as sebum, and to avoid influences of washout effects and desquamation near the skin surface, as well as to avoid Raman signals from the viable epidermis, we determined the lipid/protein ratio between depths of 4-10 μm in the SC. This was performed by calculating the ratio of the integrated signal intensity from 2866 to 2900 cm^{-1} (CH_2 asymmetric stretching of lipids) and from 2910 to 2966 cm^{-1} (CH_3 symmetric stretching of proteins, the same region as taken for the protein band for determination of the water concentration in skin²⁰) and taking into account a linear baseline between the integration boundaries. The calculated signal ratio between the lipid and protein bands is referred to as the lipid/protein ratio. Calculations were performed using SkinTools 2.0 (River Diagnostics, Rotterdam, The Netherlands).

SC isolation and lipid extraction

In order to obtain Raman spectra of human SC lipids and extracted human SC, human SC was isolated by trypsin digestion as described elsewhere²². The SC lipids were extracted according to a modified Bligh and Dyer procedure²³ with the addition of 0.25M KCl to extract polar lipids.

Tape stripping procedure

Multiple poly(phenylene sulfide) tape strips (Nichiban, Tokyo, Japan) were successively applied at the same area (4.5 cm^2) on the marked area of the ventral forearm. All tapes were applied on the targeted skin and pressed for 5 seconds at 450 g/cm^2 using a D-Squame pressure instrument (Cuderm Corp., Dallas, TX). Tweezers were used to remove the tape in a fluent stroke, using alternating directions for each subsequent tape strip. The Squamescan 850A (Heiland electronic, Wetzlar, Germany) was used to determine the dry SC mass removed by each tape strip.

The calibration procedure of the Squamescan was as follows: Immediately after measuring the absorption of the tape strip with the Squamescan, the tapes were incubated and shaken overnight in 1 mL 1M KOH, after which the extracts were neutralized with 79 μl 12M HCl. The final pH of the extract was set between 7.2-7.4 with 1M HCl and/or 1M KOH. Subsequently, 50 μl of the extract was added to 200 μl bicinchoninic acid (BCA, Pierce

BCA, Protein Assay, Perbio Science BV, Etten-Leur, The Netherlands), followed by heating for 2 hours at 37°C and determination of the absorption at 562 nm (OD₅₆₂). In this way, we obtained corresponding OD₅₆₂ values of the tape extracts with known Squamescan values. Sheets of isolated human SC with known weight (between 10-1000 µg, size ~0.05-1 cm²) were incubated overnight and treated as described above, resulting in a calibration curve of dry SC mass against OD₅₆₂. With this curve, we converted Squamescan values of the tapes via their OD₅₆₂ values into dry SC mass, which resulted in a calibration curve of Squamescan values against dry SC mass. In addition, 1/TEWL was plotted against the cumulative amount of tape stripped SC. Here, the intercept with the x-axis obtained by extrapolation is a measure for the dry SC mass per surface area²⁴. This extrapolation was only performed with curves having a $R^2 \geq 0.9$.

Statistical analysis

Statistical analysis was performed using SPSS Statistics version 17.0. As the data show a non-normal distribution, non-parametric Mann-Whitney tests were performed for comparison of different groups with a significance level of $P < 0.05$. For the paired comparison of non-lesional and lesional SC, a Wilcoxon signed rank test was used. Bivariate analysis and Spearman's ρ correlation coefficient were used to analyze correlations between parameters.

Results

From the TEWL values and the cumulative amount of stripped SC, the dry SC mass per skin area was calculated. Figure 1 shows typical examples of 1/TEWL against the cumulative amount of tape-stripped SC of three AE patients. The abscissa intercept by extrapolation is indicative for the dry SC mass per cm². In the examples in Figure 1, the dry SC mass varies between 1195.2 µg/cm² and 1802.0 µg/cm².

Figure 2a shows the dry SC mass per surface area in control SC (1619 ± 400 µg/cm²), non-lesional SC of AE patients (1407 ± 340 µg/cm²), and lesional SC of AE patients (1200 ± 168 µg/cm²). There was neither a significant difference between controls and non-lesional skin of AE, nor between non-lesional and lesional AE skin ($P > 0.08$). However, there was a difference between controls and lesional skin of AE ($P = 0.01$). Open and filled circles indicate non-carriers and carriers of *FLG* mutations, respectively. There was no difference in dry SC mass in AE patients that were carriers and non-carriers of a *FLG* mutation ($P > 0.1$). In Figure 2b, 1/TEWL values are plotted as function of the dry SC mass per surface area (µg/cm²). The correlation coefficient between these parameters is $r = 0.67$.

Raman spectroscopy was used to examine the lipid/protein ratio in the SC. Figure 3a

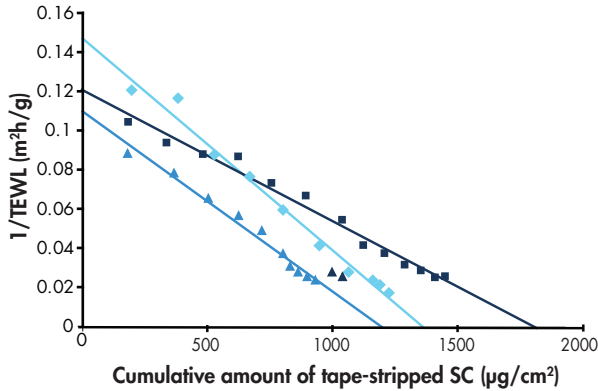


Figure 1: Three examples of $1/\text{TEWL}$ plotted against the cumulative amount of tape-stripped SC. The intercept of the line with the x-axis is indicative for the dry SC mass per cm^2 .

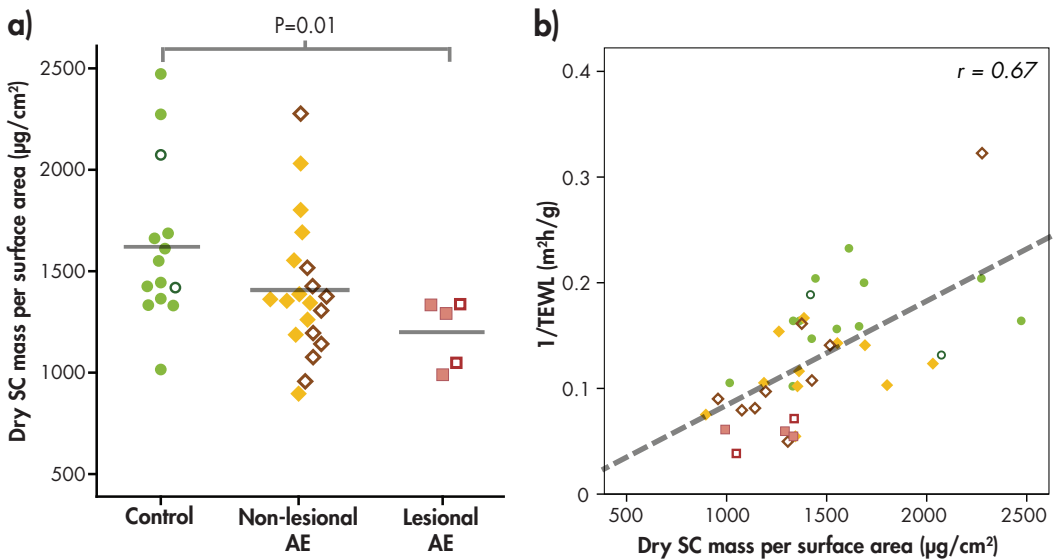


Figure 2: **a)** Dry SC mass per surface area ($\mu\text{g}/\text{cm}^2$) in control subjects, non-lesional SC of AE patients, and lesional SC of AE patients. **b)** Correlation between $1/\text{TEWL}$ and dry SC mass per cm^2 in control subjects and AE patients. Green, orange and red data points correspond to control SC, non-lesional AE SC and lesional AE SC, respectively. Open data points indicate carriers of FLG mutations, filled data points indicate non-carriers of FLG mutations. Control subjects are indicated by \bullet/\circ . Non-lesional skin and lesional skin of AE patients are indicated by \blacklozenge/\lozenge and \blacksquare/\square , respectively.

shows high wavenumber (2500-4000 cm^{-1}) Raman spectra of SC (upper), extracted SC (containing no lipids, mainly protein; middle), and extracted SC lipids (lower), respectively. The spectrum of SC exhibits peaks at 2850 cm^{-1} , 2880 cm^{-1} and 2930 cm^{-1} . The spectrum of the extracted lipids contains two characteristic peaks located at 2850 cm^{-1} and 2880 cm^{-1} . In contrast, the extracted SC spectrum consists of only one peak located at 2930 cm^{-1} . Figure 3b shows a typical example of a high wavenumber Raman spectrum of a control subject at a skin depth of 4 μm . The peaks that were used to calculate the lipid/protein ratio are shaded in red.

Figure 4a shows the lipid/protein ratio as a function of depth (between 0 and 40 μm), with a maximum between 0 and 4 μm and a gradual decrease deeper than 8 μm . Figure 4b shows the average lipid/protein ratio between 4 and 10 μm in the SC in control SC, non-lesional AE SC, and lesional AE SC. Non-lesional skin of AE patients shows a significantly lower lipid/protein ratio than the skin of control subjects (0.24 ± 0.05 and 0.28 ± 0.03 , respectively, $P < 0.005$). In lesional skin, the lipid/protein ratio is even further reduced (0.19 ± 0.03 , $P < 0.001$).

Figure 4c shows the intra-subject comparison between lesional and non-lesional skin from the same patient. In 9 out of 11 AE patients, the lipid/protein ratio is lower in lesional skin compared to non-lesional skin, which was significant ($P < 0.01$).

The lipid/protein ratio in AE patients showed no difference between carriers and non-carriers of *FLG* mutations (0.24 ± 0.04 in non-carriers and 0.23 ± 0.06 in carriers $P > 0.1$ for non-lesional AE SC; and 0.19 ± 0.02 in non-carriers and 0.18 ± 0.04 in carriers, $P > 0.1$ for lesional AE SC).

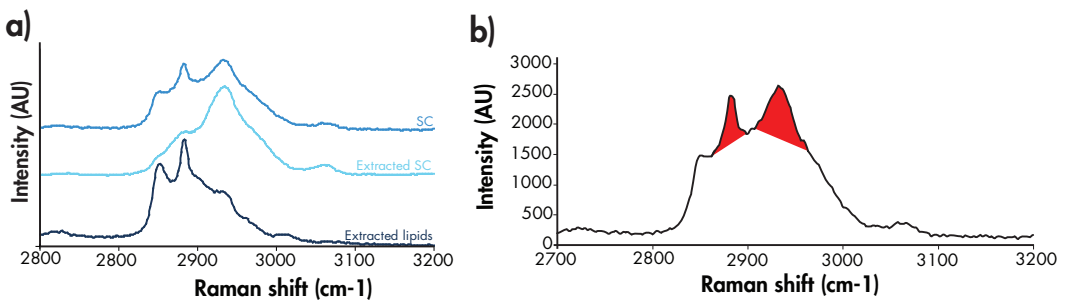


Figure 3: **a)** High wavenumber Raman spectrum of SC (upper), extracted sc (middle) and extracted SC lipids (lower). **b)** Raman spectrum between 2500-4000 cm^{-1} of control SC at a depth of 4 μm . Peaks at 2880 cm^{-1} and 2930 cm^{-1} (both colored red) belong to the lipids and proteins, respectively.

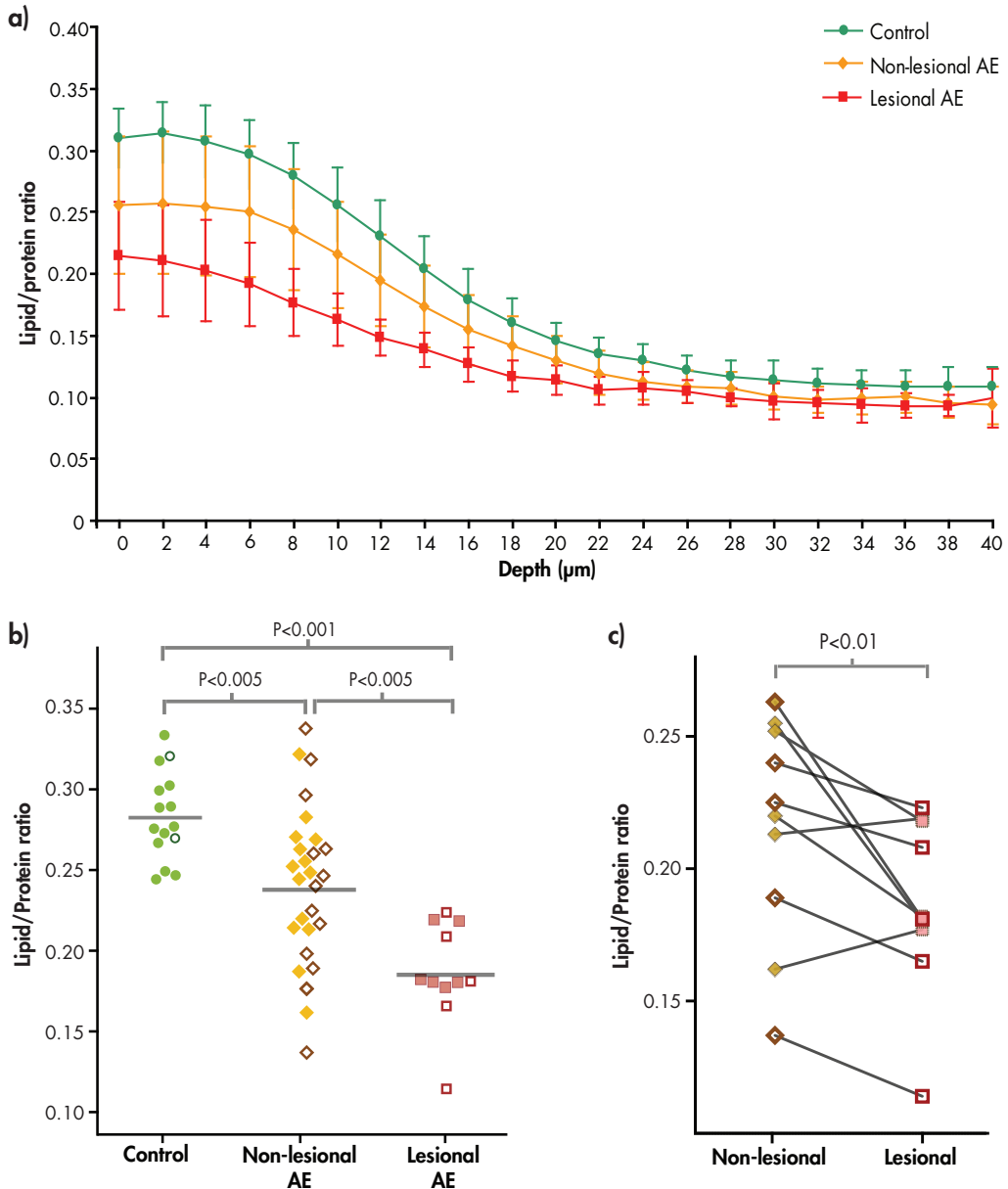


Figure 4: Lipid/protein ratio in control subjects and AE patients. **a)** Lipid/protein ratio in the range of 0–40 μm . The green, orange and red lines indicate the average ($\pm\text{SD}$) of control SC, non-lesional AE SC and lesional AE SC, respectively. **b)** Average lipid/protein ratio between 4–10 μm in the SC of the individual patients and controls. **c)** Paired lipid/protein data of non-lesional and lesional AE skin. Non-carriers and carriers of a FLG mutation are represented by filled and open data points, respectively. Control subjects are indicated by \bullet/\circ . Non-lesional skin and lesional skin of AE patients are indicated by \blacklozenge/\lozenge and \blacksquare/\square , respectively.

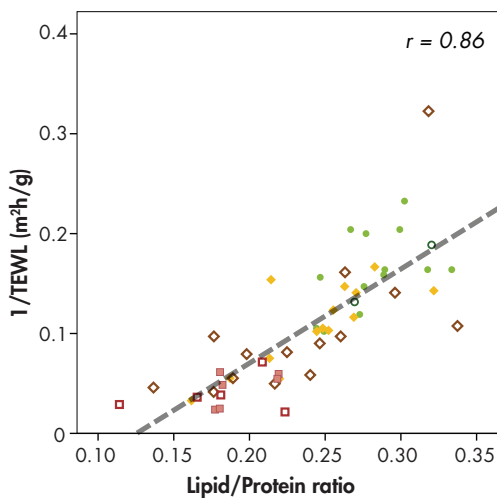


Figure 5: Correlation between lipid/protein ratio and $1/TEWL$ in control subjects and AE patients. Non-carriers and carriers of a FLG mutation are represented by filled and open data points, respectively. Control subjects are indicated by ●/○. Non-lesional skin and lesional skin of AE patients are indicated by ◆/◇ and ■/□, respectively.

The relationship between skin barrier properties and lipid/protein ratios is presented in Figure 5, showing the correlation between $1/TEWL$ and the lipid/protein ratio in control subjects and in non-lesional and lesional SC of AE patients. The correlation coefficient between $1/TEWL$ and lipid/protein ratio was 0.86 ($P < 0.001$).

Discussion

In this study, we determined the lipid/protein ratio in SC of control subjects and in non-lesional as well as lesional SC of AE patients. In addition, the dry SC mass per surface area was determined in control subjects and in non-lesional skin of AE patients. Finally, we studied the correlations of these parameters with the skin barrier function as assessed by TEWL.

The Raman spectra of extracted SC lipids and extracted SC demonstrate that the ratio between the peaks located at 2880 cm^{-1} and 2930 cm^{-1} is an excellent measure for the lipid/protein ratio in SC: the contribution of the lipids to the 2930 cm^{-1} peak as well as the contribution of the proteins to the 2880 cm^{-1} peak is negligible. The selected peak boundaries of the 2930 cm^{-1} peak were based on those used for the protein band for determination of the water concentration in the skin²⁰. A change of the baseline by broadening the peak boundaries did not have an effect on the lipid/protein ratio (not shown).

We observed that the lipid/protein ratio is significantly lower in non-lesional as well as lesional SC of AE patients, compared to SC of control subjects. This may be partly explained by changes in the SC lipid composition: previous studies have shown that the lipid composition is altered in AE patients as compared to controls^{5,14-19,25}. Some studies

revealed that the level of long-chain CERs is reduced in non-lesional AE skin and the level of very short chain CERs (with a total chain length of 34 carbon atoms, referred to as C₃₄ CERs) is increased^{16,19}. However, the level of C₃₄ CERs and long-chain CERs in non-lesional AE skin are together accounting for about 10 mol% of the total CER content in non-lesional skin¹⁹. Assuming an equimolar CER:CHOL:FFA ratio, this is only 3 mol% of the total lipids, whereas the lipid/protein level has decreased by ~1.4% in non-lesional AE and ~3.2% in lesional AE. Hence the changes in C₃₄ CERs, long-chain CERs and total CER level may not account for the complete reduction in lipid/protein ratio, which indicates a third, yet unknown factor. The reduced lipid/protein ratio may be partly explained by a delayed or incomplete lamellar body extrusion process caused by an altered peroxisome proliferator-activated receptor (PPAR) activation, which has been reported for AE²⁶⁻²⁸. PPARs can be activated by lipids, and these nuclear hormone receptors may possibly be a link for the observed changes in both the lipid chain length and lipid/keratin ratio^{29,30}.

We could perform an intra-subject comparison of non-lesional and lesional skin as eleven subjects had both skin types on their ventral forearms. In most cases the lipid/protein ratio was lower in lesional compared to non-lesional skin. These differences within a subject may primarily be attributed to inflammation, the presence of microbes and/or an altered pH. These factors may affect the lipid synthesis^{31,32} and therefore result in a lower lipid/protein ratio in lesional AE skin.

A measure of SC thickness is the total dry SC mass per surface area, which was determined by extrapolation of 1/TEWL versus the cumulative mass of tape-stripped SC. Between non-lesional AE skin and control skin no significant difference in the dry SC mass per surface area was observed, which indicates that SC thickness was comparable for both groups. In lesional AE SC the total dry SC mass per surface area was lower compared to controls. In line with our results, Voegeli *et al.*³³ have reported a decreased SC thickness in lesional AE SC. They suggested increased serine protease activity in lesional SC of AE patients as a possible explanation for the observed differences. We noticed that SC thickness does affect the TEWL values and thus the skin barrier function, as observed by the correlation between the total dry SC mass per surface area and TEWL.

An alternative method to determine SC thickness is based on the water concentration profile in the SC measured by confocal Raman spectroscopy³⁴⁻³⁷. The advantage of Raman spectroscopy is that it enables the direct monitoring *in vivo* without damaging the SC. The method determines the actual SC thickness, which includes the effects of swelling of the SC as a result of water uptake. In this study, we were interested in variations in the SC thickness as a result of changes in dry SC mass per surface area, independent of variations in water content of the SC. As the total amount of tape-stripped dry SC mass

and subsequent extrapolation does not change upon swelling, we used this method to determine the dry SC mass per surface area. In order to obtain a calibration curve we extracted small pieces of SC. During extraction of the SC, it is possible that not all proteins were extracted. Therefore, the amount of SC per tape-strip may be slightly overestimated. Both SC thickness and lipid/protein ratio are factors that affect the TEWL. However, the correlation between lipid/protein ratio and TEWL was much stronger than the correlation between dry SC mass per surface area (as a measure of SC thickness) and TEWL. This may suggest that the level of lipids in SC plays a more prominent role in the skin barrier function than the dry SC mass. In the same line, our previous study shows a strong correlation between CER chain length and skin barrier function¹⁹.

FLG mutations are the largest risk factor known to date for the development of AE^{7,38}. However, in this study the presence of *FLG* mutations was not associated with lipid/protein ratio or dry SC mass per surface area in AE patients. In our previous study it was concluded that *FLG* mutations do not influence CER composition and lipid organization¹⁹. Although *FLG* mutations are a strong risk factor in the pathogenesis of AE, the results of this study indicate that in adult AE, changes in the SC lipids seem to be the dominant factor in the reduced skin barrier.

Acknowledgements

This research is supported by the Dutch Technology Foundation STW, which is part of the Netherlands Organisation for Scientific Research (NWO), and which is partly funded by the Ministry of Economic Affairs.

References

- 1 Alanne S, Nermes M, Soderlund R *et al.* Quality of life in infants with atopic dermatitis and healthy infants: a follow-up from birth to 24 months. *Acta Paediatr* 2011; 100: e65-70.
- 2 Mozaffari H, Pourpak Z, Poursayed S *et al.* Quality of life in atopic dermatitis patients. *J Microbiol Immunol Infect* 2007; 40: 260-4.
- 3 Slattery MJ, Essex MJ, Paletz EM *et al.* Depression, anxiety, and dermatologic quality of life in adolescents with atopic dermatitis. *J Allergy Clin Immunol* 2011; 128: 668-71 e3.
- 4 van Valburg RW, Willemsen MG, Dirven-Meijer PC *et al.* Quality of life measurement and its relationship to disease severity in children with atopic dermatitis in general practice. *Acta Derm Venereol* 2011; 91: 147-51.
- 5 Di Nardo A, Wertz P, Giannetti A *et al.* Ceramide and cholesterol composition of the skin of patients with atopic dermatitis. *Acta Derm Venereol* 1998; 78: 27-30.
- 6 Yoshiike T, Aikawa Y, Sindhvananda J *et al.* Skin barrier defect in atopic dermatitis: increased permeability of the stratum corneum using dimethyl sulfoxide and theophylline. *J Dermatol Sci* 1993; 5: 92-6.
- 7 Palmer CN, Irvine AD, Terron-Kwiatkowski A *et al.* Common loss-of-function variants of the epidermal barrier protein filaggrin are a major predisposing factor for atopic dermatitis. *Nat Genet* 2006; 38: 441-6.
- 8 Brown SJ, Irvine AD. Atopic eczema and the filaggrin story. *Seminars in Cutaneous Medicine and Surgery* 2008; 27: 128-37.
- 9 Rawlings AV, Matts PJ. Stratum corneum moisturization at the molecular level: an update in relation to the dry skin cycle. *J Invest Dermatol* 2005; 124: 1099-110.
- 10 Angelova-Fischer I, Mannheimer AC, Hinder A *et al.* Distinct barrier integrity phenotypes in filaggrin-related atopic eczema following sequential tape stripping and lipid profiling. *Exp Dermatol* 2011; 20: 351-6.
- 11 Jakasa I, Koster ES, Calkoen F *et al.* Skin barrier function in healthy subjects and patients with atopic dermatitis in relation to filaggrin loss-of-function mutations. *J Invest Dermatol* 2011; 131: 540-2.
- 12 O'Regan GM, Kemperman PM, Sandilands A *et al.* Raman profiles of the stratum corneum define 3 filaggrin genotype-determined atopic dermatitis endophenotypes. *J Allergy Clin Immunol* 2010; 126: 574-80 e1.
- 13 Simonetti O, Hoogstraate AJ, Bialik W *et al.* Visualization of diffusion pathways across the stratum corneum of native and in-vitro-reconstructed epidermis by confocal laser scanning microscopy. *Arch Dermatol Res* 1995; 287: 465-73.
- 14 Bleck O, Abeck D, Ring J *et al.* Two ceramide subfractions detectable in Cer(AS) position by HPTLC in skin surface lipids of non-lesional skin of atopic eczema. *J Invest Dermatol* 1999; 113: 894-900.
- 15 Imokawa G, Abe A, Jin K *et al.* Decreased level of ceramides in stratum corneum of atopic dermatitis: an etiologic factor in atopic dry skin? *J Invest Dermatol* 1991; 96: 523-6.
- 16 Ishikawa J, Narita H, Kondo N *et al.* Changes in the ceramide profile of atopic dermatitis patients. *J Invest Dermatol* 2010; 130: 2511-4.
- 17 Matsumoto M, Umamoto N, Sugiura H *et al.* Difference in ceramide composition between "dry" and "normal" skin in patients with atopic dermatitis. *Acta Derm Venereol* 1999; 79: 246-7.
- 18 Yamamoto A, Serizawa S, Ito M *et al.* Stratum corneum lipid abnormalities in atopic dermatitis. *Arch Dermatol Res* 1991; 283: 219-23.
- 19 Mehta S, Moore RD, Graham NM. Potential factors affecting adherence with HIV therapy. *AIDS* 1997; 11: 1665-70.
- 20 Caspers PJ, Lucassen GW, Carter EA *et al.* In vivo confocal Raman microspectroscopy of the skin: noninvasive determination of molecular concentration profiles. *J Invest Dermatol* 2001; 116: 434-42.
- 21 Caspers PJ, Lucassen GW, Puppels GJ. Combined in vivo confocal Raman spectroscopy and confocal microscopy of human skin. *Biophys J* 2003; 85: 572-80.
- 22 Tanojo H, BosvanGeest A, Bouwstra JA *et al.* In vitro human skin barrier perturbation by oleic acid: Thermal analysis and freeze fracture electron microscopy studies. *Thermochemica Acta* 1997; 293: 77-85.
- 23 Bligh EG, Dyer WJ. A rapid method of total lipid extraction and purification. *Can J Biochem Physiol* 1959; 37: 911-7.
- 24 Kalia YN, Alberti I, Naik A *et al.* Assessment of topical bioavailability in vivo: the importance of stratum corneum thickness. *Skin Pharmacol Appl Skin Physiol* 2001; 14 Suppl 1: 82-6.
- 25 Janssens M, van Smeden J, Gooris GS *et al.* Lamellar lipid organization and ceramide composition in the stratum corneum of patients with atopic eczema. *J Invest Dermatol* 2011; 131: 2136-8.
- 26 Fartasch M, Bassukas ID, Diepgen TL. Disturbed extruding mechanism of lamellar bodies in dry non-eczematous skin of atopics. *Br J Dermatol* 1992; 127: 221-7.
- 27 Marsella R, Samuelson D, Doerr K. Transmission electron microscopy studies in an experimental model of canine atopic dermatitis. *Vet Dermatol* 2010; 21: 81-8.
- 28 Scharshmidt CF, Man MQ, Hatano Y *et al.* Filaggrin deficiency confers a paracellular barrier abnormality that reduces inflammatory thresholds to irritants and haptens. *J Allergy Clin Immunol* 2009; 124: 496-506, e1-6.
- 29 Feingold KR, Jiang YJ. The mechanisms by which lipids coordinately regulate the formation of the protein and lipid domains of the stratum corneum: Role of fatty acids, oxysterols, cholesterol sulfate and ceramides as signaling molecules. *Dermato-endocrinology* 2011; 3: 113-8.
- 30 Schmith M, Jiang YJ, Dubrac S *et al.* Thematic review series: skin lipids. Peroxisome proliferator-activated receptors and liver X receptors in epidermal biology. *Journal of lipid research* 2008; 49: 499-509.
- 31 Blackburn IM, Moore RG. Controlled acute and follow-up trial of cognitive therapy and pharmacotherapy in outpatients with recurrent depression. *Br J Psychiatry* 1997; 171: 328-34.
- 32 O'Sullivan DC, Averch TD, Cadeddu JA *et al.* Teleradiology in urology: comparison of digital image quality with original radiographic films to detect urinary calculi. *J Urol* 1997; 158: 2216-20.

- 33 Voegeli R, Rawlings AV, Breternitz M *et al.* Increased stratum corneum serine protease activity in acute eczematous atopic skin. *Br J Dermatol* 2009; 161: 70-7.
- 34 Boncheva M, de Sterke J, Caspers PJ *et al.* Depth profiling of Stratum corneum hydration in vivo: a comparison between conductance and confocal Raman spectroscopic measurements. *Experimental Dermatology* 2009; 18: 870-6.
- 35 Crowther JM, Sieg A, Blenkiron P *et al.* Measuring the effects of topical moisturizers on changes in stratum corneum thickness, water gradients and hydration in vivo. *British Journal of Dermatology* 2008; 159: 567-77.
- 36 Mlitz V, Latreille J, Gardinier S *et al.* Impact of filaggrin mutations on Raman spectra and biophysical properties of the stratum corneum in mild to moderate atopic dermatitis. *J Eur Acad Dermatol Venereol* 2011.
- 37 Egawa M, Tagami H. Comparison of the depth profiles of water and water-binding substances in the stratum corneum determined in vivo by Raman spectroscopy between the cheek and volar forearm skin: effects of age, seasonal changes and artificial forced hydration. *British Journal of Dermatology* 2008; 158: 251-60.
- 38 Weidinger S, Illig T, Baurecht H *et al.* Loss-of-function variations within the filaggrin gene predispose for atopic dermatitis with allergic sensitizations. *J Allergy Clin Immunol* 2006; 118: 214-9.



STUDIES ON STRATUM CORNEUM
LIPIDS FROM OTHER SKIN
SOURCES SHOWING A BARRIER
DYSFUNCTION

PART IV

CHAPTER 9

SKIN BARRIER LIPID COMPOSITION AND ORGANIZATION IN NETHERTON SYNDROME PATIENTS

J. van Smeden^{1,*}, M. Janssens^{1,*},
W.A. Boiten¹, R.J. Vreeken², A. Hovnanian³,
J.A. Bouwstra¹

¹ Division of Drug Delivery Technology,
Leiden Academic Centre for Drug Research,
Leiden University, Leiden, The Netherlands.

² Netherlands Metabolomics Centre, Leiden
Academic Centre for Drug Research,
Leiden University, Leiden, The Netherlands.

³ Pathology Department and MAGEC Center
for Rare Cutaneous Diseases, Hopital
Necker-Enfants Malades, APHP, Paris,
France.

*Both authors contributed equally to this work

Submitted

Abstract

Netherton Syndrome (NTS) is a rare genetic skin disease that is characterized by erythroderma, hair shaft defects, and severe atopic manifestations. The disease is caused by mutations in the serine protease inhibitor Kazal-type 5 (SPINK5) gene, which encodes the protease inhibitor lympho-epithelial Kazal-type-related inhibitor (LEKTI). Lack of LEKTI causes epidermal proteases hyperactivity, which results in stratum corneum (SC) detachment. NTS patients have an impaired skin barrier function. Besides barrier proteins, SC lipids are also crucial for the skin barrier. The lipids primarily consist of ceramides (CERS), free fatty acids (FFAs) and cholesterol. To date, hardly any information is available on the SC lipid composition and organization in SC of patients with NTS. Therefore, the aim of the present study is to determine the SC lipid composition and organization in NTS patients.

We investigated the SC lipids by means of mass spectrometry, infrared spectroscopy and x-ray diffraction. We studied the lipid subclasses as well as the chain length distributions. A decreased FFA chain length and an increased level of monounsaturated FFAs was observed in SC of NTS patients compared to controls. Furthermore, the level of short-chain CERS was increased in NTS patients, and in a subgroup of patients we observed a strong reduction in long-chain CER levels. The changes in lipid composition modified the lipid organization: an increased disordering of the lipids compared to the controls. This study shows that there are striking changes in the lipid composition in NTS that may contribute to the skin barrier dysfunction in NTS.

Introduction

Netherton syndrome (NTS) is a rare skin disorder with an occurrence of 1-3 in 200,000 births and a fatality rate of around 20% in the first year of life by hypernatremic dehydration, electrolyte imbalances, perturbed thermoregulation, failure to thrive, and recurrent infections¹⁻⁵. NTS is characterized by erythroderma, hair shaft defects (bamboo hair), and severe atopic manifestations⁶. In addition, NTS patients show a drastically reduced skin barrier function⁷⁻⁹. The skin barrier is primarily located in the outermost layer of the skin, the stratum corneum (SC). The SC consists of flattened corneocytes embedded in a highly ordered lipid matrix. The organization and composition of this lipid matrix seems crucial for the barrier function of the skin, but hardly any information is available on the SC lipids regarding NTS patients. The aim of the present study is therefore to unravel the composition and organization of this SC lipid matrix in NTS.

SC lipids mainly consist of ceramides (CERS), cholesterol (CHOL) and free fatty acids (FFAs). To date, 12 CER subclasses with a wide variation in chain length distribution have been identified in human SC^{10,11}. FFAs mainly consist of saturated carbon-chains with lengths varying between 16 and 36 carbon atoms, of which the most abundant chain lengths are 24 and 26 carbon atoms^{12,13}. In healthy SC, lipids form two lamellar phases with repeat distances of approximately 6 and 13 nm referred to as the short periodicity phase (SPP) and long periodicity phase (LPP), respectively^{14,15}. Within the lamellae, the lipids form a dense (orthorhombic, highly ordered lipid chains) lateral organization, although lipid domains with a less dense (hexagonal, less ordered lipid chains) lipid organization also co-exist. Both the lipid composition and lipid organization are crucial for a proper SC barrier function. Recent studies show the important role of the SC lipids in the skin barrier function of atopic eczema (AE) patients^{16,17}, a skin disease often linked to NTS because of its shared symptoms^{18,19}. We demonstrated a modified chain length distribution in CERS in SC of AE patients. This change resulted in an altered SC lipid organization, which in turn was correlated with an impaired skin barrier function.

NTS is caused by mutations in the serine protease inhibitor Kazal-type 5 (SPINK5) gene. These mutations result in loss of function of lympho-epithelial Kazal-type-related inhibitor (LEKTI)²⁰. LEKTI is described in relation to proteins involved in proliferation and differentiation of keratinocytes. In addition, several LEKTI-domains can efficiently inhibit the enzyme activity of various subtypes of kallikreins (KLKs): KLK5, KLK7 and KLK14. Lack of active LEKTI domains lead to increased activity of these KLKs, thereby affecting various biological processes that will have a detrimental effect on the skin barrier:

i) KLKs 5 and 7 are involved in the desquamation process, that is, the degradation of the corneodesmosomes linking the corneocytes in the SC²¹⁻²⁶. Reduction in the activity

of LEKTI, which inhibits the activity of these enzymes, causes epidermal proteases hyperactivity resulting in SC detachment²⁷.

ii) KLKs 5 and 14 induce cutaneous inflammation through proteinase-activated receptor 2 (PAR2) and NF- κ B pathway activation *in vitro*²⁸, leading to up-regulation of pro-Th2 cytokine thymic stromal lymphopoietin (TSLP), IL1- α , IL8, and TNF- α ^{8,23,29,30}. The production of these cytokines can in turn affect the SC lipid synthesis and thereby the skin barrier^{31,32}. Besides, PAR2 activation can lead to abnormal lamellar body secretion that also results in disrupted lipid lamellae and a reduced skin barrier function⁷.

iii) KLKs act as catalysts for the proteolysis of the enzymes β -glucocerebrosidase and acid sphingomyelinase³³. Both enzymes are involved in synthesis of CERS that play an important role in the barrier function of the SC.

iv) Increased activity of KLK5 (as a result of decreased inhibition by LEKTI) leads to hyperactivity of the epidermal protease elastase 2 (ELA2). This results in abnormal processing of filaggrin, a keratin filament-associated protein highly associated with atopic eczema³⁴. Filaggrin breakdown products, the natural moisturizing factor (NMF), are suggested to be important for maintaining the acidic nature of the SC: An increase in pH induces premature degradation of corneodesmosomes leading to a disrupted barrier and cohesion of the skin³⁵. In addition, an increase in pH can lead to altered catalytic activities of lipid processing enzymes that require an acidic pH for their optimal catalytic activity³⁶. Besides these effects of KLKs on the different aspects of the metabolic pathways, KLKs may activate each other or induce self-activation, thereby exacerbating the effects^{30,37,38}. NTS patients show different expression of proteins like loricrin, involucrin and the transglutaminases. This disturbs the assembly of the cornified envelope surrounding the corneocytes and may also reduce the SC barrier function³⁹⁻⁴¹. Altogether, this results in a drastically reduced barrier function in patients with NTS as measured by transepidermal water loss (TEWL)⁷⁻⁹.

To date, little is known about the SC lipid composition in NTS. A study of Bonnart *et al.*³⁴ with transgenic mice overexpressing ELA2 as a model for NTS reported a threefold increase in TEWL, demonstrating a decreased skin barrier function. For the first time, the lipids in total epidermis were analyzed. They observed an increased level of total glucosylceramides and a reduction of sphingomyelin, as well as significant decrease in FFA levels. In addition, it was reported that the lipids form irregular loose stacks of lamellae^{7,34,42}. However, no data were reported on individual CER and FFA subclasses and chain length distributions of the lipids. In addition, no quantitative information about the lamellar phases was provided and no information is available on the lateral packing. Therefore, the aim of this study was to perform an in depth analysis of the lipid

composition and organization in SC of patients with NTS.

Our results show that in SC of NTS patients, there is a strong increase in short chain CERs and FFAs as well as an increase in unsaturated FFAs. Furthermore, the lipid chains are more disordered and the lamellar lipid organization is altered. A subgroup of patients showed no lamellar lipid profile at all, and these patients also had the most drastic changes in their SC lipid composition.

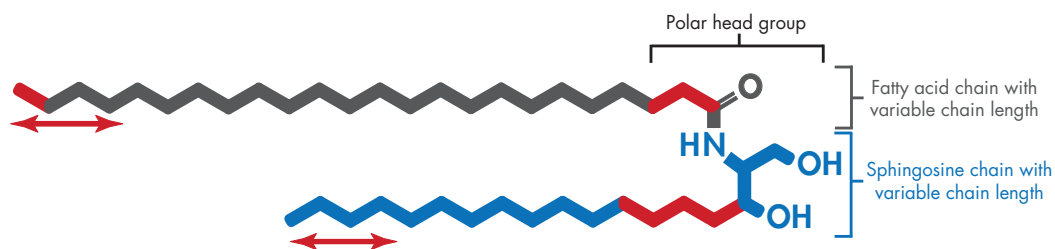
Materials and Methods

Study population

The study was conducted in accordance with the Declaration of Helsinki and was approved by the Ethical Committee of Paris Ile de France. Eight patients with classical features of Netherton syndrome were included in the study. They were from different ethnic backgrounds and their age ranged from 8 to 39 years at the time of the study. Patients included four males and four females. Patients ③ and ④, as well as ⑦ and ⑧ are siblings, respectively. Each patient presented congenital ichthyosiform erythroderma, trichorrhaxis invaginata, and eczematous like lesions. Four of them had ichthyosis linearis circumflexa (patients ④, ⑥, ⑦ and ⑧). All patients had elevated immunoglobulin E in the serum. Each patient showed negative LEKTI immunostaining on skin biopsy. SPINK5 mutations leading to premature termination codons were identified in each patient. For comparison, SC from the epidermis of 5 Caucasian subjects (36.2 ± 12.2 years; 3 males) was analyzed, which was obtained after abdominal- or mammoplasty reduction at the hospital. SC was isolated by trypsin digestion, a procedure that does not affect the lipid organization in SC⁴³ and is described previously⁴⁴.

Lipid classification and nomenclature

FFAs are classified according to their shorthand lipid number designation in which the chain length and degree of unsaturation is denoted⁴⁵. For example, octadecenoic acid (oleic acid) is denoted as C18:1. Ceramides consist of a sphingosine base linked to a fatty acid (acyl) chain. In human SC, both chains can vary in the number of carbon atoms. This results in a wide distribution in total chain length, that is, the total number of carbon atoms in both chains. In addition, both chains can have additional functional groups at specific locations. This results in 12 identified subclasses^{10,11} that are classified according to the nomenclature of Motta *et al.*⁴⁶: CER [AdS], [AH], [AP], [AS], [EODs], [EOH], [EOP], [EOS], [Nds], [NH], [NP], and [NS] (Figure 1).



	Non-hydroxy fatty acid, [N]	α -hydroxy fatty acid, [A]	Esterified ω -hydroxy fatty acid, [EO]
Dihydrosphingosine, [dS]	[NdS]	[AdS]	[EOdS]
Sphingosine, [S]	[NS]	[AS]	[EOS]
Phytosphingosine, [P]	[NP]	[AP]	[EOP]
6-hydroxy sphingosine, [H]	[NH]	[AH]	[EOH]

Figure 1: CER nomenclature and molecular structure. CERs are composed of a sphingoid base (depicted in blue) linked via an amide bond to an acyl chain (gray). Both chains show a variable carbon chain length indicated by the red arrows. This results in a wide distribution of the total CER chain length, i.e. the chain length of the sphingoid base and acyl chain combined. Both chains can have additional functional groups at the carbon positions marked in red. This results in 4 different sphingoid bases (dihydrosphingosine [dS], sphingosine [S], phytosphingosine [P], 6-hydroxy sphingosine [H]) and 3 different acyl chains (non-hydroxy fatty acid [N], α -hydroxy fatty acid [A] and esterified ω -hydroxy fatty acid [EO]). Together, this results in the presence of 12 subclasses denoted as: [NdS], [AdS], [EOdS], [NS], [AS], [EOS], [NP], [AP], [EOP], [NH], [AH], [EOH]. As an example, a CER with a non-hydroxy fatty acid of 16 carbon atoms long and a phytosphingosine base of 18 carbon atoms will be denoted as CER [NP] C34.

SC lipid extraction and analysis

An enhanced procedure of the commonly used Bligh and Dyer method was performed to extract the lipids from the SC sheets of both NTS patients and control subjects. Afterwards, lipids were analyzed by liquid chromatography coupled to mass spectrometry (LC/MS) to profile the CERs and FFAs. A detailed protocol of the lipid extraction and lipid analysis is described elsewhere^{11,47}. Briefly: a three-step sequential extraction procedure of chloroform/methanol/water (1:2:½; 1:1:0 and 2:1:0) was performed to extract all extracellular SC lipids. To enable proper analysis by LC/MS, samples were reconstituted in chloroform/methanol/heptane (2½:2½:95) to obtain a final concentration of 1.0 mg/

mL. Two injections of 10 μ L of each lipid sample were performed to analyze sequentially FFAs and CERS, using an Alliance 2695 HPLC system (Waters Milford, MA). The HPLC was coupled to a mass spectrometer (TSQ Quantum, Thermo Finnigan, San Jose, CA) equipped with an APCI ionization source. FFAs were separated using a C18 reverse phase column (Purospher Star LiChroCART, Merck, Darmstadt, Germany) and analyzed in negative ion mode, while separation of CERS was achieved using a normal phase column (PVA-sil, YMC, Kyoto, Japan) while analyzing in positive ion mode. Xcalibur software version 2.0 was used for data acquisition.

Small angle x-ray diffraction measurements

SC sheets were analyzed by small angle x-ray diffraction (SAXD), performed at the European Synchrotron Radiation Facility (ESRF, Grenoble, France) using station BM26B. SC was hydrated over a 27% NaBr solution during 24h before the measurements. SC sheets were oriented parallel to the primary x-ray beam in order to obtain high quality diffraction patterns. SAXD patterns were detected with a Frelon 2000 charge-couple device (CCD) detector at room temperature for a period of 10 minutes using a microfocus beam, similarly as described elsewhere⁴⁸. The exposure time to the x-rays was kept to a minimum and samples showed no evidence of radiation damage. From the scattering angle, the scattering vector (q) was calculated by $q = 4\pi \sin \theta / \lambda$, in which λ is the wavelength of the x-rays at the sample position and θ the scattering angle. The repeat distance of a lamellar phase can be calculated from the diffraction peaks by $d = n \cdot 2\pi / q_n$, in which n is the order of the peak. This means that a shift in peak position to higher q values results in a shorter repeat distance.

Conformational ordering of the lipids

A high conformational ordering is an indication that the lipids adopt the properties of a crystalline phase, whereas a low conformational ordering indicate that the lipids form a liquid phase. To obtain information on the conformational ordering, Fourier transform infrared (FTIR) spectra were recorded using a Varian 670-IR spectrometer (Varian Inc., Santa Clara, CA) equipped with a broad band liquid nitrogen cooled mercury-cadmium-telluride (MCT) detector and an external sample compartment containing a GladiATR (Pike, Madison, WI) attenuated total reflection (ATR) accessory with a single reflection diamond. The spectra of patients were collected in attenuated total reflectance (ATR) mode and transmission mode (as a control), and no difference between both methods was observed. SC samples were hydrated over a 27% NaBr solution during 24h. SC was mounted between two ZnSe windows when measured in transmission mode. Samples

were put under a purge of continuous dry air starting 30 minutes before data acquisition. Spectra were acquired as a co-addition of 256 scans at 1 cm^{-1} resolution during 4 minutes. When measuring in ATR mode, 150 spectra were acquired and averaged. The spectral resolution was 2 cm^{-1} . Resolutions Pro 4.1 (Varian Inc.) was used for data acquisition.

Statistical analysis

Statistical analysis was performed using SPSS Statistics. Non-parametric Mann-Whitney tests were performed when comparing 2 groups, unless explicitly noted elsewhere. Differences were considered either weakly significant ($P < 0.1$), moderately significant ($P < 0.05$), or highly significant ($P < 0.005$), and are denoted throughout the manuscript as *, **, and ***, respectively.

Results

Decreased FFA chain length and increased degree of unsaturation in patients with Netherton syndrome

Figure 2 shows data on the FFA composition of NTS patients (red) compared to the control subjects (green). The presence of FFAs < 20 carbon atoms, being abundantly present in patients, were not taken into account in the present study as these FFAs are most probably present due to contamination of topical treatments of the NTS patients. It is impossible to distinguish between native FFAs and those from topical formulations. The relative abundance of saturated FFAs and mono-unsaturated FFAs (MUFAs) is shown in Figure 2a. In NTS patients, there is a lower level of saturated FFAs compared to SC of controls ($71.3 \pm 24.1\%$ and $97.0 \pm 1.1\%$, respectively), and a higher level of MUFAs compared to controls ($28.7 \pm 24.1\%$ and $3.0 \pm 1.1\%$, respectively). Figure 2b shows the relative chain length distribution of saturated FFAs in NTS patients (red) and in controls (green). The most abundant chain lengths in controls are C24:0 and C26:0. The large standard deviations of the NTS patients are caused by inter-subject variation and not due to methodological variation.

Compared to control subjects, lipids of SC in NTS patients show a shift to shorter FFA chain length: there is a significant increase in FFA C20:0 and C21:0 and a significant decrease in FFAs C24:0, C25:0 and C26:0. Figure 2c shows the chain length distribution of MUFAs. No odd chain length MUFAs were detected in SC from either NTS or control. SC of NTS patients show a significant level of MUFAs C20:1, C22:1, C24:1. On the contrary, control subjects did not show a detectable level of MUFAs $\leq C24$ (C20:1, C22:1, C24:1) and only very low levels of C26:1, C28:1, C30:1 and $> C30:1$. From the abundance of both the saturated FFAs and MUFAs, the average chain length for each patient and control was

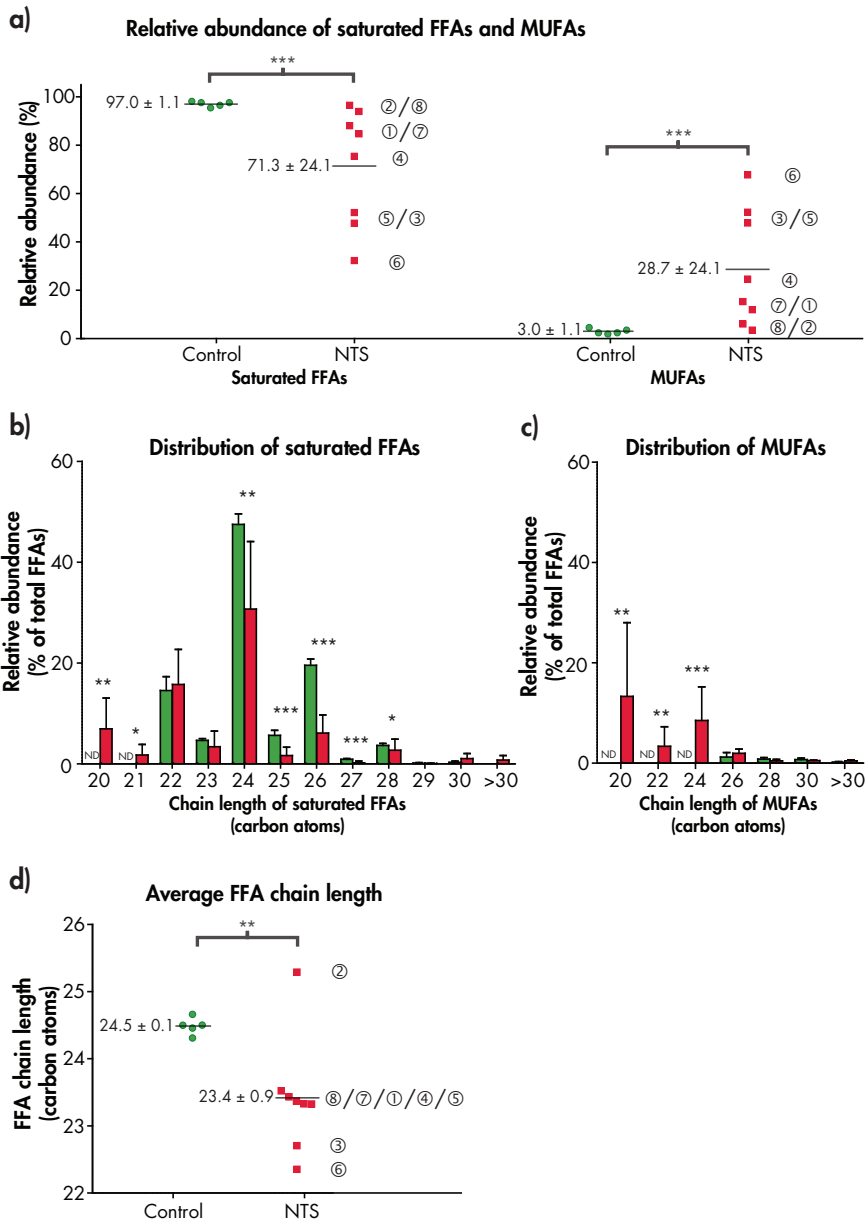


Figure 2: **a)** Scatter dot plot showing the relative abundance of saturated FFAs (left) and MUFAs (right). **b)** and **c)** present bar graphs showing the relative abundance of respectively saturated FFAs and MUFAs. The total abundance of saturated FFAs and MUFAs together was set to 100%. **d)** Scatter dot plot showing the average FFA chain length. Controls ($n=5$) and NTS patients ($n=8$) are presented as green and red bars/dots, respectively. Error bars represent SD values; Horizontal lines indicate averages. ND means 'not detected'. Individual NTS patients are labeled ①-⑧.

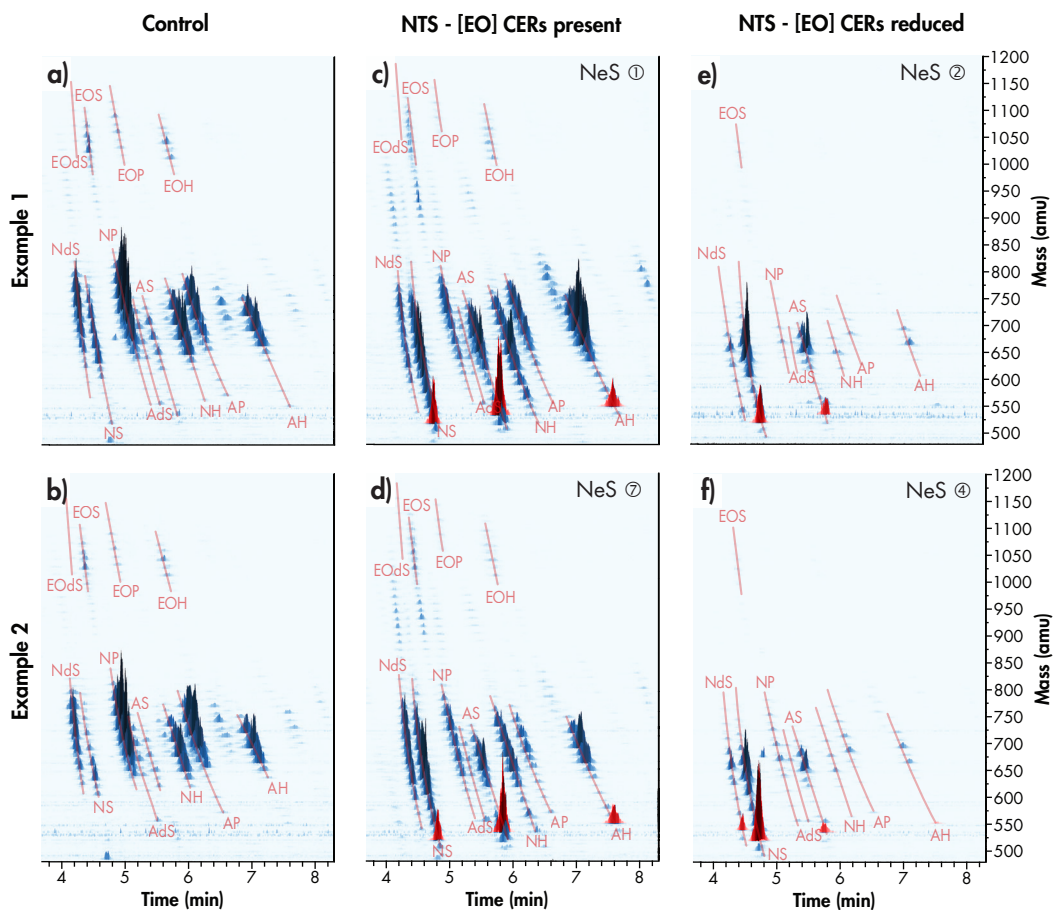


Figure 3: 3D ion chromatograms of control SC (a and b) and NTS patients (c, d, e and f). Retention time (3.6-8.3 min), mass (480-1200 amu), and relative intensity of each peak are shown on the x-, y- and 'z'-axis, respectively. Chromatograms are normalized to their most abundant peak. The chromatograms of the NTS patients show a decreased chain length of the CERs. In addition, in (e) and (f) there is a decrease in acyl-CERs ([EO] CERs) and a narrower chain length distribution in all other CER subclasses. NTS patients also show an increase in short chain CERs, in particular CERs with a chain length of 34 carbon atoms (C₃₄ CERs), which are indicated in the chromatograms by red peaks. The 3D ion chromatograms of the other controls and NTS patients are listed in Supplementary Figure 1.

calculated. These results are provided in Figure 2d and show that the average FFA chain length is significantly reduced in NTS patients versus controls (23.4 ± 0.9 and 24.5 ± 0.1 carbon atoms, respectively).

Altered levels of acyl-CERs and short-chain CERs in SC of NTS patients

The CER profiles of 5 controls and 8 NTS patients were studied. The CER profiles of two representative examples of controls and 4 examples of NTS patients are presented in the 3D ion chromatograms in Figure 3. An overview of 3D ion chromatograms of the remaining

NTS patients and control subjects is provided in Supplementary Figure 1. Figures 3a and b show two examples of the CER profiles of control SC. As there was very little difference in the profile of all control subjects, these two pictures closely resemble those of all 5 controls. There are at least 12 CER subclasses depicted, as reported before¹¹. Within each CER subclass, a large number of peaks can be observed. Each peak indicates a CER specie with a different chain length: The difference in molecular mass of two sequential CER species within one subgroup is 14 mass units, representing a reduction of one CH₂-group. In all 12 CER subclasses in human SC a wide distribution in their total carbon chain length is observed. The CERs with higher mass values in the upper part of the 3D mass spectrogram belong to the CER [EO] subclasses (also noted as acyl-CERs) and show a chain length distribution between 63-78 carbon atoms. The α -hydroxy [A] and non-hydroxy [N] CER subclasses have shorter chains and therefore lower masses. The carbon chain lengths of these subclasses are between 34-52 and 32-56 carbon atoms, respectively. The 3D ion chromatograms of NTS patients are provided in Figures 3c, d, e and f.

In general, of all CER subclasses, CER [NP] was most significantly reduced, whereas CER subclasses [AS], [NS], and [AH] were least affected. Furthermore, there is a shift in the lipid chain length distribution of NTS patients to lower mass values compared to controls: increased peak intensities in the molecular range between 550 and 650 amu are observed in chromatograms of NTS patients (labeled as red peaks in Figure 3).

The chromatograms of Figures 3c and d are representative for 5 NTS patients (①, ⑤, ⑥, ⑦, and ⑧). In the SC of these patients, all CER subclasses are observed. There is a clear shift to a higher abundance of short-chain CERs. This is particularly the case for CER subclasses [NS], [AS] and [AH], for which a very high peak was observed corresponding to CERs with a very short total carbon chain length of 34 carbon atoms (referred to as C₃₄ CERs). Figures 3e and f show the ion chromatograms representative for the other 3 NTS patients (②, ③ and ④). These patients show a clearly distinguishable pattern compared to the other NTS patients: There is a narrow chain length distribution in [A] and [N] subclasses. In addition, the level of acyl-CERs is drastically decreased and the C₃₄ CERs are strongly increased. NTS subject ⑥ also shows a clearly distinguishable pattern in the CER subclasses, but in contrast to the other 3 patients, acyl-CERs were present in this subject (Supplementary Figure 1).

Quantitative results on the relative abundance of acyl-CERs and short-chain CERs are shown in Figures 4a and b, respectively. Control subjects show on average a relative abundance of $8.4 \pm 1.9\%$ acyl-CERs. This abundance was comparable for 5 out of 8 NTS patients, but 3 patients show a drastic reduction to $\sim 2.5\%$. Regarding the abundance of very short chain CERs with a mass lower than 600 amu (corresponding to a total chain

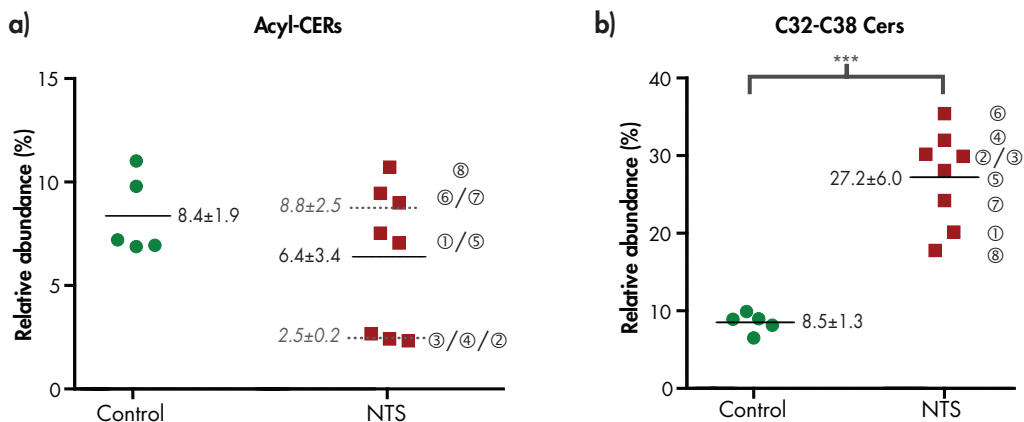


Figure 4: Dot plots showing the relative abundance of **a)** acyl-CERs and **b)** short chain CERs (C₃₂-C₃₈). Black horizontal lines and the corresponding values indicate mean values (±SD). Gray dotted lines indicate averages for two different categories observed: 5 NTS patients with normal acyl-CER levels and 3 NTS patients with reduced acyl-CER levels. Individual NTS patients are labeled ①-⑧.

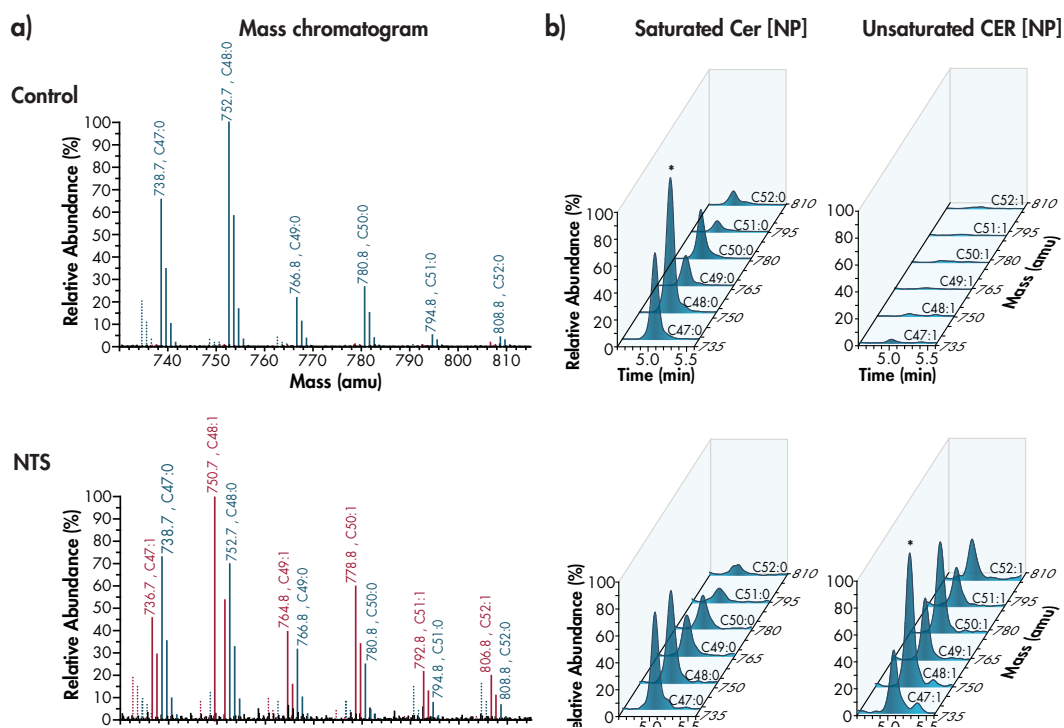


Figure 5: **a)** Mass chromatograms of a subsection (730-815 amu) of CER [NP] in a representative control subject (upper chromatogram) and NTS patient (lower chromatogram). Peak labels indicate the mass (amu) and to which CER chain length and degree of unsaturation it corresponds. Red lines indicate the unsaturated CERs observed in NTS patients. Although $[M+H]^+$ was the main ion observed, also the $[M+H-H_2O]^+$ is detected and shown in the chromatograms as dotted lines. These have a mass that is 18 amu lower than their main $[M+H]^+$ counterpart. **Figure b)** shows the 3D ion chromatograms of **Figure a)**. Saturated and unsaturated chromatograms are presented separately in the left and right column respectively. Chromatograms are normalized to their highest peak in the sample and marked by *: i.e. CER [NP] C_{48:0} in the control subject and CER [NP] C_{48:1} in NTS patient.

length of about ≤ 38 carbon atoms), all NTS patients show an increase compared to control subjects ($27.2 \pm 6.0\%$ and $8.5 \pm 1.3\%$, respectively).

A closer examination of the mass spectra led to the observation of unidentified peaks present in many CER subclasses, with a mass of exactly 2 amu lower compared to the identified CERs. As an example, this is illustrated in the mass chromatogram of Figure 5a, in which a subsection of the mass spectrum of CER [NP] is shown. These peaks correspond to CERs with one degree of unsaturation. The increase in unsaturated CERs in NTS is high, and the example of CER [NP] is illustrated in Figure 5b: The 3D ion chromatograms show the same subsection of CER [NP] in a control sample and a NTS patient. No unsaturated CERs were observed in control subjects, and the most abundant peak in this subsection corresponded to a saturated CER with a chain length of 48 carbon atoms. On the contrary, multiple peaks corresponding to unsaturated CERs of different chain length were observed in the NTS patient. In this subsection of CER [NP], unsaturated C48:1 was the most abundant peak. When comparing all the lipid profiles, it becomes apparent that NTS subject ⑥ does show the highest abundance of unsaturated CERs.

Altered lamellar lipid organization in Netherton syndrome

Figure 6 shows diffraction patterns of controls and NTS patients. The positions of the peaks are indicative for the periodicity of the lipid lamellae: a shift to higher q -values in the figure is indicative for a shorter periodicity (d) of the lipid lamellae. Figure 6a shows diffraction patterns of control SC. In previous studies, the diffraction patterns were analyzed and attributed to the two lamellar phases with repeat distances of around 13 (LPP) and 6 nm (SPP). All controls show clear peaks at scattering vector values (q) of 1.00 ± 0.01 and $1.45 \pm 0.01 \text{ nm}^{-1}$. The 1.00 nm^{-1} diffraction peak is attributed to the 2nd order peak of the LPP and the 1st order peak of the SPP, whereas the 1.45 nm^{-1} peak is attributed to the 3rd order of the LPP. In addition, some controls also show the 1st order of the LPP as a weak shoulder at a q -value located at $\sim 0.50 \text{ nm}^{-1}$. Figures 6b and 6c show diffraction patterns of NTS patients. SAXD patterns of NTS patients (numbers ①, ⑤, ⑥, ⑦, and ⑧), who clearly showed acyl-CERs present in their 3D ion chromatograms of Figure 3 and Supplement 1, are depicted in Figure 6b. The presence of a diffraction peak at 0.5 nm^{-1} , but also the presence of peak '2' and '3' in patients ①, ⑤, ⑦, and ⑧ suggests that the LPP is present. The diffraction pattern of patient ⑧ is very similar to that of the controls, although the peak position indicated by '2' is shifted to slightly higher q -values suggesting a reduction in the repeat distances of the lamellar phases. The other diffraction patterns show distinct differences. In the SAXD pattern of SC from patients ①, ⑤, and ⑦, the peak indicated as '3' has a higher intensity compared that that in the controls and shifted to

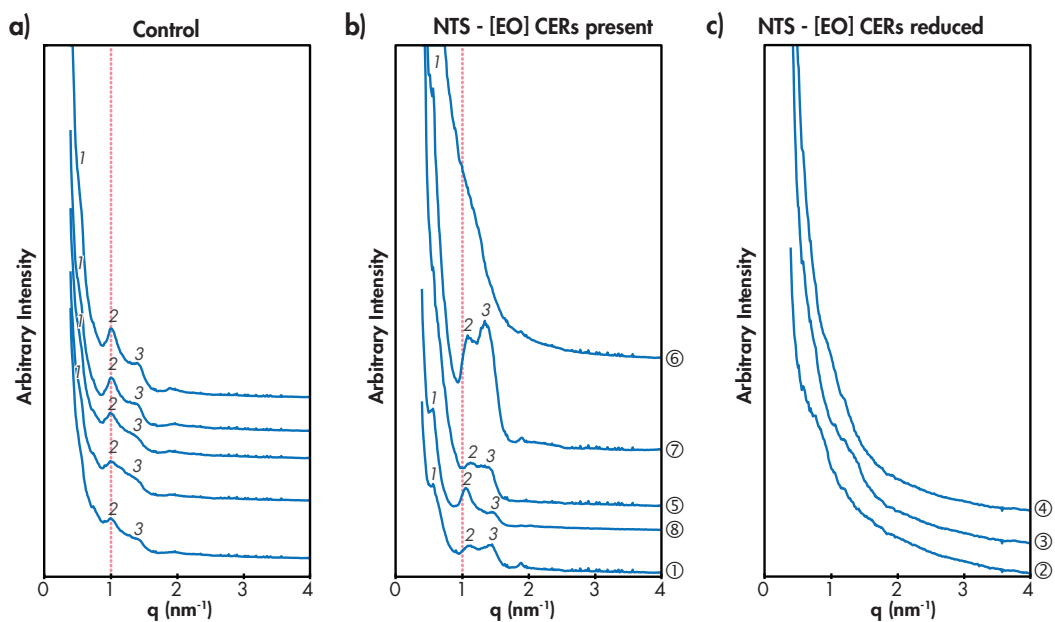


Figure 6: SAXD patterns of controls **a)** and NTS patients (**b** and **c**). The positions of the peaks (q) are indicative for the periodicity of the lipid lamellae. Figure **b)** shows NTS patients with a normal level of acyl-CERs, while Figure **c)** presents diffraction patterns of NTS patients with a reduced level of acyl-CERs. From the scattering angle, the scattering vector (q) was calculated by $q = 4\pi \sin \theta / \lambda$, in which λ is the wavelength of the X-rays at the sample position and θ the scattering angle. Individual NTS patients are labeled ①-⑧.

either lower or higher q -values. The most likely explanation for this increased intensity and changed shape of the peak is the formation of additional phases. The diffraction pattern of patient ⑥ does not show any diffraction peak. Figure 6c shows the SAXD curves of the NTS patients (numbers ②, ③, and ④) that have a low level of acyl-CERs present in the 3D ion chromatograms in Figure 3. No peaks are observed in the diffraction patterns of these NTS patients.

Higher degree of disordering of the lipid chains in NTS

Figure 7 shows the CH_2 symmetric stretching peak position of the SC lipids in controls (green) and NTS patients (red). A higher peak position indicates a higher degree of conformational disordering of the lipid chains. The average peak position of the NTS patients is $2850.0 \pm 0.6 \text{ cm}^{-1}$, which is significantly higher compared to the control samples, showing an average value of $2849.4 \pm 0.1 \text{ cm}^{-1}$. In addition, a larger variability between NTS patients compared to controls was observed when performing a non-parametric Levene's test ($P < 0.05$).

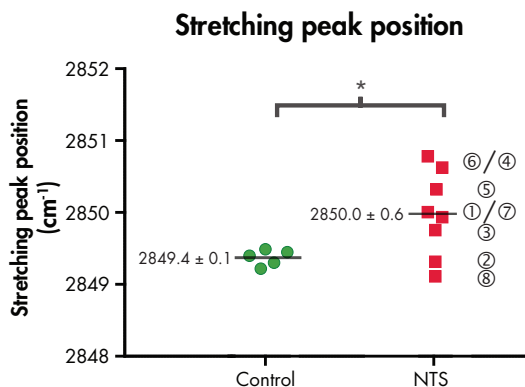


Figure 7: CH_2 symmetric stretching peak position in SC of controls (green dots) and NTS patients (red dots). A higher peak position indicates a higher degree of conformational disordering of the lipid chains. Individual NTS patients are labeled ①-⑧.

Discussion

In this study, we investigated the SC lipid composition and organization in 8 NTS patients and compared this to control SC. Recently, Bonnart *et al.* studied the lipid composition in transgenic mice overexpressing ELA2 as a model for NTS³⁴. They observed a decreased level of FFAs and an increased total level of glucosylceramide and reduction of sphingomyelin. Electron microscopy studies revealed the presence of unprocessed lipids in the intercellular space of the SC. However, no further details on lipid subclasses and chain length distributions were provided, which is the focus of the present study. In addition we analyzed the lipid organization. Both the lipid composition and organization in SC of NTS patients show large deviations from that in control subjects. More precisely, we show that in SC of NTS patients there is an increase in the levels of MUFAs and in short-chain FFAs. Similar changes were observed in the CER composition: increased levels of unsaturated CERS as well as short-chain CERS were abundantly present in SC of NTS patients compared to control subjects. We also observed changes in the lipid organization in SC of NTS patients: a higher degree in conformational disordering of the lipid chains as well as an altered lamellar organization. In a subgroup of NTS patients almost no acyl-CERS were present.

The changes in the lipid composition correlated to changes in the lipid organization. NTS patients (①, ⑤, ⑦, and ⑧) with normal levels of acyl-CERS in their SC, revealed a diffraction pattern indicating the presence of the LPP. In contrast, NTS patients with low levels of acyl-CERS (②, ③, and ④) did not show any proper SC lamellar organization, as no diffraction peaks were observed in the corresponding SAXD profile. The exception is NTS patient ⑥: Despite a high level of acyl CERS present in the SC, no peaks were detected in the

SAXD profile of this patient. However, this patient shows a clearly distinguishable profile in most CER subclasses and has the highest level of short chain CERs and unsaturated CERs. In addition, the highest level of MUFAs as well as the shortest average FFA chain length was observed in this patient. The abundant presence of shorter and unsaturated lipid chains enhances disordering of the lipid organization and may therefore explain the lack of regularly stacked lipid lamellae⁴⁹. Finally, only one patient (Ⓢ) showed a diffraction profile very similar to the controls. This patient exhibits the least deviation in SC lipid composition compared to the control subjects.

It has been reported that NTS patients show a drastic reduction in skin barrier function, as indicated by increased TEWL values⁷⁻⁹. As the lipids play a crucial role in the skin barrier function, an altered lipid composition and thus a change in lipid organization may contribute to the increased TEWL values in NTS patients: In previous studies using model lipid systems, we observed that both an absence of acyl-CERs as well as short chain FFAs results in an increased permeability^{49,50}. Furthermore, very recently we also reported an excellent correlation between a reduction in chain length of CERs and an increase in TEWL in patients with AE, demonstrating that the lipids may play a role in the impaired skin barrier function¹⁷.

NTS and AE are both inflammatory diseases with some genetic association. Patients with NTS show many symptoms comparable to AE patients^{18,19}. Therefore, a comparison in lipid profiling between NTS and AE is also of interest. Several changes in lipid composition in NTS were also observed in SC of patients with AE, but in the latter less pronounced. These changes are: *i*) A reduction in the level of acyl-CERs; *ii*) Increased levels of CER [AS] and CER [NS] and a reduced level of CER [NP]; *iii*) Increased levels in C₃₄ CERs; *iv*) A shift to shorter chain lengths in FFAs and CERs; *v*) Increased levels in MUFAs. In AE, these changes in lipid composition correlated very well with an increased TEWL^{16,17,51}. Therefore, also in NTS these changes in lipid composition and organization may contribute to the impaired skin barrier. In AE we observed that changes in the SC lipids were more pronounced in lesional skin compared to non-lesional skin, which may indicate that either inflammation and/or the presence of surface bacteria may play a role in changes in the lipid composition.

Several changes in epidermal processing may contribute to a change in the lipid composition in NTS. *i*) An increased pH in SC of NTS patients, which may be caused by an ELA-2 hyperactivity and lower NMF levels. This may lead to alterations in SC CER subclass levels in NTS^{33,36,52} as the activity of both sphingomyelinase and β -glucocerebrosidase are both highly dependent on the pH in their microenvironment. Furthermore, a pH increase induces high serine proteases activity that in turn degrades lipid processing enzymes³³. Upregulation of KLK activity has also been reported to affect these enzymes³³. As CER

[AS] and CER [NS] both have sphingomyelin as precursor, an imbalance in the activity of these enzymes may increase the relative levels of these ceramides. ii) Park *et al.* showed a downregulation of elongases 1, 4 and 6 (ELOVL1, 4 and 6) and a subsequent reduction in CER chain length in a murine atopic eczema model⁵³, demonstrating that these enzymes may be involved in the reduction of CER chain length in this model. In addition, it is known that ELOVL-4 knockout mice show a strong reduction in long chain FFAs, especially beyond C24; increased presence of unsaturated FFAs; and absence of acyl-CERs⁵⁴. Therefore, the reduction in chain length of the lipids in SC of NTS patients may be related to a decreased activity of ELOVLs.

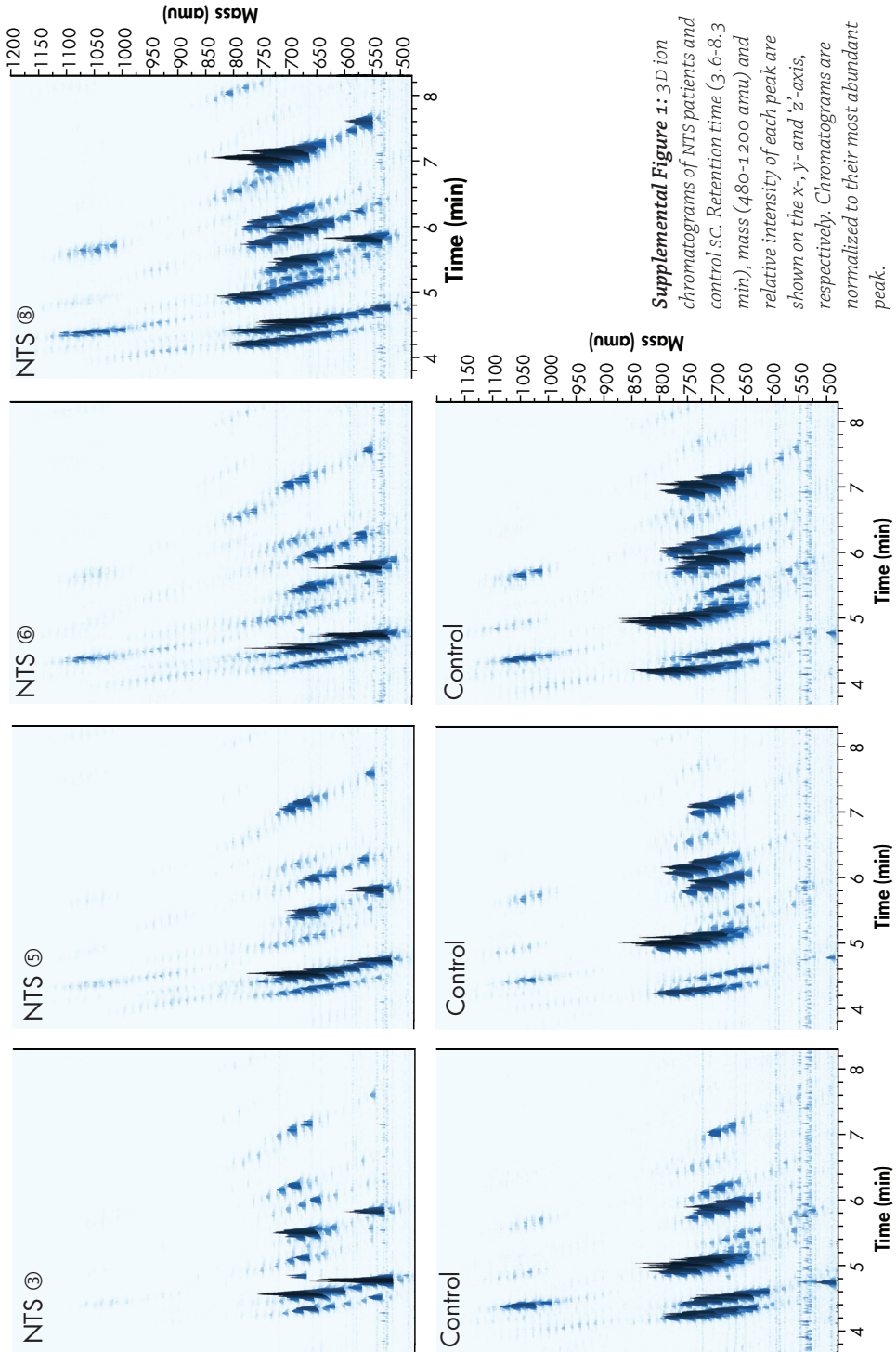
In conclusion, this study indicates for the first time that the SC lipid composition and organization are both altered in NTS patients. These alterations in SC lipids may at least partly explain the skin barrier dysfunction in NTS. It is of interest to study the activity of the abovementioned enzymes in NTS patients *in vivo* as the SC lipid barrier is likely impaired due to altered epidermal enzyme activities in NTS patients.

References

- 1 Bitoun E, Chavanas S, Irvine AD *et al*. Netherton syndrome: disease expression and spectrum of SPINK5 mutations in 21 families. *J Invest Dermatol* 2002; 118: 352-61.
- 2 Hausser I, Anton-Lamprecht I, Hartschuh W *et al*. Netherton's syndrome: ultrastructure of the active lesion under retinoid therapy. *Arch Dermatol Res* 1989; 281: 165-72.
- 3 Pruszkowski A, Bodemer C, Fraitag S *et al*. Neonatal and infantile erythrodermas: a retrospective study of 51 patients. *Arch Dermatol* 2000; 136: 875-80.
- 4 Smith DL, Smith JG, Wong SW *et al*. Netherton's syndrome: a syndrome of elevated IgE and characteristic skin and hair findings. *J Allergy Clin Immunol* 1995; 95: 116-23.
- 5 Sun JD, Linden KG. Netherton syndrome: a case report and review of the literature. *Int J Dermatol* 2006; 45: 693-7.
- 6 Greene SL, Muller SA. Netherton's syndrome. Report of a case and review of the literature. *J Am Acad Dermatol* 1985; 13: 329-37.
- 7 Fartasch M, Williams ML, Elias PM. Altered lamellar body secretion and stratum corneum membrane structure in Netherton syndrome: differentiation from other infantile erythrodermas and pathogenic implications. *Arch Dermatol* 1999; 135: 823-32.
- 8 Hachem JP, Wagberg F, Schmutz M *et al*. Serine protease activity and residual LEKTI expression determine phenotype in Netherton syndrome. *J Invest Dermatol* 2006; 126: 1609-21.
- 9 Moskowitz DG, Fowler AJ, Heyman MB *et al*. Pathophysiologic basis for growth failure in children with ichthyosis: an evaluation of cutaneous ultrastructure, epidermal permeability barrier function, and energy expenditure. *J Pediatr* 2004; 145: 82-92.
- 10 Masukawa Y, Narita H, Sato H *et al*. Comprehensive quantification of ceramide species in human stratum corneum. *J Lipid Res* 2009; 50: 1708-19.
- 11 van Smeden J, Hoppel L, van der Heijden R *et al*. LC/MS analysis of stratum corneum lipids: ceramide profiling and discovery. *J Lipid Res* 2011; 52: 1211-21.
- 12 Norlen L, Nicander I, Lundsjo A *et al*. A new HPLC-based method for the quantitative analysis of inner stratum corneum lipids with special reference to the free fatty acid fraction. *Arch Dermatol Res* 1998; 290: 508-16.
- 13 Ponem M, Gibbs S, Pilgram G *et al*. Barrier function in reconstructed epidermis and its resemblance to native human skin. *Skin Pharmacol Appl Skin Physiol* 2001; 14 Suppl 1: 63-71.
- 14 Madison KC, Swartzendruber DC, Wertz PW *et al*. Presence of intact intercellular lipid lamellae in the upper layers of the stratum corneum. *J Invest Dermatol* 1987; 88: 714-8.
- 15 Bouwstra JA, Gooris GS, van der Spek JA *et al*. Structural investigations of human stratum corneum by small-angle X-ray scattering. *J Invest Dermatol* 1991; 97: 1005-12.
- 16 Ishikawa J, Narita H, Kondo N *et al*. Changes in the ceramide profile of atopic dermatitis patients. *J Invest Dermatol* 2010; 130: 2511-4.
- 17 Janssens M, van Smeden J, Gooris GS *et al*. Increase in short-chain ceramides correlates with an altered lipid organization and decreased barrier function in atopic eczema patients. *J Lipid Res* 2012; 53: 2755-66.
- 18 Elias PM. Therapeutic Implications of a Barrier-based Pathogenesis of Atopic Dermatitis. *Ann Dermatol* 2010; 22: 245-54.
- 19 Krol A, Krafchik B. The differential diagnosis of atopic dermatitis in childhood. *Dermatol Ther* 2006; 19: 73-82.
- 20 Chavanas S, Bodemer C, Rochat A *et al*. Mutations in SPINK5, encoding a serine protease inhibitor, cause Netherton syndrome. *Nat Genet* 2000; 25: 141-2.
- 21 Simon M, Bernard D, Minondo AM *et al*. Persistence of both peripheral and non-peripheral corneodesmosomes in the upper stratum corneum of winter xerosis skin versus only peripheral in normal skin. *J Invest Dermatol* 2001; 116: 23-30.
- 22 Komatsu N, Saijoh K, Otsuki N *et al*. Proteolytic processing of human growth hormone by multiple tissue kallikreins and regulation by the serine protease inhibitor Kazal-Type5 (SPINK5) protein. *Clin Chim Acta* 2007; 377: 228-36.
- 23 Komatsu N, Saijoh K, Sidiropoulos M *et al*. Quantification of human tissue kallikreins in the stratum corneum: dependence on age and gender. *J Invest Dermatol* 2005; 125: 1182-9.
- 24 Komatsu N, Takata M, Otsuki N *et al*. Elevated stratum corneum hydrolytic activity in Netherton syndrome suggests an inhibitory regulation of desquamation by SPINK5-derived peptides. *J Invest Dermatol* 2002; 118: 436-43.
- 25 Borgono CA, Michael IP, Komatsu N *et al*. A potential role for multiple tissue kallikrein serine proteases in epidermal desquamation. *J Biol Chem* 2007; 282: 3640-52.
- 26 Egelrud T, Brattsand M, Kreutzmann P *et al*. hK5 and hK7, two serine proteinases abundant in human skin, are inhibited by LEKTI domain 6. *Br J Dermatol* 2005; 153: 1200-3.
- 27 Deraison C, Bonnart C, Lopez F *et al*. LEKTI fragments specifically inhibit KLK5, KLK7, and KLK14 and control desquamation through a pH-dependent interaction. *Mol Biol Cell* 2007; 18: 3607-19.
- 28 Stefansson K, Brattsand M, Roosterman D *et al*. Activation of proteinase-activated receptor-2 by human kallikrein-related peptidases. *J Invest Dermatol* 2008; 128: 18-25.
- 29 Briot A, Deraison C, Lacroix M *et al*. Kallikrein 5 induces atopic dermatitis-like lesions through PAR2-mediated thymic stromal lymphopoietin expression in Netherton syndrome. *J Exp Med* 2009; 206: 1135-47.
- 30 Brattsand M, Stefansson K, Lundh C *et al*. A proteolytic cascade of kallikreins in the stratum corneum. *J Invest Dermatol* 2005; 124: 198-203.
- 31 Hatano Y, Terashi H, Arakawa S *et al*. Interleukin-4 suppresses the enhancement of ceramide synthesis and cutaneous permeability barrier functions induced by tumor necrosis factor-alpha and interferon-gamma in human epidermis. *J Invest Dermatol* 2005; 124: 786-92.
- 32 Jung YJ, Jung M, Kim M *et al*. IL-1 alpha Stimulation Restores Epidermal Permeability and Antimicrobial Barriers Compromised by Topical Tacrolimus. *Journal of Investigative Dermatology* 2011; 131: 698-705.

- 33 Hachem JP, Man MQ, Crumrine D *et al.* Sustained serine protease activity by prolonged increase in pH leads to degradation of lipid processing enzymes and profound alterations of barrier function and stratum corneum integrity. *J Invest Dermatol* 2005; 125: 510-20.
- 34 Bonnart C, Deraison C, Lacroix M *et al.* Elastase 2 is expressed in human and mouse epidermis and impairs skin barrier function in Netherton syndrome through filaggrin and lipid misprocessing. *J Clin Invest* 2010; 120: 871-82.
- 35 Rippke F, Schreiner V, Schwanitz HJ. The acidic milieu of the horny layer: new findings on the physiology and pathophysiology of skin pH. *Am J Clin Dermatol* 2002; 3: 261-72.
- 36 Mauro T, Elias PM, Feingold KR. SC pH: measurement, origins, and functions. In "Skin Barrier". New York: Taylor & Francis. 2006.
- 37 Emami N, Diamandis EP. Human kallikrein-related peptidase 14 (KLK14) is a new activator component of the KLK proteolytic cascade. Possible function in seminal plasma and skin. *J Biol Chem* 2008; 283: 3031-41.
- 38 Michael IP, Pampalakis G, Mikolajczyk SD *et al.* Human tissue kallikrein 5 is a member of a proteolytic cascade pathway involved in seminal clot liquefaction and potentially in prostate cancer progression. *J Biol Chem* 2006; 281: 12743-50.
- 39 Raghunath M, Tontsidou L, Oji V *et al.* SPINK5 and Netherton syndrome: novel mutations, demonstration of missing LEKTI, and differential expression of transglutaminases. *J Invest Dermatol* 2004; 123: 474-83.
- 40 Di WL, Hennekam RC, Callard RE *et al.* A heterozygous null mutation combined with the G1258A polymorphism of SPINK5 causes impaired LEKTI function and abnormal expression of skin barrier proteins. *Br J Dermatol* 2009; 161: 404-12.
- 41 Hitomi K. Transglutaminases in skin epidermis. *Eur J Dermatol* 2005; 15: 313-9.
- 42 Hausser I, Anton-Lamprecht I. Severe congenital generalized exfoliative erythroderma in newborns and infants: a possible sign of Netherton syndrome. *Pediatr Dermatol* 1996; 13: 183-99.
- 43 Schreiner V, Gooris GS, Pfeiffer S *et al.* Barrier characteristics of different human skin types investigated with X-ray diffraction, lipid analysis, and electron microscopy imaging. *J Invest Dermatol* 2000; 114: 654-60.
- 44 Tanojo H, BosvanGeest A, Bouwstra JA *et al.* In vitro human skin barrier perturbation by oleic acid: Thermal analysis and freeze fracture electron microscopy studies. *Thermochimica Acta* 1997; 293: 77-85.
- 45 International Union of Pure and Applied Chemistry. Commission on the Nomenclature of Organic Chemistry., Rigaudy J, Klesney SP *et al.* *Nomenclature of organic chemistry, 4th edn.* Oxford ; New York: Pergamon Press. 1979.
- 46 Motta S, Monti M, Sesana S *et al.* Ceramide composition of the psoriatic scale. *Biochim Biophys Acta* 1993; 1182: 147-51.
- 47 Bligh EG, Dyer WJ. A rapid method of total lipid extraction and purification. *Can J Biochem Physiol* 1959; 37: 911-7.
- 48 Bras W, Dolbnya IP, Detollenaere D *et al.* Recent experiments on a combined small-angle/wide-angle X-ray scattering beam line at the ESRF. *Journal of Applied Crystallography* 2003; 36: 791-4.
- 49 Groen D, Poole DS, Gooris GS *et al.* Is an orthorhombic lateral packing and a proper lamellar organization important for the skin barrier function? *Biochim Biophys Acta* 2011; 1808: 1529-37.
- 50 de Jager M, Groenink W, Bielsa i Guivernau R *et al.* A novel in vitro percutaneous penetration model: evaluation of barrier properties with p-aminobenzoic acid and two of its derivatives. *Pharm Res* 2006; 23: 951-60.
- 51 van Smeden J, Janssens M, Kaye EC *et al.* The essence of the lipid chain length for skin barrier function and its relation to atopic eczema. To be submitted.
- 52 Hachem JP, Crumrine D, Fluhr J *et al.* pH directly regulates epidermal permeability barrier homeostasis, and stratum corneum integrity/cohesion. *J Invest Dermatol* 2003; 121: 345-53.
- 53 Park YH, Jang WH, Seo JA *et al.* Decrease of ceramides with very long-chain fatty acids and downregulation of elongases in a murine atopic dermatitis model. *J Invest Dermatol* 2012; 132: 476-9.
- 54 Vasireddy V, Uchida Y, Salem N, Jr. *et al.* Loss of functional ELOVL4 depletes very long-chain fatty acids (> or =C28) and the unique omega-O-acylceramides in skin leading to neonatal death. *Hum Mol Genet* 2007; 16: 471-82.

Supplementary Figure



Supplemental Figure 1: 3D ion chromatograms of NTS patients and control sc. Retention time (3.6-8.3 min), mass (480-1200 amu) and relative intensity of each peak are shown on the x-, y- and z-axis, respectively. Chromatograms are normalized to their most abundant peak.

CHAPTER 10

INCREASED PRESENCE OF MONO- UNSATURATED FATTY ACIDS IN THE STRATUM CORNEUM OF HUMAN SKIN EQUIVALENTS

Jeroen van Smeden^{1,*},
Varsha S. Thakoersing^{1,*},
Aat Mulder¹, Rob Vreeken^{2,3},
Abdoelwaheb El Ghalbzouri⁴,
Joke A. Bouwstra¹

¹ Division of Drug Delivery Technology,
Leiden Academic Centre for Drug Research,
Leiden University, Leiden, The Netherlands.

² Division of Analytical Biosciences, Leiden
Academic Centre for Drug Research,
Leiden University, Leiden, The Netherlands.

³ Netherlands Metabolomics Centre, Leiden
Academic Centre for Drug Research,
Leiden University, Leiden, The Netherlands.

⁴ Department of Dermatology, Leiden
University Medical Center, Leiden,
The Netherlands

*Both authors contributed equally to this work

Adapted from Journal of Investigative
Dermatology. 2013. 133:59–67

Abstract

Previous results showed that our in-house human skin equivalents (HSEs) differ in their stratum corneum (SC) lipid organization compared with human SC. To elucidate the cause of the altered SC lipid organization in the HSEs, a recently developed liquid chromatography/mass spectrometry method was used to study the free fatty acid (FFA) and ceramide (CER) composition in detail. In addition, the SC lipid composition of the HSEs and human skin was examined quantitatively with high-performance thin layer chromatography. For the first time our results reveal that all our HSEs have an increased presence of mono-unsaturated FFAs compared with human SC. Moreover, the HSEs display the presence of CER species with a mono-unsaturated acyl chain, which are not detected in human SC. All HSEs also exhibit an altered expression of stearyl-CoA desaturase, the enzyme that converts saturated FFAs to mono-unsaturated FFAs. Furthermore, the HSEs show the presence of twelve CER subclasses, similar to native human SC. However, the HSEs have increased levels of CERS [EOS] and [EOH] and CER species with short total carbon chains and a reduced FFA level compared with human SC. The presence of unsaturated lipid chains in HSE offers new opportunities to mimic the lipid properties of human SC more closely.

Introduction

Human skin equivalents (HSEs) provide a valuable tool to predict the permeation of substances through the skin^{1–8} or to determine whether compounds are toxins, irritants, or sensitizers for the skin^{9–12}. However, to obtain a reliable *in vitro* – *in vivo* correlation, it is a prerequisite that HSEs have a comparable skin barrier function as native human

skin. The main barrier for compound penetration is located in the lipid matrix of the stratum corneum (SC). This lipid matrix is mainly composed of cholesterol, free fatty acids (FFAs), and ceramides (CERs)^{13,14}. The lipid composition determines the lipid organization in the SC and is therefore a key factor in determining the skin barrier function¹⁵. We have previously investigated the SC lipid organization of four of our in-house HSEs, namely the fibroblast derived matrix model (FDM), Leiden epidermal model (LEM), full-thickness collagen model (FTM), and full-thickness outgrowth (FTO). The LEM is a skin equivalent with only an epidermal compartment. The FDM is a model wherein fibroblasts produce their own extracellular matrix, whereas the FTM contains a dermal compartment that consists of rat tail collagen populated with human fibroblasts. In the FTO, a full thickness explant of native human skin is placed onto rat tail collagen and is allowed to expand and develop an epidermis. The skin models mimic many aspects of native human skin. However, they display some differences in their SC lipid organization. These differences may have an important role in their decreased permeability barrier compared with human SC^{16,17}. As the lipid organization is dictated by the lipid composition, we determined the SC lipid composition of each HSE in detail to unravel the cause of their altered SC lipid organization. For this purpose, we quantitatively assessed the SC lipid composition of our in-house HSEs and native human SC with high-performance thin layer chromatography (HPTLC). Nine CER subclasses have been identified in native human SC using HPTLC¹⁸, whereas twelve CER subclasses have been identified using a recently developed liquid chromatography/mass spectrometry (LC/MS) method¹⁹. In this study, we used LC/MS to determine whether all identified CER subclasses in native human SC are also present in the SC of our HSEs. In addition, detailed information on the chain length distribution and degree of saturation of each CER subclass and FFAs is provided and compared with the SC of native human skin. The expression pattern of several enzymes involved in the FFA and CER synthesis was also investigated to examine the biological cause of the altered SC lipid properties observed in the HSEs. This study has led to the identification of previously unreported targets that offer previously unreported opportunities to optimize the SC lipid properties of HSEs and mimic the barrier properties of native human skin even more closely.

Materials and Methods

Cell culture

Native human mammary or abdomen skin was obtained from adults undergoing surgery. Human skin left over from surgery was collected after written informed consent of the skin donors and institutional approval was obtained. The Declaration of Helsinki

Principles were followed when using human tissue. Normal human keratinocytes (NHKs) and human dermal fibroblasts were isolated as described before²⁰. A detailed description of the required media is provided as supplementary information. NHKs used to create HSEs with only an epidermal compartment were cultured with the Dermalife K medium complete kit (Lifeline Cell Technology, Walkersville, MD) supplemented with 1% penicillin/streptomycin (Sigma, Zwijndrecht, The Netherlands) until they reached a maximum confluency of 80%. First and second passage NHKs were used to generate HSEs.

Dermal equivalents

Collagen-type I containing dermal equivalents: Collagen-type I containing dermal equivalents were generated as described earlier²⁰. Details regarding the generation of the dermal equivalents are provided as Supplementary Information.

Fully human dermal equivalents: The dermal matrices for the FDMs were generated as described previously²¹. Details regarding the generation of the FDMs are provided as Supplementary Information.

Generation of HSEs

HSEs generated on collagen dermal equivalents referred to as FTM: One week after preparation of the collagen type I containing dermal equivalents $0.5 \cdot 10^6$ NHKs were seeded on top of each dermal equivalent. On the first two days, the HSEs were kept submerged in a medium consisting of DMEM and Ham's F12 (Invitrogen, Leek, The Netherlands) (3:1 v/v), 5% fetal bovine serum (FBS), 1% penicillin/streptomycin, $0.5 \mu\text{M}$ hydrocortisone, $1 \mu\text{M}$ isoproterenol and $0.5 \mu\text{g/mL}$ insulin. The following two days the HSEs were kept submerged in a similar medium, except that the FBS was reduced to 1% and $0.053 \mu\text{M}$ selenious acid (Johnson Matthey, Maastricht, The Netherlands), 10 mM L-serine (Sigma), $10 \mu\text{M}$ L-carnitine (Sigma), $1 \mu\text{M}$ α -tocopherol acetate (Sigma), 25 mM vitamin C and a lipid mixture of $3.5 \mu\text{M}$ arachidonic acid (Sigma), $30 \mu\text{M}$ linoleic acid (Sigma), $25 \mu\text{M}$ palmitic acid (Sigma) were added to the medium. Hereafter, the HSEs were lifted to the air/liquid interface and were nourished with a medium in which the FBS was omitted and the arachidonic acid concentration was increased to $7 \mu\text{M}$. The medium was refreshed twice a week. The HSEs were harvested 16 days after seeding of the NHKs onto the dermal equivalents.

HSEs generated on fully human dermal equivalents referred to as FDM: Three weeks after seeding fibroblasts onto filter inserts $0.5 \cdot 10^6$ NHKs were seeded onto each dermal equivalent. The HSEs were further cultured as described for the FTMs.

HSEs generated on inert filter, referred to as Leiden epidermal model (LEM): LEMs were

generated as described previously¹⁰ with slight modifications. $0.2 \cdot 10^6$ NHKs were seeded onto cell culture inserts (Corning tranwell cell culture inserts, membrane diameter 12 mm, pore size $0.4 \mu\text{M}$, Corning Life Sciences, Amsterdam, The Netherlands). The cells were kept submerged for 2-3 days in Dermalife medium until confluency. On the following 2 days, the HSEs were kept submerged in CnT medium (CellnTec, Bern, Switzerland) supplemented according to the manufacturer's protocol and 1% penicillin/streptomycin solution, $1 \mu\text{M}$ α -tocopherol acetate, $25 \mu\text{M}$ vitamin C, and a lipid mixture of $7 \mu\text{M}$ arachidonic acid, $30 \mu\text{M}$ linoleic acid, and $25 \mu\text{M}$ palmitic acid. Hereafter, the cells were nourished with the same medium, but were grown at the air/liquid interface. The LEMs were harvested 16 days after seeding the NHKs onto the inserts.

Full thickness cultures (FTO): Full-thickness (4 mm) fat free punch biopsies obtained from abdomen or mammary skin were gently pushed into freshly generated collagen type 1 containing dermal equivalents. These HSEs were cultured similarly as described for the FTMs and FDMS, except that they were directly cultured at the air/liquid interface. The FTOs were grown for approximately 16 days.

Morphology and immunohistochemistry

Harvested HSEs were fixed in 4% (w/v) paraformaldehyde (Lommerse Pharma, Oss, The Netherlands), dehydrated and subsequently embedded in paraffin. $5 \mu\text{m}$ sections were cut and used for immunohistochemical staining of human SCD1 (100 \times dilution; Sigma), serine palmitoyltransferase (SPT; 400 \times dilution; Cayman Chemicals, Ann Arbor, MI) and CER synthase 3 (CERS3; 10 \times dilution; Atlas Antibodies, Stockholm, Sweden). Immunohistochemical stainings of the samples were performed with the R.T.U. Vectastain Elite ABC reagent kit (Vector Laboratories, Burlingame, CA). Details of the staining procedure are provided as Supplementary Information.

SC Isolation and lipid extraction

The SC of human abdomen or mammary skin was isolated as described previously¹⁹. The SC lipids were extracted according to the Bligh and Dyer procedure²² with a series of chloroform/methanol mixtures (1:2, 1:1 and 2:1 v/v) for 1 hour each. The extracts were combined and treated with 0.25M KCl and water. The organic phase was collected and evaporated under a stream of nitrogen at 40°C . The obtained lipids were reconstituted in a suitable volume of chloroform/methanol (2:1 v/v) and stored at -20°C until use. To obtain enough lipids for quantification, the lipid extracts of 2-4 HSEs from the same experiment and donor were pooled. The SC lipid composition of the full-thickness explant could not be determined, because there was not enough material to extract.

HPTLC lipid quantification

The extracted SC lipids were quantified using HPTLC. The used solvent system to separate the lipids is provided elsewhere²³. Co-chromatography of serial dilutions of standards was used to identify and quantify each lipid class. The standards consisted of cholesterol, palmitic acid, stearic acid, arachidic acid, tricosanoic acid, behenic acid, lignoceric acid, cerotic acid, and CERS [EOS], [NS], [NP], [EOH], and [AP]. CER nomenclature according to terminology of Motta *et al.*²⁴ and Masukawa *et al.*²⁵. The CERS were provided by Cosmoferm (The Netherlands). All other compounds were purchased from Sigma (The Netherlands). The lipid fractions were visualized and quantified as described before²⁶. For quantification, SC lipid samples of two donors were used of each HSE type and native human skin.

LC/MS lipid analysis

The SC lipid species in the pooled lipid extracts of the HSEs and native human skin were analyzed by LC/MS according to the method described elsewhere¹⁹. Briefly: an Alliance 2695 HPLC (Waters Corp., Milford, MA) was coupled to a TSQ Quantum MS (Thermo Finnigan, San Jose, CA) measuring in APCI mode. The total lipid concentration of all samples was around 1 mg/ml and the injection volume was set to 10 µl for the analysis of both CERS and fatty acids. CERS were separated using a PVA-Sil analytical column (5 µm particle size, 100 × 2.1 mm i.d. YMC, Kyoto, Japan) using a gradient mobile phase from heptane to heptane/isopropanol/ethanol at a flow rate of 0.8 mL/min. The scan range of the MS was set between 500-1200 amu, measuring in positive ion mode. FFAs were analyzed by introducing some adaptations to the setup used for CER analysis as will be described in detail elsewhere (van Smeden *et al*, submitted): separation was achieved using a LichroCART Purospher STAR analytical column (55 × 2 mm i.d. Merck, Darmstadt, Germany) under a flow rate of 0.6 ml/min using a gradient system from acetonitril/H₂O to methanol/heptane. 1% CHCl₃ and 0.2% acetic acid (HAc) were added to both mobile phases as ionization enhancers. The ionization mode and scan range was altered to negative mode and 200-600 amu, respectively.

Results

HPTLC analysis reveals that the HSEs have a reduced SC FFA content compared with human skin

The SC lipids of the HSEs and human skin were extracted and quantified with HPTLC to determine whether the HSEs show differences in their lipid composition compared with human skin. Figure 1a shows that SC of the HSEs contains cholesterol, FFAs, and all CER

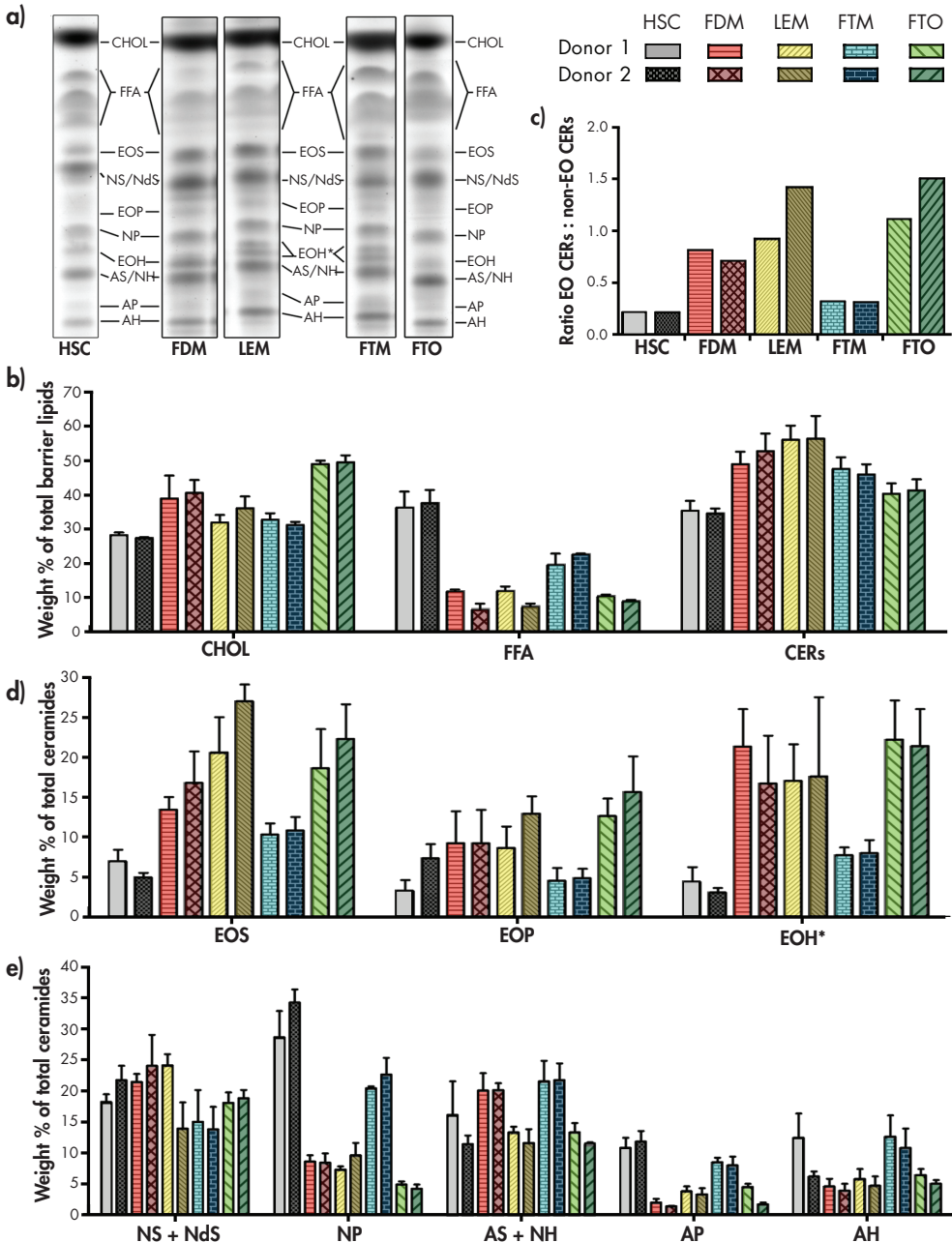


Figure 1: Stratum corneum barrier lipids content. Barrier lipids of human stratum corneum (HSC), FDM, LEM, FTM, and FTO were fractionated and quantified by HPTLC and photo densitometry. **a)** Barrier lipid composition of human SC and HSEs. **b)** Relative level of each SC lipid class, **c)** ratio of acyl-CERs ([EO] CERs) and non-acyl-CERs (non-[EO] CER), **d)** relative level of acyl-CERs, **e)** relative level of α -hydroxy and non-hydroxy CERs. The data represents the sample mean \pm SD of at least 3 analytical points. CHOL = cholesterol, FFA = free fatty acids, CERs = CERs, * unidentified lipid. CER nomenclature: A = α -hydroxy fatty acid, E = ester-linked fatty acid, N = non-hydroxy fatty acid, O = ω -hydroxy fatty acid, ds = dihydrosphingosine, H = 6-hydroxysphingosine, P = phytosphingosine, S = sphingosine.

subclasses, which are also observed in human SC. In the LEM and FTM, an additional band of an unidentified lipid, with an R_f -value close to that of CER [EOH], can be observed. This unidentified lipid, which may represent an unidentified CER, was also occasionally observed in the FDM and FTO.

Figure 1b shows that human SC consists of approximately equal amounts of cholesterol, FFAs and CERs. All HSEs, however, show a different distribution of the SC barrier lipids (Figure 1b). The relative FFA content in the HSEs, especially in the FDM, LEM, and FTO, is much lower compared with human SC. The SC lipid quantification also indicates that the CER/cholesterol ratio (Supplementary Table 1) in the LEM is increased and reduced in FTO compared to human SC. This indicates that the relative CER and/or cholesterol levels in the SC of the LEM and FTO differ from the levels determined in human SC.

Most of the HSEs have an increased acyl-CER content compared with native human SC

In human SC twelve CER subclasses are identified. Each subclass is named according to its chemical structure^{24,25}. In short, CERs with a sphingosine (S), phytosphingosine (P), 6-hydroxysphingosine (H), or dihydrosphingosine (ds) backbone are linked via an amide to a fatty acid chain, which can either be an esterified ω -hydroxy (EO), α -hydroxy (A), or non-hydroxy (N) fatty acid. Figure 1c shows the ratio between the total acyl-CERs ([EO] CERs) and the other CER classes (sum of all α -hydroxy + non-hydroxy CERs) in the HSEs and native human skin. This figure clearly shows that the total acyl-CERs level is much higher in the FDM, LEM, and FTO compared with native human skin. Focusing on the individual acyl-CER levels, it is evident that the FDM, LEM and FTO have a higher content of CERs [EOS] and [EOH]* compared with human SC. The difference in EOP level between FDM, LEM, FTO and human SC is somewhat smaller compared with the other acyl-CERs (Figure 1d). FTM has a small increase in CER [EOS] and [EOH]* level compared with human SC, while the [EOP] level is very similar (Figure 1d).

On the TLC plate, an unidentified lipid close to CER [EOH] is observed in the LEM and FTM (Figure 1a). In the LC/MS CER profiles of the HSEs, an unidentified group of lipids, which have a molecular weight similar to acyl-CERs, is also observed close to CER [EOH] (Figure 2b, indicated by **). This suggests that the lipid band on the TLC plate most likely represents an acyl-CER class. For this reason, the unidentified lipid was quantified together with CER [EOH] (the two bands together are represented as [EOH]*).

The comparison of the α -hydroxy and non-hydroxy CERs also shows some differences in the distribution of these CER subclasses between the HSEs and human SC (Figure 1e). CER [NP] is the most abundant CER in human SC. Compared with human SC, the CER [NP] content is reduced in the FTM and an even further reduction is observed in the FDM,

LEM, and FTO. In addition, the CER [AP] content in the FTM is close to the CER content in human SC, but reduced in the FDM, LEM and FTO. The relative content of CERS [NS] + [Nds], CERS [AS] + [NH], and CER [AH] are similar in the HSEs and human SC. CERS [NS] + [Nds], and [AS] + [NH] were grouped together for quantification, because they comigrate and therefore have a similar R_f -value when using HPTLC.

All twelve CER subclasses detected in human SC are also observed in the HSEs

LC/MS analysis of native human SC lipids shows the presence of at least twelve CER subclasses, as reported previously¹⁹ (Figure 2a). In addition, within one CER subclass a large number of peaks are observed in the multi-mass chromatogram. Each peak represents a CER specie that has the same head group, but a different total carbon chain length and therefore a different molecular weight. In descending order, each specie has 14 mass units less, which represents a reduction in one CH_2 -group compared with the previous specie. All twelve CER subclasses in human SC show a large variation in their total carbon chain length distribution. In human SC the acyl-CERs have a total chain length varying from 63 to 78 carbon atoms. The α -hydroxy and non-hydroxy CER subclasses have shorter total carbon chains, which range from 34 to 50 and 34 to 56 carbon atoms, respectively. In addition to the twelve identified CER subclasses, human SC also shows the presence of some unidentified lipid classes. These unidentified lipid classes also consist of several species, indicated by the variation in total carbon chain length. The molecular structure of these lipids remains to be elucidated. The CER subclasses present in the FDM, including the total chain length distribution of each subclass, is provided in the multi-mass chromatogram in Figure 2b. This figure shows that all twelve CER subclasses present in native human SC are also detected in FDM. The other HSEs show a very similar LC/MS profile as the FDM and also show the presence of all twelve CER subclasses (Supplementary Figure 1). Each CER subclass in the HSEs shows a wide variation in total chain length distribution, similar to native human SC. In the HSEs the acyl-CERs have a total carbon chain that varies between 64 and 78 carbon atoms, which is almost similar to the chain length distribution observed for native human SC. The α -hydroxy and non-hydroxy CER subclasses have a total carbon chain between 32 and 50 and 34 and 56 carbon atoms, respectively. When focusing in more detail on the LC/MS profiles of the HSEs and native human SC, some differences are observed. In the multi-mass chromatograms of the HSEs, a weak lipid band is located just below the stronger peaks of the CER species (Figure 2c), which is observed for all CER subclasses. These additional weak lipid bands always have a mass of two units less than that of stronger band of the CER specie above them (Figure 2c and d). This specific difference of two mass units suggests that the lipid band

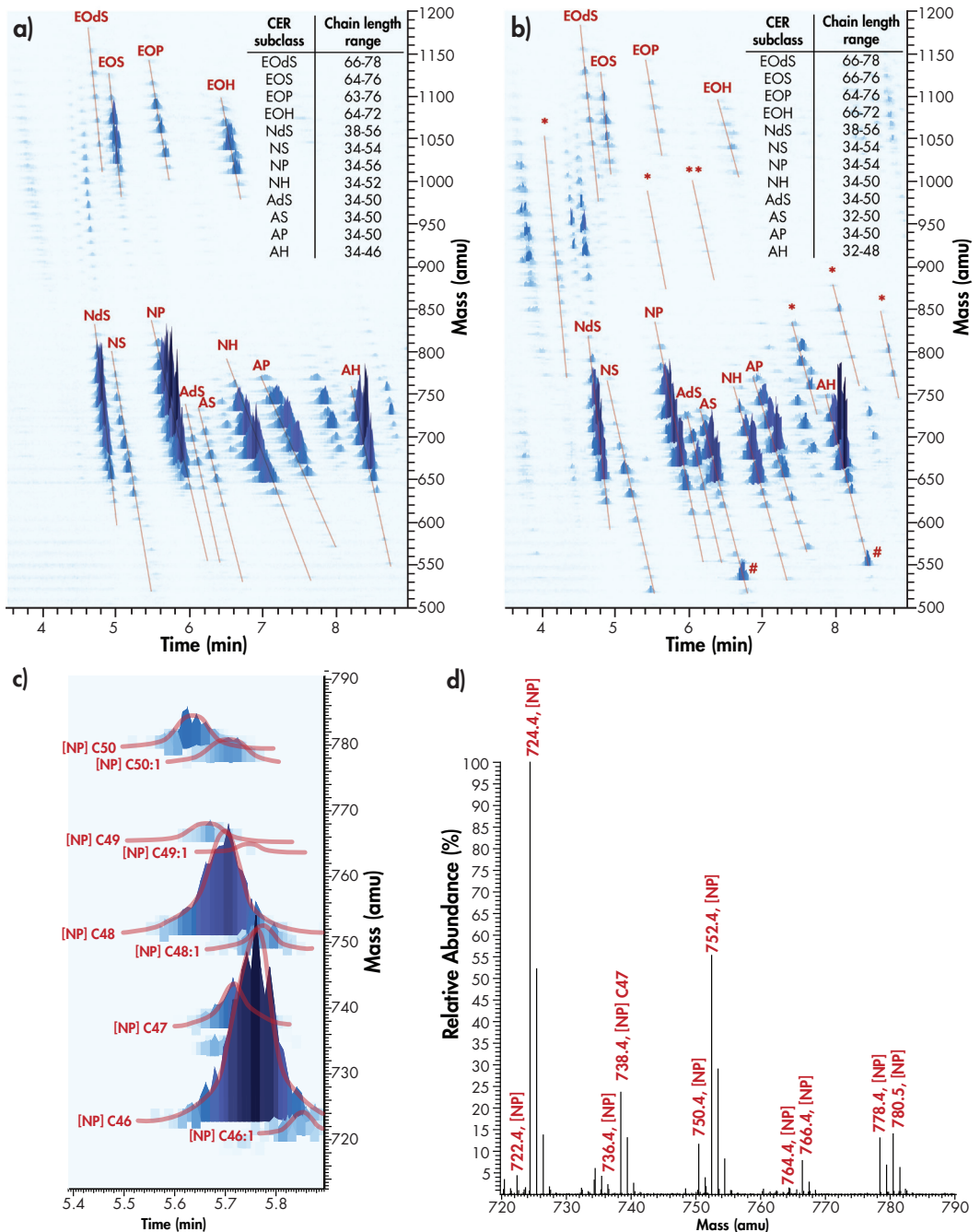


Figure 2: CER chain length distribution. LC/MS chromatogram of CER subclasses in human SC **a)** and FDM **b)**. The retention time, mass and intensity of each peak are shown on the x-axis, y-axis and 'z'-axis, respectively. The total carbon chain length variation of each CER subclass is provided in the inset. CERs with a low total carbon chain length, which are present in lower quantities in human SC, are indicated by # in the chromatogram of FDM. Unidentified lipids only observed in the chromatogram of FDM are specified with *. The unidentified lipid quantified together with CER [EOH] using HPTLC is indicated by **. Examples of CER species containing a MUFA chain are shown in **c)**. The masses of CER species with a saturated or MUFA chain are shown in **d)**.

represents a CER specie that contains a mono-unsaturated fatty acyl chain. The multi-mass chromatograms of the HSEs also show low molecular weight CER species that are not detected in human SC. Furthermore, some low molecular weight CER species, which have a mass below approximately 620 amu have a higher intensity in the multi-mass chromatograms of the HSEs compared with human skin. This is mainly observed for species of CERs [AS] and [AH], which have a total chain length of 34 carbon atoms (Figure 2b, indicated by #). The HSEs show the presence of several unidentified lipids, of which some are not present in the multi mass chromatogram of native human SC (Figure 2b, indicated by *).

HSEs show an increased presence of mono-unsaturated FFAs compared to native human SC

Figure 3 depicts the FFA chain length distribution and degree of saturation in human SC and FDM. The other HSEs showed a similar FFA composition as the FDM (Supplementary Figure 1). Human SC shows a FFA chain length distribution from C16:0 to C30:0. All HSEs contain FFAs with chain lengths varying from C16:0 to C28:0. This indicates that the HSEs are able to synthesize similar FFAs as native human skin. However, the FFA LC/MS profiles

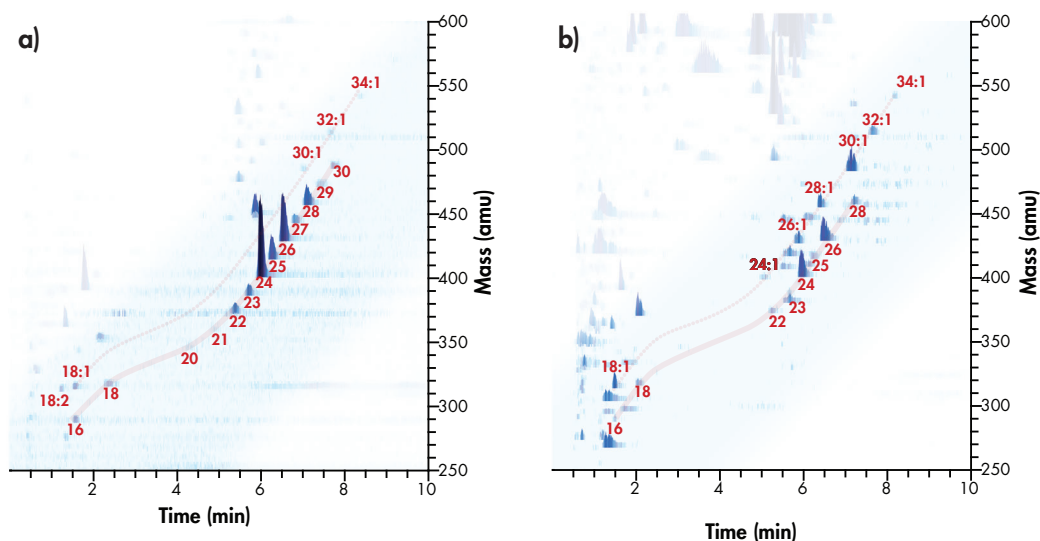


Figure 3: Fatty acid chain length distribution. Three dimensional multi-mass LC/MS chromatogram of FFAs in native human SC **a**) and FDM **b**) are shown. The retention time is shown on the x-axis, the mass (in amu) is provided on the y-axis and the intensity of each peak is depicted on the 'z'-axis. In human SC the FFA chain length distribution varies from C16:0 to C30:0. The FDM has a very similar FFA chain length distribution as human SC, but shows an increase in MUFAs with chain lengths varying from C16:1 to C34:1. Additionally, the odd chain length FFAs show a lower intensity in the chromatogram of FDM compared to human SC.

of all HSEs additionally show the presence of mono-unsaturated fatty acids (MUFAs), which are hardly detected in human SC. The MUFAs detected in the LC/MS profiles of the HSEs have a chain length varying from C16:1 up to C34:1. All HSEs also show a reduced level of FFAs with an odd carbon chain length compared with human SC.

The HSEs show an altered expression of stearoyl-CoA desaturase 1

To investigate the biological cause of the altered SC lipid organization of the HSEs, the expression pattern of some enzymes involved in the FFA and CER synthesis was examined. Stearoyl-CoA desaturase (SCD) is the rate-limiting enzyme that catalyzes the synthesis of MUFAs from saturated fatty acids^{27,28}. In native human epidermis, SCD1 is only expressed in the basal layer (Figure 4). In all HSEs, the expression of SCD is observed in the basal layer, as well as in the differentiated layers of the viable epidermis (Figure 4). This indicates that the expression of SCD1 is altered in the HSEs compared with human skin.

The first step in CER synthesis is the coupling of serine to palmitic acid by serine palmitoyltransferase (SPT)²⁹. In human skin, SPT expression is observed in the entire viable epidermis, showing both nucleic and cytoplasmic staining. No difference in expression pattern between human skin and the HSEs is observed (Figure 4). CER synthase 3 (CERS3) is one of the key enzymes involved in de novo CER synthesis pathway. CERS3 has a broad fatty acyl-CoA preference and therefore *n*-acylates both long and very-long chain fatty acyl-CoAs to a sphingoid base. Among the six CERS members (CERS 1-6), the mRNA expression of CERS3 is found to be the highest in differentiated keratinocytes *in vitro*³⁰. In addition, a recent publication by Jennemann *et al.*³¹ demonstrated that CERS3 is responsible for the synthesis of very-long chain CERs in the skin. In human skin and in all HSEs, CERS3 is expressed in the entire viable epidermis (Figure 4). It should be noted that the expression of SCD, SPT, and CERS3 was weaker in the FTO samples compared with the other HSEs.

Discussion

In previous studies, we have investigated the SC lipid organization of four in-house HSEs and native human skin. These studies showed that our in-house HSEs have a mainly hexagonal packing¹⁷, whereas human SC has the dense orthorhombic packing (a schematic representation of the SC lipid organization is depicted in Supplementary Figure 2). The presence of a hexagonal lipid organization has been correlated to a decreased skin barrier function as monitored by transepidermal water loss compared with the orthorhombic packing³². We examined the SC lipid composition of our HSEs in detail to verify the cause

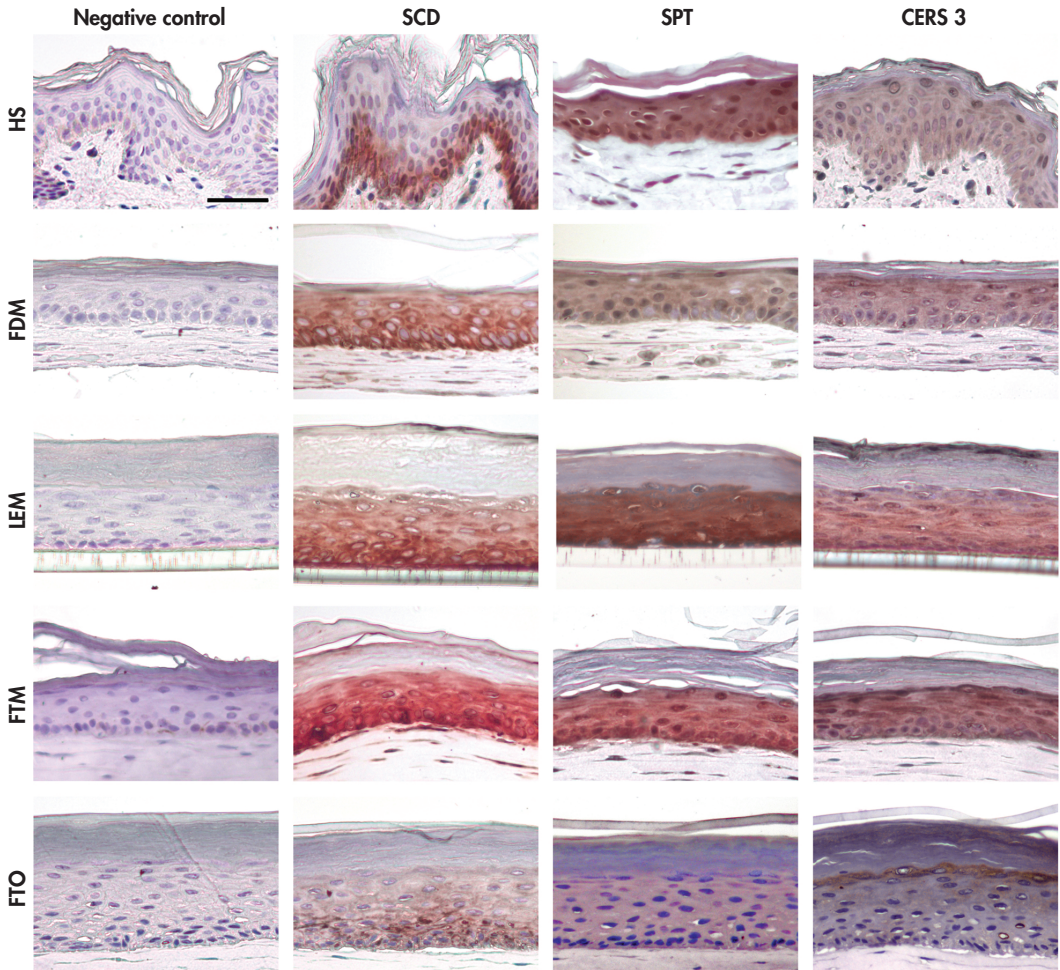


Figure 4: Expression pattern of enzymes involved in free fatty acid desaturation and de novo CER synthesis. Immunohistochemical staining showing the expression pattern of stearoyl-CoA desaturase (SCD), serine palmitoyltransferase (SPT) and CER synthase 3 (CERS3) in human skin (HS), FDM, LEM, FTM and FTO. The negative control represents sections on which only the secondary antibody was applied. The micrographs were taken at a 20x magnification. Scale bar represents 50 μm .

of their altered SC lipid properties and to determine how the latter can be optimized.

To our knowledge, it previously unreported that the SC of HSEs contain MUFAs, which may be a key factor for their altered SC lipid organization. The increase in MUFA content in the SC of HSEs coincides with the altered expression of SCD1 in the viable epidermis of the HSEs compared with human epidermis. It has been demonstrated that lipid mixtures containing an equimolar ratio of cholesterol, FFAs, and human CERS predominantly form an orthorhombic packing³³. However, a reduction in FFAs or the addition of MUFAs in such

mixtures enhances the formation of a hexagonal lateral packing . This indicates that the reduction in FFA level and an increased presence of MUFAs contribute to the formation of the hexagonal packing in our HSEs and thus may be key factors in the observed increased benzocaine penetration across the SC of HSEs compared with native human skin. With respect to the lamellar phases, the HSEs show the predominant presence of the long periodicity phase (LPP)¹⁷, whereas in human SC both the LPP and short periodicity phase (SPP) are formed³⁴. All HSEs have an increased relative content of CERs [EOS] and [EOH]. As suggested in previous studies, these high acyl-CER levels may favor the formation of the LPP in HSEs³⁵, but does not make the HSEs more permeable.

We show that all twelve CER subclasses observed in native human SC are also present in the SC of all HSEs. This indicates that the keratinocytes in our HSEs retain their ability to synthesize all CER subclasses that are also present in human SC. This observation represents a big step forward in the characterization of the SC lipid properties of HSEs, considering that until now a maximum of nine CER subclasses were detected in HSEs, whereas in the commercial HSEs even those nine CER classes were not always present^{18,36,37}.

Masukawa *et al.* quantified the CER composition in native human SC using LC/MS³⁸. The relative prevalence of each CER class determined in this study and the study of Masukawa *et al.* are very similar. In this study, five synthetic CERs are used for quantification of the SC lipids in the HSEs and native human SC. The use of several CER subclasses for quantification is very important, as the charring intensities of the CER subclasses differ considerably when equal amounts are sprayed on TLC plates (Supplementary Figure 3). The different composition of CER subclasses in the FDM, LEM, and FTO compared with human skin is indicative of an altered CER subclass synthesis in these HSEs. The reason for this difference remains to be elucidated.

Our results demonstrate that the HSEs show a similar expression of CERS3 as human skin. The LC/MS multi mass chromatograms indeed show that the HSEs are able to synthesize CERs with a large variety in total carbon chain lengths, which are very similar to human skin. The expression of SCD1 in the proliferating and differentiating layers of the epidermis of the HSEs may result in an increased activity of SCD1 in the differentiated epidermal layers and thus an increased intracellular content of MUFAs in the keratinocytes. Because of the increase in intracellular MUFA content, the CERS enzymes, including CERS3, *n*-acylate both MUFAs and saturated FFAs to the sphingoid bases. The observation that an increase in MUFA content in the SC is accompanied by the presence of CER species with a mono-unsaturated fatty acyl chain suggests that fatty acids present in the SC and the fatty acyl chains of CERs have a common source or synthetic pathway.

The results of this study indicate that the SC lipid properties of the HSEs can be improved

by increasing the FFA content in the SC. The culture medium used to generate the HSEs is supplemented with FFAs. Optimization of FFA supplementation to the culture medium may lead to SC FFA levels that more closely resemble the SC FFA level of native human skin. At present it is unclear why the HSEs show an altered expression of SCD1 compared to human skin. It is possible that the culture conditions or certain media components which are known to affect SCD expression or activity, such as insulin, glucose and fatty acids^{27,39} lead to an increased MUFA level in HSEs. However, it remains to be established whether increased expression of SCD1 in the suprabasal layers of the HSEs is truly associated with an increased activity of SCD1 compared with native human epidermis. If this appears to be true, the SC lipid properties can additionally be improved by reducing SCD1 activity and thereby the MUFA level in the SC of HSEs. SCD1 activity in the HSEs may therefore be reduced by using, e.g., SCD inhibitors^{27,40} in the culture medium. Studies performed by Miyazaki *et al* 41 have demonstrated that SCD-deficient mice show skin permeability barrier defects, such as an insufficient lipid deposition in the SC due to the presence of immature lamellar bodies with a reduced lipid content, and a reduction in acyl-CER content. The reduction in SCD1 activity should therefore be performed with care to prevent different types of SC barrier defects in HSEs that may occur by a too severe suppression of SCD1 activity. Optimization of the FFA content in the SC of HSEs will be the subject of future studies.

Acknowledgements

The authors thank Maria Ponec for helpful suggestions during the meetings. We like to thank Evonik (Essen, Germany) for providing the CERs. This research is supported by the Dutch Technology Foundation STW, which is part of the Netherlands Organisation for Scientific Research (NWO), and which is partly funded by the Ministry of Economic Affairs.

References

- 1 Ackermann K, Borgia SL, Kortling HC *et al.* The Phenion full-thickness skin model for percutaneous absorption testing. *Skin Pharmacol Physiol* 2010; 23: 105-12.
- 2 Asbill C, Kim N, El-Kattan A *et al.* Evaluation of a human bio-engineered skin equivalent for drug permeation studies. *Pharm Res* 2000; 17: 1092-7.
- 3 Batheja P, Song Y, Wertz P *et al.* Effects of growth conditions on the barrier properties of a human skin equivalent. *Pharm Res* 2009; 26: 1689-700.
- 4 Marjukka Suhonen T, Pasonen-Seppanen S, Kirjavainen M *et al.* Epidermal cell culture model derived from rat keratinocytes with permeability characteristics comparable to human cadaver skin. *Eur J Pharm Sci* 2003; 20: 107-13.
- 5 Netzlaff F, Kaca M, Bock U *et al.* Permeability of the reconstructed human epidermis model EpiSkin in comparison to various human skin preparations. *Eur J Pharm Biopharm* 2007; 66: 127-34.
- 6 Schafer-Kortling M, Bock U, Diembeck W *et al.* The use of reconstructed human epidermis for skin absorption testing: Results of the validation study. *Altern Lab Anim* 2008; 36: 161-87.
- 7 Schmoock FP, Meingassner JG, Billich A. Comparison of human skin or epidermis models with human and animal skin in in-vitro percutaneous absorption. *Int J Pharm* 2001; 215: 51-6.
- 8 Zghoul N, Fuchs R, Lehr CM *et al.* Reconstructed skin equivalents for assessing percutaneous drug absorption from pharmaceutical formulations. *Altex* 2001; 18: 103-6.
- 9 Alepee N, Tornier C, Robert C *et al.* A catch-up validation study on reconstructed human epidermis (SkinEthic RHE) for full replacement of the Draize skin irritation test. *Toxicol In Vitro* 2009; 24: 257-66.
- 10 El Ghalbzouri A, Siamari R, Willemze R *et al.* Leiden reconstructed human epidermal model as a tool for the evaluation of the skin corrosion and irritation potential according to the ECVAM guidelines. *Toxicol In Vitro* 2008; 22: 1311-20.
- 11 Gibbs S. In vitro irritation models and immune reactions. *Skin Pharmacol Physiol* 2009; 22: 103-13.
- 12 Netzlaff F, Lehr CM, Wertz PW *et al.* The human epidermis models EpiSkin, SkinEthic and EpiDerm: an evaluation of morphology and their suitability for testing phototoxicity, irritancy, corrosivity, and substance transport. *Eur J Pharm Biopharm* 2005; 60: 167-78.
- 13 Feingold KR. The outer frontier: the importance of lipid metabolism in the skin. *J Lipid Res* 2009; 50 Suppl: S417-22.
- 14 Wertz PW. Lipids and barrier function of the skin. *Acta Derm Venereol Suppl (Stockh)* 2000; 208: 7-11.
- 15 Bouwstra JA, Ponc M. The skin barrier in healthy and diseased state. *Biochim Biophys Acta* 2006; 1758: 2080-95.
- 16 Thakoersing VS, Gooris GS, Mulder A *et al.* Unraveling barrier properties of three different in-house human skin equivalents. *Tissue engineering. Part C, Methods* 2012; 18: 1-11.
- 17 Thakoersing VS, Gooris G, Mulder AA *et al.* Unravelling Barrier Properties of Three Different In-House Human Skin Equivalents. *Tissue Eng Part C Methods* 2011.
- 18 Ponc M, Weerheim A, Lankhorst P *et al.* New acylCER in native and reconstructed epidermis. *J Invest Dermatol* 2003; 120: 581-8.
- 19 Van Smeden J, Hoppel L, van der Heijden R *et al.* LC/MS analysis of stratum corneum lipids: CER profiling and discovery. *J Lipid Res* 2011; 52: 1211-21.
- 20 Bouwstra JA, Groenink HW, Kempenaar JA *et al.* Water distribution and natural moisturizer factor content in human skin equivalents are regulated by environmental relative humidity. *J Invest Dermatol* 2008; 128: 378-88.
- 21 El Ghalbzouri A, Commandeur S, Rietveld MH *et al.* Replacement of animal-derived collagen matrix by human fibroblast-derived dermal matrix for human skin equivalent products. *Biomaterials* 2009; 30: 71-8.
- 22 Bligh EG, Dyer WJ. A rapid method of total lipid extraction and purification. *Can J Biochem Physiol* 1959; 37: 911-7.
- 23 Thakoersing VS, Ponc M, Bouwstra JA. Generation of human skin equivalents under submerged conditions-mimicking the in utero environment. *Tissue Eng Part A* 2010; 16: 1433-41.
- 24 Motta S, Monti M, Sesana S *et al.* CER composition of the psoriatic scale. *Biochim Biophys Acta* 1993; 1182: 147-51.
- 25 Masukawa Y, Narita H, Shimizu E *et al.* Characterization of overall CER species in human stratum corneum. *J Lipid Res* 2008; 49: 1466-76.
- 26 Rissmann R, Groenink HW, Weerheim AM *et al.* New insights into ultrastructure, lipid composition and organization of vernix caseosa. *J Invest Dermatol* 2006; 126: 1823-33.
- 27 Ntambi JM, Miyazaki M, Dobrzyn A. Regulation of stearoyl-CoA desaturase expression. *Lipids* 2004; 39: 1061-5.
- 28 Zhang L, Ge L, Parimoo S *et al.* Human stearoyl-CoA desaturase: alternative transcripts generated from a single gene by usage of tandem polyadenylation sites. *Biochem J* 1999; 340 (Pt 1): 255-64.
- 29 Gault CR, Obeid LM, Hannun YA. An overview of sphingolipid metabolism: from synthesis to breakdown. *Adv Exp Med Biol* 2010; 688: 1-23.
- 30 Mizutani Y, Mitsutake S, Tsuji K *et al.* CER biosynthesis in keratinocyte and its role in skin function. *Biochimie* 2009; 91: 784-90.
- 31 Jennemann R, Rabionet M, Gorgas K *et al.* Loss of CER synthase 3 causes lethal skin barrier disruption. *Hum Mol Genet* 2012; 21: 586-608.
- 32 Damien F, Boncheva M. The extent of orthorhombic lipid phases in the stratum corneum determines the barrier efficiency of human skin in vivo. *J Invest Dermatol* 2010; 130: 611-4.
- 33 Bouwstra J, Pilgram G, Gooris G *et al.* New aspects of the skin barrier organization. *Skin Pharmacol Appl Skin Physiol* 2001; 14 Suppl 1: 52-62.
- 34 Bouwstra JA, Gooris GS, van der Spek JA *et al.* Structural investigations of human stratum corneum by small-angle X-ray scattering. *J Invest Dermatol* 1991; 97: 1005-12.
- 35 De Jager M, Gooris G, Ponc M *et al.* AcylCER head group architecture affects lipid organization in synthetic CER

- mixtures. *J Invest Dermatol* 2004; 123: 911-6.
- 36 Ponc M, Boelsma E, Gibbs S *et al*. Characterization of reconstructed skin models. *Skin Pharmacol Appl Skin Physiol* 2002; 15 Suppl 1: 4-17.
- 37 Ponc M, Weerheim A, Kempenaar J *et al*. The formation of competent barrier lipids in reconstructed human epidermis requires the presence of vitamin C. *J Invest Dermatol* 1997; 109: 348-55.
- 38 Masukawa Y, Narita H, Sato H *et al*. Comprehensive quantification of CER species in human stratum corneum. *J Lipid Res* 2009; 50: 1708-19.
- 39 Mauvoisin D, Mounier C. Hormonal and nutritional regulation of SCD1 gene expression. *Biochimie* 2011; 93: 78-86.
- 40 Liu G. Stearoyl-CoA desaturase inhibitors: update on patented compounds. *Expert Opin Ther Pat* 2009; 19: 1169-91.
- 41 Miyazaki M, Dobrzyn A, Elias PM *et al*. Stearoyl-CoA desaturase-2 gene expression is required for lipid synthesis during early skin and liver development. *Proc Natl Acad Sci U S A* 2005; 102: 12501-6.

Supplementary information – Materials & Methods

Cell culture

Human dermal fibroblasts were cultured in DMEM (Invitrogen, Leek, The Netherlands) supplemented with 5% fetal bovine serum (FBS; Hyclone, Logan, UT) and 1% penicillin/streptomycin (Sigma). Normal human keratinocytes were grown in medium consisting of DMEM and Hams's F12 (Invitrogen, Leek, The Netherlands) (3:1 v/v), 5% FBS, 1% penicillin/streptomycin, 1 μM hydrocortisone (Sigma), 1 μM isoproterenol (Sigma) and 0.5 $\mu\text{g}/\text{mL}$ insulin (Sigma).

Dermal equivalents

Collagen-type I containing dermal equivalents: a 1 mg/mL collagen, isolated from rat tails, solution was obtained by mixing a 4 mg/mL collagen solution in 0.1% acetic acid with Hank's buffered salt solution (Invitrogen, Leek, The Netherlands), 0.1% acetic acid, 1M NaOH and FBS (Hyclone, Logan, UT) on ice. One mL of this mixture was pipetted into a filter insert (Corning transwell cell culture inserts, membrane diameter 24 mm, pore size 3 μm , Corning Life Sciences, Amsterdam, The Netherlands) and polymerized for 15 minutes at 37°C. Hereafter, a 2 mg/mL collagen layer was prepared as described, with the addition of fibroblasts to the FBS solution (final fibroblast cell density of $0.4 \cdot 10^5$ cells/mL collagen solution). Three mL of this fibroblast-populated collagen mixture was pipetted onto the previous collagen layer and polymerized as described. The dermal equivalents were transferred to a 6-well deep-well plate (Organogenesis, Canton, MA) and cultured under submerged conditions in medium consisting of Dulbecco's Modified Eagle medium (DMEM; Invitrogen, Leek, The Netherlands), 5% FBS, 1% penicillin/streptomycin (Sigma) and fresh supplementation of 45 mM vitamin C (Sigma). The medium was refreshed twice a week.

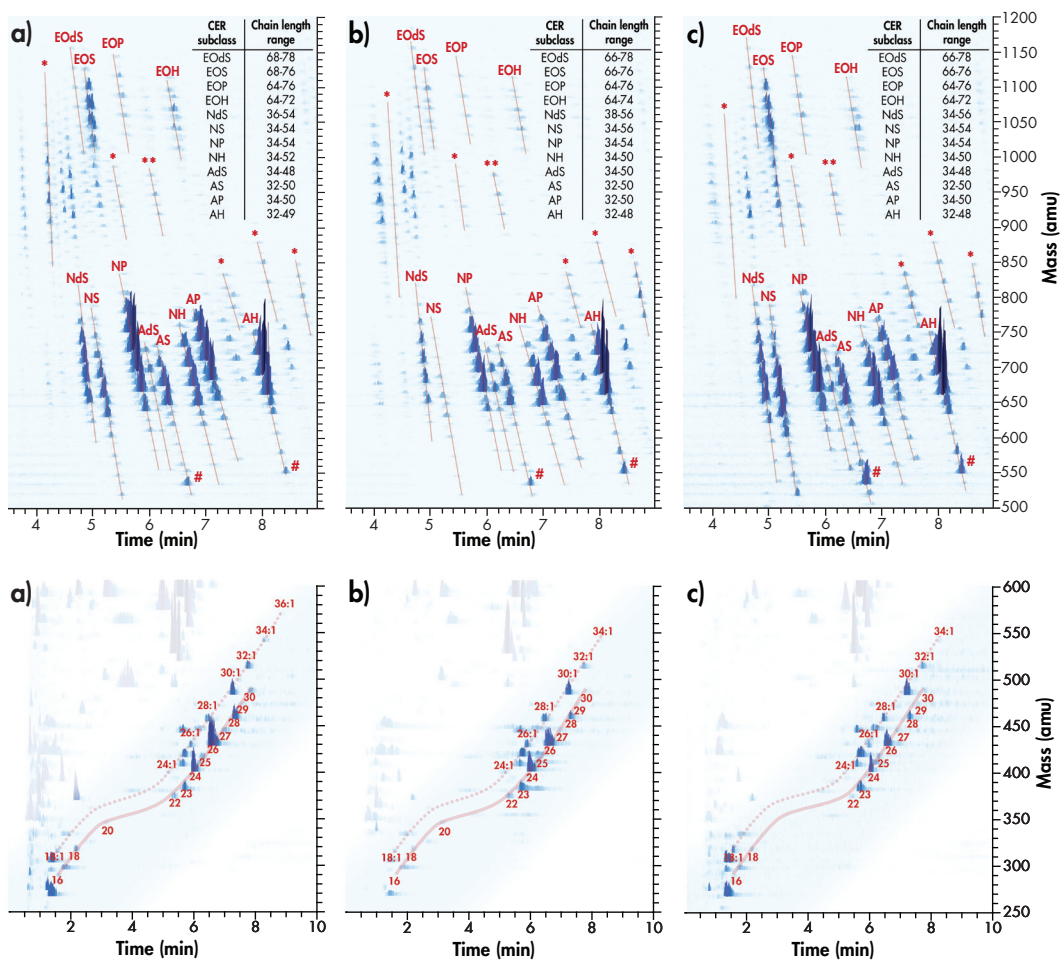
Fully human dermal equivalents: $0.4 \cdot 10^6$ fibroblasts were seeded onto filter inserts (Corning Transwell culture inserts, membrane diameter 24 mm, pore size 0.4 μm ; Corning Life Sciences, Amsterdam, The Netherlands) and were nourished with a similar medium described for the collagen type I containing dermal equivalents. The fibroblasts were allowed to generate their own extracellular matrix for 3 weeks. The medium was refreshed twice a week.

Morphology and immunohistochemistry

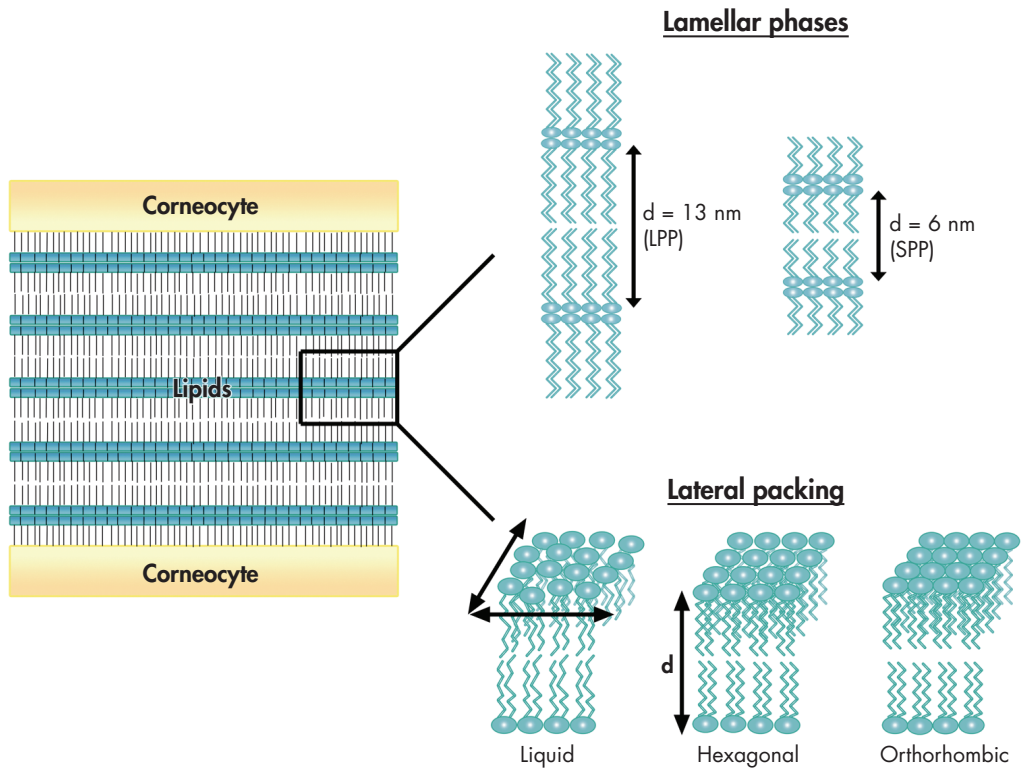
The paraffin sections were deparaffinized and rehydrated through xylene and graded

ethanol series and finally washed with PBS. Antigen retrieval was performed by immersion in sodium citrate buffer (pH 6) for 30 minutes close to the boiling point. After cooling the sections were blocked with normal horse serum for 20 min, followed by incubation with the primary antibody (diluted to the appropriate concentration in 1% BSA in PBS) overnight at 4°C. After washing with PBS the sections were incubated with the secondary antibody for 30 minutes, washed again and incubated with ABC reagent for 30 minutes. The sections were consecutively washed with PBS, 0.1 M sodium acetate buffer and incubated for 30 minutes in amino-ethylcarbazole (Sigma) dissolved in N,N-dimethylformamide (1 g/250 mL) (Sigma) supplemented with 0.1% hydrogen peroxide and finally with water. Counterstaining was performed with haematoxylin. Incubation with normal horse serum, secondary antibody and ABC reagent were performed with the R.T.U. Vectastain Elite ABC reagent kit (Vector Laboratories, Burlingame, CA).

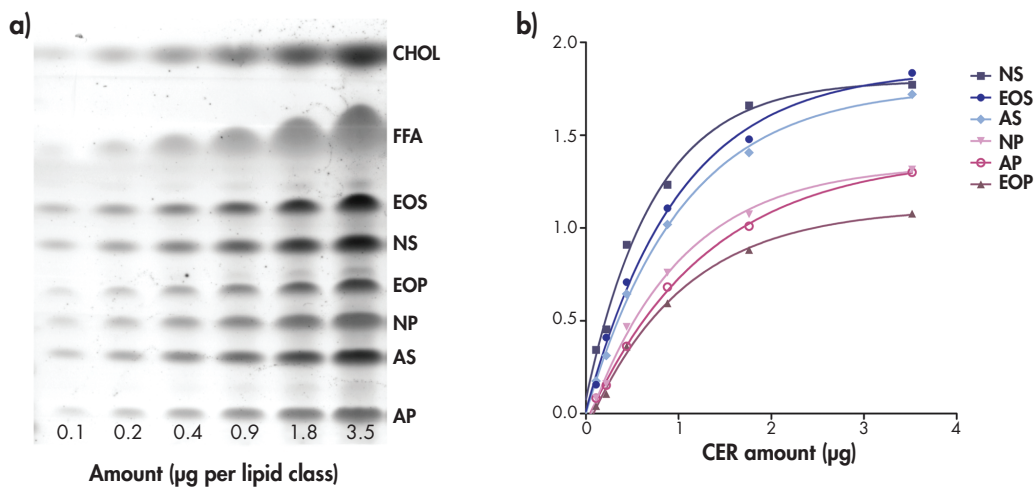
Supplementary information – Figures and Table



Supplementary Figure 1: Ceramide and FFA chain length distribution in LEM, FTM and FTO. Three dimensional multi-mass LC/MS chromatogram of ceramide subclasses in LEM **a)**, FTM **b)** and FTO **c)**. The retention time is shown on the x-axis, the mass is provided on the y-axis and the intensity of each peak is depicted on the 'z'-axis. The total carbon chain length variation of each ceramide subclass is indicated in the inset. Ceramides with a low total carbon chain length which are present in lower quantities in human SC are indicated by #. Unidentified lipids observed in the chromatogram of the LEM, FTM and FTO which are not observed in human SC are specified with *. The unidentified lipid quantified together with ceramide [EOH] using HPTLC is indicated by **. The FFA chain length distribution and degree of saturation of LEM, FTM and FTO are shown in **d)**, **e)** and **f)**, respectively.



Supplementary Figure 2: Stratum corneum lipid organization. In human SC the lamellar phases refer to the stack of lipid layers (i.e. lipid lamellae) between the corneocytes. The distance over which one lipid layer is repeated is referred to as the repeat distance d . In human SC the lipid lamellae have a repeat distance of approximately 13 or 6 nm, the long and short periodicity phase (LPP and SPP), respectively. The lateral packing discloses the density of the lipids within the lipid lamellae. The orthorhombic packing has the highest lipid density and the liquid packing the lowest. In human SC the lipids are arranged in the orthorhombic packing, although some lipid domains also form the hexagonal or liquid packing.



Supplementary Figure 3: Charring differences of ceramide standards. Figure a) shows the charring intensities of the lipid standards used for the quantification of the SC lipid composition. The lipid standard contains equal weight amounts of each standard. The charring intensity of each spot was determined by densitometry and plotted against the amount sprayed to construct a calibration curve b).

Supplementary Table 1

Skin source	Ceramide/Cholesterol ratio
HSC	Donor 1 1.3
	Donor 2 1.3
FDM	Donor 1 1.3
	Donor 2 1.3
LEM	Donor 1 1.8
	Donor 2 1.6
FTM	Donor 1 1.5
	Donor 2 1.5
FTO	Donor 1 0.8
	Donor 2 0.8



PART V

SUMMARY AND APPENDICES



SUMMARY AND PERSPECTIVES

Rationale

Atopic eczema (AE) is one of the most common types of inflammatory skin diseases. It is characterized by eczematous lesions (lesional skin), whereas other areas of the body may visually appear normal (non-lesional skin). The diagnosis of AE is based on a constellation of clinical findings, as there is currently no biomarker characteristic for diagnosis of AE. The disease is often referred to as atopic dermatitis, neurodermatitis, and endogenous eczema. Because up to 60 percent of patients with the clinical phenotype do not have elevation of total or allergen-specific IgE levels in serum, there is still a controversy in the terminology of 'atopic'. The inflammation is primarily related to penetration of allergens into the skin that provoke an immune response, resulting in clinical symptoms like erythema (red skin) and pruritus (itch)¹⁻³. Also xerosis (dry skin) is one of the main symptoms of AE, indicating a dysfunction in skin hydration, regulated by the skin's natural moisturizing factors (NMF)⁴⁻⁶. The NMF are breakdown products of the filaggrin protein. Mutations in the filaggrin gene (*FLG*) are to date the single most predisposing factor for developing AE⁷, although it can only explain 20-50% of all occurrences^{8,9}. This subscribes the heterogeneity of AE and implies the role of other genetic and environmental factors in the pathophysiology of AE. One of these is the importance of a reduced barrier function that facilitates the penetration of exogenous compounds into the skin¹⁰⁻¹⁵.

The main barrier of the skin is located in the outermost layer of the skin, the stratum corneum (SC)¹⁶⁻¹⁸. It consists of corneocytes embedded in a highly ordered lipid matrix, and prevents the penetration of environmental substances into the

skin¹⁹. In addition, it protects the body from excessive transepidermal water loss (TEWL).

In AE, the SC barrier is impaired, and allergens can penetrate through the extracellular lipids into the lower layers of the epidermis^{2,11,13,20}. This stresses the importance of the SC lipids for a proper skin barrier function. SC lipids consist of free fatty acids (FFAs), ceramides (CERs) and cholesterol (CHOL)^{21,22}. Both FFAs and CERs contain respectively 1 and 2 long carbon chains. These may differ in their molecular structure: FFAs are predominantly saturated, although mono-unsaturated FFAs (MUFAs) are present as well^{23,24}. CERs consist of a sphingoid base and a fatty acid (acyl) chain. Variations in both carbon chains (chain length and head group structure) lead to 12 CER subclasses^{25,26}. In addition to these structural variations, both FFAs and CERs show a wide distribution in their carbon chain lengths. The variation in carbon chain length and chemical structure is unique for SC lipids and results in a distinctive lipid organization: the lipid lamellae^{27,28}. These stacked lipid layers have a repeat distance of approximately 6 nm and 13 nm, referred to as the short periodicity phase (SPP) and long periodicity phase (LPP)²⁹⁻³¹. Besides this lamellar lipid organization, SC lipids are packed in a lateral lipid organization: Human SC lipids are mainly present in a very dense – orthorhombic – organization, although a subpopulation is packed in a less dense – hexagonal – organization³²⁻³⁶.

Analytical methods to study the lipid composition are limited, and no methods are currently available to study the chain length of the SC lipids. This is one of the reasons that the role of the SC lipids in AE remains inconclusive: Reports on the CER composition give conflicting information³⁷⁻⁴⁵; hardly any information is available on the composition of the FFAs^{46,47}; and only one study in a limited number of AE patients is present that studies the lipid organization, only mentioning the lateral packing⁴⁸. The lack of knowledge about the SC barrier lipids in relation to the impaired skin barrier function of AE was the basis for the aims of this thesis.

Aims

The primary aim of this thesis is to study in detail the SC lipid composition and organization as well as their role in the skin barrier function in eczematous patients. This is achieved by pursuing the following challenges:

1. Developing robust methods that enables quantitative analysis of all main SC lipid classes in detail.
2. Determine the comprehensive SC lipid composition of both lesional and non-lesional skin in AE patients and compare the lipid profile to healthy controls.
3. Establish how changes in the SC lipid composition of AE patients are related to changes observed in the lipid organization, and how those affect the skin barrier function.

4. Determine the relationship between SC lipid composition and organization with respect to other SC sources that show a reduced skin barrier function (i.e. Netherton syndrome (NTS) and human skin equivalents (HSEs)).

Part I: Method development for detailed stratum corneum lipid analysis

Part I addresses the first aim in which a novel method was developed that would permit detailed analysis on all main SC lipids (CERS, CHOL and FFAs) in a single setup. To achieve this, liquid chromatography coupled to mass spectrometry (LC/MS) was preferred, as it can analyze the SC lipid classes and subclasses as well as the chain length of each individual lipid.

The development of such a method was started with the analysis of CERS, reported in **Chapter 3**. It describes a quick and robust LC/MS method that enables quantitative analysis of all human SC CER subclasses using only limited sample preparation. The combination of normal phase LC in combination with atmospheric pressure chemical ionization (APCI) MS is uncommon. Nevertheless, it proved to be an excellent choice for the analysis of SC CERS, as all subclasses and chain lengths were adequately separated and could easily be identified. Human SC shows the presence of 11 known CER subclasses. In addition, unidentified lipid subclasses were discovered. Using high mass accuracy MS as well as by acquiring fragmentation data (MS/MS), one of these lipid subclasses was identified as the 12th (missing) CER subclass: the ester-linked ω -hydroxy acyl chain linked to a dihydrosphingosine base (CER [EODs]). The method appeared successful in analyzing all 12 CER subclasses from both *ex-vivo* skin, SC obtained by tape stripping and SC from human skin equivalents (HSEs).

The development of the second major SC lipid class, FFAs is described in **Chapter 4**. The first challenge was to develop and subsequently validate an LC/MS method for quantitative analysis of SC FFAs. Such a method has not been reported before for SC FFAs, as gas chromatography is the most common method. Besides, LC/MS of underivatized FFAs results usually in unstable ions or is not sensitive. Using reverse phase LC in combination with APCI-MS in negative ion mode as well as the addition of chloroform as an ionization enhancer contributed to a large extent to the formation of stable chloride adducts. A quantitative validation protocol demonstrated that the method is robust, reproducible, sensitive, fast, whereas ion suppression was negligible. This method was therefore suitable for analysis of human SC FFAs and could be combined with the analysis of CERS, as the same ionization source (APCI) was used. The second challenge was to enable quantitative analysis of CHOL, which was achieved by optimizing the LC-gradient for the CER method. The combined methods enable (semi-)quantitative analysis of all major SC lipid classes

in a single setup. The last part of the chapter describes the application on *ex vivo* human SC, human SC obtained from tape stripping and human skin substitutes (porcine SC and human skin equivalents). In conjunction with CER profiles, clear differences in FFA profiles were observed between these different SC sources.

Now that the developed LC/MS methods enable the analysis of all major SC lipids, this method was used in several studies in which the role of the SC lipids was investigated with respect to the skin barrier function. These studies are described in Part II and III.

Part II: Stratum corneum lipid composition in atopic eczema and its role in the skin barrier function

Using the LC/MS methods developed in part I, the second aim of the study was tackled, in which the SC lipid composition of AE patients was examined and compared to healthy subjects (controls). Part II describes 4 chapters that investigate different aspects of the SC lipid composition. These chapters also cover the third aim of the thesis, in which the relation between the lipid composition and the lipid organization was studied, as well as their involvement in the reduced skin barrier function of AE patients.

The first, explorative, study in AE patients is described in **Chapter 5**. The composition of the CER subclasses as well as the lamellar lipid organization of SC from six AE patients was compared to that of 6 control subjects. Only non-lesional skin of the ventral forearms was investigated. The CER composition was examined by tape stripping and successively analyzed by the newly developed LC/MS method. Skin biopsies were harvested in order to examine the lamellar lipid organization by small-angle X-ray diffraction studies. Regarding the CER composition, all 12 CER subclasses were observed in AE patients. However, a significant decrease in the level of CER [EO] subclasses (those with an ester-linked ω -hydroxy acyl chain linked to a sphingoid base, also referred to as acyl-CERs) and CER subclass [NP] (CERs with a non-hydroxy acyl chain linked to a phytosphingosine base) was observed. Interestingly, subjects with the strongest reduction in acyl-CERs also show the most pronounced deviations in their SAXD-profiles. This suggests that changes in CER composition are related to an altered lamellar lipid organization in AE patients.

These findings were the starting point for a comprehensive study in 28 AE patients and 14 control subjects, described in **Chapter 6**. Both the CER composition and lipid organization in non-lesional SC was determined by means of LC/MS, Fourier transform infrared spectroscopy (FTIR) and small angle X-ray diffraction. In addition, the skin barrier and clinical state of the disease as well as the effect of *FLG* mutations were examined. SC of AE patients showed an increased level of CERs with a very short total chain length of 34 carbon atoms (fatty acid + sphingoid base, C₃₄ CERs), whereas the level of very long acyl-

CERs was decreased. These changes reduced the overall CER chain length significantly, and induced an altered lipid organization that correlated to a decreased skin barrier function in these AE patients. Moreover, the changes in SC CERs also correlated with disease severity. The CERs were the first of the main lipid classes analyzed in SC of AE. Because the results show that the lipids seem to play an important role for the barrier function in AE, other main SC lipid classes were analyzed as well.

A consecutive study in AE patients focused on the second main SC lipid class, the FFAs. As no studies have been reported so far that studied the FFA composition and its chain length in SC of AE patients, **Chapter 7** presents a study that focuses on the extracellular SC FFA composition in both lesional and non-lesional AE skin, and describes how changes in FFA composition are related to the observed changes in the CER composition. In addition, it was studied how the changes in lipid composition affect the lipid organization as well as the skin barrier function. An increased abundance of MUFAs at the expense of hydroxy-FFAs was observed in SC of AE patients. Moreover, the FFA chain length distribution is shifted towards shorter chain lengths. These findings were already observed in non-lesional skin, but much more pronounced in lesional skin. The reduced FFA chain length matches the shorter chain length observed for the CERs, which is a strong indication that the CERs and FFAs share a common synthetic pathway. The chain length of the lipids was strongly associated with the lateral lipid organization: An increase in lipids with shorter chain length results in the increased presence of a hexagonal lipid organization, while longer chain length lipids contribute to the orthorhombic organization. The increased presence of a less densely packed lipid organization also correlated to the reduced skin barrier function, as monitored by TEWL.

Both Chapters 6 and 7 described the effect of FLG mutations on the lipid parameters. These mutations are a major predisposing factor for development of AE, and are therefore of interest to study regarding their relation to the SC lipids. Also the NMF – degradation products of filaggrin – are taken into account, as these play an important role in the hydration and establishing a pH gradient of the SC. The lipid composition and organization show a clear correlation with NMF levels, but not with FLG mutations. This discrepancy illustrates that between FLG genotype and filaggrin metabolites, other factors may play an important role (like filaggrin expression), and demonstrates the importance of studying filaggrin at the phenotype level in addition to profiling FLG genotype.

The studies described in the previous chapters make clear that the lipid composition and its organization play an important role in the reduced skin barrier function of AE patients. **Chapter 8** describes a study in AE patients in which the importance of the lipid to protein level was studied. This was achieved by determining for each AE patient and

control subject the dry SC mass per surface area as well as the ratio between lipid and protein bands in the Raman spectra, which is a measure for the relative lipid/protein ratio. The results demonstrate that the dry SC mass per skin area is to a minor extent changed in AE patients compared to control subjects. In contrast, the lipid/protein ratio is much more reduced in SC of AE patients, both in non-lesional skin and even more pronounced at lesional skin sites. These changes correlated with the skin barrier function and indicate that, besides lipid composition, also the lipid/protein ratio plays an important role in the reduced skin barrier function in AE.

Overall, the studies described in Part II illustrate the importance of the altered lipid composition and organization for the impaired barrier function of the skin in AE. The findings obtained in these studies formed the basis to investigate other SC sources in which a reduced barrier function is present, which are described in Part III.

Part III: Studies on SC lipids from other skin sources showing a barrier dysfunction

In part II the relevance of the SC lipids for the skin barrier function and its biological relevance to AE has been demonstrated. In part III, we expanded the scope beyond AE to pursue the fourth aim of this thesis. Two additional studies were performed on the SC lipids from different skin sources in which a reduced skin barrier is present: patients with Netherton syndrome (NTS) and human skin equivalents (HSEs).

Chapter 9 describes a study in 8 NTS patients. NTS is an exceptional form of dermatitis and share similarities with AE. NTS is caused by rare specific genetic mutations in the SPINK 5 gene, which encodes for a specific protease inhibitor (LEKTI). In NTS, lack of this inhibitor results in increased activity of epidermal proteases, leading to severe SC detachment. The aim of the study was to determine the SC lipid composition and organization in NTS patients, as hardly any information on these matters is currently available. NTS patients showed a decrease in their SC FFA chain length as well as an increased amount of MUFAs compared to controls. In addition, the level of C₃₄ CERs was increased in NTS patients whereas a subgroup of patients showed a strong reduction in long-chain CER levels. NTS patients also showed the presence of high levels of unsaturated CERs, which had not been observed in any other SC source studied so far. These changes in the lipid composition increased the disordering of the lipid packing: both the lamellar and lateral lipid organization showed significant changes. The results demonstrated that acyl-CERs are crucial for the long periodicity phase in the lamellar lipid organization. The changes in lipid composition and organization are expected to contribute to the barrier dysfunction in NTS.

Chapter 10 describes a study on the SC lipids of human skin HSEs. These are

bioengineered skin models that mimic many features for native human SC, but they show an impaired skin barrier and a different SC lipid organization. To elucidate, in detail, the cause of the altered SC lipid organization, analysis by LC/MS was performed to determine the FFA and CER composition as well as the chain length distribution in detail. The results reveal that all HSEs *i*) show the presence of 12 CER subclasses (similar to native human SC), although CER species with short total carbon chains were significantly increased compared to human SC. *ii*) display the presence of CER species with a monounsaturated acyl chain, which are not detected in human SC (except for NTS patients); *iii*) have an increased presence of MUFAs compared with human SC, whereas the total amount of FFAs was drastically decreased; *iv*) exhibit an altered expression of stearoyl-CoA desaturase, the enzyme that converts saturated FFAs to MUFAs.

Conclusions

The studies described in this thesis reveal that SC lipids play a crucial role for a proper skin barrier function in humans. *In vivo* studies in AE and NTS patients reveal that changes in the composition of the lipids negatively affect the lamellar and lateral lipid organization. In particular the lipid chain length excellently correlated to the organization of the lipids: shorter FFA and CER chain lengths contribute to a more hexagonal lipid organization, while longer lipid carbon chains will result in a more densely packed, orthorhombic organization. From the results in AE and NTS patients, it can also be concluded that the acyl-CERs are crucial for the long periodicity phase in the lamellar lipid organization. The use of LC/MS proved to be essential for these findings, as no other method to date can analyze the SC lipid chain lengths in all its detail. Besides, the sensitivity of MS reduced the amount of sample necessary for analysis, which permitted harvesting SC lipids in a non-invasive way by means of tape-stripping.

In addition, the level of SC lipids may be important for a proper skin barrier function, as the reduced lipid/protein ratio in AE subjects correlate to a high extent with a reduced skin barrier function. Chapters 5-7 report that TEWL correlates with the lipid composition (particularly lipid chain length), whereas chapter 8 reports a strong correlation between TEWL and the lipid/protein ratio. This raises the question whether changes in lipid composition correlate with the changes observed in lipid/protein ratio, in AE. Indeed, a high correlation is observed between the lipid chain length and the lipid/protein ratio ($r_{\text{spearman}}=0.79$). This could indicate that the changes observed in the lipid chain length and lipid/protein ratio may share a common factor in lipid metabolism that is altered in AE (discussed below).

The SC barrier lipids in AE, NTS and HSEs showed similar changes in their composition:

a reduced lipid chain length and increase in unsaturated lipids. Comparing SC from non-lesional AE with lesional AE skin and NTS reveals that more severe changes in the composition of the lipids result in more severe changes in the lipid organization. This may explain why previous studies on NTS patients show a drastic reduction in the SC barrier function. The relation between the composition of the FFAs and CERS is remarkable: the chain length and the degree of unsaturation of the FFAs complement the composition of the CERS. This is of fundamental relevance as it supports the hypothesis that human SC CERS and FFAs share a common synthetic pathway^{49,50}. It is also of clinical importance, as it implies that normalizing the FFA chain length distribution in AE skin may also contribute to normalization of the CER chain length.

These studies give relevant information regarding possible changes in the epidermal lipid metabolism: *i*) The reduced FFA chain length observed in AE, NTS and HSEs suggest that FFA elongation is impaired⁵¹; *ii*) the changes in the relative abundances of the CER subclasses indicate that the enzymes involved in synthesis of one particular subclass may either be up- or downregulated. Two enzymes that are likely to be involved in the altered epidermal lipid metabolism are β -glucocerebrosidase and acid sphingomyelinase, which convert CER precursors into their final CER structure⁵²⁻⁵⁵. Both enzymes, however, do not have the same affinity to all CER precursors, and changes in the activity of one of these enzymes may partly explain the increase in certain CER subclasses at the expense of others⁵⁶; *iii*) the correlation between lipid chain length and lipid/protein ratio may indicate that the changes share a common factor that is altered in AE. It goes beyond the current knowledge to speculate about these factors, but enzymes involved in *de novo* synthesis of the lipids are definitely a target of interest for future studies.

Moreover, the studies in AE patients contributed to a better understanding of the role of FLG and NMF with respect to the SC lipids and barrier function. Filaggrin at the phenotype and metabolic (NMF) level seems more closely related than at the genotype level, which supports the hypothesis that changes in filaggrin expression may be an important factor in AE^{57,58}.

Overall, the studies performed throughout this thesis increased the knowledge of the SC barrier function from both a biophysical perspective (the relation between lipid composition, lipid organization, and barrier function) as well as a clinical perspective (the essence of the SC barrier lipids in relation to AE and NTS).

Prospects

Despite the fact that the aims set at the very beginning of this thesis may have been accomplished, the studies have raised additional questions and may serve as a basis for future studies in multiple directions. The most prominent ones will be discussed below.

Exploiting the possibilities of LC/MS for analysis of SC lipids

Although an adequate method was developed for qualitative and quantitative analysis of all major SC lipid classes, many possibilities remain unexploited. The main advantages of the current LC/MS method compared to other methods are that it is quick (<20 minutes analysis time to acquire data on all main SC lipids), robust, sensitive, and gives detailed information on the lipid chain length. However, the main bottleneck for high-throughput analysis is currently the lipid extraction protocol (taking several hours) and manual data-processing (several hours per sample). Regarding an alternative extraction protocol, experiments that replace the current 3-step Bligh and Dyer extraction protocol with a 1-step heptane/isopropanol extraction of 20 minutes provided similar results on the lipid composition. Future validation of such an improved extraction protocol may therefore significantly reduce the amount of time spent on sample preparation. With respect to data-processing, currently automatic data-processing results in proper quantification in ~90% of the assigned peaks. With a number of >250 designated peaks, this needs to be improved for reliable automatic quantification. One way to do this is by analyzing lipids in MRM mode. Two additional advantages are that sensitivity is (usually) increased, and it may also provide more structural information, for example on the individual chains of the sphingoid base and acyl chain of the CERS. The sensitivity may also be greatly enhanced when changing from the current HPLC method to UPLC. Last but not least, it is preferable to use only a single injection for analysis of all lipid classes at once. Currently, CERS and CHOL are analyzed in positive ion mode and NPLC, whereas FFAs are analyzed in negative ion mode and RPLC. Because CERS are also observed when analyzing FFAs in negative ion mode, it may be worthwhile to analyze all SC lipids in negative ion mode, using NPLC for adequate separation of all CER subclasses and optimize it to include proper analysis of FFAs and CHOL.

Another aspect for future studies concerns the identification of additional lipid peaks that were noticed in Chapters 3 and 4. Among these are probably the glucosyl-CERS, di- and triglycerides, CHOL esters, and probably others which are yet unknown. In particular the unknown lipid species that elute in between the different CER subclasses (e.g. between CER [AP] and CER [AH]) may be of interest. Their mass and hydrophobicity may indicate that they have comparable molecular structures, but fragmentation studies (MS/MS) may

fully elucidate the molecular structure of these lipids. It is likely that some of these ions are isomers of the alpha-hydroxy fatty acid CER subclasses ([AS], [AdS], [AP], [AH]), but that the hydroxyl group in the acyl chain is located at the ω -position. This would slightly increase the polarity but not the mass, something which matches the unidentified CER located between CER [AP] and [AH]. These so-called ω -hydroxy fatty acid CERs are already known to be present in the SC as bound lipids⁵⁹, and it is therefore plausible that these could also be observed with the current method as free lipids.

Elucidating the epidermal lipid metabolism

It was concluded from the *in vivo* studies performed in patients with AE and NTS, but also the *in vitro* studies with HSEs, that changes in the synthesis of epidermal lipids are the underlying cause of the altered SC lipid composition. Future studies may therefore focus on the enzymes that elongate the FFAs (ELOVLs), as these may be a probable reason for the reduced lipid chain length. Since a lower level of FFAs with a chain length of 24 carbon atoms and higher was observed in AE and NTS, ELOVL4 activity may be reduced, as this enzyme is involved in elongation of FFAs ≥ 24 carbon atoms. Recent murine studies support this hypothesis, demonstrating that SC lipids of ELOVL knockout mice show reduced levels of long chain FFAs⁶⁰⁻⁶². The increased amount of MUFAs suggests that expression of stearoyl-CoA desaturase (the enzyme that converts saturated FFAs to MUFAs) may be increased in AE⁶³.

In general, studying the enzymes in eczematous patients will give valuable information about the altered epidermal lipid pathways and may lead to more fundamental knowledge about epidermal lipid synthesis and the relation to AE. Also the role of inflammation on these epidermal lipid enzymes needs to be elucidated, as it is known that inflammatory cytokines affect the epidermal lipid synthesis in several ways. Studies related to the inflammatory aspects of AE may therefore focus on *i*) metabolic enzymes involved in CER synthesis (like β -glucocerebrosidase and acid sphingomyelinase)⁵²⁻⁵⁵; *ii*) cytokines like TNF- α as well as several interleukins (IL-17, IL-22, IL-25, IL-31) that are related to downregulation of filaggrin expression⁶⁴⁻⁶⁸; and *iii*) nuclear receptors (peroxisome proliferator-activated receptors) that are involved in SC barrier formation and have anti-inflammatory capabilities⁶⁹⁻⁷⁵.

SC barrier repair

Restoring the SC barrier function has become one of the main challenges in AE. Two fundamentally different approaches can be pursued to achieve this: *i*) one can compensate for the reduced barrier function by application of topical formulations; *ii*) Another

approach is to restore the epidermal lipid synthesis.

With respect to the former approach, our studies give new insights in possible topical formulations which may be beneficial to the SC barrier. In particular the finding of the reduced lipid chain length in AE is something that offers a new perspective. An interesting study in AE subjects would therefore be to compensate for the reduced lipid chain length by topical application of a formulation containing long carbon chain CERs and/or FFAs for at least several weeks, and subsequently analyze the lipid composition and organization of these patients and investigate whether these lipids will be incorporated in the native SC lipid matrix and improve the lipid organization and skin barrier function. One can improve such formulations even further by analyzing the SC lipid composition at forehand. There is a large individual variation in the CER and FFA composition of AE subjects, and one specific formulation may not be suitable as a treatment for all patients. Based on deteriorations in the lipid profile, it can be decided which formulation and dose should lead to an optimal barrier recovery. This approach of individual dose/formulation regimen is something that has increased attention for pharmaceutical companies as it proves to be more beneficial to the patient.

The second approach, to restore the epidermal lipid synthesis, may be much more difficult to achieve, and needs much more knowledge on the fundamentals of AE. In order to target the enzymes that may lead to normalization of the lipid synthesis, one need to normalize the metabolic processes that take place in the cytosol and endoplasmatic reticulum of the keratinocytes, where de novo syntheses of respectively FFAs and CERs primarily take place. A proper skin hydration, pH gradient, and keratinocyte differentiation are factors that should be taken into account for proper SC barrier repair using this approach.

It should not be overlooked that AE is mainly related to the western society, and relatively simple, non-clinical/pharmaceutical adaptations can already significantly improve the barrier. For example, a proper level of the environmental humidity, or the moderate use of soap, preferably with a skin-neutral to acid pH, may already reduce the prevalence of AE.

Additional studies in AE may elucidate fundamental questions on the disease.

One of the most frequently asked questions with respect to AE and the barrier function, is whether the inflammatory response (inside-to-outside model) or the reduced SC barrier function (outside-to-inside model) is the primary cause of the disease^{20,76-78}. Although a definite answer cannot be given at the current time, it should be noted that future studies can lead to small progressions that may stepwise unravel this question. For example, studies in newborns with a high risk of developing AE (e.g. carriers of *FLG* mutations; parents with AE) but without any clinical appearance of the disease may be monitored

for a longer period of time and regularly checked on markers for skin inflammation and SC barrier function. If the onset of AE is imminent in such a newborn, one can study changes in some of these biomarkers that led to the onset of AE. This will lead to a better understanding of the disease. However, it should be mentioned that AE is a multifactorial disease and that this ‘chicken-or-egg’ question may well prove to be a ‘chicken-and-egg question’, as discussed by Elias *et al.*, suggesting the ‘outside-to-inside and back-to-outside’ model^{11,20}.

The role of *FLG* mutations, filaggrin protein, and filaggrin breakdown products (i.e. the NMF) for the SC barrier function of AE may be another aspect for future studies. Studying the SC lipids in patients with ichthyosis vulgaris may therefore be of interest, as these patients carry loss-of-function mutations in the *FLG* gene. In addition, studies in subjects that carry a *FLG* mutation and have low NMF levels but normal SC barrier properties may give a better insight in the role of *FLG* and the SC barrier function in a diseased state.

References

- 1 Leung DY, Bieber T. Atopic dermatitis. *Lancet* 2003; 361: 151-60.
- 2 Oyoshi MK, He R, Kumar L *et al*. Cellular and molecular mechanisms in atopic dermatitis. *Adv Immunol* 2009; 102: 135-226.
- 3 Wollenberg A, Rawer HC, Schaubert J. Innate immunity in atopic dermatitis. *Clin Rev Allergy Immunol* 2011; 41: 272-81.
- 4 Voegeli D. The role of emollients in the care of patients with dry skin. *Nursing standard* 2007; 22: 62, 4-8.
- 5 Takahashi M, Tezuka T. The content of free amino acids in the stratum corneum is increased in senile xerosis. *Archives of Dermatological Research* 2004; 295: 448-52.
- 6 Sandilands A, O'Regan GM, Liao H *et al*. Prevalent and rare mutations in the gene encoding filaggrin cause ichthyosis vulgaris and predispose individuals to atopic dermatitis. *The Journal of investigative dermatology* 2006; 126: 1770-5.
- 7 Palmer CN, Irvine AD, Terron-Kwiatkowski A *et al*. Common loss-of-function variants of the epidermal barrier protein filaggrin are a major predisposing factor for atopic dermatitis. *Nature Genetics* 2006; 38: 441-6.
- 8 Jakasa I, Koster ES, Calkoen F *et al*. Skin barrier function in healthy subjects and patients with atopic dermatitis in relation to filaggrin loss-of-function mutations. *J Invest Dermatol* 2011; 131: 540-2.
- 9 Akiyama M. FLG mutations in ichthyosis vulgaris and atopic eczema: spectrum of mutations and population genetics. *The British journal of dermatology* 2010; 162: 472-7.
- 10 Elias PM. Barrier repair trumps immunology in the pathogenesis and therapy of atopic dermatitis. *Drug Discov Today Dis Mech* 2008; 5: e33-e8.
- 11 Elias PM, Steinhoff M. "Outside-to-inside" (and now back to "outside") pathogenic mechanisms in atopic dermatitis. *The Journal of investigative dermatology* 2008; 128: 1067-70.
- 12 Seidenari S, Giusti G. Objective assessment of the skin of children affected by atopic dermatitis: A study of pH, capacitance and TEWL in eczematous and clinically uninvolved skin. *Acta Dermato-Venereologica* 1995; 75: 429-33.
- 13 Elias PM, Schmutz M. Abnormal skin barrier in the etiopathogenesis of atopic dermatitis. *Current Opinion in Allergy and Clinical Immunology* 2009; 9: 437-46.
- 14 Werner Y, Lindberg M. Transepidermal water loss in dry and clinically normal skin in patients with atopic dermatitis. *Acta Derm Venereol* 1985; 65: 102-5.
- 15 Yoshiike T, Aikawa Y, Sindhvananda J *et al*. Skin barrier defect in atopic dermatitis: increased permeability of the stratum corneum using dimethyl sulfoxide and theophylline. *J Dermatol Sci* 1993; 5: 92-6.
- 16 Elias PM, Choi EH. Interactions among stratum corneum defensive functions. *Experimental Dermatology* 2005; 14: 719-26.
- 17 Elias PM. Stratum corneum defensive functions: an integrated view. *The Journal of investigative dermatology* 2005; 125: 183-200.
- 18 Irvine AD, McLean WH. Breaking the (un)sound barrier: filaggrin is a major gene for atopic dermatitis. *The Journal of investigative dermatology* 2006; 126: 1200-2.
- 19 Bouwstra JA, Dubbelaar FE, Gooris GS *et al*. The lipid organisation in the skin barrier. *Acta dermato-venereologica. Supplementum* 2000; 208: 23-30.
- 20 Elias PM, Hatano Y, Williams ML. Basis for the barrier abnormality in atopic dermatitis: outside-inside-outside pathogenic mechanisms. *The Journal of allergy and clinical immunology* 2008; 121: 1337-43.
- 21 Wertz PW, Downing DT. Epidermal lipids. In: *Physiology, biochemistry, and molecular biology of the skin* (Goldsmith LA, ed), 2nd edn. New York: Oxford University Press. 1991; 205-36.
- 22 Bouwstra JA, Gooris GS, Cheng K *et al*. Phase behavior of isolated skin lipids. *Journal of lipid research* 1996; 37: 999-1011.
- 23 Ansari MN, Nicolaidis N, Fu HC. Fatty acid composition of the living layer and stratum corneum lipids of human sole skin epidermis. *Lipids* 1970; 5: 838-45.
- 24 Norlen L, Nicander I, Lundsjo A *et al*. A new HPLC-based method for the quantitative analysis of inner stratum corneum lipids with special reference to the free fatty acid fraction. *Arch Dermatol Res* 1998; 290: 508-16.
- 25 Motta S, Monti M, Sesana S *et al*. Ceramide composition of the psoriatic scale. *Biochim Biophys Acta* 1993; 1182: 147-51.
- 26 Masukawa Y, Narita H, Shimizu E *et al*. Characterization of overall ceramide species in human stratum corneum. *J Lipid Res* 2008; 49: 1466-76.
- 27 Madison KC, Swartzendruber DC, Wertz PW *et al*. Presence of intact intercellular lipid lamellae in the upper layers of the stratum corneum. *The Journal of investigative dermatology* 1987; 88: 714-8.
- 28 Bouwstra JA, Gooris GS, van der Spek JA *et al*. Structural investigations of human stratum corneum by small-angle X-ray scattering. *The Journal of investigative dermatology* 1991; 97: 1005-12.
- 29 Groen D, Gooris GS, Bouwstra JA. New insights into the stratum corneum lipid organization by X-ray diffraction analysis. *Biophysical Journal* 2009; 97: 2242-9.
- 30 McIntosh TJ, Stewart ME, Downing DT. X-ray diffraction analysis of isolated skin lipids: reconstitution of intercellular lipid domains. *Biochemistry* 1996; 35: 3649-53.
- 31 Bouwstra J, Pilgram G, Gooris G *et al*. New aspects of the skin barrier organization. *Skin Pharmacology and Applied Skin Physiology* 2001; 14 Suppl 1: 52-62.
- 32 Pilgram GS, Engelsma-van Pelt AM, Bouwstra JA *et al*. Electron diffraction provides new information on human stratum corneum lipid organization studied in relation to depth and temperature. *The Journal of investigative dermatology* 1999; 113: 403-9.
- 33 Damien F, Boncheva M. The extent of orthorhombic lipid phases in the stratum corneum determines the barrier efficiency of human skin *in vivo*. *The Journal of investigative dermatology* 2010; 130: 611-4.
- 34 Goldsmith LA, Baden HP. Uniquely oriented epidermal lipid. *Nature* 1970; 225: 1052-3.
- 35 de Jager MW, Gooris GS, Dolbnya IP *et al*. The phase behaviour of skin lipid mixtures based on synthetic ceramides. *Chemistry and physics of lipids* 2003; 124: 123-34.
- 36 Bouwstra JA, Gooris GS, Dubbelaar FE *et al*. Phase behavior

- of lipid mixtures based on human ceramides: coexistence of crystalline and liquid phases. *Journal of lipid research* 2001; 42: 1759-70.
- 37 Bleck O, Abeck D, Ring J *et al.* Two ceramide subfractions detectable in Cer(AS) position by HPTLC in skin surface lipids of non-lesional skin of atopic eczema. *J Invest Dermatol* 1999; 113: 894-900.
- 38 Farwanah H, Raith K, Neubert RH *et al.* Ceramide profiles of the uninvolved skin in atopic dermatitis and psoriasis are comparable to those of healthy skin. *Arch Dermatol Res* 2005; 296: 514-21.
- 39 Angelova-Fischer I, Mannheimer AC, Hinder A *et al.* Distinct barrier integrity phenotypes in filaggrin-related atopic eczema following sequential tape stripping and lipid profiling. *Exp Dermatol* 2011; 20: 351-6.
- 40 Ishibashi M, Arikawa J, Okamoto R *et al.* Abnormal expression of the novel epidermal enzyme, glucosylceramide deacylase, and the accumulation of its enzymatic reaction product, glucosylsphingosine, in the skin of patients with atopic dermatitis. *Laboratory investigation; a journal of technical methods and pathology* 2003; 83: 397-408.
- 41 Matsumoto M, Umemoto N, Sugiura H *et al.* Difference in ceramide composition between "dry" and "normal" skin in patients with atopic dermatitis. *Acta Dermato-Venereologica* 1999; 79: 246-7.
- 42 Di Nardo A, Wertz P, Giannetti A *et al.* Ceramide and cholesterol composition of the skin of patients with atopic dermatitis. *Acta Derm Venereol* 1998; 78: 27-30.
- 43 Jungersted JM, Scheer H, Mempel M *et al.* Stratum corneum lipids, skin barrier function and filaggrin mutations in patients with atopic eczema. *Allergy* 2010; 65: 911-8.
- 44 Imokawa G, Abe A, Jin K *et al.* Decreased level of ceramides in stratum corneum of atopic dermatitis: an etiologic factor in atopic dry skin? *J Invest Dermatol* 1991; 96: 523-6.
- 45 Holleran WM, Takagi Y, Uchida Y. Epidermal sphingolipids: metabolism, function, and roles in skin disorders. *Febs Letters* 2006; 580: 5456-66.
- 46 Takigawa H, Nakagawa H, Kuzukawa M *et al.* Deficient production of hexadecenoic acid in the skin is associated in part with the vulnerability of atopic dermatitis patients to colonization by *Staphylococcus aureus*. *Dermatology* 2005; 211: 240-8.
- 47 Macheleidt O, Kaiser HW, Sandhoff K. Deficiency of epidermal protein-bound omega-hydroxyceramides in atopic dermatitis. *J Invest Dermatol* 2002; 119: 166-73.
- 48 Pilgram GS, Vissers DC, van der Meulen H *et al.* Aberrant lipid organization in stratum corneum of patients with atopic dermatitis and lamellar ichthyosis. *J Invest Dermatol* 2001; 117: 710-7.
- 49 Ohno Y, Suto S, Yamanaka M *et al.* ELOVL1 production of C24 acyl-CoAs is linked to C24 sphingolipid synthesis. *Proc Natl Acad Sci U S A* 2010; 107: 18439-44.
- 50 Uchida Y. The role of fatty acid elongation in epidermal structure and function. *Dermatoendocrinol* 2011; 3: 65-9.
- 51 Guillou H, Zadravec D, Martin PG *et al.* The key roles of elongases and desaturases in mammalian fatty acid metabolism: Insights from transgenic mice. *Prog Lipid Res* 2010; 49: 186-99.
- 52 Holleran WM, Ginns EI, Menon GK *et al.* Consequences of beta-glucocerebrosidase deficiency in epidermis. Ultrastructure and permeability barrier alterations in Gaucher disease. *The Journal of clinical investigation* 1994; 93: 1756-64.
- 53 Holleran WM, Takagi Y, Menon GK *et al.* Processing of epidermal glucosylceramides is required for optimal mammalian cutaneous permeability barrier function. *The Journal of clinical investigation* 1993; 91: 1656-64.
- 54 Jensen JM, Schutze S, Forl M *et al.* Roles for tumor necrosis factor receptor p55 and sphingomyelinase in repairing the cutaneous permeability barrier. *The Journal of clinical investigation* 1999; 104: 1761-70.
- 55 Schmuth M, Man MQ, Weber F *et al.* Permeability barrier disorder in Niemann-Pick disease: sphingomyelin-ceramide processing required for normal barrier homeostasis. *The Journal of investigative dermatology* 2000; 115: 459-66.
- 56 Briot A, Deraison C, Lacroix M *et al.* Kallikrein 5 induces atopic dermatitis-like lesions through PAR2-mediated thymic stromal lymphopoietin expression in Netherton syndrome. *J Exp Med* 2009; 206: 1135-47.
- 57 Brown SJ, Irvine AD. Atopic eczema and the filaggrin story. *Seminars in Cutaneous Medicine and Surgery* 2008; 27: 128-37.
- 58 Brown SJ, McLean WH. One remarkable molecule: filaggrin. *The Journal of investigative dermatology* 2012; 132: 751-62.
- 59 Farwanah H, Pierstorff B, Schmelzer CE *et al.* Separation and mass spectrometric characterization of covalently bound skin ceramides using LC/APCI-MS and Nano-ESI-MS/MS. *Journal of chromatography. B, Analytical technologies in the biomedical and life sciences* 2007; 852: 562-70.
- 60 Vasireddy V, Uchida Y, Salem N, Jr. *et al.* Loss of functional ELOVL4 depletes very long-chain fatty acids (> or =C28) and the unique omega-O-acylceramides in skin leading to neonatal death. *Hum Mol Genet* 2007; 16: 471-82.
- 61 Cameron DJ, Tong Z, Yang Z *et al.* Essential role of Elov14 in very long chain fatty acid synthesis, skin permeability barrier function, and neonatal survival. *Int J Biol Sci* 2007; 3: 111-9.
- 62 Li W, Sandhoff R, Kono M *et al.* Depletion of ceramides with very long chain fatty acids causes defective skin permeability barrier function, and neonatal lethality in ELOVL4 deficient mice. *Int J Biol Sci* 2007; 3: 120-8.
- 63 Miyazaki M, Ntambi JM. Chapter 7 - Fatty acid desaturation and chain elongation in mammals. In: *Biochemistry of Lipids, Lipoproteins and Membranes (Fifth Edition)* (Dennis EV, Jean EV, eds). San Diego: Elsevier. 2008; 191-V.
- 64 Gutowska-Owsiak D, Schaupp AL, Salimi M *et al.* IL-17 downregulates filaggrin and affects keratinocyte expression of genes associated with cellular adhesion. *Experimental Dermatology* 2012; 21: 104-10.
- 65 Cornelissen C, Marquardt Y, Czaja K *et al.* IL-31 regulates differentiation and filaggrin expression in human organotypic skin models. *The Journal of allergy and clinical immunology* 2012; 129: 426-33, 33 e1-8.
- 66 Kim BE, Howell MD, Guttman-Yassky E *et al.* TNF-alpha downregulates filaggrin and lorcinr through c-Jun N-terminal kinase: role for TNF-alpha antagonists to improve skin barrier. *J Invest Dermatol* 2011; 131: 1272-9.
- 67 Hvid M, Vestergaard C, Kemp K *et al.* IL-25 in atopic

- dermatitis: a possible link between inflammation and skin barrier dysfunction? *J Invest Dermatol* 2011; 131: 150-7.
- 68 Gutowska-Owsiak D, Schaupp AL, Salimi M *et al.* Interleukin-22 downregulates filaggrin expression and affects expression of profilaggrin processing enzymes. *Br J Dermatol* 2011; 165: 492-8.
- 69 Sertznig P, Seifert M, Tilgen W *et al.* Peroxisome proliferator-activated receptors (PPARs) and the human skin: importance of PPARs in skin physiology and dermatologic diseases. *Am J Clin Dermatol* 2008; 9: 15-31.
- 70 Staumont-Salle D, Abboud G, Brenuchon C *et al.* Peroxisome proliferator-activated receptor alpha regulates skin inflammation and humoral response in atopic dermatitis. *J Allergy Clin Immunol* 2008; 121: 962-8 e6.
- 71 Plager DA, Leontovich AA, Henke SA *et al.* Early cutaneous gene transcription changes in adult atopic dermatitis and potential clinical implications. *Exp Dermatol* 2007; 16: 28-36.
- 72 Hanley K, Jiang Y, Crumrine D *et al.* Activators of the nuclear hormone receptors PPARalpha and FXR accelerate the development of the fetal epidermal permeability barrier. *J Clin Invest* 1997; 100: 705-12.
- 73 Jiang YJ, Barish G, Lu B *et al.* PPARdelta activation promotes stratum corneum formation and epidermal permeability barrier development during late gestation. *J Invest Dermatol* 2010; 130: 511-9.
- 74 Man MQ, Barish GD, Schmuth M *et al.* Deficiency of PPARbeta/delta in the epidermis results in defective cutaneous permeability barrier homeostasis and increased inflammation. *J Invest Dermatol* 2008; 128: 370-7.
- 75 Schmuth M, Jiang YJ, Dubrac S *et al.* Thematic review series: skin lipids. Peroxisome proliferator-activated receptors and liver X receptors in epidermal biology. *J Lipid Res* 2008; 49: 499-509.
- 76 Boguniewicz M, Leung DY. Recent insights into atopic dermatitis and implications for management of infectious complications. *The Journal of allergy and clinical immunology* 2010; 125: 4-13; quiz 4-5.
- 77 Elias PM, Feingold KR. Does the tail wag the dog? Role of the barrier in the pathogenesis of inflammatory dermatoses and therapeutic implications. *Archives of dermatology* 2001; 137: 1079-81.
- 78 Chesney C. Canine atopy - inside out, or outside in? *The Veterinary record* 2011; 168: 533-4.

Deel I: Introductie

Een van de meest voorkomende huidziekten is constitutioneel eczeem (in de volksmond ook wel atopisch eczeem genoemd). De oorzaak van de ziekte is tot op heden onduidelijk, maar kenmerkend zijn de rode, jeukende plekken – de aangedane huid¹. De rest van de huid ziet er op het oog normaal uit, en wordt de niet-aangedane huid genoemd (zie Figuur 1). De aangedane huid is ontstoken doordat **allergenen** de huid zijn binnengedrongen en daar een ontstekingsreactie in gang hebben gezet, waarbij sprake kan zijn van een atopie: een verhoging van **allergeen-specifiek immunoglobuline-E (IgE)**^{2,3}. Echter, het gebruik van het woord ‘atopisch’ is met betrekking tot deze ziekte controversieel, omdat een groot deel (tot wel 60%) van de patiënten geen verhoging in IgE laat zien⁴.

De vraag blijft waardoor allergenen de huid kunnen binnendringen. Een belangrijke eigenschap van deze aandoening is droge huid. Dit betekent dat het watergehalte in de huid verlaagd is. Dit watergehalte wordt gereguleerd door onder meer de natuurlijke



Figuur 1: Een kind met constitutioneel eczeem. Herkenbaar zijn de rode plekken (aangedane, rode huid) naast huid dat er op het oog gezond uitziet (niet-aangedane huid).

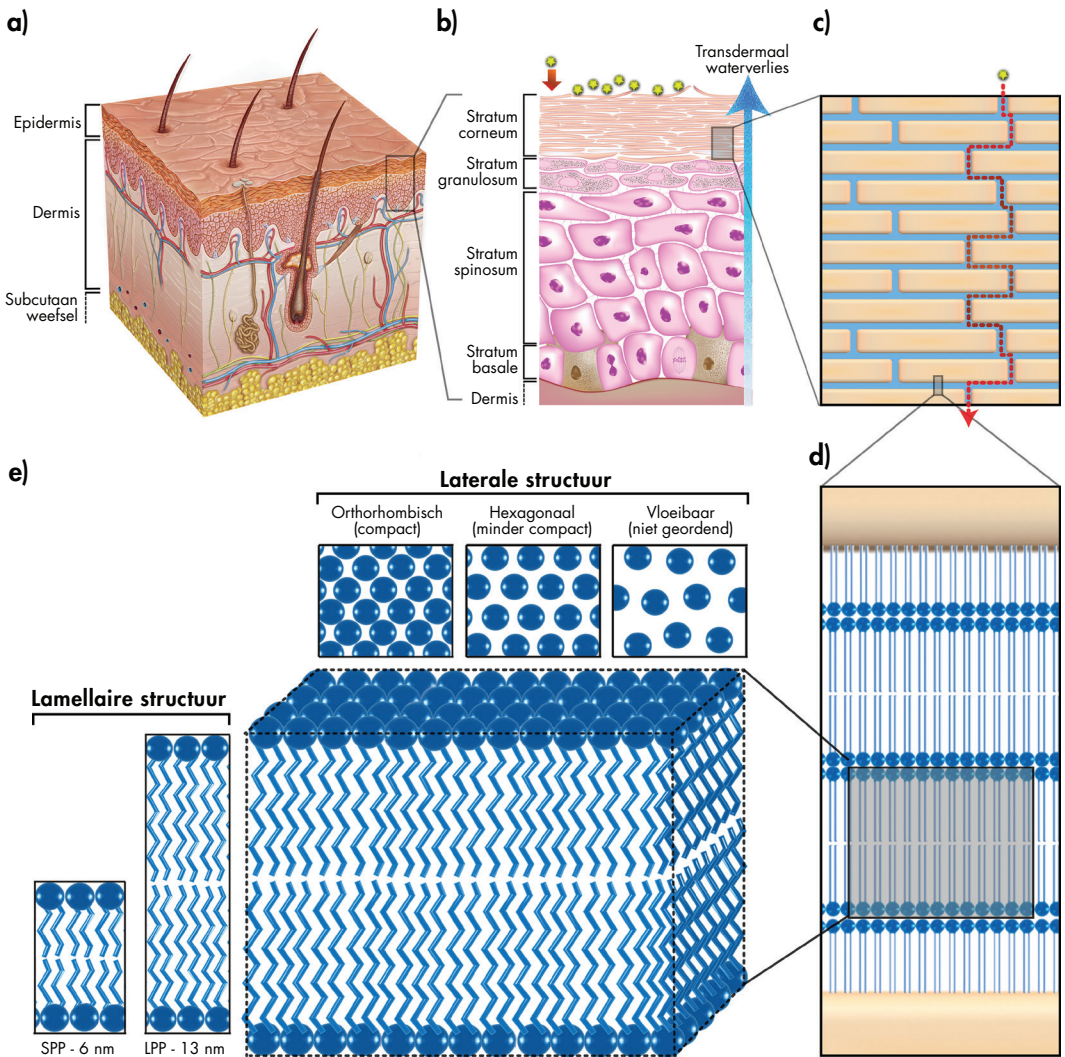
*Roodgedrukte woorden zijn opgenomen in een verklarende woordenlijst

hydratatiefactor van de huid, de NMF (natural moisturizing factor)^{5,6}. Deze NMF zijn **metaboliëten** van het eiwit **filaggrine**. Het is bekend dat **mutaties** in het filaggrine-gen een grote risicofactor vormen voor de ontwikkeling van constitutioneel eczeem⁷. Echter, deze mutaties komen bij constitutioneel eczeem maar in 20 tot 50 procent van de patiënten voor, en kan de ziekte daarom niet volledig verklaren^{8,9}. Dit laat het belang zien van andere factoren die een rol spelen bij deze ziekte. Eén van deze factoren is de barrièrefunctie van de huid, welke verstoord is bij mensen met constitutioneel eczeem¹⁰⁻¹⁴.

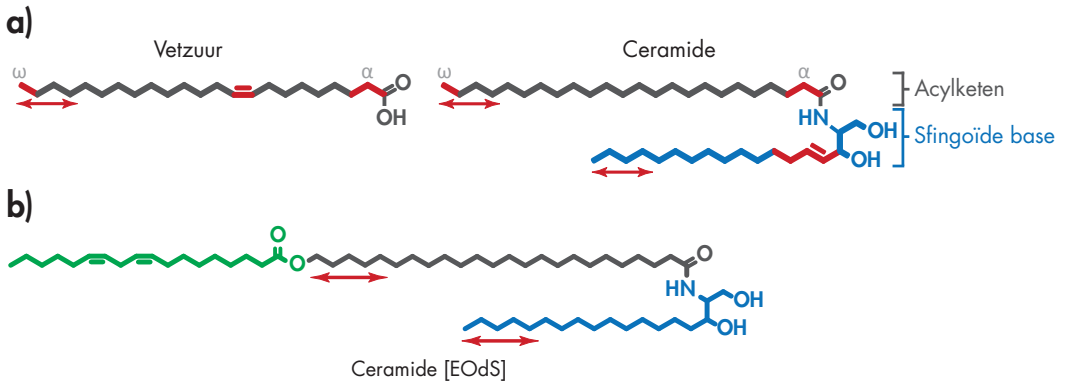
De huidbarrière bevindt zich in de buitenste huidlaag. Dit is de hoornlaag, ook wel het **stratum corneum** genoemd^{15,16}, verder afgekort tot SC. Deze laag bestaat voornamelijk uit dode huidcellen (corneocyten) die worden omsloten door **lipiden**. Deze lipiden vormen een sterk geordende structuur, en voorkomen het binnendringen van allergenen uit de omgeving (zie Figuur 2a-c)¹⁷. Daarnaast beschermt het SC het lichaam tegen overmatig **transdermaal waterverlies**, en dus uitdroging. In constitutioneel eczeem is de barrièrefunctie van het SC verminderd en kunnen allergenen via de lipiden door het SC penetreren en de dieper gelegen huidlagen bereiken^{2,10,13,18}. Dit duidt erop dat de lipiden in het SC een belangrijke functie vervullen voor een goede huidbarrière.

De lipiden in het SC bestaan uit vetzuren, ceramides, en cholesterol^{19,20}. Op moleculair niveau hebben vetzuren en ceramides respectievelijk één en twee lange koolstofketens, zoals uitgelegd in Figuur 3a. Echter, de molecuulstructuur van deze lipiden kan verschillen: vetzuren zijn voornamelijk verzadigd, maar **onverzadigde vetzuren** zijn ook aangetoond^{21,22}. Ceramides bestaan uit een sfincoïde base en een vetzuurketen (acylketen genoemd). Beide ketens kunnen verschillen in hun chemische structuur, wat resulteert in ceramidesubklassen^{23,24}. Naast deze variaties in functionele groepen hebben zowel vetzuren als ceramides een grote variatie in de ketenlengte. Deze variatie in zowel ketenlengte en functionele groepen is uniek voor lipiden in het SC en resulteert in een karakteristiek geordende structuur van de lipiden: lipidenlagen die geordend op elkaar gestapeld zijn (Figuur 2d,e)^{25,26}. In humaan SC bevinden zich twee soorten gestapelde lipidenlagen (lamellaire lipidenstructuren genoemd), die zich over een afstand van 6 of 13 nanometer herhaalt, respectievelijk de SPP (short periodicity phase) en LPP (long periodicity phase) genoemd²⁷⁻²⁹. Naast deze **lamellaire lipidenstructuur** zijn de lipiden in deze lipidenlagen ook geordend met een bepaalde dichtheid, bekend als de **laterale lipidenstructuur**³⁰⁻³⁴: humane SC-lipiden zijn voornamelijk zeer compact geordend – orthorombisch genoemd. Een klein deel van de lipiden is echter geordend in een minder compacte – hexagonale – lipidenstructuur, of zelfs een structuur die veel minder geordend, en vloeibaar is.

Bekend is dat lipiden in het SC een cruciale rol spelen bij een goed functionerende



Figuur 2: Verklaring van de lipidenstructuur in de huid. **a)** Dwarsdoorsnede van de huid met daarin de opperhuid (epidermis), lederhuid (dermis), en het onderhuids vet- en bindweefsel. **b)** De epidermis is onderverdeeld in een aantal lagen waarvan het SC (hoornlaag) de buitenste is. Deze beschermt het lichaam tegen het binnendringen van allergenen van buitenaf, en voorkomt tevens excessievelijk transepidermaal waterverlies van binnen het lichaam. **c)** Het SC is opgebouwd als een bakstenen muur, bestaande uit corneocyten (bakstenen) omgeven door lipiden (cement). De corneocyten zijn veelal ondoordringbaar, en stoffen van buitenaf dringen de huid daarom binnen via de intercellulaire route (via de lipiden, aangegeven met de rode pijl). **d)** Ingezoomd op de lipiden zijn daar de lipide lamellen: gestapelde lipidelagen met een driedimensionale ordening, weergegeven in **e)**. Ten eerste kunnen de lipiden onderzocht worden naar hun lamellaire structuur (vooraanzicht in de figuur), en inzicht worden verkregen in de lengte van de repeterende afstanden. Daarnaast kan ook de dichtheid van de lipiden bestudeerd worden, de laterale structuur (bovenaanzicht in de figuur). Hiermee kijkt men hoe compact en geordend de lipiden zijn gestructureerd.



Figuur 3: Molecuulstructuur van vetzuren en ceramides. **a)** Vetzuren bestaan uit een lange koolstofketen en een zuurgroep. Daarnaast kunnen vetzuren één of meerdere dubbele bindingen in de koolstofketen hebben en daarmee respectievelijk enkelvoudig onverzadigd of meervoudig onverzadigd zijn. Vetzuren kunnen ook een extra hydroxylgroep hebben op de alpha- of omegapositie in het molecuul (met rood aangegeven). Ceramides bestaan uit twee koolstofketens: een vetzuurketen (acylketen genoemd, aangegeven in grijs) gekoppeld aan een sfingoïde base (in blauw). Ook bij ceramides kan de molecuulstructuur van beide ketens variëren en kan een extra hydroxylgroep op de met rood gemarkeerde plaatsen voorkomen. Daarnaast kunnen zowel vetzuren als ceramides verschillen in de lengte van de koolstofketens (aangegeven met rode pijlen). Vetzuren in het SC kunnen een ketenlengte hebben variërend van ongeveer 16 tot 36 koolstofatomen. Ceramides hebben een totale ketenlengte (beide ketens samen) tussen de 32 en 56 koolstofatomen, uitgezonderd de [EO]-subklasse (zie hieronder). **b)** De molecuulstructuur van de twaalfde, ontdekte ceramide: de ester-gebonden ω -hydroxy acylketen gekoppeld aan een dihydrosfingosine base. Deze behoort tot de [EO]-subklasse, waarin een extra vetzuur vastgekoppeld is (aangegeven in het groen) via een esterbinding aan de vetzuurketen van de ceramide. Dit maakt dat ceramides die behoren tot deze subklasse uitzonderlijk lang zijn, met een totale ketenlengte die ligt tussen de 62 en 78 koolstofatomen. Ook bij deze subklasse komen variaties in ketenlengte voor (aangegeven met rode pijlen).

huidbarrière. Onduidelijk is echter welke rol de samenstelling van de lipiden (en de ordening ervan) spelen in constitutioneel eczeem. Wetenschappelijke studies geven gebrekkige of tegenstrijdige informatie als het gaat om de samenstelling van de lipiden³⁵⁻⁴⁵. Dit komt onder meer doordat de analytische methoden om de samenstelling nauwkeurig te bepalen erg gelimiteerd zijn en vaak weinig gedetailleerde informatie geven. Ook over de mate van ordening van de lipiden is bijna geen informatie beschikbaar. Er is slechts één studie bekend waarin de laterale lipidenstructuur is onderzocht in relatie tot constitutioneel eczeem⁴⁶. Het kleine aantal patiënten in die studie maakt de interpretatie echter beperkt, en tevens geeft dit geen inzicht in de lamellaire structuur van de lipiden. Het gebrek aan kennis over de lipiden in het SC belemmert de ontwikkeling van mogelijke behandelingen en medicatie voor mensen met constitutioneel eczeem. Het uitgangspunt van dit proefschrift is om meer inzicht te verkrijgen over de functie van de SC-lipiden en hun rol in de verstoorde huidbarrière bij mensen met constitutioneel eczeem.

Doelstellingen

Het hoofddoel van dit proefschrift is om in detail de samenstelling en de ordening van de lipiden in het SC te bepalen, en te onderzoeken wat de rol van deze lipiden is met betrekking tot de verminderde huidbarrière in eczeempatiënten. Om dit doel te verwezenlijken moest aan een viertal wetenschappelijke doelstellingen worden voldaan:

1. Het ontwikkelen van een robuuste methode die het mogelijk maakt om in detail de lipiden van het SC **kwantitatief** te analyseren.
2. Het bepalen van de lipidenamenstelling in zowel aangedane als niet-aangedane huid van constitutioneel eczeempatiënten, en deze vergelijken met een gezonde controlegroep.
3. Verklaren hoe veranderingen in de samenstelling van SC-lipiden in constitutioneel eczeempatiënten gerelateerd zijn aan veranderingen in de ordening van de lipiden, en hoe dit effect heeft op de barrièrefunctie van de huid.
4. De relatie onderzoeken tussen de samenstelling en de ordening van de SC-lipiden in patiënten met Netherton syndroom en in **humane huidmodellen**.

Deel II: methodeontwikkeling voor het analyseren van SC-lipiden

Deel II van het proefschrift richt zich op de eerste doelstelling waarin een nieuwe methode is ontwikkeld die het mogelijk maakt om alle lipiden in het SC (de ceramides, vetzuren, en cholesterol) tot in detail te analyseren. Dit is uitgevoerd met behulp van **vloeistofchromatografie** gekoppeld aan **massaspectrometrie** (LC/MS). Met deze techniek is het mogelijk om alle lipidenklassen en subklassen te scheiden en vervolgens te analyseren, evenals de ketenlengte van elk afzonderlijk lipide te bepalen.

De ontwikkeling van deze methode staat beschreven in Hoofdstuk 3, waarin het analyseren van de ceramides centraal staat. In dit hoofdstuk wordt een snelle en robuuste LC/MS methode beschreven die het mogelijk maakt om kwantitatief alle ceramides te analyseren met een geringe **monstervoorbewerking**. De ongebruikelijke combinatie van **normale fase LC** met **atmosferische druk chemische ionisatie (APCI) MS** bleek een uitstekende keus voor de analyse van ceramides, aangezien alle subklassen en ketenlengtes afdoende werden gescheiden en makkelijk konden worden gedetecteerd. In humaan SC werden alle 11 tot dusverre bekende ceramidesubklassen gedetecteerd. Daarnaast werden onbekende subklassen ontdekt. Met behulp van **hoge-resolutie MS** en door middel van **fragmentatie-MS** (MS/MS) werd een twaalfde ceramide-subklasse geïdentificeerd: Ceramide [EOds] (ester-gebonden ω -hydroxy acylketen gekoppeld aan een dihydrosfingosine base; zie Figuur 3b). De methode bleek niet alleen succesvol in het

analyseren van *ex-vivo*huid, maar ook voor SC verkregen door middel van *tape-strippen* en SC geïsoleerd uit humane huidmodellen.

De methodeontwikkeling van de andere twee lipidenklassen, de vetzuren en cholesterol, is beschreven in Hoofdstuk 4. Hierin wordt eerst de analyse van vetzuren beschreven. Door gebruik te maken van *omgekeerde fase LC* in combinatie met APCI-MS konden vetzuren worden gescheiden en gedetecteerd. Toevoeging van chloroform verbeterde in sterke mate de *ionisatie* en leidde tot de formatie van stabiele *chloride-adducten*. Een kwantitatief *validatieprotocol* liet zien dat de methode robuust, reproduceerbaar, gevoelig en snel is, terwijl *ionsuppressie* verwaarloosbaar klein bleek. Deze methode is daarom zeer geschikt voor de analyse van SC-vetzuren, en kan gecombineerd worden met de methode voor de analyse van ceramides beschreven in Hoofdstuk 3, omdat dezelfde ionisatiebron (APCI) is gebruikt. Deze methode voor het analyseren van ceramides werd op enkele punten aangepast, waardoor cholesterol ook gedetecteerd en kwantitatief geanalyseerd kan worden. De gecombineerde methode maakt het nu mogelijk om alle belangrijke lipiden (ceramides, vetzuren, en cholesterol) in het SC gezamenlijk te analyseren. Het laatste onderdeel van Hoofdstuk 4 beschrijft hoe de methode gebruikt kan worden voor SC afkomstig van: 1) *ex-vivo*huid; 2) *in-vivo*huid verkregen met behulp van *tape-strippen*; 3) humane huidmodellen, en; 4) varkenshuid. De verschillende soorten huid laten tal van verschillen zien in de lipidenprofielen van zowel de ceramides als de vetzuren.

Nadat de LC/MS-methode ontwikkeld was, is deze toegepast in een aantal studies waarin de rol van deze lipiden op de barrièrefunctie van de huid werd onderzocht. Deze studies worden beschreven in Deel III en IV.

Deel III: Samenstelling van de SC-lipiden in constitutioneel eczeem, en de rol van deze lipiden voor de barrièrefunctie van de huid.

Met behulp van de ontwikkelde LC/MS-methode is de samenstelling van de lipiden bepaald in patiënten met constitutioneel eczeem onderzocht, en vergeleken met de samenstelling in gezonde vrijwilligers (controle-groep). Daarnaast is de relatie tussen de samenstelling en de ordening van deze lipiden onderzocht, en hoezeer de lipiden betrokken zijn bij de verminderde huidbarrière in constitutioneel eczeem.

De eerste, verkennende studie in patiënten met constitutioneel eczeem is beschreven in Hoofdstuk 5. Hierin is de samenstelling van de ceramideklassen bepaald in 6 patiënten en vergeleken met een controlegroep van 6 gezonde vrijwilligers. In dit hoofdstuk wordt enkel de lipidenamenstelling besproken van niet-aangedane huid. Door middel van het *tape-strippen* van de onderarmen werd SC verkregen. Daarnaast werden *huidbiopten* afgenomen om met behulp van *röntgen-diffractie* (SAXD) de lamellaire lipidenstructuur

te onderzoeken. Uit dit onderzoek blijkt dat de SC-lipiden van patiënten met constitutioneel eczeem een veranderde ceramidesamenstelling hebben. Evenals bij de gezonde controlegroep, zijn alle 12 ceramidesubklassen aanwezig. Echter, de onderlinge verhouding in subklassen verschilt: Percentueel gezien hebben patiënten significant minder ceramides die behoren tot de [EO]-subklassen. Deze worden acylceramides genoemd en hebben een uitzonderlijk lange koolstofketen, zoals uitgelegd in Figuur 3b. Daarnaast werd duidelijk dat patiënten met de grootste afname in deze acylceramides ook de grootste afwijkingen hadden in de lamellaire structuur van de lipiden. Hieruit blijkt dat er een relatie bestaat tussen de ordening en de samenstelling van de ceramides.

De resultaten beschreven in Hoofdstuk 5 vormden het uitgangspunt voor een uitvoerige studie in 28 patiënten met constitutioneel eczeem en een controlegroep van 14 gezonde vrijwilligers, beschreven in Hoofdstuk 6. In deze studie is de ceramidesamenstelling bepaald en daarnaast de ordening van de SC-lipiden onderzocht: door gebruik te maken van SAXD werd informatie verkregen over de lamellaire structuur, terwijl de laterale ordening onderzocht is met behulp van **Fourier transform infrarood spectroscopie (FTIR)**. Ook werd de rol van de lipiden in relatie tot huidbarrière en het klinisch ziektebeeld onderzocht. Omdat mutaties in het filaggrine-gen een belangrijk risicofactor vormen voor de ontwikkeling van constitutioneel eczeem, is ook de relatie tussen dit gen en de samenstelling en ordening van de SC-lipiden onderzocht. Uit de resultaten kwamen een aantal opvallende aspecten naar voren. Allereerst blijkt dat SC van patiënten met constitutioneel eczeem een verhoogd gehalte hebben aan ceramides met een korte ketenlengte, in het bijzonder ceramides met een ketenlengte van (slechts) 34 koolstofatomen. Daarnaast blijkt het gehalte aan acylceramides verlaagd te zijn in patiënten. Deze twee veranderingen veroorzaken een verlaging van de gemiddelde ketenlengte van ceramides in patiënten met constitutioneel eczeem. Ook leiden deze veranderingen tot een andere ordening van de lipiden: Uit de laterale lipidenstructuur blijkt dat een groter deel van de lipiden geordend is in een minder compacte (hexagonale) structuur. Daarnaast laat de lamellaire ordening zien dat de afstand waarover de structuur zich herhaalt kleiner is. Alle bovengenoemde afwijkingen in samenstelling en ordening van lipiden gingen gepaard met een verminderde barrièrefunctie van de huid en correleerden daarnaast ook met de mate waarin de ziekte zich manifesteert in deze patiënten.

Uit deze studie, waar de ceramide samenstelling en de lipidenordering in het SC centraal staat, blijkt dat de veranderingen in de lipiden een zeer belangrijk aspect vormen voor de verstoorde huidbarrière in constitutioneel eczeem. Voor het eerst werd aangetoond dat met name de ketenlengte van de totale ceramideklassen een rol spelen in de verminderde

barrièrefunctie. Naast ceramides zijn vetzuren een andere belangrijke SC-lipidenklasse. Bovendien zijn vetzuren essentieel voor de biosynthese van ceramides, en veranderingen in vetzuurketenlengte zou mogelijk ten grondslag kunnen liggen aan de verandering in ketenlengte van de ceramides.

Omdat tot dusverre de ketenlengte van de vetzuren in het SC van patiënten met constitutioneel eczeem niet onderzocht is, werd deze lipidenklasse ook bepaald. Hierbij zijn zowel verzadigde, onverzadigde, en hydroxyvetzuren geanalyseerd. Deze studie is beschreven in Hoofdstuk 7, waarin de lipidsamenstelling in zowel aangedane als niet-aangedane eczeemhuid is onderzocht. Tevens werd de correlatie tussen veranderingen in de ketenlengte van de vetzuursamenstelling en ceramidesamenstelling bestudeerd. Daarnaast is onderzocht hoe veranderingen in de lipidsamenstelling kunnen bijdragen aan veranderingen in de ordening van de lipiden, en zo de barrièrefunctie van de huid kunnen verminderen. Het bleek dat in het SC van patiënten met constitutioneel eczeem een verhoogde hoeveelheid aanwezig is van onverzadigde vetzuren ten koste van hydroxyvetzuren. Daarnaast was er een verschuiving te zien in de vetzuurketenlengte: patiënten hadden een verhoging aan vetzuren met kortere ketens en een verlaging van vetzuren met lange ketens. Deze veranderingen waren al aanwezig in niet-aangedane huid, maar komen duidelijker naar voren in aangedane huid. De kortere vetzuurketenlengte correleert met een verkorte ketenlengte voor de ceramides. Dit bevestigt de hypothese dat de vetzuren en ceramides een gedeeltelijk gezamenlijke biosynthese hebben. De ketenlengte van de lipiden – zowel de vetzuren als de ceramides – blijkt sterk geassocieerd te zijn met de ordening van de lipiden: een verhoging in de hoeveelheid lipiden met een kortere ketenlengte leidt tot een minder compacte, hexagonale, lipidenstructuur. Daarentegen dragen langere ketenlengtes bij aan een compactere, orthorombische, ordening. Ook werd in dit hoofdstuk aangetoond dat een minder compacte lipidenstructuur samenvalt met verminderde huidbarrièrefunctie. Dit was zeer duidelijk te zien in aangedane huid, maar al waarneembaar in niet-aangedane huid.

Zowel in Hoofdstuk 6 als 7 wordt het effect van mutaties in het filaggrine-gen op de lipiden beschreven. Ook de NMF, metaboliëten van filaggrine, worden meegenomen in het onderzoek omdat deze een belangrijke rol spelen in de hydratatie van de huid en zorgen voor de juiste pH van het SC. Zowel de lipidsamenstelling als de ordening laten een duidelijk verband zien met de NMF: Patiënten met een sterker afwijkend lipidenprofiel laten ook een sterkere afname zien in de hoeveelheid NMF in het SC. Daarentegen is er geen enkele correlatie gevonden met mutaties in het filaggrine-gen. Deze discrepantie laat zien dat tussen het filaggrine-genotype en de filaggrine-metaboliëten andere factoren een belangrijke rol spelen (zoals filaggrine-expressie), en maakt duidelijk dat onderzoek naar

flaggrine op **fenotypisch** niveau naast dat van flaggrine genotypering erg belangrijk is.

Uit de studies beschreven in de voorgaande hoofdstukken blijkt dat de samenstelling van de lipiden – en de daaruitvoortkomende ordening – een belangrijke rol spelen in de verminderde barrièrefunctie van het SC in patiënten met constitutioneel eczeem. Een laatste studie in deze patiëntengroep was gericht om het effect van de totale hoeveelheid aan lipiden in het SC op de barrièrefunctie te onderzoeken. Om hierin inzicht te verkrijgen kan men het drooggewicht van het SC vergelijken met de **lipide/eiwit-ratio**, verkregen via **Ramanspectroscopie**. Dit onderzoek is beschreven in Hoofdstuk 8, en laat zien dat het drooggewicht van het SC nauwelijks veranderd is in patiënten met constitutioneel eczeem ten opzichte van de gezonde controlegroep. De lipide/eiwit-ratio was daarentegen wel significant afgenomen in eczeempatiënten, zowel in aangedane huid als – in mindere mate – in niet-aangedane huid. Ook deze veranderingen correleren met een verminderde huidbarrière in de patiëntengroep. De resultaten impliceren dat de hoeveelheid lipiden binnen het SC (en niet de hoeveelheid SC) een belangrijke rol spelen bij de verstoorde huidbarrière in constitutioneel eczeem.

Samenvattend: de studies beschreven in Deel III van dit proefschrift illustreren het belang van de lipiden voor de verstoorde huidbarrière in patiënten met constitutioneel eczeem. Deze conclusies vormden de basis om de lipiden van andere huidsoorten te onderzoeken waarin eveneens sprake is van een verminderde huidbarrière. Dit is uitvoerig beschreven in Deel IV.

Deel IV: Onderzoek naar SC-lipiden afkomstig van andere huidsoorten met een verminderde huidbarrière

In Deel III is een sterke relatie tussen de lipidensamentelling, de lipidenstructuur, en een verminderde huidbarrière in patiënten met constitutioneel eczeem beschreven. Daarom werd besloten om ook SC te onderzoeken van patiënten met Netherton syndroom en humane huidmodellen. Van beide is bekend dat er sprake is van een verminderde barrièrefunctie van de huid, maar informatie over de SC-lipiden is er niet of nauwelijks.

Hoofdstuk 9 beschrijft de samenstelling en ordening van de SC-lipiden in 8 patiënten met Netherton syndroom, een zelfdzame en zeer ernstige huidziekte die veel gelijkenissen vertoont met constitutioneel eczeem. Het syndroom wordt veroorzaakt door mutaties in het **SPINK5** gen. Dit gen codeert voor het eiwit **LEKTI**, een specifieke **proteaseremmer**. Bij patiënten is er geen of nauwelijks expressie van dit eiwit, wat leidt tot een verhoogde activiteit van **epidermale proteases** en daardoor extreme schilfering van het SC. De barrièrefunctie van de huid is dan ook ernstig verstoord bij mensen die lijden aan Netherton syndroom. Het doel van dit onderzoek was om te bepalen of er

afwijkingen zijn in de samenstelling en de ordening van de lipiden in het SC van deze patiënten. Er is nagenoeg geen informatie bekend over de lipideneigenschappen van het SC van deze patiënten. Uit het door ons uitgevoerde onderzoek blijkt dat patiënten met Netherton syndroom een lipidenprofiel hebben die veel overeenkomsten vertoont met constitutioneel eczeem: ten opzichte van de controlegroep is de ketenlengteverdeling van de vetzuren verschoven naar kortere ketens, en tevens is er een verhoging in het aantal onverzadigde vetzuren. Ook is het gehalte aan ceramides met een korte keten verhoogd en is er in een aantal patiënten een drastische verlaging van ceramides met een zeer lange keten (acylceramides). Naast deze overeenkomsten met constitutioneel eczeem zijn er in patiënten met Netherton syndroom hoge gehalten aan onverzadigde ceramides gemeten. De veranderingen in de samenstelling van de lipiden komt overeen met een verandering in de ordening ervan: zowel de lamellaire als de laterale structuur lieten significante veranderingen zien. Het ligt voor de hand dat de bovengenoemde veranderingen in lipidenstructuur en lipidenstructuur bijdragen aan de verminderde barrièrefunctie van de huid bij deze patiënten.

Hoofdstuk 10 beschrijft een studie waarin de SC-lipiden van vier verschillende (humane) huidmodellen onderzocht is. Deze gekweekte huid afkomstig van geïsoleerde huidcellen lijkt in veel opzichten op de eigenschappen van menselijke huid, maar vertoont desalniettemin een verminderde huidbarrière en een afwijkende lipidenstructuur. Om de oorzaak van deze afwijkingen in huidmodellen te achterhalen, is de samenstelling van de vetzuren en ceramides geanalyseerd. Uit de resultaten blijkt dat in alle huidmodellen dezelfde 12 ceramidesubklassen aanwezig zijn als in humaan SC. Echter, ceramides met kortere koolstofketens zijn significant verhoogd ten opzichte van humaan SC. Daarnaast zijn in de huidmodellen ook onverzadigde ceramides aanwezig. Deze zijn nooit eerder waargenomen in humaan SC, uitgezonderd de patiënten met Netherton syndroom. Ook bleek de totale hoeveelheid vetzuren drastisch verlaagd, en vertonen de huidmodellen een verhoogde hoeveelheid onverzadigde vetzuren ten opzichte van humaan SC. Dit laatste kan verklaard worden door een verhoogde expressie van het enzym stearoyl-CoA desaturase (SCD), het enzym dat verzadigde vetzuren omzet tot onverzadigde vetzuren.

Deel V: Conclusies

Uit de studies beschreven in dit proefschrift blijkt dat lipiden in het SC een cruciale rol spelen in de barrièrefunctie van de huid. Uit studies in patiënten met constitutioneel eczeem en Netherton syndroom blijkt dat veranderingen in de samenstelling van de lipiden een negatief effect hebben op de lamellaire en laterale lipidenstructuur. In het bijzonder de ketenlengte van de lipiden blijkt uitstekend te correleren met de ordening

van de lipiden: kortere vetzuur- en ceramideketenlengtes dragen bij aan een minder compacte, hexagonale, lipidenordering, terwijl langere lipidenketens resulteren in een meer compacte, orthorombische, lipidenstructuur.

Uit de studies blijkt ook dat acylceramides (ceramides met een zeer lange koolstofketen, behorende tot de [EO] subklasse) essentieel zijn voor een lange periodiciteitsfase (LPP) in de lamellaire lipidenstructuur. De aanwezigheid van deze LPP heeft een positieve bijdrage op de barrièrefunctie van de huid. Het gebruik van LC/MS als analytische methode bleek essentieel voor deze bevindingen, omdat geen enkele andere methode tot op heden alle SC-lipiden en de ketenlengtes ervan kan analyseren. Daarnaast is de gevoeligheid van massaspectrometrie ongeëvenaard, waardoor de hoeveelheid huidmateriaal die nodig is voor analyse zeer beperkt blijft. Hierdoor was het mogelijk om lipiden uit het SC te verkrijgen op een non-invasieve manier door middel van tape-strippen.

Het SC van patiënten met constitutioneel eczeem, Netherton syndroom, en van huidmodellen laten allemaal dezelfde soort veranderingen zien in hun lipiden samenstelling: een verkorte ketenlengte in de lipiden en een verhoging van het gehalte aan onverzadigde lipiden. Een sterkere afwijking in de lipiden samenstelling – zoals aangedane huid in constitutioneel eczeem of huid van patiënten met Netherton syndroom – leidt tot een sterkere afwijking in de ordening van de lipiden en een ernstigere verstooring van de huidbarrière.

Uit deze studies blijkt dat er een duidelijk verband is tussen de samenstelling van de vetzuren en de ceramides: zowel de ketenlengte als de hoeveelheid onverzadigde lipiden correleert voor beide lipidenklassen. Deze bevinding is biologisch gezien relevant, omdat dit de hypothese ondersteunt dat vetzuren en ceramides in het SC een overlappende biosynthese hebben^{47,48}. Ook is de bevinding van klinische waarde, omdat het impliceert dat de ceramidesamenstelling gedeeltelijk hersteld kan worden door het normaliseren van de vetzuursamenstelling.

Tevens is er meer inzicht verkregen in het epidermaal lipidenmetabolisme: Allereerst suggereren de kortere vetzuurketenlengtes – waargenomen in constitutioneel eczeem, Netherton syndroom, en de huidmodellen – dat de verlenging (**elongatie**) van vetzuurketens verstoord is⁴⁹; Ten tweede laten de veranderingen in de relatieve hoeveelheid van bepaalde ceramidesubklassen zien dat de enzymen die betrokken zijn bij de synthese van deze subklassen meer- of minder actief zijn. Twee enzymen die wellicht deels ten grondslag liggen aan dit veranderde lipidenmetabolisme zijn **β -glucocerebrosidase** en **sphingomyelinase**. Beiden zijn betrokken bij de omzetting van ceramide-precursors naar hun uiteindelijke ceramidestructuur⁵⁰⁻⁵³. Beide enzymen hebben echter niet dezelfde **affiniteit** voor alle precursors, en verandering in de activiteit van één van deze enzymen kan deels verklaren

waarom bepaalde ceramidesubklassen verhoogd zijn ten koste van andere subklassen⁵⁴.

De studies in constitutioneel eczeempatiënten geven een beter inzicht in de rol van filaggrine en NMF met betrekking tot de lipiden in het SC en de barrièrefunctie van de huid. Filaggrine op fenotypisch en metabolisch (NMF) niveau zijn hier meer aan gerelateerd dan op het genotypisch (DNA) niveau. Dit ondersteunt de hypothese dat veranderingen in filaggrine-expressie een belangrijke factor vormen in constitutioneel eczeem^{55,56}.

Concluderend, de studies die beschreven zijn in dit proefschrift dragen bij aan meer kennis omtrent de barrièrefunctie van het SC vanuit zowel een biofysisch perspectief (de relatie tussen lipidensamenstelling, lipidenstructuur, en barrièrefunctie van de huid), maar ook vanuit een klinisch perspectief, namelijk het belang van de SC-lipiden in relatie tot constitutioneel eczeem en Netherton syndroom. Toekomstig onderzoek zou zich kunnen richten op het herstellen van de huidbarrière bij mensen met (constitutioneel) eczeem, of meer inzicht verschaffen naar de oorzaak en de mechanismen van de ziekte. Daarnaast kan men ook breder kijken door fundamenteel onderzoek te verrichten naar het lipidenmetabolisme van de huid, of de mogelijkheden benutten die liggen op het gebied van de analytische technieken als LC/MS.

References

- 1 Leung DY, Bieber T. Atopic dermatitis. *Lancet* 2003; 361: 151-60.
- 2 Oyoshi MK, He R, Kumar L *et al*. Cellular and molecular mechanisms in atopic dermatitis. *Adv Immunol* 2009; 102: 135-226.
- 3 Wollenberg A, Rawer HC, Schaubert J. Innate immunity in atopic dermatitis. *Clin Rev Allergy Immunol* 2011; 41: 272-81.
- 4 Flohr C, Johansson SG, Wahlgren CF *et al*. How atopic is atopic dermatitis? *J Allergy Clin Immunol* 2004; 114: 150-8.
- 5 Voegeli D. The role of emollients in the care of patients with dry skin. *Nurs Stand* 2007; 22: 62, 4-8.
- 6 Sandilands A, O'Regan GM, Liao H *et al*. Prevalent and rare mutations in the gene encoding filaggrin cause ichthyosis vulgaris and predispose individuals to atopic dermatitis. *J Invest Dermatol* 2006; 126: 1770-5.
- 7 Palmer CN, Irvine AD, Terron-Kwiatkowski A *et al*. Common loss-of-function variants of the epidermal barrier protein filaggrin are a major predisposing factor for atopic dermatitis. *Nat Genet* 2006; 38: 441-6.
- 8 Jakasa I, Koster ES, Calkoen F *et al*. Skin barrier function in healthy subjects and patients with atopic dermatitis in relation to filaggrin loss-of-function mutations. *J Invest Dermatol* 2011; 131: 540-2.
- 9 Akiyama M. FLG mutations in ichthyosis vulgaris and atopic eczema: spectrum of mutations and population genetics. *Br J Dermatol* 2010; 162: 472-7.
- 10 Elias PM, Hatano Y, Williams ML. Basis for the barrier abnormality in atopic dermatitis: Outside-inside-outside pathogenic mechanisms. *J Allergy Clin Immunol* 2008; 121: 1337-43.
- 11 Elias PM. Barrier repair trumps immunology in the pathogenesis and therapy of atopic dermatitis. *Drug Discov Today Dis Mech* 2008; 5: e33-e8.
- 12 Seidenari S, Giusti G. Objective assessment of the skin of children affected by atopic dermatitis: A study of pH, capacitance and TEWL in eczematous and clinically uninvolved skin. *Acta Dermato-Venereologica* 1995; 75: 429-33.
- 13 Elias PM, Schmutz M. Abnormal skin barrier in the etiopathogenesis of atopic dermatitis. *Current Opinion in Allergy and Clinical Immunology* 2009; 9: 437-46.
- 14 Yoshiike T, Aikawa Y, Sindhvananda J *et al*. Skin barrier defect in atopic dermatitis: increased permeability of the stratum corneum using dimethyl sulfoxide and theophylline. *J Dermatol Sci* 1993; 5: 92-6.
- 15 Elias PM, Choi EH. Interactions among stratum corneum defensive functions. *Exp Dermatol* 2005; 14: 719-26.
- 16 Elias PM. Stratum corneum defensive functions: An integrated view. *Journal of Investigative Dermatology* 2005; 125: 183-200.
- 17 Bouwstra JA, Dubbelaar FER, Gooris GS *et al*. The lipid organisation in the skin barrier. *Acta Dermato-Venereologica* 2000; 23-30.
- 18 Elias PM, Steinhoff M. "Outside-to-Inside" (and now back to "Outside") pathogenic mechanisms in atopic dermatitis. *Journal of Investigative Dermatology* 2008; 128: 1067-70.
- 19 Wertz P, Downing D, Goldsmith L. Physiology, Biochemistry and Molecular Biology of the Skin. *Oxford University Press; Oxford* 1991.
- 20 Bouwstra JA, Gooris GS, Cheng K *et al*. Phase behavior of isolated skin lipids. *J Lipid Res* 1996; 37: 999-1011.
- 21 Ansari MN, Nicolaides N, Fu HC. Fatty acid composition of the living layer and stratum corneum lipids of human sole skin epidermis. *Lipids* 1970; 5: 838-45.
- 22 Norlen L, Nicander I, Lundsjo A *et al*. A new HPLC-based method for the quantitative analysis of inner stratum corneum lipids with special reference to the free fatty acid fraction. *Arch Dermatol Res* 1998; 290: 508-16.
- 23 Motta S, Monti M, Sesana S *et al*. Ceramide composition of the psoriatic scale. *Biochim Biophys Acta* 1993; 1182: 147-51.
- 24 Masukawa Y, Narita H, Shimizu E *et al*. Characterization of overall ceramide species in human stratum corneum. *J Lipid Res* 2008; 49: 1466-76.
- 25 Madison KC, Swartzendruber DC, Wertz PW *et al*. Presence of intact intercellular lipid lamellae in the upper layers of the stratum corneum. *J Invest Dermatol* 1987; 88: 714-8.
- 26 Bouwstra JA, Gooris GS, van der Spek JA *et al*. Structural investigations of human stratum corneum by small-angle X-ray scattering. *J Invest Dermatol* 1991; 97: 1005-12.
- 27 Groen D, Gooris GS, Bouwstra JA. New insights into the stratum corneum lipid organization by X-ray diffraction analysis. *Biophys J* 2009; 97: 2242-9.
- 28 McIntosh TJ, Stewart ME, Downing DT. X-ray diffraction analysis of isolated skin lipids: reconstitution of intercellular lipid domains. *Biochemistry* 1996; 35: 3649-53.
- 29 Bouwstra J, Pilgram G, Gooris G *et al*. New aspects of the skin barrier organization. *Skin Pharmacol Appl Skin Physiol* 2001; 14 Suppl 1: 52-62.
- 30 de Jager MW, Gooris GS, Dolbnya IP *et al*. The phase behaviour of skin lipid mixtures based on synthetic ceramides. *Chem Phys Lipids* 2003; 124: 123-34.
- 31 Bouwstra JA, Gooris GS, Dubbelaar FE *et al*. Phase behavior of lipid mixtures based on human ceramides: coexistence of crystalline and liquid phases. *J Lipid Res* 2001; 42: 1759-70.
- 32 Goldsmith LA, Baden HP. *Uniquely oriented epidermal lipid*. *Nature* 1970; 225: 1052-3.
- 33 Damien F, Boncheva M. The extent of orthorhombic lipid phases in the stratum corneum determines the barrier efficiency of human skin in vivo. *J Invest Dermatol* 2010; 130: 611-4.
- 34 Pilgram GS, Engelsma-van Pelt AM, Bouwstra JA *et al*. Electron diffraction provides new information on human stratum corneum lipid organization studied in relation to depth and temperature. *J Invest Dermatol* 1999; 113: 403-9.
- 35 Bleck O, Abeck D, Ring J *et al*. Two ceramide subfractions detectable in Cer(AS) position by HPTLC in skin surface lipids of non-lesional skin of atopic eczema. *J Invest Dermatol* 1999; 113: 894-900.
- 36 Farwanah H, Raith K, Neubert RH *et al*. Ceramide profiles of the uninvolved skin in atopic dermatitis and psoriasis are comparable to those of healthy skin. *Arch Dermatol Res* 2005; 296: 514-21.

- 37 Angelova-Fischer I, Mannheimer AC, Hinder A *et al.* Distinct barrier integrity phenotypes in filaggrin-related atopic eczema following sequential tape stripping and lipid profiling. *Exp Dermatol* 2011; 20: 351-6.
- 38 Ishibashi M, Arikawa J, Okamoto R *et al.* Abnormal expression of the novel epidermal enzyme, glucosylceramide deacylase, and the accumulation of its enzymatic reaction product, glucosylsphingosine, in the skin of patients with atopic dermatitis. *Lab Invest* 2003; 83: 397-408.
- 39 Matsumoto M, Umemoto N, Sugiura H *et al.* Difference in ceramide composition between "dry" and "normal" skin in patients with atopic dermatitis. *Acta Derm Venereol* 1999; 79: 246-7.
- 40 Di Nardo A, Wertz P, Giannetti A *et al.* Ceramide and cholesterol composition of the skin of patients with atopic dermatitis. *Acta Derm Venereol* 1998; 78: 27-30.
- 41 Jungersted JM, Scheer H, Mempel M *et al.* Stratum corneum lipids, skin barrier function and filaggrin mutations in patients with atopic eczema. *Allergy* 2010; 65: 911-8.
- 42 Imokawa G, Abe A, Jin K *et al.* Decreased level of ceramides in stratum corneum of atopic dermatitis: an etiologic factor in atopic dry skin? *J Invest Dermatol* 1991; 96: 523-6.
- 43 Holleran WM, Takagi Y, Uchida Y. Epidermal sphingolipids: metabolism, function, and roles in skin disorders. *FEBS Lett* 2006; 580: 5456-66.
- 44 Takigawa H, Nakagawa H, Kuzukawa M *et al.* Deficient production of hexadecenoic acid in the skin is associated in part with the vulnerability of atopic dermatitis patients to colonization by *Staphylococcus aureus*. *Dermatology* 2005; 211: 240-8.
- 45 Macheleidt O, Kaiser HW, Sandhoff K. Deficiency of epidermal protein-bound omega-hydroxyceramides in atopic dermatitis. *J Invest Dermatol* 2002; 119: 166-73.
- 46 Pilgram GS, Vissers DC, van der Meulen H *et al.* Aberrant lipid organization in stratum corneum of patients with atopic dermatitis and lamellar ichthyosis. *J Invest Dermatol* 2001; 117: 710-7.
- 47 Ohno Y, Suto S, Yamanaka M *et al.* ELOVL1 production of C24 acyl-CoAs is linked to C24 sphingolipid synthesis. *Proc Natl Acad Sci USA* 2010; 107: 18439-44.
- 48 Uchida Y. The role of fatty acid elongation in epidermal structure and function. *Dermatoendocrinol* 2011; 3: 65-9.
- 49 Guillou H, Zadravec D, Martin PG *et al.* The key roles of elongases and desaturases in mammalian fatty acid metabolism: Insights from transgenic mice. *Prog Lipid Res* 2010; 49: 186-99.
- 50 Holleran WM, Ginns EI, Menon GK *et al.* Consequences of beta-glucocerebrosidase deficiency in epidermis. Ultrastructure and permeability barrier alterations in Gaucher disease. *J Clin Invest* 1994; 93: 1756-64.
- 51 Holleran WM, Takagi Y, Menon GK *et al.* Processing of epidermal glucosylceramides is required for optimal mammalian cutaneous permeability barrier function. *J Clin Invest* 1993; 91: 1656-64.
- 52 Jensen JM, Schutze S, Forl M *et al.* Roles for tumor necrosis factor receptor p55 and sphingomyelinase in repairing the cutaneous permeability barrier. *J Clin Invest* 1999; 104: 1761-70.
- 53 Schmuth M, Man MQ, Weber F *et al.* Permeability barrier disorder in Niemann-Pick disease: sphingomyelin-ceramide processing required for normal barrier homeostasis. *J Invest Dermatol* 2000; 115: 459-66.
- 54 Briot A, Deraison C, Lacroix M *et al.* Kallikrein 5 induces atopic dermatitis-like lesions through PAR2-mediated thymic stromal lymphopoietin expression in Netherton syndrome. *J Exp Med* 2009; 206: 1135-47.
- 55 Brown SJ, Irvine AD. Atopic eczema and the filaggrin story. *Seminars in Cutaneous Medicine and Surgery* 2008; 27: 128-37.
- 56 Brown SJ, McLean WH. One remarkable molecule: filaggrin. *J Invest Dermatol* 2012; 132: 751-62.

Figure 1 was used with permission from Rachmat Tubagus, doktermudatrader.blogspot.nl (2012)

Figure 2a was purchased from iStockphoto

Figure 2b was purchased from Shutterstock

Verklarende woordenlijst

Deze verklarende woordenlijst fungeert als supplement bij de Nederlandse Samenvatting, en dient in de context gelezen te worden. De termen zijn op alfabetische wijze vermeld.

Affiniteit: Aantrekkingskracht tussen het molecuul (ligand) en het enzym. Een ligand met een hogere affiniteit voor een bepaald enzym zal makkelijker een binding vormen met het enzym en vervolgens omgezet worden.

Allergeen-specifiek immunoglobuline-E (IgE): Lichaamseigen antistof dat een rol speelt bij overgevoeligheid. IgE bindt aan de allergene stof en zet een immuunreactie in werking. In het geval van een allergie is er sprake van een overreactie.

Allergenen: Stoffen (van buitenaf) die een allergie kunnen veroorzaken. Het lichaam reageert hierop hevig met een overgevoelige reactie en (eventueel) de aanmaak van IgE. Bekende voorbeelden zijn pollen en huisstofmijt, maar ook pinda's en koemelkeiwitten kunnen een IgE-gemedieerde immuunreactie in gang zetten.

Atmosferische druk chemische ionisatie (APCI): Een methode om geladen deeltjes (ionen) te verkrijgen via verdamping en het gebruik van elektrische ontladingen met een hoog voltage (waarbij plasma ontstaat). Deze ionen zijn nodig om met een massaspectrometer te kunnen detecteren.

β -glucocerebrosidase: Enzym dat een suikergroep 'losknijpt' van een glucosylceramide-molecuul, waardoor een ceramide ontstaat.

Biosynthese: Natuurlijke aanmaak van stoffen in het lichaam via enzymatische reacties.

Chloride-adducten: Een geladen deeltje (ion) gevormd uit de koppeling van het oorspronkelijke molecuul met een chloor-atoom. Adducten worden gebruikt in massaspectrometrie omdat het oorspronkelijke molecuul bijvoorbeeld erg instabiel of niet goed detecteerbaar is.

Elongatie: Natuurlijke manier om koolstofketens (zoals het geval bij vetzuren) te verlengen met behulp van enzymen (zogenoemde elongases).

Epidermale proteases: enzymen in de huid die eiwitbindingen afbreken.

Ex-vivo huid: Huid waarop onderzoek gedaan wordt, maar buiten het lichaam. In dit geval gaat het om huid dat via plastische chirurgie is verwijderd en vervolgens geprepareerd is om experimenteel werk op te kunnen verrichten.

Expressie: Het proces waarin het DNA van een gen wordt gekopieerd en tot uiting komt (fenotype), vaak als een eiwit (in dit geval filaggrine). Of een gen ook daadwerkelijk tot expressie komt hangt af van vele factoren, waaronder de omgeving. Het genotype (DNA) bepaalt dus maar in beperkte mate de uiterlijke vorm en hoeveelheid van een eiwit (fenotype).

Fenotypisch: Waarneembaar/Meetbare resultaat van een genotype (DNA). Iets wat in het DNA zit hoeft niet altijd tot uiting te komen in een fenotype ('zichtbaar te worden'), omdat ook andere factoren een rol spelen zoals de omgeving (zie 'Expressie'). In dit geval gaat het om het filaggrine-gen (genotype), dat uiteindelijk tot uiting kan komen in het eiwit filaggrine (fenotype).

Filaggrine: Eiwit in de huid met twee belangrijke functies. Allereerst zorgt het voor het bij elkaar houden van keratinefillamenten, 'eiwitdraden' die zorgen voor de compactheid en stevigheid van huidcellen. Daarnaast wordt filaggrine afgebroken in moleculen die belangrijk zijn voor de hydratatie van de huid, de NMF.

Fourier transform

infraroodspectroscopie (FTIR):

Analytische techniek waarbij met behulp van infrarode straling gekeken wordt naar specifieke trillingen van moleculen.

Hiermee kan de laterale structuur van de lipiden onderzocht worden, omdat de lipiden met een andere frequentie trillen als de ordening verandert.

Fragmentatie-MS:

Een massaspectrometrische techniek waarbij de ionen worden gefragmenteerd. Uit de massa van deze fragmenten kan de molecuulstructuur van het ion herleidt worden.

Genotype: De erfelijke eigenschappen (genen) die zich bevinden in het DNA.

Hoge-resolutie MS: Met een massaspectrometer met hoge resolutie kan de massa van ionen bepaald worden tot op 5 à 6 decimalen achter de komma.

Huidbiopten: Stukjes huidweefsel dat is weggesneden zodat het gebruikt kan worden voor onderzoek.

Humane huidmodellen: gekweekte huid dat grote gelijkenissen vertoont met menselijke huid.

Hydroxy-vetzuren: Vetzuren met een extra hydroxyl-groep (OH-groep) in het molecuul.

In-vivo huid: Huid waarop onderzoek verricht wordt in een levend organisme. In dit geval waren het de onderarmen van vrijwilligers waarop onderzoek gedaan is.

Ionsuppressie: Bij massaspectrometrie kunnen meerdere ionen met verschillende massa's tegelijkertijd gemeten worden. Het signaal van het ene ion kan echter wel het signaal van het andere ion verstoren, waardoor het signaal gedeeltelijk of zelfs geheel weg kan vallen. Dit gebeurt voornamelijk als de detector teveel ionen in een te korte tijd krijgt te verwerken.

Kwantitatief: Iets dat uit te drukken is in een bepaalde hoeveelheid (bijvoorbeeld gram, milliliter, of percentage). Dit is tegengesteld aan kwalitatief, wat alleen ingaat op de vraag OF iets aanwezig is of niet.

Lamellaire lipidenstructuur: Een structuur tussen de corneocyten dat bestaat uit repeterende lagen (fasen) van lipiden. In humaan stratum corneum komt een lange en korte periodiciteitsfase voor. Niet te verwarren met de molecuulstructuur, wat een weergave is van alle atomen in een molecuul.

Laterale lipidenstructuur: Lateraal betekent letterlijk zijkant. Men bekijkt de lipiden vanuit het vlak dat loodrecht op de lamellaire structuur staat. Niet te verwarren met de molecuulstructuur, wat een weergave is van alle atomen in een molecuul.

LEKTI: Een eiwit dat staat voor Lympho-epithelial Kazal-type-related inhibitor. Dit eiwit bindt zich aan specifieke proteases, enzymen die eiwitbindingen doorknippen (zie Epidermale Proteases). Doordat LEKTI bindt aan de proteases, kunnen andere eiwitten niet meer binden en geknipt worden. Op deze manier inhibeert (verhindert) LEKTI de werking van bepaalde proteases in de epidermis, waardoor de huid niet overmatig schilfert.

Lipiden: vetachtige stoffen die slecht oplossen in water. Lipiden hebben in het menselijk lichaam velerlei functies, waaronder de barrièrefunctie in de huid. Lipiden die voorkomen in het stratum corneum zijn cholesterol, vetzuren en ceramides.

Lipide/eiwit ratio: Verhouding van het aantal lipiden ten opzichte van de hoeveelheid eiwit. Omdat het stratum corneum bestaat uit lipiden en corneocyten (dode cellen bestaande uit voornamelijk keratine, een eiwit), is de ratio een goede maat voor het aantal lipiden ten opzichte van het totaal aan stratum corneum.

Massaspectrometrie: Een analytische techniek waarbij moleculen eerst omgezet worden in ionen (geladen deeltjes), waarna het mogelijk is om de exacte molecuulmassa te kunnen meten van deze ionen.

Metabolieten: Natuurlijke afbraakproducten. Filaggrine wordt in de huid afgebroken tot kleinere moleculen – zoals de NMF – die een eigen functie hebben.

Monstervoorbewerking: Voordat een (huid)monster gemeten kan worden met analytische apparatuur, moeten er eerst een aantal stappen genomen worden om goede metingen te kunnen verrichten en vervuiling te voorkomen. Zo moeten de lipiden eerst uit de cellen geëxtraheerd worden en het lipidenextract opgezuiverd worden.

Mutaties: veranderingen in het DNA. In het geval van filaggrine kunnen mutaties leiden tot (onder andere) minder synthese van het eiwit filaggrine.

NMF: Natuurlijke hydratatiefactor van de huid, de zogenaamde Natural Moisturizing Factor. Deze is belangrijk voor een goede waterhuishouding in de huid, en bestaat uit onder meer afbraakproducten van het eiwit filaggrine.

Normale fase LC: Een manier van vloeistofchromatografie waarbij de vaste fase een polaire stof is. Deze vorm van chromatografie is tegenwoordig ongebruikelijk.

Omgekeerde fase LC: Een manier van vloeistofchromatografie waarbij de vaste fase een apolaire stof is, vaak een lange koolstofketen. Dit is tegenwoordig de meestvoorkomende vorm van chromatografie.

Onverzadigde vetzuren: Vetzuren met een dubbele binding in hun molecuulstructuur. Vetzuren kunnen enkelvoudig onverzadigd, maar ook meervoudig onverzadigd zijn. Laatstgenoemde komen nauwelijks voor in humaan stratum corneum.

Precursors: Uitgangsstoffen die als voorloper dienen voor de uiteindelijk stof.

Proteaseremmer: Een eiwit dat bindt aan een protease (enzym dat eiwitbindingen doorknipt), waardoor andere eiwitten niet meer geknipt kunnen worden en de werking van de protease dus wordt geremd (geïnhibeert).

Ramanspectroscopie: Analytische techniek waarbij met behulp van een laser met monochromatisch licht (licht met één golflengte) gekeken wordt naar de Raman-verstrooiing van dit licht. Deze verstrooiing hangt samen met specifieke trillingen van moleculen. Hiermee kan onder meer de verhouding tussen lipiden en eiwit in het stratum corneum bepaald worden omdat de lipiden met een andere frequentie trillen dan de eiwitten.

Röntgen-diffractie: Analytische techniek waarbij Röntgenstraling wordt gebruikt om de lamellaire structuur van in dit geval lipiden in het stratum corneum te onderzoeken.

Sfingomyelinase: Enzym dat een fosfocholine 'losknijpt' van een sfingomyeline-molecuul, waardoor een ceramide ontstaat.

SPINK5 gen: Het gen wat codeert voor het eiwit LEKTI (zie LEKTI), en wat gemuteerd is bij mensen met Netherton syndroom. De naam staat voor serine peptidase inhibitor, Kazal type 5.

Stratum corneum: Beter bekend als de hoornlaag van de huid, die bestaat uit dode cellen met daartussen de lipiden. Deze dunne huidlaag fungeert als belangrijkste barrière tegen het binnendringen van stoffen van buitenaf. Daarnaast voorkomt het uitdroging.

Tape-strippen: methode om met behulp van 'tape' snel en op een niet belastende manier laagjes stratum corneum te verkrijgen.

Transdermaal waterverlies: De hoeveelheid water dat vanuit het lichaam via de huid wordt afgegeven aan de omgeving. Niet te verwarren met zweet, dat via zweetklieren wordt afgegeven.

Validatieprotocol: Een protocol waarin getest wordt of de ontwikkelde methode voldoet aan de eisen die vooraf gesteld zijn.

Vloeistofchromatografie: Een techniek waarbij stoffen gescheiden worden op basis van hun affiniteit met een vaste fase ten opzichte van een bewegende vloeistoffase: Stoffen worden meegeleid in een vloeistof langs een analytische kolom met een vaste fase. Stoffen die chemisch gezien meer overeenkomst vertonen met de vaste fase worden vertraagd en worden op deze manier in de mobiele fase gescheiden van stoffen die minder overeenkomst vertonen met de vaste fase.

Ionisatie: Het proces waarbij een ongeladen molecuul een geladen atoom (of elektron) meer of minder krijgt en zo een positieve of negatieve lading krijgt.



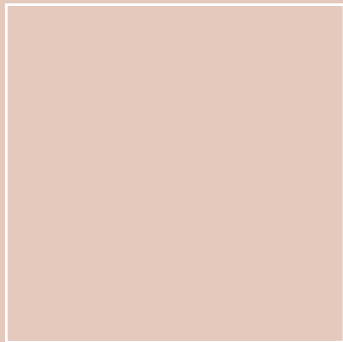
CURRICULUM VITAE

Jeroen van Smeden was born on the 28th of August in 1984 in Leidschendam. After graduating from the Oranje Nassau College in Zoetermeer in 2003, he started his study Bio-Pharmaceutical Sciences at the University of Leiden. During his study he did two internships. The first one he performed at the division of Drug Delivery Technology at the LACDR, entitled “Transdermal iontophoretic delivery of a dopamine agonist – Characterisation of 5-OH-DPAT and two esterified prodrugs”. Afterwards, he went to Octopus N.V. for his second internship, working on the topic of “Study on Locteron™ content – Characterisation of IFN- α 2b”. On the 9th of September 2008, he obtained his Master’s degree with honour. He started his PhD one month later at the division of Drug Delivery Technology under the supervision of Prof. Dr. Joke Bouwstra and Dr. Rob. J. Vreeken from the division of Analytical Biosciences, which resulted in this thesis. In March 2013 he continued as a postdoc to advance the knowledge achieved on the PhD project.

List of Publications:

- J. van Smeden, W.A. Boiten, T. Hankemeier, R. Rissmann, J.A. Bouwstra and R.J. Vreeken.
Combined LC/MS-assay for analysis of all major stratum corneum lipids, and the analysis of skin substitutes. (submitted)
- V.S. Thakoersing, J. van Smeden, W. Boiten, G.S. Gooris, A. Mulder, R.J. Vreeken, A. El Ghalbzouri, J.A. Bouwstra.
Modulation of barrier properties of human skin equivalents by specific medium supplements. (prepared for submission)
- J. van Smeden*, M. Janssens*, W.A. Boiten, R.J. Vreeken, A. Hovnanian, J.A. Bouwstra.
Skin barrier lipid composition and organization in Netherton Syndrome patients. (submitted)
- J. van Smeden*, M. Janssens*, E.C.J. Kaye, P. J. Caspers, A.P. Lavrijsen, R.J. Vreeken and J.A. Bouwstra.
The essence of free fatty acid chain length for the skin barrier function in atopic eczema patients. (submitted)
- M. Janssens, J. van Smeden, G.J. Puppels, A.P.M. Lavrijsen, P.J. Caspers, J.A. Bouwstra.
Lipid to protein ratio plays an important role in the skin barrier function of patients with atopic eczema. (submitted)
- M. Janssens, A.A. Mulder, J. van Smeden, G.S. Pilgram, R. Wolterbeek, A.P. Lavrijsen, R.I. Koning, A.J. Koster, J.A. Bouwstra.
Electron diffraction study of lipids in non-lesional stratum corneum of atopic eczema patients. *Biochim Biophys Acta.* 2013.
- J. van Smeden*, M. Janssens*, A.P. Lavrijsen, S. Kezic, R.J. Vreeken, J.A. Bouwstra.
Skin barrier dysfunction in non-lesional atopic eczema: the role of stratum corneum lipids. *Eur J Dermatol.* 2013.
- J. van Smeden*, M. Janssens*, G.S. Gooris, W. Bras, G. Portale, P.J. Caspers, R.J. Vreeken, T. Hankemeier, S. Kezic, R. Wolterbeek, A.P. Lavrijsen, J.A. Bouwstra.
Increase in short-chain ceramides correlates with an altered lipid organization and decreased barrier function in atopic eczema patients. *J Lipid Res.* 2012.
- J. van Smeden*, V.S. Thakoersing*, A.A. Mulder, R.J. Vreeken, A. El Ghalbzouri, J.A. Bouwstra.
Increased presence of monounsaturated fatty acids in the stratum corneum of human skin equivalents. *J Invest Dermatol.* 2013.
- J. van Smeden*, M. Janssens*, G.S. Gooris, W. Bras, G. Portale, P.J. Caspers, R.J. Vreeken, S. Kezic, A.P. Lavrijsen, J.A. Bouwstra.
Lamellar lipid organization and ceramide composition in the stratum corneum of patients with atopic eczema. *J Invest Dermatol.* 2011.
- J. van Smeden, L. Hoppel, R. van der Heijden, T. Hankemeier, R.J. Vreeken, J.A. Bouwstra.
LC/MS analysis of stratum corneum lipids: ceramide profiling and discovery. *J Lipid Res.* 2011.
- O.W. Ackaert, J. van Smeden, J. de Graan, D. Dijkstra, M. Danhof, J.A. Bouwstra.
Mechanistic studies of the transdermal iontophoretic delivery of 5-OH-DPAT in vitro. *J Pharm Sci.* 2010.

* Contributed equally as first authors.



DANKWOORD

Aan het einde van dit proefschrift rest er nog 1 belangrijke taak: het bedanken van de mensen die dit proefschrift tot stand hebben gebracht. Hoewel ik iedereen kan – en ook nadrukkelijk wil – noemen die mij de afgelopen vier jaar hebben bijgestaan (familie, (pizza-)vrienden, fysiotherapeut, en meer van diens), blijf ik mij hier beperken tot de mensen met een direct wetenschappelijk gerelateerde bijdrage aan dit proefschrift.

Allereerst Michelle. We kunnen terugkijken op een succesvolle samenwerking tijdens de afgelopen jaren. Zonder jou was de planning waarschijnlijk uitgemond in een geordende chaos, als er al überhaupt een planning was geweest. Ik denk dat er weinig PhD's kunnen zeggen dat zo'n hechte samenwerking heeft geleid tot zo veel mooie artikelen.

Natuurlijk wil ik ook jou, Varsha, apart vermelden. Jouw bijdrage met betrekking tot de kweekhuid is van heel veel waarde, en waarschijnlijk meer dan je zelf denkt. Daarnaast zijn daar die 'unieke' momenten op bijvoorbeeld de conferenties als de Gordon. Het is jammer dat aan dat tijdperk een einde heeft moeten komen.

Gelukkig heb je een hele lieve opvolger gekregen. Lolu, ik ben blij dat de huidkweek wordt doorgezet, en dat je kon voortborduren op dit gebied waar wij nu nauw samen aan verbonden zijn.

Ook jij, Aat, mag hier natuurlijk niet ontbreken, aangezien je Michelle en mij zo veelvuldig hebt geholpen. Niet alleen voor de ontelbare keren dat er tape-strips gestanst moesten worden, maar ook bij de BCA-assay, waar het woord microliterpipetteren een nieuwe dimensie heeft gekregen. En dan heb ik het niet eens over ED, excelsheets, en gewoon de gezelligheid op de kamer.

Daarnaast kan ik natuurlijk ook mijn 9-maanden

stagestudenten en de enige echte LC/MS analist niet vergeten. Walter, Edward en Hannah, jullie hebben eraan bijgedragen dat de vakgroep een LC/MS methode voor het analyseren van huidlipiden heeft die op dit moment zonder twijfel tot de meest vooraanstaande behoort in de wereld.

Aansluitend wil ik ook twee andere analisten noemen: Gert en Gerwin. Als alles zou zijn gegaan zonder problemen, zouden jullie waarschijnlijk minder bij het project betrokken zijn geweest. Maar uiteraard vraagt wetenschappelijke apparatuur meer tijd, inspanning en onderhoud dan je zou wensen, en laten we eerlijk wezen, zonder jullie zou er de afgelopen vier jaar überhaupt weinig te meten zijn geweest. En dan heb ik nog niet eens jullie bijdrage genoemd tijdens de nuttige conversaties.

Lieve Connie, ook jij moet even apart genoemd worden. De afgelopen vier jaren ben jij als secretaresse vaak bij ons project betrokken geweest voor die kleine dingetjes die toch elke keer weer geregeld moesten worden. Afspraken met het LUMC, meetings tussen Joke en Rob, zaken voor mijn promotie, et cetera. Heel erg bedankt voor al die uren die je eraan hebt gespendeerd.

Laat ik dan ook zeker Robert niet vergeten. Jij hebt mij al weer meer dan 4 jaar terug ingewerkt in het hele project waar dit proefschrift uit voortgekomen is. Ik ben blij dat jij me hebt geholpen de eerste maanden als PhD succesvol (hoop ik) door te zijn gekomen.

Enamul en Koen, als Paranimfen ben ik blij dat jullie aan mijn zijde staan tijdens de verdediging van mijn proefschrift. Jullie hebben ervoor gezorgd dat ook het einde van mijn PhD tot een feest geworden is.

Eveneens wil ik iedereen van de vakgroep kort vermelden. De individuele discussies, vragen tijdens de presentaties, of scherpe opmerkingen tijdens de koffiepauzes hebben mij veelvuldig aan het denken. Daar waar wetenschap soms een zwart gat lijkt en moeilijk te doorgronden valt, kan een simpele opmerking licht brengen en tot nieuwe inzichten leiden.

En dan wil ik ook Melina noemen. Iedereen die dit proefschrift leest kan dat alleen maar lezen dankzij de urenlange inspanningen die jij hebt verricht om dit proefschrift tot zoiets moois, unieks, en bovenal waanzinnig stijlvol weten te maken. Heel, héél veel dank daarvoor.

Rest mij te besluiten met de allerlaatsten, en tevens de meest dierbaren die niet mogen ontbreken: mijn naaste familie, in het bijzonder mijn lieve Bianca. Vaak heb ik mijn thuissituatie tot 's avonds laat moeten achterlaten in dienst van de wetenschap. Los van het feit dat jij ook hebt bijgedragen aan de uiteindelijke versie van het proefschrift, ben ik zo ontzettend dankbaar dat jij mij altijd gesteund hebt!



LIST OF ABBREVIATIONS

ACN	- acetonitrile
AE	- atopic eczema
(A)GPAT	- (acyl)glycerol-3-phosphate
ANOVA	- analysis of variance
APCI	- atmospheric pressure chemical ionization
aSMASE	- acid sphingomyelinase
ATR	- attenuated total reflectance
AU	- arbitrary units
β -GCase	- β -glucocerebrosidase
BCA	- bicinchoninic acid assay
BSA	- bovine serum albumin
CCD	- charge-coupled detector
CER	- ceramide
CERS	- ceramide synthase family (1 to 6)
CERS3	- ceramide synthase 3
CHCl ₃	- chloroform
CHOL	- cholesterol
DES	- dihydroceramide desaturase (1 and 2)
ELA2	- protease elastase 2
ELOVL	- elongation of very long chain fatty acids
ESI	- electrospray ionization
EtOH	- ethanol
FAS	- fatty acid synthase
FDM	- fibroblast derived matrix model
FFA	- free fatty acid
FLG	- filaggrin gene
FT-ICR	- Fourier transform ion cyclotron resonance
FTIR	- Fourier transform infrared spectroscopy
FTM	- full-thickness collagen model
FTO	- full thickness outgrowth
FWHM	- full width at half maximum
GC	- gas chromatography

GCS	- glucosylceramide synthase	PAR2	- proteinase-activated receptor 2
GLC	- gas-liquid chromatography	PLA-2	- phospholipase
H ₂ O	- water	PPAR	- peroxisome proliferator-activated receptor
HAC	- acetic acid	PUFA	- polyunsaturated fatty acid
HPLC	- high performance liquid chromatography	PVA	- polyvinyl alcohol
HPTLC	- high performance thin layer chromatography	RPLC	- reversed phase liquid chromatography
HSE	- human skin equivalents	S/N	- signal to noise ratio
IFN	- interferon	SAXD	- small angle X-ray diffraction
IgE	- immunoglobulin E	SC	- stratum corneum
IL	- interleukin	SCD	- stearyl-CoA desaturase
IPA	- isopropanol	SCORAD	- scoring atopical dermatitis
IT	- ion trap	SD	- standard deviation
KLK	- kallikrein	SEM	- standard error of the mean
KSR	- 3-ketosphinganine reductase	SMS	- sphingomyelin synthase
LB	- lamellar body	SPINK5	- serine protease inhibitor Kazal-type 5
LC/MS	- liquid-chromatography-mass-spectrometry	SPP	- short periodicity phase
LEKTI	- lympho-epithelial Kazal-type-related inhibitor	SPT	- serine palmitoyltransferase
LEM	- Leiden epidermal model	SULT2B1b	- cholesterol sulfotransferase type 2B isoform 1B
LOD	- limit of detection	TEWL	- transepidermal water loss
LOQ	- limit of quantification	TLC	- thin layer chromatography
LPP	- long periodicity phase	TQ	- triple quad
LXR	- liver X receptor	TSLP	- thymic stromal lymphopoietin
MCT	- mercury-cadmium-telluride		
MeOH	- methanol		
MS	- mass spectrometry		
MUFA	- monounsaturated fatty acid		
NES	- Netherton syndrome		
NMF	- natural moisturizing factor		
NMR	- nuclear magnetic resonance		
NPLC	- normal phase liquid chromatography		
OH-FFAs	- hydroxyl-fatty acids		

